Identification and Characterization of SdbA, a Novel Thiol-Disulfide Oxidoreductase in *Streptococcus gordonii*

by

Lauren Davey

Submitted in partial fulfilment of the requirements
for the degree of Doctor of Philosophy

at

Dalhousie University
Halifax, Nova Scotia
March 2016

Table of Contents

List of Tables

List of Figures

Abstract

Disulfide bonds are important for the stability of certain extracellular proteins, including bacterial virulence factors. Thiol disulfide oxidoreductases (TDORs) catalyze disulfide bond formation. Although these enzymes have been well characterized in some organisms, little is known about how disulfide bonds are formed in Gram-positive bacteria, particularly among facultative anaerobes such as streptococci. An analysis of the *Streptococcus gordonii* sequenced genome found five putative TDORs. These TDORs were systematically investigated for their affect on autolysis, extracellular DNA release, biofilm formation, bacteriocin production, and genetic competence. This revealed a single TDOR with a pleiotropic phenotype that we named ***S****treptococcus* **d**isulfide **b**ond protein **A** (**SdbA**). SdbA was demonstrated to catalyze disulfide bond formation, and using an *in silico* approach, we identified the major autolysin AtlS as a natural substrate.

The low homology of SdbA to known TDORs prompted us to investigate its catalytic mechanism. TDORs catalyze disulfide bonds using a CXXC motif. Typically, the N-terminal cysteine interacts with substrates, while the C-terminal cysteine is buried, and both are essential for activity. We show that SdbA functions differently, and that mutants with a single, buried C-terminal cysteine of the CXXC motif can complement a Δ*sdbA* mutant, and restore disulfide bond formation to recombinant and natural substrates. These results distinguish SdbA from previously described TDORs.

Finally, we found that mutation of SdbA generated an activating signal for the CiaRH two-component system. CiaRH is involved in stress response and affects virulence in pathogenic streptococci. Our results suggest that CiaRH can sense disulfide bond formation in *S. gordonii*. Activation of CiaRH repressed a second signaling system, ComDE, and eliminated bacteriocin production. Together, CiaRH and ComDE regulate >100 genes. By modulating the activity of CiaRH, SdbA can influence a broad spectrum of bacterial physiological processes that are not directly related to disulfide bond formation.

In summary, this study establishes SdbA as a novel TDOR that catalyzes disulfide bond formation in *S. gordonii* and is important for the normal physiology of the cell.

List of Abbreviations Used

AP	alkaline phosphatase
BCIP	5-bromo-4-chloro-3'-indolyphosphate p-toluidine salt
BHI	brain heart infusion
BHIS	brain heart infusion with 5% serum
cCMP	cytidine 2':3'-cyclic monophosphate monosodium salt
CHAP	cysteine, histidine-dependent amidohydrolase/peptidase
CSP	competence stimulating peptide
csRNA	cia-dependent small RNAs
DEAE	diethylaminoethyl
Dsb	disulfide bond
DSF	differential scanning fluorimetry
DTNB	5, 5'-dithio-bis(2-nitrobenzoic acid)
DTT	dithiothreitol
eDNA	extracellular DNA
EDTA	ethylenediaminetetraacetic acid
ELISA	enzyme-linked immunosorbent assay
FAD	flavin adenine dinucleotide
FBS	fetal bovine serum
GH25	glycosyl hydrolase 25
GSH	reduced glutathione
GSSG	oxidized glutathione
HEPES	4-(2-hydroxyethyl)-1-piperazineethanesulfonic acid
His_6	hexahistidine
HTVG	HEPES-buffered tryptone-vitamins glucose media
IAM	iodoacetamide
IPTG	isopropyl-β-D-thiogalactopyranoside
LB	Luria-Bertani

LC	liquid chromatography
Mal	maleimide
MOPS	3-(N-morpholino) propanesulfonic acid
MS	mass spectrometry
NBT	nitro-blue tetrazolium
PBS	phosphate buffered saline
PBST	phosphate buffered saline, 0.1% Tween 20
PCR	polymerase chain reaction
PEG	polyethylene glycol
PMSF	phenylmethylsulfonyl fluoride
qPCR	quantitative real-time PCR
RT-PCR	reverse transcription PCR
scFv	single chain variable fragment
SEM	scanning electron microscopy
TCA	trichloroacetic acid
TDOR	thiol-disulfide oxidoreductase
TE	Tris EDTA
Tris	Tris (hydroxymethyl) aminomethane

Acknowledgments

This project was possible thanks to the help of many people along the way. Foremost are my supervisors and mentors, Drs. Song Lee and Scott Halperin. They have been a continual source of motivation and sound advice. Their input and support kept the project on track, even during difficult periods. Dr. Lee's enthusiasm for research is infectious, and he sets a great example for all of his students. I have learned a lot from him and I truly appreciate his encouragement of my career.

Thank you to my committee members, Drs. John Rohde, Nikhil Thomas, and Raphael Garduno. Their great suggestions really helped to improve the project. Dr. Rohde also helped with critically reading our manuscript and helped us to establish our collaboration with Drs. Alexi Shevchenko and Peter Stogios (University of Toronto). I appreciate their collaboration, and thanks to their hard work we can finally see what SdbA looks like. I also thank my external advisors Dr. Dennis Cvitkovitch (University of Toronto) and Dr. Neale Ridgway.

Some of the initial experiments that helped to shape the direction of the project were carried out Crystal Ng, who worked on *S. gordonii* TDORs for her Honours thesis. Her work characterizing all of the TDOR mutants was a significant contribution to the project. I thank Alejandro Cohen for all of his help with our mass spectrometry experiments, and for taking the extra time to explain the process and teach me about data analysis. I also thank Jason LeBlanc for his help with analyzing our proteins and with the preparation of our manuscript. And thank you to Ann MacMillan for her help with our mouse experiments, and for being so great to work with. I also thank Dr. Ping Li and Patricia Scallion for their help with electron microscopy.

The CCfV lab is vibrant work environment, and the students and staff have made even the longest days in the lab enjoyable. I am thankful to Badii Al-Bana for his advice and for reading my comprehensive essays. I have really enjoyed working with all of the past and present students in the Lee lab including Farhan, Maram, Yunnuo, Hilary, Naif, Chih Chen, and Sarah, and all of the other students that have worked in the lab.

Thank you to Drs. J. Weiser (New York University), G. Tompkins (University of Otago), M. Vickerman (University at Buffalo), and R. Glockshuber (ETH Zurich,

Institute of Molecular Biology and Biophysics) for providing bacterial strains and antibodies.

I also thank my funding sources: the Natural Sciences and Engineering Research Council of Canada, Nova Scotia Health Research Foundation, and the Izaak Walton Killam Health Centre.

Chapter 1: Introduction

1.1 Protein Disulfide Bonds

Background

The production and maintenance of functional proteins is essential for viability. Cells employ a host of chaperones, enzymes, and proteases dedicated to protein production and quality control (1). Remarkably, organisms from all three domains of life have evolved to use disulfide bonds to stabilize their proteins. Structural disulfide bonds enable proteins to achieve their proper conformation, while conferring stability and resistance to degradation (1, 2).

Protein disulfide bonds are covalent bonds formed between the sulfur atoms of cysteine residues. Their formation is an oxidation reaction that involves the loss of two electrons and two protons, and is generally referred to as oxidative protein folding (3). At one time, disulfide bonds were thought to form spontaneously in the presence of oxygen. Anfinsen's classic experiments on RNase A refolding, which led to a Nobel prize, showed that the primary amino acid sequence contains all the information needed to generate the final, native protein (4). Although this is true *in vitro*, spontaneous disulfide bond formation lacks the efficiency and accuracy required for living cells, and it is now clear that disulfide bond formation is a catalyzed process *in vivo* (1). The enzymes that catalyze disulfide bond formation are referred to as thiol-disulfide oxidoreductases (TDORs).

For most organisms, from humans to *Escherichia coli*, disulfide bonds are primarily found as extracytoplasmic proteins. Outside of the regulated environment of the cytoplasm, secreted proteins are vulnerable to potentially damaging conditions, and disulfide bonds are thought to provide added resilience. In eukaryotes, disulfide bond formation occurs in the endoplasmic reticulum (ER) and the intermembrane space of mitochondria (3, 5). A similar scenario occurs in Gram-negative bacteria, where disulfide bond formation occurs in the periplasmic space between the inner and outer cell

membranes (6). Gram-positive bacteria, on the other hand, lack an outer membrane and periplasm, and therefore carry out disulfide bond formation directly at the cell wall (7). In contrast, the cytoplasm is actively maintained as a reducing environment by enzymes such as thioredoxin and glutaredoxin (8). A rare exception to this trend is the hyperthermophilic Archaea, which are predicted to have an abundance of disulfide bonded cytoplasmic proteins, presumably as an adaptation to the harsh conditions of their niche (9).

Characteristics of Thioredoxin Family Enzymes

The thioredoxin superfamily is a conserved and ancient group of enzymes, thought to date back billions of years to the last common universal ancestor (10). These enzymes are found in all organisms and participate in a range of redox reactions including oxidation, reduction, and isomerization (rearrangement) of disulfide bonds (11). Although the enzymes share very little sequence homology, they all have a characteristic thioredoxin fold structure, with a four-stranded β-sheet with three flanking α-helices, and a C-X-X-C active site motif (8, 12, 13). The only conserved amino acid, aside from the cysteines of the CXXC motif, is a *cis*-proline residue that localizes to the active site in the tertiary structure. This proline is involved in substrate release and prevents metal binding at the active site (14, 15). With few conserved amino acids, it can be difficult to predict the function of thioredoxin family proteins based on sequence alone.

Several biochemical properties of thioredoxin family proteins are used to describe their activity. A key factor affecting activity is the pK_a of the N-terminal cysteine in the CXXC motif. The pK_a value refers to the pH where 50% of the sulfur atoms in the protonated, thiol form (SH), and 50% are in the thiolate anion form (S^-). This is an important indicator of reactivity because a thiolate anion is much more reactive than a thiol (16). Typical cysteines have a basic pK_a (~9), whereas the cysteines of thioredoxin family proteins are unusually acidic. Generally, enzymes that participate in reduction reactions have a pK_a value around 7, while those that catalyze oxidation reactions have a pK_a value as low as 3 (16, 17).

A second measure of enzyme activity is the redox potential. This value is calculated based on an equilibration reaction with glutathione, and gives an indication of the reactivity of an enzyme. Electrons will travel from the enzyme with the more negative redox potential to those that are more positive (3). For example, the reducing enzyme thioredoxin has a redox potential of -270 mV, whereas the oxidizing enzyme DsbA has a redox potential of -121 mV (8, 18). However, it has been observed that enzymes with opposite functions can have similar redox potentials, and that it may not correlate with activity (19). For example, the reductase/isomerase DsbC has a redox potential of -129 mV, similar to the oxidase DsbA (13, 18). In addition, mutations that lower the redox potential of DsbA to that of thioredoxin do not eliminate its oxidizing activity (19). Thus, it is important to combine *in vitro* and *in vivo* assays to get a clear picture of enzyme function.

1.2 Disulfide Bond Formation in Eukaryotes

In eukaryotes, disulfide bond formation occurs primarily in the lumen of the endoplasmic reticulum. Here, a multifunctional enzyme called protein disulfide isomerase (PDI) catalyzes both disulfide bond formation and isomerization. PDI is a thioredoxin family protein with two CXXC active sites, and both are required for efficient activity (3). PDI works by binding to the cysteines of reduced protein substrates as they are translocated from the cytosol. This results in a mixed disulfide bond between the active site of PDI and its substrate. The substrates then fold into their native conformation, and as the final step of the folding process, PDI catalyzes disulfide bond formation (20). PDI is maintained as a mixture of oxidized and reduced forms. The reduced form has isomerase activity to rearrange disulfide bonds, while the oxidized form catalyzes disulfide bond formation (3).

During the catalytic cycle, a disulfide bond between the active site cysteines of PDI is transferred to substrate proteins in redox reaction that couples the oxidation of the substrate with reduction of PDI. A redox partner, ERO1, regenerates the PDI active site disulfide bond. ERO1 is an integral membrane protein that generates disulfide bonds

from molecular oxygen with the help of a FAD cofactor (21). During the reaction, electrons are passed from PDI to cysteines in ERO1, on to the FAD cofactor, and finally to molecular oxygen, with H_2O_2 produced as a byproduct (1). In humans, there are two ERO1 proteins and at least 20 different types of PDI-family enzymes (3).

A separate set of enzymes that catalyze disulfide bond formation are present in mitochondria. Mia40 is a disulfide bond catalyst located in the intermembrane space, and like PDI, it uses a FAD dependent redox partner, Erv1. Mia40 is an unusual disulfide bond catalyst because it is not a thioredoxin family protein and it acts on a specific set of substrates with CX3C or CX9C motifs (5). Substrates traverse the mitochondrial membrane through the translocase of the outer membrane (TOM) complex in a reduced state, and once inside, disulfide bond formation by Mia40 folds them into a conformation that traps them within (22). Like PDI, Mia40 has both oxidase and isomerase activity (23).

1.3 Disulfide Bond Formation in Bacteria

Bacteria also use dedicated enzymes to catalyze disulfide bond formation, and the *E. coli* Dsb system is considered the archetype of oxidative protein folding. As information emerges regarding the disulfide bond pathways of other types of bacteria, it is becoming clear that there is considerable diversity in the prevalence and mechanisms of disulfide bond formation (24). Understanding how disulfide bonds are formed is of interest from a biotechnological perspective, to enhance recombinant protein production, as well as from a health perspective since pathogens often use disulfide bonds to stabilize their virulence factors (25).

The enzymes that catalyze disulfide bond formation play a pivotal role in virulence (25, 26). Examples of well characterized virulence factors that require disulfide bonds for activity include toxins from *Bordetella pertussis* and *Staphylococcus aureus*, secreted enzymes from *Pseudomonas aeruginosa*, pili and flagella in *E. coli* and *Salmonella*, and the type III and type IV secretions systems of various pathogens including *Shigella flexneri, Yersinia pestis*, and *Legionella pneumophila* (25, 27–34). Consequently,

disulfide oxidoreductases are often essential for virulence, and there is an active effort to develop small molecule inhibitors against them (35–37).

Disulfide oxidoreductases also have the potential to enhance recombinant protein production. Some eukaryotic proteins require many disulfide bonds, for example, an IgM pentamer has over 100, and this can be a rate limiting step in production (2, 38). Over-expression of enzymes that catalyze disulfide bond formation and isomerization has been used to enhance yields of recombinant proteins (39–41). Similarly, inactivating reductases can enhance protein production by permitting disulfide bond formation in the cytoplasm (38, 42). Commercial *E. coli* strains that lack thioredoxin and glutaredoxin (Origami, Novagen), and express a cytoplasmic version of the disulfide isomerase DsbC (SHuffle, New England Biolabs) have been developed to facilitate recombinant protein production (38, 43).

Whether the goal is to enhance disulfide bond formation for recombinant protein production, or to stop it to prevent infection, it is essential to first understand the basic mechanisms involved. Since the initial discovery of the *E. coli* system, new oxidoreductases have been identified in all phyla of bacteria.

1.3.1 Gram-Negative Bacteria

In Gram-negative bacteria, disulfide bond formation occurs in the periplasm. Nascent proteins are translocated from the cytoplasm via the sec pathway in a reduced and unfolded state, and disulfide bonds are introduced as the proteins enter the periplasm (44). Within the periplasmic space, a host of enzymes catalyze the formation, reduction, and rearrangement of disulfide bonds to ensure properly folded proteins. This process is best understood in *E. coli*.

1.3.1.1 *Escherichia coli* K-12

Disulfide Bond Formation by DsbAB

E. coli DsbA was the first bacterial disulfide bond catalyst to be discovered (45). Although the discovery was made by Jonathan Beckwith's laboratory in 1991, almost 30

years after the discovery of PDI, it has since become the best characterized disulfide bond catalyst. DsbA is among the most oxidizing enzymes discovered to date, with a redox potential of -121 mV, and it is estimated to form disulfide bonds in hundreds of substrates, or around 40% of secreted proteins (46). Surprisingly, however, DsbA is not essential, which has facilitated extensive investigation the disulfide bond pathway. Several structures for DsbA have been reported, including both the oxidized and reduced conformations (47, 48), as well as complexes of DsbA with its redox partner, DsbB (49), and with a peptide substrate (50). These structures, along with detailed mutational analyses, have contributed to the basic understanding of how DsbA works and the factors that affect the enzymatic activity of oxidoreductases (13, 18).

DsbA is a 21 kDa monomeric protein located in the periplasm, where it introduces disulfide bonds into substrate proteins (14). The catalytic mechanism involves oxidation of a substrate coupled with reduction of DsbA. DsbA has a Cys^{30}-Pro^{31}-His^{32}-Cys^{33} active site motif, which contains a disulfide bond between Cys30 and Cys33 (Fig. 1.1). The interaction between DsbA and a substrate is initiated when a reduced cysteine in the substrate attacks the DsbA active site disulfide bond, resulting in a mixed disulfide between the substrate and DsbA Cys30. A second cysteine in the substrate then reacts to resolve the mixed disulfide bond. This completes the reaction, generating a new disulfide bond in the substrate protein, while leaving DsbA in a reduced state (6).

Before DsbA can oxidize another substrate, its active site disulfide bond must be regenerated. A partner enzyme located at the inner membrane, DsbB, is responsible for the reoxidation of DsbA. DsbB is a 20 kDa integral inner membrane protein with four transmembrane domains, and two periplamsic domains. Each of the periplasmic domains contains two cysteine residues, Cys41 and Cys44, and Cys104 and Cys130, all of which participate in reoxidation of DsbA (51). Although more than one reaction mechanism has been proposed for DsbB, the primary mechanism involves the generation of a disulfide bond between Cys41 and Cys44, which is subsequently transferred to Cys104 and Cys130 (49). DsbA Csy30, the N-terminal cysteine of the DsbA active site, then attacks DsbB Cys104 resulting in a mixed disulfide complex. Finally, the second cysteine of the

DsbA active site, DsbA Cys33, resolves the mixed disulfide, to form the active site disulfide bond. At this point, DsbA is ready to catalyze another round of disulfide bond formation.

Unlike DsbA, which transfers an existing disulfide bond from its active site to a substrate, DsbB is capable of generating disulfide bonds *de novo* by reducing molecular oxygen, and it is the main generator of disulfide bonds in the cell (52). DsbB achieves this with the help of a quinone cofactor that binds to a transmembrane region near Cys44 (49). The quinone accepts electrons from DsbB and funnels them into the electron transport chain, via cytochromes, to a final electron acceptor (53). Under aerobic conditions, DsbB transfers electrons to ubiquinone, and ultimately uses oxygen as a final electron acceptor (53), whereas under anaerobic conditions, DsbB associates with menaquinone and uses alternative electron acceptors, such as fumerate and nitrate reductase (54).

Reactivity of DsbA

DsbA is a highly reactive enzyme and analysis of its structure and biochemistry has identified several contributing factors. The reactivity of DsbA is attributed largely to the highly acidic pK_a of its N-terminal active site cysteine, which is around 3.5 (55). DsbA has one of the lowest cysteine pK_a values known. This means that at physiological pH, all of DsbA will be in the reactive thiolate anion form.

A second factor contributing to the reactivity of DsbA is the unusual structural instability of its active site disulfide bond. Unlike most proteins, where disulfide bonds enhance structural stability, the disulfide bond in DsbA is energetically destabilizing (47, 56). The instability of the oxidized form enhances reactivity towards substrate proteins. Interestingly, there is little structural difference between the reduced and oxidized forms of DsbA, and the difference in stability has been attributed to the His32 residue located in the CPHC active site motif (47). Similarly, His32, along with other nearby residues, contributes to the acidic nature of Cys30 (47).

Given the influence of His32 on the activity of DsbA, it is not surprising that the CXXC active site dipeptide influences enzyme activity (18, 57–59). Mutational analysis of DsbA and the isomerase DsbC (discussed below) have shown that, depending on the identity of the amino acid substitutes, activity can be abolished or enhanced above wild type levels (58). The observed changes in activity have been attributed to the dipeptide's affect on redox potential and on the pK_a of the active site cysteines (17, 57, 58). Changes to the active site dipeptide can also alter the nature of the redox reactions catalyzed by an enzyme. For example, mutation of the active site dipeptide in thioredoxin can convert it from a reductase to an oxidase (18). This indicates that the variable amino acids of the CXXC motif have evolved to fine tune enzyme function.

Aside from the CXXC motif, only one amino acid has been found to affect the activity thioredoxin family enzymes. This is the amino acid located on the N-terminal side of the conserved *cis*-proline. This amino acid affects the pK_a of the active site cysteine, as well as interactions with substrates and redox partners (13). Thus, the activity of DsbA is dictated by just a few specific amino acids, in combination with its structural features.

Substrate Recognition

Structural analysis of DsbA shows a deep groove adjacent to the active site that was once thought to be involved in substrate binding (48). However, the structure of DsbA in complex with its redox partner, DsbB, indicated that the groove is involved in binding its redox partner rather than substrates (49). Instead, DsbA is thought to interact with substrates via hydrophobic surface features surrounding the active site, referred to as a hydrophobic patch (48, 50). This mechanism of substrate binding has been postulated to contribute to the enzyme's broad substrate range (50). An analysis of the amino acid sequences in 45 confirmed DsbA substrates showed no homology, aside from cysteines requiring disulfide bonds, indicating that DsbA does not recognize a specific motif in its substrates (50). However, DsbA does not react with all thiols equally, and it has been shown to preferentially oxidize unfolded proteins (55, 60). This is consistent with the

idea that hydrophobic interactions contribute to substrate recognition, since hydrophobic regions are typically exposed in unfolded proteins.

Since DsbA is both highly reactive and non-specific, it has the potential to introduce incorrect disulfide bonds, particularly in proteins with multiple cysteines. DsbA is thought to bind to its substrates during translocation. Thus, it tends to introduce disulfide bonds sequentially, between consecutive cysteines, as they emerge into the periplasm (61). For proteins with non-consecutive disulfide bonds, an additional enzyme, DsbC, is required to achieve the correct connectivity of their cysteines (62, 63).

Disulfide Isomerization by DsbCD

Unlike the dual oxidase/isomerase activity of PDI, these functions are separated in *E. coli*, which uses a dedicated isomerase called DsbC (Fig. 1.2). Although DsbA can fold certain proteins with non-consecutive disulfide bonds (61, 64), a few are dependent on DsbC to achieve their native conformation (62, 63). These substrates include proteins with multiple disulfide bonds, such as RNase I, MepA, and phytase (62, 63). DsbC probably becomes more important under certain growth conditions, and has been found to be important for resistance to copper stress (65).

DsbC is a soluble homodimer with one catalytic CGYC motif in each subunit (66). Upon encountering a misoxidized protein, DsbC forms a mixed disulfide between the N-terminal cysteine of its active site and a substrate cysteine, thus breaking the incorrect disulfide bond. From here there are two alternative pathways to resolve the mixed disulfide bond between DsbC and its substrate: (1) A second cysteine within the substrate can attack the mixed disulfide, generating the correct bond in a single step; or (2) the C-terminal cysteine of the DsbC CXXC motif can attack the bond, resulting in reduction of the substrate to allow another cycle of oxidation by DsbA (67). Interestingly, only a single CXXC site is required for activity, and dimerization of DsbC serves to prevent interactions with DsbB to keep the oxidation and isomerization pathways separated (68).

In reactions that leave the DsbC active site oxidized, it must be reduced by its redox partner, DsbD, before it can continue another catalytic cycle (69, 70). DbsD is an integral inner membrane protein that transfers reducing equivalents from the cytoplasm to periplasm (71). DsbD consists of three domains, an N-terminal periplasmic domain with an immunoglobulin fold (DsbDα), a membrane domain with eight transmembrane helices (DsbDβ), and a C-terminal periplasmic thioredoxin domain (DsbDγ). Each of the three domains has two cysteines that are required for activity (72). The pathway for electron transfer by DsbD has been well characterized, and the structures of the DsbDα and DsbDγ domains have been solved (73, 74), as well as the DsbDβ domain homolog, CcdA (75). Electrons originating from NADPH in the cytoplasm are transferred via thioredoxin reductase to thioredoxin, and then on the cysteines of the transmembrane DsbDβ domain (71, 75, 76). Through a series of conformation changes, DsbDβ shuttles electrons across the inner membrane, and passes them through a disulfide cascade first to DsbDγ, and then to DsbDα (75, 77). Finally, the DsbDα domain transfers electrons to DsbC to maintain DsbC in its reduced and active state (41).

Reducing Pathways

DsbD is central to the reducing pathways in the periplasm. In addition to DsbC, DsbD also reduces the sulfenic acid reductase DsbG (79) and the cytochrome c maturation protein CcmG (DsbE) (80). DsbG is a dimer that is structurally similar to DsbC, but rather than isomerization, it catalyzes reduction of single cysteines that have been oxidized to sulphenic acid (79). CcmG on the other hand, functions in an entirely different pathway, and is a component of the cytochrome c maturation system I (CCMI). The CCMI system employs at least ten proteins to ligate heme to apocytochrome c, and the cysteines of apocytochrome c must be reduced for the reaction to occur. CcmG is part of a disulfide bond relay that transfers electrons from the cytoplasm via DsbD, on to CcmG, followed by CcmH and finally to apocytochrome c (81). Reduced apocytochrome c binds heme to produce mature cytochrome c.

Interestingly, the necessity for both DsbC and CcmG is to counteract oxidation that is primarily mediated by DsbA. This cooperation between the oxidizing and reducing pathways maintains the characteristically oxidizing environment of the periplasm, while preventing incorrect disulfide bond formation and oxidative damage.

1.3.1.2 Other Gram-Negative Species

The key role of disulfide bond formation in bacterial physiology and virulence has driven investigations of diverse species. This has revealed a number of deviations from the model system, ranging from differences in substrate specificity, to species that use entirely different enzymes. Among Gram-negative species, DsbA homologs are the predominant disulfide bond catalysts, and DsbAB systems are predicted to be used by most Proteobacteria (24). Nevertheless, some notable variations have been observed.

Some species use multiple DsbA homologs with varying substrate specificities. For example, uropathogenic *E. coli* CFT073 encodes additional DsbAB homologs, called DsbLI, which specifically oxidize arylsulfate sulfotransferase (82). *Salmonella enterica* encodes three DsbA homologs, two with homology to *E. coli* DsbA and DsbL, along with a third called SrgA encoded on a virulence plasmid. Both DsbA and SrgA contribute to virulence and production of the type III secretion systems (33). However, the enzymes have different substrate specificity, and only SrgA is capable of oxidizing PefA fimbria subunits (83, 84).

Other species encode multiple DsbA homologs with more marked differences. *Neisseria meningitidis* has three DsbA homologs, two of which are lipoproteins located at the inner membrane, while the third is a soluble periplasmic protein like *E. coli* DsbA (27). Surprisingly, the lipoproteins, NmDsbA1 and NmDsbA2, are the primary disulfide bond forming enzymes in the cell, whereas periplasmic NmDsbA3 is thought to have a limited substrate range (27, 85). NmDsbA1 and NmDsbA2 share a single redox partner and both are involved in virulence, although they exhibit different substrate specificities that have been attributed to subtle structural variations (86). Similarly, *Pseudomonas*

aeruginosa encodes two DsbA homologs, PaDsbA1 and PaDsbA2, along with two DsbB homologs. PaDsbA1 is similar to *E. coli* DsbA and appears to be the primary oxidoreductase in the cell, while PaDsbA2 has four cysteine residues and its function is unknown (87). PaDsbA1 and PaDsbA2 have different expression profiles, and conditions for PaDsbA2 expression have not been identified (87).

Species more distantly related to *E. coli* use more divergent types of oxidoreductases. For example, *Helicobacter pylori* HP0231 (DsbK) is a periplasmic dimer that is structurally similar to the *E. coli* sulfenic acid reductase DsbG, yet functions as a oxidase (88–90). Many intracellular pathogens, particularly those with type IV secretion systems, use a dimeric DsbA homolog called DsbA2. This is a dual function enzyme that catalyzes both oxidation and isomerization, reminiscent eukaryotic PDI (34, 91). The activity of DsbA2 has been investigated experimentally in *Legionella* and *Francisella*, where it is essential for virulence (34, 91). *Legionella* DsbA2 partners with two DsbB and two DsbD homologs. The opposing oxidizing and reducing activities of DsbB and DsbD maintain DsbA2 as a mixture of oxidized and reduced states that enables it to carryout both oxidation and isomerization (92, 93). This is similar to PDI, which is also partially reduced *in vivo* (3). DsbA2 enzymes are predicted to be widely distributed among intracellular pathogens including *Brucella, Rickettsia, Bartonella, Coxiella*, and *Agrobacterium* among others (34, 91, 92).

Although most studies focus on DsbA homologs, their redox partners are also critical players in the formation disulfide bonds. Bioinformatic analysis showed three general trends in DsbA redox partners, and most bacteria either encode DsbB, VKOR, or lack both DsbB and VKOR (24, 25). VKOR is homologous to mammalian vitamin K epoxide reductase (VKORC1), which transfers electrons to the quinone vitamin K (94). Its role as a redox partner was discovered through a pattern of co-association with DsbA homologs among divergent groups of bacteria, including Cyanobacteria, Proteobacteria, Actinobacteria, and Spirochaetes (24). Despite its lack of homology with DsbB, VKOR and DsbB have the same function and share key structural features (94, 95).

1.3.2 Gram-Positive Bacteria

Disulfide bond formation in Gram-positive bacteria has not been investigated to the same extent as in Gram-negatives, and the majority of Gram-positive TDORs have only been identified within the past five years (96–101). Many Gram-positive species either lack homologs to archetypical DsbA proteins entirely, or the homology is so low that they go undetected in bioinformatic screens. This may be a result of the fundamental differences between Gram-positive and Gram-negative cell envelopes. In Gram-negative bacteria, the periplasmic compartment houses soluble disulfide oxidoreductases and isomerases required for oxidative protein folding. In contrast, Gram-positive bacteria lack a periplasmic space and must carry out disulfide bond formation directly at the cell wall. Nevertheless, Gram-positive bacteria do form disulfide bonds, and adaptations such as anchoring oxidoreductases to the membrane facilitates oxidative protein folding in the absence of a periplasm (7, 97, 102, 103).

Recent analyses of the prevalence of disulfide bonded proteins and DsbA homologs has revealed stark differences in the frequency and mechanism of disulfide bond formation among all groups of bacteria, and particularly in Gram-positive species (24, 96). Using an *in silico* approach, Dutton et al. (24) analyzed trends in bacterial disulfide bond formation by correlating the frequency of secreted proteins with even numbers of cysteines (where pairs of cysteines are indicative of disulfide bonds) with the presence of DsbAB homologs. The results revealed that certain subsets of bacteria produce few disulfide-bonded proteins and lack enzymes for disulfide bond formation. This study was subsequently supported by the work of Daniels et al. (96), which found that among the two major phyla of Gram-positive bacteria, Actinobacteria stabilize up to 60% of their secreted proteins with disulfide bonds, more than any other group, whereas Firmicutes are at the opposite end of the spectrum with a tendency to exclude cysteines altogether.

In addition to differences in the prevalence of disulfide-bonded proteins, Gram-positive organisms display considerable diversity in their disulfide catalysts. While DsbA/DsbB homologs appear to be typical of disulfide bond formation in Gram-negative

species, there is growing evidence that some Gram-positive species use enzymes with little homology to the archetypical *E. coli* DsbA/DsbB system.

1.3.2.1 Actinobacteria

Most of the TDORs among this group of bacteria have only recently been investigated. Many encode DsbA homologs that use VKOR proteins as their redox partners, and with their high number of disulfide-bonded proteins, it is not surprising that some species encode DsbA homologs that are essential for growth. It has been suggested that the high prevalence of disulfide bond formation in some Actinobacteria might be related to periplasm-like compartment formed by their mycolic acid layer (104, 105).

Mycobacterium

M. tuberculosis is predicted to stabilize the majority of its secreted proteins with disulfide bonds, and it encodes at least three oxidoreductases (99, 100, 106–108) (Fig. 1.3). Although the structures have been solved for each of the enzymes, their biological roles and natural substrates remain poorly understood.

The first *M. tuberculosis* oxidoreductase to be characterized was DsbE, a homolog of the *E. coli* cytochrome c maturation protein CcmG. However, unlike CcmG, DsbE lacked the reductase activity typical of cytochrome maturation proteins, and instead efficiently catalyzed the oxidation of reduced hirudin, a common test substrate for oxidase activity (108). The biochemical properties of DsbE were also consistent with an oxidase, including an active site cysteine with an acidic pK_a of 5, a destabilizing active site disulfide bond, and a redox potential of -128 mV (108). Further supporting the notion that DsbE of is functionally distinct its from Gram-negative homolog, a different protein, CcsX, has since been demonstrated to fulfill the role of CcmG in *M. tuberculosis* cytochrome c maturation (109).

A second enzyme with homology to DsbE, called DsbF, was subsequently identified and found to have similar structural and biochemical properties (99). In one of

the only studies to examine expression levels in an organism encoding multiple oxidoreductases, Chim et al. (99) conducted a meta-analysis of *M. tuberculosis* expression data and found that DsbE and DsbF were inversely regulated, indicating that the proteins were involved in different biological processes. DsbF expression was correlated with peroxidase expression, while DsbE expression was correlated with an extracellular sigma factor required for virulence. Based on these findings, DsbF is hypothesized to be linked to oxidative stress resistance, while DsbE is involved in virulence. Investigation of DsbE and DsbF has been limited to *in vitro* characterization and their role *in vivo* has not been examined.

More recently, an essential DsbA homolog called MtbDsbA (Rv2969c) was identified (35). Unlike DsbE and DsbF, MtbDsbA is a homolog of *E. coli* DsbA that uses a VKOR redox partner (35, 94). MtbDsbA is structurally similar to *E. coli* DsbA, with a typical CXXC catalytic motif, but also contains a second disulfide bond required for stability (100, 106, 107). *In vitro* analyses of MtbDsbA activity have produced conflicting results. MtbDsbA was inactive in standard oxidase assays using hirudin (100) and RNase A (106), but successfully oxidized a peptide substrate (107). Similarly conflicting results have also been reported for isomerase activity (100, 107). Attempts to investigate MtbDsbA by expressing it in *E. coli* and *Corynebacterium diptheriae* have been unsuccessful (94, 98). MtbDsbA does not interact with DsbB (107), which likely explains why it was inactive in its foreign hosts, and although it has not been tested, production of active MtbDsbA might require co-expression with VKOR.

Despite these inconsistencies, there is indirect evidence that MtbDsbA catalyzes disulfide bond formation *in vivo*, based on the activity of VKOR. For example, VKOR complements *E. coli* DsbB mutants for motility, an assay that is indicative of disulfide bond formation in the flagellar protein FlgI (94, 107). In addition, mutation of VKOR suppresses the growth defect of Δ*ccmG* mutants, which is a phenotype associated with disulfide bond catalysts in other organisms (109, 110). Furthermore, both MtbDsbA and VKOR are essential in *M. tuberculosis* and *M. smegmatis*, possibly because Mycobacteria are predicted to form disulfide bonds in the majority of their secreted proteins (100, 107).

Additional investigation of the all of the enzymes that comprise the disulfide bond formation pathway will be required to determine their biological functions and natural substrates. However, work to understand these processes in *Mycobacterium* has been hindered by a lack of assays to detect disulfide bond formation *in vivo* and growth defects associated with the mutants (94).

Corynebacterium

Aside from *Mycobacterium* spp., disulfide bond formation in Actinobacteria had gone uncharacterized until Daniels *et al*. identified three novel enzymes in *C. glutamicum* (96). Two of these putative oxidoreductases, A-DsbA and CG2799, were active in *in vitro* oxidase and reductase assays (96). Although the enzymes were initially identified through their homology to *E. coli* DsbA, they exhibit significant differences, such as functioning as a dimer and using a VKOR redox partner (24, 96). Neither CG2799 or A-DsbA were investigated *in vivo* and their biological functions in *C. glutamicum* remain unknown. However, A-DsbA homologs were identified a range of other Actinobacteria, including *Corynebacterium, Rhodococcus*, and *Streptomyces* (96), and a CG2799 homolog in *C. diphtheriae* (MdbA) has been investigated in detail (98, 111).

Functional analysis of *C. diphtheriae* MdbA revealed that it plays an important role in growth and virulence. Natural substrates of MdbA include SpaA pilin subunits that are required for pili production, and diphtheria toxin (98). MdbA mutants also had growth defects at 37°C, and showed reduced virulence in a guinea pig model of infection (98). Like other Gram-positive oxidoreductases, MdbA is anchored to the membrane by a transmembrane domain. Interestingly, despite sequence similarity to CG2799 and structural similarity to MtbDsbA, two enzymes with VKOR redox partners, MdbA is predicted to use a DsbB-like redox partner (24, 98).

C. diphtheriae also encodes a oxidoreductase similar to *M. tuberculosis* DsbF. The structure for the enzyme has been solved, but its enzymatic activity and biological functions have not been investigated (112).

Actinomyces

A. oris also encodes an MdbA enzyme (97). Although MdbA is essential in *A. oris*, its VKOR redox partner is not, thus, the biological roles of MdbA are inferred from a VKOR mutant. MdbA forms disulfide bonds in FimP and FimA, the pilus shaft proteins of types 1 and 2 fimbriae. As an inhabitant of the human oral microbiota, *A. oris* uses its pili for biofilm formation and coaggregation with *Streptococcus oralis*. Accordingly, VKOR mutants were defective in coaggregation and biofilm formation, and also showed an altered cell morphology (97). The fact that MdbA was essential for growth suggests that it might have additional substrates.

1.3.2.2 Firmicutes

In general, Firmicutes form disulfide bonds in a much smaller fraction of their proteins compared to other groups of bacteria (96). They are also known to use other types of covalent bonds to stabilize extracellular proteins, such as isopeptide and thioether bonds (113). Many of the disulfide catalysts identified in this group appear to be more specialized than their Gram-negative counterparts, with enzymes dedicated to specific substrates or pathways, such as genetic competence and bacteriocin production. Although there may be a limited number of Firmicute proteins with disulfide bonds, those that do contain them often have important functions, and include the most lethal toxins known.

A common theme among staphylococci, clostridia, and streptococci is that they all secrete toxins that contain disulfide bonds, but nothing is known about how these bonds are formed. One possibility is spontaneous oxidation. However, this seems unlikely since the toxins from Gram-negative species and Actinobacteria require enzymes to catalyze their disulfide bonds (25, 98, 114, 115). In addition, many toxin producers are facultative or obligate anaerobes that live in low oxygen conditions. This suggests that novel oxidoreductases might exist in these species.

The first Gram-positive disulfide catalysts to be discovered were identified in aerobic Firmicutes, and the disulfide bond pathway of *Bacillus subtilis* is still one of the best characterized systems. In contrast, understanding of disulfide bond formation in facultative anaerobes and anaerobic Firmicutes remains murky, and there has been little disulfide bond related research in this group.

Bacillus

B. subtilis encodes two DsbA homologs, BdbD and BdbA, and two DsbB homologs, BdbB and BdbC (116, 117) (Fig. 1.4). Among these, BdbD and BdbC appear to be the primary disulfide catalysts in the cell, and are important for production of recombinant disulfide bonded proteins, such as alkaline phosphatase and β-lactamase, as well as natural substrates (7, 116–119). BdbDC are encoded on the core genome and have homologs in other *Bacillus* species (102, 120), whereas BdbA and BdbB are encoded on a prophage and are specific to *B. subtilis* 168 (121). Although there is some substrate overlap between the two systems, they are not redundant.

BdbD is structurally similar to *E. coli* DsbA, except that it is tethered to the membrane by a transmembrane domain. Also, unlike all other DsbA-like proteins described to date, BdbD binds a calcium cofactor. The Ca^{2+} cofactor enhances oxidizing power by increasing redox potential, but is not essential for function (102). BdbC is a DsbB homolog and the main redox partner for BdbD, although the mechanism of interaction between the two has not been studied. BdbDC is essential for genetic competence, and it catalyzes disulfide bond formation in the pilin-like protein ComGC that makes up the competence pseudopilus (117, 122), as well as the ComEC channel protein required for DNA uptake (123). Likewise, BdbD is also involved in sporulation (124) and cytochrome c maturation (110). There is also preliminary evidence to suggest BdbDC oxidizes several integral membrane proteins, including ProA, an enzyme involved in proline biosynthesis, and Pyr proteins involved in pyrimidine metabolism (119).

The functions of BdbA and BdbB are more ambiguous, and they do not oxidize BdbDC substrates. The genes encoding BdbA and BdbB are located next to the bacteriocin sublancin and its transporter, *sunT,* as part of the Spβ prophage locus. Therefore BdbAB is probably a specialized redox pair for the oxidation of the bacteriocin sublancin, which contains four cysteines that form two disulfide bonds. Although only BdbB is required for sublancin production (7, 125), the genetic location of BdbA and its homology to DsbA suggest that it participates in disulfide bond formation. However, the enzymatic activity of BdbA has not been tested, and disulfide bonding in sublancin has only been investigated indirectly (7, 125).

While the Bdb proteins constitute an oxidative pathway, *B. subtilis* also has a reducing pathway in its cell envelope. This system works by transferring electrons from cytoplasmic thioredoxin across the membrane via CcdA, an integral membrane protein (126). CcdA is functionally similar to the β-domain of DsbD proteins in Gram-negative bacteria, but lacks the DsbDα and DsbDγ domains (127). Instead, CcdA passes electrons to intermediate oxidoreductases, StoA and ResA, both of which reduce specific downstream substrates (126).

ResA is the *B. subtilis* equivalent of *E. coli* CcmG (128–130). The cytochrome c maturation system of Gram-positive bacteria, CCMII, consists of ResABC and CcdA. CcdA transfers electrons from the cytoplasm to ResA, which reduces apocytochorme c, while ResB and ResC transfer heme (126, 131). The ResA CcdA pair counteracts oxidation of apocytochrome c by BdbDC (110). As described above, this phenomenon also occurs Gram-negative bacteria, and both systems use reductases to counteract their own oxidizing enzymes (81). The function of this seemingly inefficient pathway is unclear and disulfide bond formation is not essential for cytochrome c maturation, although it is required for optimal levels of cytochrome c production (81).

The second CcdA substrate, StoA, is a reductase involved in sporulation that also reduces a disulfide bond formed by BdbD. StoA specifically reduces a disulfide bond in the penicillin binding protein SpoVD, which is required for endospore cortex synthesis

(124). This bond acts like an on/off switch that modulates SpoVD activity. The disulfide bond formed by BdbD blocks the SpoVD active site and maintains it in an off state, until it is reduced by StoA to become activated and participate in cortex formation (124). Accordingly, mutation of SpoVD cysteines locks it in an active state that eliminates the need for StoA (132). Like ResA, StoA is thought to have high substrate specificity and SpoVD is its only known substrate.

As a model organism, disulfide bond formation in *B. subtilis* has been well characterized. However, as more information becomes available, it is evident that the *Bacillus* pathway might not be representative of other Firmicutes.

Staphylococcus

Unlike *Bacillus*, only one TDOR has been identified in *Staphylococcus*. *S. aureus* has a DsbA homolog called SaDsbA, which is predicted to be conserved among staphyloccocci (103). Although structurally similar to *E. coli* DsbA, SaDsbA is a lipoprotein.

SaDsbA is the only disulfide catalyst that functions autonomously, without the need for a redox partner. *S. aureus* does not encode DsbB or VKOR homologs, and it successfully complements *E. coli dsbAB* (103) and *B. subtilis bdbDC* mutants (7). Instead, SaDsbA has been shown to use medium components, such as cystine, for reoxidation (133). The ability of SaDsbA to function without a partner has been attributed the unusual structural stability of its active site cysteines (133). *Listeria* and *Enterococcus* also lack DsbB/VKOR homologs and might use enzymes similar to SaDsbA, although disulfide bond formation has not been investigated in these organisms (24, 133).

Although SaDsbA was first characterized in 2005 (103), its biological function remained unknown until recently, when it was discovered to play a role in genetic competence (134). Similar to BdbD in *Bacillus*, SaDsbA catalyzes disulfide bond formation in ComGC pseudopilins, and SaDsbA mutants produce less pseudopilin protein (134). The link between SaDsbA and competence probably went undetected

because competence in Staphylococcus is not fully understood, and laboratory growth conditions to allow competence induction have only recently been identified (135). ComGC is the only SaDsbA substrate identified to date (103). Despite its relatively strong oxidizing activity, SaDsbA does not have any other phenotypes and it does not contribute to virulence *in vitro* or *in vivo* (103).

SaDsbA is the only oxidoreductase identified in *S. aureus*, however, there is evidence to suggest that it might have additional disulfide bond catalysts. *S. aureus* produces multiple disulfide bonded virulence factors that are independent of SaDsbA (103). Notably, it produces a large group of secreted toxins, the superantigen enterotoxins, that contain a characteristic disulfide loop that is needed for function and stability (136–142). Disulfide bonds also stabilize other, structurally unrelated toxins, such as β-toxin sphingomyelinase which requires two intramolecular disulfide bonds (143, 144). The enzymes that form these bonds are unknown. Given that certain strains can produce up to 23 different superantigen enterotoxins (136), identification of disulfide bond catalysts in *S. aureus* could reveal important antimicrobial targets.

Clostridium

Nothing is known about disulfide bond formation in clostridia. In general, there is evidence that most clostridial proteins lack disulfide bonds, and they do not encode DsbA or DsbB/VKOR homologs (24). Nevertheless, many species produce important disulfide bonded proteins, suggesting that they do possess some sort of disulfide bond formation machinery. All clostridial neurotoxins, including the seven types of botulinum neurotoxins from *Clostridium botulinum* and tetanus toxin from *Clostridium tetani*, contain disulfide bonds that are crucial for function (29, 145–150). These toxins are derived from a single precursor protein that is cleaved to produce a heavy chain and a light chain that are linked by a disulfide bond. An intact disulfide bond is required for the light chain to translocate into host cells (151). It is not known how the disulfide bonds are formed, and even the mechanisms of toxin release from the cell are poorly understood (152). Considering that clostridia are obligate anaerobes, and therefore inhabit reducing

environments, it seems unlikely that the disulfide bonds are formed by spontaneous oxidation.

Another hint that *Clostridium* species have disulfide catalysts is that they encode homologs to *Bacillus subtilis* StoA and SpoVD (153). As described above, *B. subtilis* uses StoA to reduce a disulfide bond in the sporulation protein SpoVD, which is formed by the disulfide bond catalyst BdbD (124). Interestingly, SpoVD, including the disulfide bond forming cysteines, and StoA are both conserved in clostridia (153). This suggests that although clostridia do not encode a BdbD homolog, they might have a functionally similar protein that would necessitate StoA. Whether or not clostridia use TDORs for toxin production or sporulation remains to be determined.

Streptococcus

Disulfide bond formation in streptococci is also poorly understood. Several members of this group use specialized oxidoreductases for bacteriocin production, but enzymes with broad substrate specificity like DsbA, BdbD, or MdbA have not been identified.

Many streptococci and related lactic acid bacteria produce disulfide-bonded bacteriocins. For example, *S. thermophilus* LMD-9 uses an oxidoreductase, $BlpG_{ST}$, to catalyze disulfide bond formation in its bacteriocin thermophillin 9 (154). *S. bovis* also produces a bacteriocin with disulfide bonds required for activity, bovicin HJ50 (155–157). Bacteriocins similar to bovicin HJ50, all of which contain a disulfide bond, are produced in multiple species including *Bacillus thuringiensis, Bacillus cereus, Clostridium perfringens, and Streptococcus suis* (158). There is an oxidoreductase located within the bovicin gene cluster, Sdb1, although it is not essential for bovicin production (156, 158). *S. dysgalactiae* also produces a disulfide bonded bacteriocin (159). Likewise, bacteriocins with disulfide bonds are widely produced by other lactic acid bacteria, such as *Lactobacillus* spp. (160, 161), *Enterococcus* spp. (162) and *Pediococcus* spp. (163). The mechanism of disulfide bond formation has been determined for pediocin, and involves an oxidoreductase associated with the bacteriocin ABC-

transporter, which is required to generate the correct connectivity of pediocin's two disulfide bonds (164).

A second group of streptococcal proteins that contain disulfide bonds are the superantigen exotoxins produced primarily by *S. pyogenes* and *S. dysgalactiae* (165). Streptococcal superantigens are major virulence factors that contribute to invasive disease, such as necrotizing fasciitis, and streptococcal toxic shock syndrome (136, 165, 166). The success of the current epidemic clone of *S. pyogenes* has been attributed to its acquisition of the SpeA superantigen (167, 168). Staphylococcal and streptococcal superantigens share a similar structure, with a disulfide loop that is required for stability and activity (136, 169, 170). However, like *S. aureus*, the mechanism of disulfide bond formation is unknown.

Another important pathogen, *S. pneumoniae*, lacks DsbA homologs, but does have a reducing pathway. To counter oxidative stress at the cell envelope, *S. pneumoniae* uses an extracellular methionine sulfoxide reductase, MsrAB2. MsrAB2 has two domains, A and B, that reduce the R and S enantiomers of methionine sulfoxide (70, 171). Similar to the reducing pathway in *B. subtilis, S. pneumoniae* uses a series of enzymes to transfer reducing equivalents from the cytoplasm. CcdA proteins pass electrons from cytoplasmic thioredoxin to extracellular thioredoxins (Etrx1 and Etrx2) at the cell surface. Etrx1 then passes electrons to the MsrA domain, while Etrx2 passes electrons to both MsrAB2 domains (171). Oxidation of methionine residues can alter protein hydrophobicity, or otherwise damage or inactivate proteins unless they are reduced by MsrAB2 (70). The CcdA-Etrx-MsrAB system is required for full virulence (171).

Interestingly, the CcdA and Etrx proteins appear to be homologs of the *Bacillus* cytochrome c maturation system, yet streptococci do not produce c-type cytochromes (172). Instead, CcdA-Etrx-MsrAB functions in oxidative stress resistance, which is particularly important for *S. pneumoniae,* because it secretes H_2O_2 as a metabolic byproduct and lacks catalase (173). H_2O_2 can oxidize cysteine residues unless they are

part of a disulfide bond (174) (Fig. 1.5). Although DsbA homologs have not been identified in *S. pneumoniae* yet, it is conceivable that it would use enzymes to ensure efficient disulfide bond formation and prevent oxidative damage. Alternatively, it might exclude disulfide bonds from its proteins entirely (96).

1.4 An Investigation of Gram-positive Disulfide Bond Formation in *Streptococcus gordonii*

1.4.1 Challenges to Identifying Disulfide Bond Catalysts

It is difficult to determine the function of thioredoxin family enzymes based on their sequence. These enzymes display surprising plasticity in the nature of their activity. For example, the cytoplasmic reductases thioredoxin (19, 59) and glutaredoxin (175) gain oxidase activity when they are expressed in the periplasm of *E. coli*. Similarly, DsbA can gain isomerase activity when overexpressed (176), and a single point mutation in DsbC is sufficient to convert it from an isomerase to an oxidase (13, 68). This suggests that subcellular localization and redox partners are important determinants of enzyme function, independent of protein sequence.

Although some general trends have been observed in the sequences of Gram-negative thioredoxin family enzymes, the patterns do not apply to Gram-positive enzymes. For example, Ren *et al*. surveyed the CXXC active site dipeptide of DsbA homologs from 180 different species and found that 79% have a histidine in the second position (18), while DsbC homologs typically have a tyrosine (13). Similarly, the identity of the residue next to the conserved *cis*-proline shows a clear pattern based on enzyme activity: valine in DsbA, isoleucine in thioredoxin, and threonine in DsbC (13). In comparison, the limited number of Gram-positive homologs do not follow the same trends. The CXXC dipeptide of Gram-positive disulfide oxidoreductases appears more variable, and none of the enzymes have valine next to the cis-proline. Rather, based on sequence alone, Gram-positive oxidases appear more similar to Gram-negative isomerases (Table 1.1). In addition, our work (Chapter 4), and that of others has indicated that disulfide bond catalysts can differ from conventional thioredoxin family enzymes,

and that some can function using a single cysteine (177), and possibly without any (178). This unpredictability stresses the need for *in vivo* assays to understand enzyme function.

An obstacle to studying disulfide bond formation in Gram-positive bacteria is the lack of functional assays. Investigations in Actinobacteria have been hindered by the fact that they have many substrates and are essential for growth (94), while the opposite issue, a lack of substrates and phenotypes, has posed a challenge in Firmicutes (103). One strategy to investigate disulfide bond formation in Firmicutes, which are predicted to have few disulfide bonded proteins, is to use a model organism with many testable phenotypes to maximize the likelihood of identifying a processes affected by oxidative protein folding. *Streptococcus gordonii* is an excellent model for the study of disulfide bond formation because it is easy to grow and, as an adaptation to its natural habitat in oral biofilms, it has many easily testable phenotypes, namely biofilm formation, genetic competence, bacteriocin production, extracellular DNA release, and autolysis (Fig. 1.6).

1.4.2 *Streptococcus gordonii*

S. gordonii is a facultative anaerobe that inhabits oral biofilms (179). As a pioneer colonizer, *S. gordonii* and related streptococci, such as *S. mitis* and *S. oralis*, form the base of oral biofilms. *S. gordonii* produces a range of adhesins that contribute to biofilm formation, and allow it to bind directly to host salivary proteins (180, 181). These include proteins such as SspA and SspB that bind salivary agglutinin glycoproteins (182), AbpA that binds α-amylase (183), and others with multiple substrates, such as CshA and Hsa (181). *S. gordonii* also binds to other oral bacteria, in a process called co-adhesion, that facilitates colonization by species that are unable to bind to directly to host proteins (181). While *S. gordonii* is natural component of dental plaque, it is generally associated with oral health, and through a combination of secreted proteases, bacteriocins, and H_2O_2 it can inhibit biofilm formation by cariogenic species (184, 185).

Genetic Competence and Bacteriocin Production

The ComDE two component signaling system regulates genetic competence in *S. gordonii*, and is similar to the well characterized system of *S. pneumoniae* (186) (Fig. 1.7). ComD is a histidine kinase located at the cell surface and ComE is its cognate response regulator. The system works through a quorum sensing mechanism, and is activated by a small autoinducer called competence-signaling peptide (CSP) (187). ComDE forms an operon with *comC*, the gene that encodes CSP.

CSP is a small peptide derived from a larger precursor protein. The peptide has a double glycine motif signal peptide that targets it to a specific ABC-transporter, ComAB (188). ComAB cleaves the CSP precursor during translocation, to generate the active form of CSP (189). Competence is induced when the extracellular concentration of CSP reaches a threshold level. ComD senses extracellular CSP, resulting auto-phosphorylation, and subsequent phosphorylates its cognate response regulator ComE (190). An auto-inducing loop drives the expression of the *comCDE* operon, along with two copies of an alternative sigma factor, called *comR1* and *comR2*, that are similar to *comX* in *S. pneumoniae* (191). ComR activates expression of over 100 genes, including those encoding the DNA uptake machinery required for transformation to occur (187). In *S. gordonii*, genetic competence occurs during a brief period in the early exponential growth phase.

The DNA uptake machinery in *S. gordonii* is considered to be similar to that of other Gram-positive bacteria (186, 187, 192). The machinery consists of a pseudopilus structure and a dedicated channel for DNA transport. Although it has not been visualized in *S. gordonii*, the pseudopilus structure might be similar to the pilus of *S. pneumoniae* (193). This pseudopilus is thought to bind exogenous double stranded DNA in the environment and help it to gain access ComEA (CelA), a DNA receptor protein at the cell surface (193). From here, an exonuclease, EndA, generates single stranded DNA to be taken up by the cell via the ComEC (CelB) channel (186).

In addition to genetic competence, the ComDE system also regulates bacteriocin production. *S. gordonii* Challis produces two unmodified peptide bacteriocins, Sth1 and Sth2, that inhibit the growth of closely related species including *S. oralis, S. mitis*, and other strains of *S. gordonii* (188, 194). Bacteriocin gene expression is driven by the alternative sigma factor ComR and occurs concomitantly with genetic competence. Like CSP, Sth1 and Sth2 also have double glycine signal peptides and are secreted by the ComAB transporter (188). Although it has not been tested, the coordination of bacteriocin production and genetic competence might serve to increase the amount of exogenous DNA available for transformation.

Extracellular DNA (eDNA)

S. gordonii not only takes up exogenous DNA, but it also releases DNA into the environment. This extracellular DNA (eDNA) is an important component of the biofilm matrix and serves as a source of genetic material for recombination (195, 196). The mechanisms of eDNA release are not fully understood, although it is known to occur during aerobic growth and without cell lysis (195). Under aerobic conditions, pyruvate oxidase (Pox) catalyzes the conversion of pyruvate to acetyl phosphate, in a reaction that generates H_2O_2 and carbon dioxide as byproducts. H_2O_2 is essential for eDNA production, and Pox mutants are deficient in eDNA (195). While the mechanism of secretion is unclear, a murein hydrolase, LytF, has been identified as the main factor responsible for eDNA release (197). Interestingly, LytF is part of the competence regulon, suggesting that eDNA may be used in recombination (198).

Autolysis

Autolysins are large surface proteins that hydrolyze peptidoglycan and play important roles in cell wall turnover, growth, and division. AtlA, the major autolysin of *S. mutans*, is required for normal biofilm formation, surface protein biogenesis, and genetic competence (199, 200). Interestingly, although AtlA does not contain disulfide bonds, its activity is modulated by an upstream CXXC motif protein (199). *S. gordonii* encodes a homolog to AtlA, called AtlS. AtlS affects multiple phenotypes, including cell

separation, resistance to pH and oxidative stress, hydrogen peroxide production, biofilm formation, and eDNA production (197, 201). As would be expected, AtlS mutants are also highly resistant to lysis (201).

1.4.3 *S. gordonii* as Model Organism to Study Disulfide Bond Formation

Several traits make *S. gordonii* a good model to study disulfide bond formation. Foremost, it is easy to grow and amenable to genetic manipulation. Secondly, it displays testable phenotypes that can be used to assess the cell's physiology. This is particularly useful for the study of disulfide bond formation when there are no known disulfide bonded proteins to target for investigation. Some of these phenotypes, such as natural genetic competence and bacteriocin production, are associated with disulfide bond formation in other Gram-positive species (117, 134, 154). *S. gordonii* also forms biofilms (202), releases extracellular DNA (197), and has autolytic activity (201) that can be tested with simple assays. These phenotypes are fundamental to *S. gordonii* biology. If mutation of a potential disulfide oxidoreductase affects these processes, it can give clues to an enzyme's biological function.

As a facultative anaerobe, *S. gordonii* represents a group of organisms in which disulfide bond formation is particularly poorly understood. Streptococci and lactococci do not have homologs to DsbAB and lack a complete electron transport chain (24), which suggests that any pathways for disulfide bond formation may be quite different from those in *E. coli* and *B. subtilis*. In general, this group of organisms is believed to produce a limited number of disulfide bonded proteins, which adds to the challenge of identifying potential oxidoreductases and their substrates (96). Importantly, however, there are examples of these species producing recombinant proteins, such as antibodies and cytokines, that contain multiple disulfide bonds (203, 204). *S. gordonii* SecCR1 produces a recombinant single chain variable fragment antibody with two disulfide bonds (204). Since antibodies require disulfide bonds for stability, it strongly suggests that *S. gordonii* has a mechanism to catalyze disulfide bond formation (205, 206).

Investigating disulfide bond formation in *S. gordonii* has the potential to give insight into disulfide bond formation in related Gram-positive species, including important pathogens. It also has biotechnological value, since it could lead to new strategies to enhance recombinant protein production. *S. gordonii* is a candidate live vaccine vector that can be engineered to secrete recombinant vaccine antigens, however, insufficient antigen production has hindered development. By understanding the fundamental aspects of protein production, we will be in a better position to overcome this obstacle.

1.5 Rationale, Hypothesis, and Objectives

The process of disulfide bond formation remains largely unexplored among Gram-positive facultative anaerobes. The goal of this project was to use *S. gordonii* as a representative Gram-positive facultative anaerobe to study disulfide bond formation.

Hypothesis: Gram-positive facultative anaerobes have novel enzymes to catalyze disulfide bond formation in secreted proteins.

Objectives:

- Identify an enzyme that catalyzes disulfide bond formation in *S. gordonii*
- Chacterize how this novel enzyme works by investigating the active site
- Investigate the role of disulfide bond formation in bacteriocin production

Rationale: Since certain bacteria, including Gram-positive facultative anaerobes, lack homologs to known disulfide bond catalysts, it has been suggested that they might not have enzymes to form disulfide bonds. However, there are known examples of disulfide-bonded proteins produced by this group of organisms, including important virulence factors. This suggests that Gram-positive facultative anaerobes do have a mechanism for disulfide bond formation, but that it has gone undetected. Understanding how disulfide bonds are formed has potential health and biotechnological benefits. Previously, we had observed that *S. gordonii* was capable of producing a recombinant disulfide bonded

protein. We sought to identify the enzyme responsible, and to investigate its biological functions, natural substrates, and catalytic mechanism.

Chapter Summaries

In Chapter 3, we start by characterizing five putative thioredoxin family proteins. By assessing the phenotypes associated with each of these proteins, we identified a single enzyme that a plays a key role in *S. gordonii* biology. This enzyme was named *Streptococcus* disulfide bond protein A, SdbA. Using a combination of computational, genetic, and biochemical approaches we demonstrate that SdbA catalyzes disulfide bond formation, and identify the major autolysin AtlS is a natural substrate.

In Chapter 4, we focus on the catalytic mechanisms of SdbA. Mutational analysis of the active site revealed that SdbA functions differently from other oxidoreductases. Mutants with a single active site cysteine of the CXXC motif retained catalytic activity, and were able to oxidize disulfide bonds *in vitro* and in *S. gordonii*.

In Chapter 5 we focus on the biological functions of SdbA by investigating its role in bacteriocin production. SdbA affects bacteriocin production indirectly, by activating the CiaRH two component signaling system. CiaRH is associated with stress tolerance and antibiotic resistance in streptococci. We show that activation of CiaRH inhibits the ComDE pathway, thereby preventing bacteriocin production. Thus, even in organisms with few disulfide-bonded proteins, inactivation of a disulfide catalyst like SdbA can have significant effects on the cell.

Finally, Chapter 6 provides a brief discussion and conclusion, and possible directions for future invesitgation.

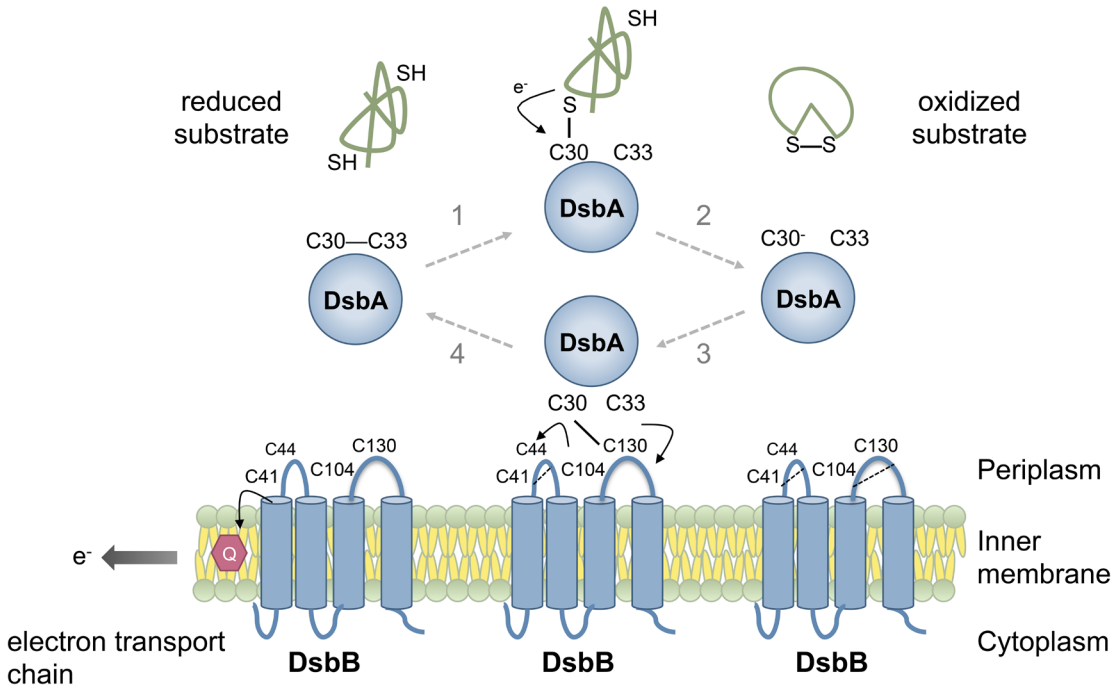

Figure 1.1 Interactions between DsbA and DsbB

DsbA has a Cys^{30}-Pro^{31}-His^{32}-Cys^{33} active site motif, which contains a disulfide bond between Cys30 and Cys33. The interaction between DsbA and a substrate is initiated when a reduced cysteine in a substrate protein attacks the DsbA active site disulfide, resulting in a mixed disulfide between the substrate and DsbA Cys30. A second cysteine in the substrate then reacts to for a bond in the substrate, leaving DsbA in a reduced state. To regenerate the DsbA active site, DsbA C30 attacks a disulfide bond between DsbB C104 and C130. The DsbA active site disulfide is formed by DsbA C33. Electrons transferred from DsbA to DsbB are passed to quinones and on to a final electron acceptor (adapted from (6, 50)). Arrows show the movement of electrons.

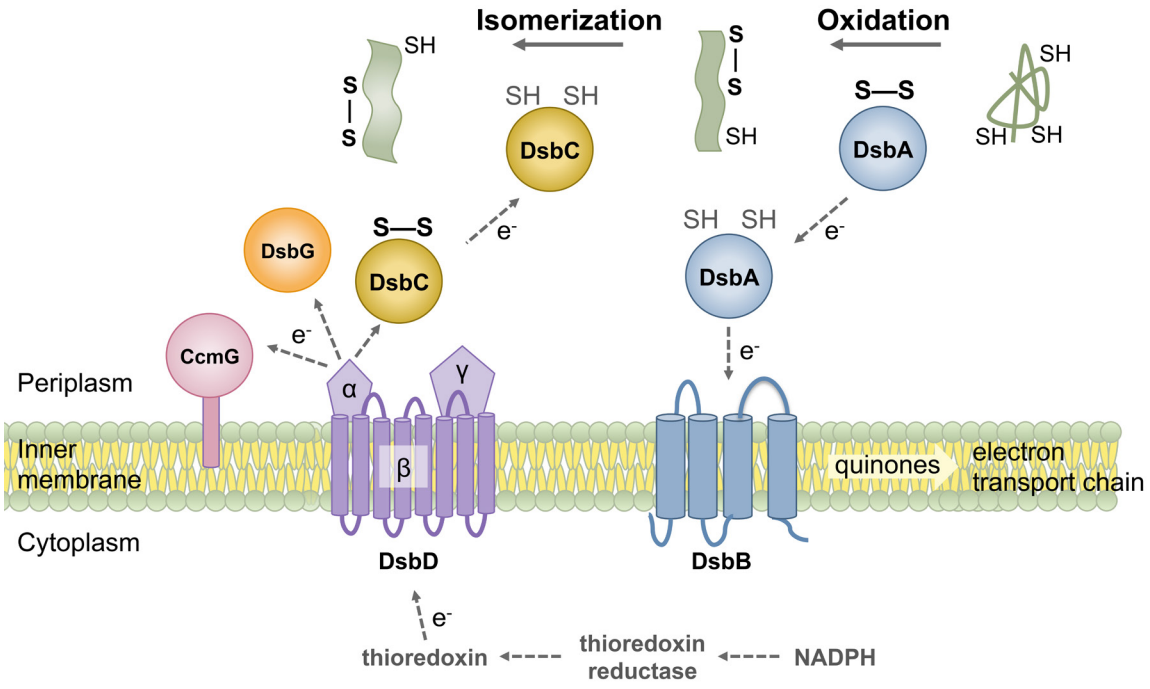

Figure 1.2 Reducing and oxidizing pathways of extracytoplasmic proteins

DsbA is highly reactive and can make errors when generating disulfide bonds. A second enzyme, DsbC, can reduce incorrect disulfide bonds and rearrange their connectivity. DsbC receives electrons from its redox partner DsbD. DsbD transfers electrons from the cytoplasm using its intermembrane DsbDβ domain. Electrons are passes to the DsbDγ subunit first, and then to the DsbDα domain. DsbDα reduces several substrates, including DsbC, DsbG, and CcmG (70).

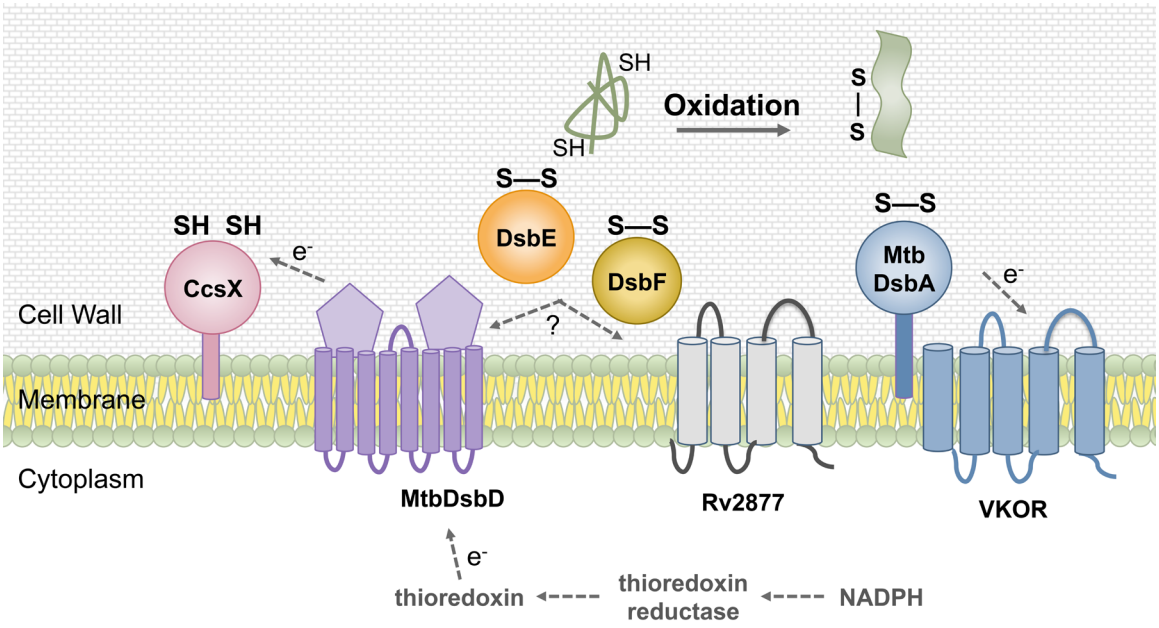

Figure 1.3 Oxidoreductases in *M. tuberculosis*

Three potential disulfide bond forming enzymes have been identified in *M. tuberculosis*. DsbE and DsbF catalyze disulfide bond formation *in vitro*, and they are predicted to use the membrane proteins MtDsbD and Rv2877c as redox partners (99). DsbE is predicted to have a cleavable signal sequence (108). Another redox pair, MtbDsbA and VKOR, also catalyzes disulfide bond formation, and both proteins are essential (100, 107). CcsX is a reductase involved in cytochrome c maturation (109).

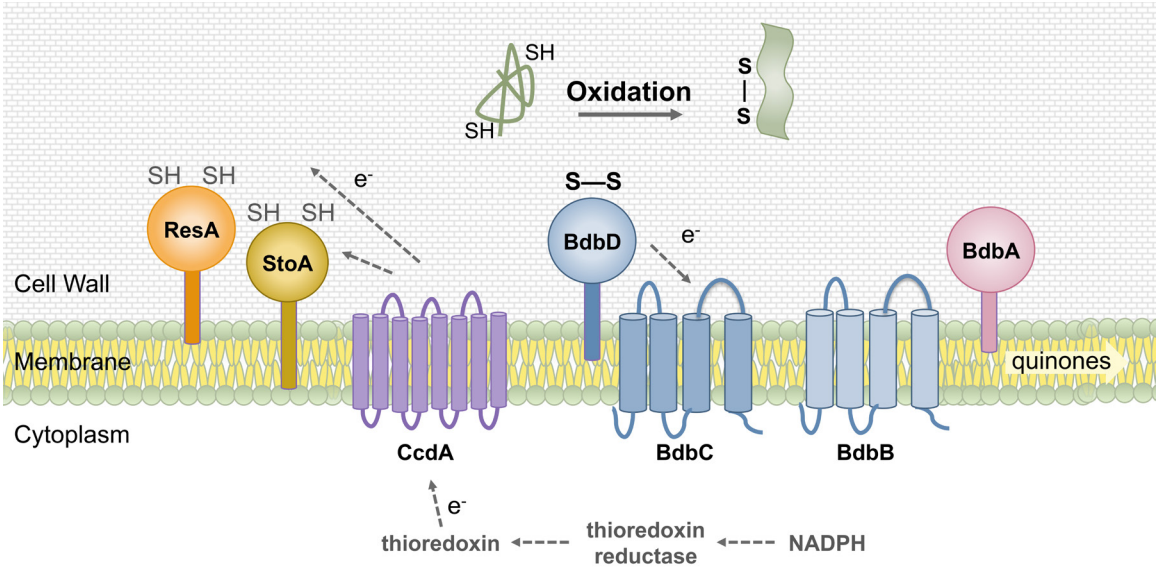

Figure 1.4 Oxidoreductases in *B. subtilis*

The oxidizing pathway of *B. subtilis* consists of BdbDC and BdbAB. BdbD is a DsbA-like enzyme that is tethered to the cell membrane. It primarily uses the integral membrane protein BdbC as its redox partner, but can also be reoxidized by BdbB (7). BdbA is a second DsbA-like enzyme with unknown function. There is also a reducing pathway that resembles the DsbD system of *E. coli*. CcdA transfers electrons from the cytoplasm to its partners at the cell surface. These include two membrane bound reductases: StoA, a sporulation protein, and ResA, a cytochrome c reductase (124, 129).

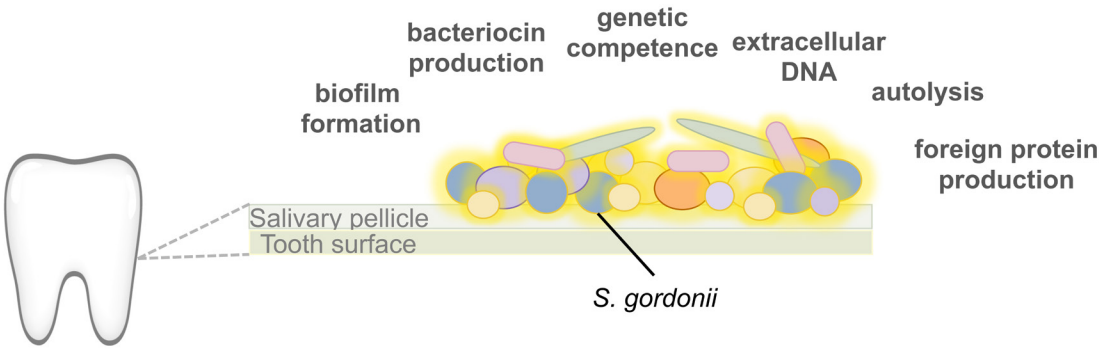

Figure 1.5 The readily phenotypes of *S. gordonii*

S. gordonii is a useful model to study disulfide bond formation without prior knowledge of substrate proteins. It displays many easily testable phenotypes that can be used to assess changes in physiology associated with mutations to a disulfide catalyst. This can be a clue to how an enzyme functions and can be used to generate leads on potential substrates. As part of the oral microbiota, *S. gordonii* forms biofilms, releases DNA, and produces bacteriocins, among other phenotypes. The strain used in this study also produces a recombinant protein that requires disulfide bonds for stability. This test protein can be used to detect changes to oxidoreductase activity.

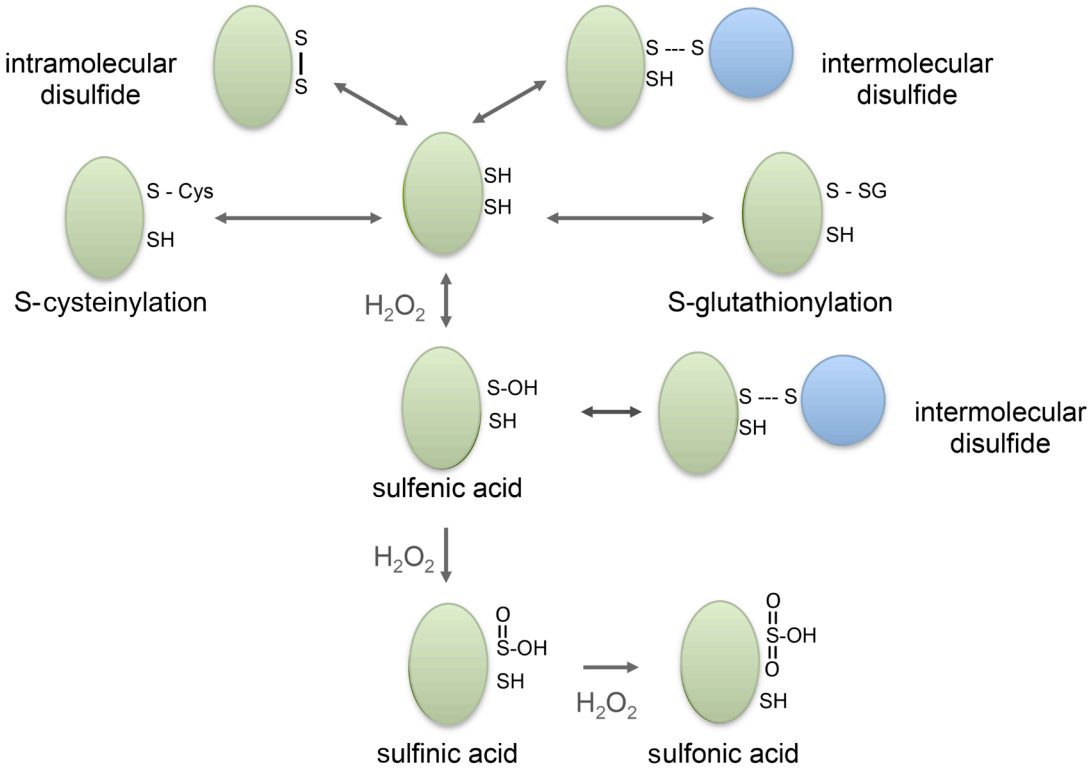

Figure 1.6 Cysteine oxidation

The sulfur of cysteine residues is reactive and vulnerable to oxidative damage. Cysteine oxidation can result in disulfide bond formation, in the formation of mixed disulfides with low molecular weight thiols, such as cysteine and glutathione, or in oxidative damage. Oxidation by hydrogen peroxide initially generates sulfenic acid, which is reversible. Sulfenic acid can be reduced back to a thiol or react with another cysteine to form a disulfide bond. Further oxidation generates sulfininc and sulfonic acid, which is irreversible (adapted from (207)).

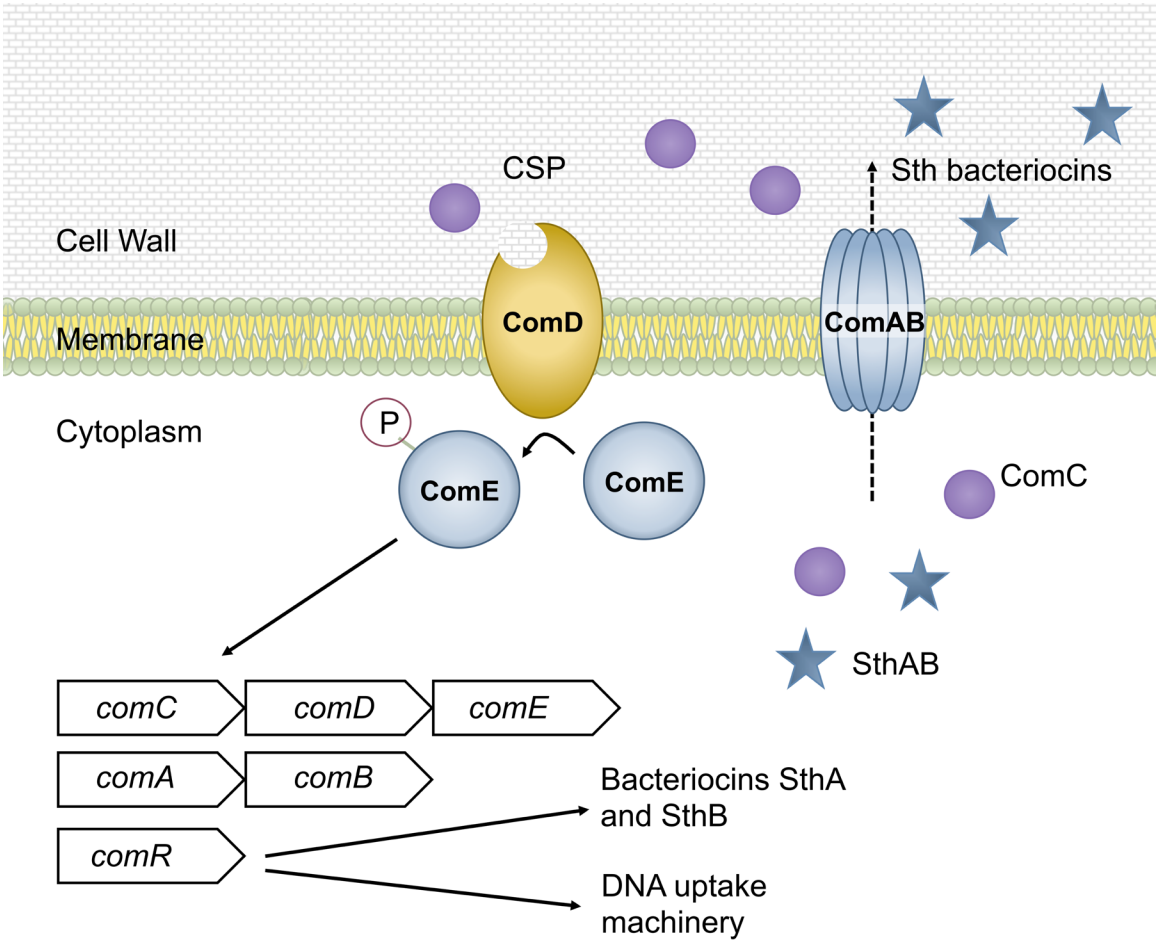

Figure 1.7 The *S. gordonii* ComDE signaling system

Genetic competence and bacteriocin production are both controlled by the ComDE two component system (187). The histidine kinase ComD is activated when it senses accumulating CSP autoinducer at the cell surface. This triggers autophosphorylation of ComD, leading phosphorylation of its response regulator, ComE. ComE drives transcription of *comCDE*, as well as the alternative sigma factor *comR*. Finally, ComR activates transcription of the bacteriocin genes, *sthAB*, and the genes required for genetic competence (188, 191). Both CSP and Sth are processed and transported by ComAB (188).

Table 1.1 Disulfide oxidoreductases in Gram-positive bacteria

				Activity				
Species	**Enzyme**	**CXXC**	***cis*-pro**[a]	**Oxidase**	**Isomerase**	**Reductase**	**Substrates**	**Reference**
M. tuberculosis	DsbA	CPAC	T	Y	Y	N		(100, 106, 107)
M. tuberculosis	DsbE	CPFC	Q	Y	N	N		(108)
M. tuberculosis	DsbF	CPTC	Q	Y	N	N		(99)
A. oris	Mdb	CSHC	T	Y	-	-	FimA, FimP	(97)
C. diphtheriae	Mdb	CPHC	S	Y	-	-	SpaA, diphtheria toxin	(98)
C. glutamicum	CG26	CPFC	T	Y	-	Y		(96)
C. glutamicum	CG2799	CSHC	S	Y	-	Y		(96)
S. aureus	SaDsbA	CPYC	T	Y	N	N	ComGC	(133, 134)
B. subtilis	BdbD	CPSC	T	Y			ComGC, ComEC, SpoVD, ProA*	(117, 119, 123, 124)
B. subtilis	BdbA*	CPPC	T	-	-	-	Sublancin	(116)
B. brevis	Bdb	CGYC	T	Y	-	Y		(120)
S. thermophilus	$BlpG_{St}$	CYYC	T	Y	-	-	Thermophilin	(154)
S. gordonii	SdbA	CPDC	I	Y	N	N	AtlS	(101)
P. acidilactici	PedC	CPYC	T	Y	-	-	Pediocin	(164)

(Y) enzyme activity confirmed *in vitro* or by complementation of *E. coli* DsbA; (N) tested, but inactive; (-) not determined
[a]Identity of the amino acid adjacent (N-terminal) to the conserved *cis*-proline (located outside of the active site);
*Disulfide bond formation has not been confirmed

Species	**Enzyme**	**CXXC**	***cis*-pro**
E. coli	DsbA	CPHC	V
	DsbC	CGYC	T
	DsbG	CPYC	T
	CcmG	CPTC	A
	Trx	CGPC	I

Chapter 2: Methods

2.1 Bacterial Strains and Culture Conditions

Experiments were carried out using *S. gordonii* SecCR1 or *S. gordonii* Challis DL-1 as the parent strain. *S. gordonii* SecCR1 is a recombinant strain of *S. gordonii* Challis DL-1 that secretes a single chain variable fragment antibody (scFv) against complement receptor 1 (CR1) (204). All other strains are described in Table 2.1. Unless otherwise noted, *S. gordonii* was grown in HTVG (per 100 ml: 0.5 g glucose, 3.5 g tryptone, 100 mM HEPES, 4 mg *p*-aminobenzoic acid, 20 mg thiamine-HCl, 0.1 mg nicotinamide and 0.02 mg riboflavin, pH 7.6) (208) at 37°C, 5% CO_2, without shaking. *Streptococcus oralis* 34 and *Streptococcus mitis* I18 were grown in Brain Heart Infusion medium (BHI, Difco). Cysteine free minimal medium (MM) was prepared as described previously (209) (56 mM glucose, 13.6 mM L-glutamic acid, 7mM L-leucine, 19 mM NH_4Cl, 20 mM K_2HPO_4, 11 mM KH_2PO_4, 50 mM Na_HCO_3, 4.9 mM $MgSO_4 \cdot 7H_2O$, 0.1 mM $MnCl_2 \cdot 4H_2O$, 72 μM $FeSO_4 \cdot 7\ H_2O$, 5.5 mM sodium pyruvate, 2.6 μM riboflavin, 1.4 μM thiamine HCl, 0.4 μM biotin, 8 μM nicotinic acid, 0.7 μM *p*-aminobenzoic acid, 1 μM calcium pantothenate, and 5 μM pyridoxal HCl) and buffered with 0.05 M Tris–maleate (pH 7.4) to a final pH of 7.1). Biofilm medium was prepared as described by Loo *et al*. (58 mM K_2HPO_4, 15 mM KH_2PO_4, 10 mM $(NH_4)_2SO_4$, 35 mM NaCl, 0.8% (wt/vol) glucose, 0.2% (wt/vol) casamino acids, and 10 μM $MnCl_2 \cdot 4H_2O$ (pH 7.4) and was supplemented with filter-sterilized vitamins (0.04 mM nicotinic acid, 0.1 mM pyridoxine HCl, 0.01 mM pantothenic acid, 1 μM riboflavin, 0.3 μM thiamin HCl, and 0.05 μM D-biotin), amino acids (4 mM L-glutamic acid, 1 mM L-arginine HCl, 1.3 mM L-cysteine HCl, and 0.1 mM L-tryptophan), and 2 mM $MgSO_2 \cdot 7H_2O$.).

E. coli was grown in Luria-Bertani medium (LB; per 100 ml: 1 g tryptone, 1 g NaCl, 0.5 g yeast extract) at 37°C with shaking.

Antibiotics (Sigma) were used at the following concentrations: for *S. gordonii*, erythromycin 10 μg/ml, tetracycline 10 μg /ml, spectinomycin 250 μg /ml, kanamycin

250 μg /ml, rifampin 100 μg /ml and chloramphenicol 5 μg/ml; for *E. coli*, ampicillin 100 μg /ml, tetracycline 10 μg/ml and chloramphenicol 20 μg/ml.

2.2 Genetic Manipulations

2.2.1 Transformation of *S. gordonii*

Overnight cultures of *S. gordonii* were diluted 1:40 into pre-warmed BHI supplemented with 5% heat inactivated calf serum (Gibco) and grown to an OD_{600} of ~0.150. DNA was added to 0.75 ml aliquots of competent cells and incubated at 37°C for 30 min. Following the addition 0.75 ml of fresh medium, the cells were incubated for another 90 min. The cells were then concentrated by centrifugation at 10 000 x g for 1 min and resuspended in 0.5 ml supernatant. Transformants were selected on BHI agar containing the appropriate antibiotics and incubated for 24 h at 37°C, 5% CO_2.

2.2.2 Transformation of *E. coli*

To prepare competent cells, 1 ml of an overnight culture was used to inoculate 45 ml of LB medium. Cultures were grown at 37°C, 180 rpm, to an OD_{600} of 0.35, and the cells were harvested by centrifugation at 10 000 x g, 10 min, 4°C. The cell pellet was washed with 50 ml of transformation buffer 1 (10 mM Tris, 150 mM NaCl, pH 7.5), followed by centrifugation. The resulting pellets were suspended in transformation buffer 2 (50 mM $CaCl_2$) and incubated on ice for 45 min. The cells were harvested by centrifugation and suspended in 3 ml transformation buffer 2 and 2 ml of 50% glycerol. Aliquots were stored at -80°C.

DNA was mixed with 200 μl competent cells and 100 μl transformation buffer 3 (10 mM Tris, 50 mM $CaCl_2$, and 10 mM, $MgSO_4$, pH 7.5) and incubated on ice for 45 min. The transformation mixture was heat shocked at 37°C for 2 min, followed by incubation at room temperature for 10 min. Fresh LB medium (0.5 ml) was added and the cells were incubated for an additional 60 min at 37°C. Transformants were grown for 24 h at 37°C on LB agar with appropriate antibiotics.

2.2.3 DNA Isolation

Genomic DNA

DNA for PCR was isolated from *S. gordonii* and *E. coli* using the same procedure. Cultures (1.5 ml) were grown overnight and the cells were harvested by centrifugaction at 14 000 x g, 5 min. The resulting pellets were suspended in 100 μl TE buffer (10 mM Tris, 10 mM EDTA, pH 8.0), 100 μl chloroform, and 100 mg glass beads (600 μm, Sigma), and vortexed for 1 min. Cell debris was removed by centrifugation at 14 000 x g, 5 min. Supernatants were transferred to new 1.5 ml tubes and ethanol precipitated at described above. Pellets were suspended in 10 μl TE buffer.

Genomic DNA used in transformation frequency experiments was isolated from *S. gordonii* Wicky WK1. To prepare the DNA, overnight cultures (100 ml) were mixed 1:1 with fresh BHI medium and grown for 2 h at 37°C. Solid glycine powder was added to the cultures to a final concentration of 5% (w/v) and the mixture was incubated for an additional 2 h at 37°C. Cells were then harvested by centrifugation for 10 min at 10 000 x g and washed with phosphate buffered saline (PBS). The pellets were suspended in GTE buffer (50 mM glucose, 25 mM Tris, 10 mM EDTA, pH 8.0) containing 10 mg/ml lysozyme, 10 μl RNase A (10 mg/ml), 10 U/ml mutanolysin (Sigma), and 12.5 mM EDTA, pH 8.0, and incubated for 2 h at 37°C to digest the cell wall. The cells were subsequently lysed with 2% (w/v) sodium dodecyl sulphate (SDS) at room temperature for 30 min. The mixture was vortexed to separate the DNA from cell debris, followed by centrifugation at 14 000 xg, 10 min. The DNA was extracted with one volume phenol and one volume chloroform by centrifugation at 14 000 x g for 5 min, followed extraction with an additional two volumes of chloroform. The aqueous layer was then precipitated with 95% ethanol, 2.5 mM potassium acetate for 30 min at -80°C. DNA was sedimented by centrifugation at 14 000 xg, 10 min, 4˚C, and washed with 70% ethanol. The resulting pellet was suspended in 3 ml TE buffer and aliquots were stored at -20°C. To estimate the DNA concentration, 1 μl was separated by gel electrophoresis and the concentration was estimated using image analysis to compare pixel intensity to a known standard (1 kb DNA ladder N3232S, New England Biolabs).

Plasmid DNA

Plasmids were isolated from *E. coli* by alkaline lysis. Cells were grown overnight in 2 ml LB mediumand harvested by centrifugation at 14 000 x g, 5 min. The pellets were suspended in 100 μl GTE buffer, 186 μl MilliQ water, 2 μl RNase A (10 mg/ml), 10 μl of 20% SDS, 4 μl NaOH (10 M). The tubes were gently mixed by inversion and incubated at ambient temperature for 5 min. The pH was neutralized with 150 μl of cold potassium acetate solution (60% (v/v) 5 M potassium acetate , 28.5% (v/v) ddH2O and 11.5% (v/v) glacial acetic acid), mixed by inversion, and incubated on ice for 10 min. This was followed by centrifugation at 14 000 x g, 10 min, 4°C. Supernatants were transferred to new 1.5 ml tubes, chloroform extracted, and precipitated with ethanol. The resulting pellets were suspended in 15 μl TE buffer.

2.2.4 Mutant Construction

TDORs

The TDOR mutants were constructed by insertional inactivation with an erythromycin resistance cassette (*ermAM*) (210) with the primers listed in Table 2.2. PCR products were digested with restriction enzymes as indicated in Table 2.2 and ligated together with T4 DNA ligase (New England Biolabs). The ligation products were amplified using the outside primers and the resulting constructs were used to transform *S. gordonii* SecCR1 and *S. gordonii* RJM4 as described above. Transformants were selected on BHI agar containing the appropriate antibiotics and insertion of the *ermAM* cassette was confirmed by PCR.

SdbA

Inactivation of *sdbA* was achieved by insertion with *ermAM* as described above using the primers listed in Table 2.2. Construction of a *sdbA*-complemented mutant was achieved by introducing a functional *sdbA* gene back onto the chromosome. To this end, the entire *sdbA* reading frame and a portion of the upstream gene, *nusG*, was amplified with the primer pair SL756/SL803. This fragment was digested with BamHI and ligated to a kanamycin resistance cassette (*aphA3*) amplified from plasmid pDL276 (211). The ligation product was amplified by PCR and digested with EcoRI. This construct was then

ligated to a 557 bp segment of *sdbA* and the downstream gene, *padA*, amplified with the primers SL758/SL759. The resulting construct was used to transform the *sdbA* mutant, replacing the *ermAM* cassette with a functional *sdbA* gene and *aphA3* by double crossover homologous recombination. Transformants were selected on BHI with kanamycin, and replica plating was used to identify erythromycin sensitive, kanamycin resistant colonies. Complementation of the *sdbA* gene was confirmed by PCR analysis and Western blotting using anti-SdbA antisera.

DegP

DegP-deficient mutants were constructed in the *S. gordonii* SecCR1 parent and *ΔsdbA* mutant using the primers listed in the Table 2.2. A single *ΔdegP* mutant was constructed by insertional inactivation with *ermAM*, and a *ΔsdbAΔdegP* double mutant was constructed using *aphA3* amplified from pDL276. Inactivation of *degP* in the SdbA cysteine point mutants was achieved by insertion of the *ermAM* gene. PCR products were digested with restriction enzymes as indicated in Table 2.2 and ligated together with T4 DNA ligase. The ligation products were amplified using the outside primers and the resulting constructs were used to transform *S. gordonii* SecCR1 and *S. gordonii ΔsdbA* mutants. Transformants were selected on BHI containing the appropriate antibiotics and insertion of the resistance cassettes was confirmed by PCR. The same strategy was used to mutate *spxB* with the *ermAM* cassette.

Construction of a *degP*-complemented mutant was achieved by introducing a functional *degP* gene back onto the chromosome. The entire *degP* reading frame and a portion of the upstream intergenic region was amplified with the primer pair SL752/SL993. This fragment was digested with BamHI and ligated to *aphA3*. The ligation product was amplified by PCR and digested with KpnI. This construct was then ligated to a 531 bp segment of the downstream portion of *degP* amplified with the primers SL822/SL755. The resulting construct was used to transform the *ΔdegP* mutant, replacing the *ermAM* cassette with a functional *degP* gene and *aphA3* by double crossover homologous recombination. Complementation of the *degP* gene was confirmed

by PCR analysis and Western blotting using anti-HtrA (DegP) antisera (1:500 dilution, a gift from Dr. Jeffrey Weiser, University of Pennsylvania).

CiaRH

ΔciaRH mutants were constructed by creating a clean deletion of *ciaRH* and replacing the genes with *aphA3*. Polymerase chain reaction (PCR) was carried out using Phusion high-fidelity DNA polymerase (New England Biolabs, Whitby, ON, Canada) to amplify 425 bp of the upstream gene *sgo.1071* and 525 bp of the downstream gene *sgo.1074* using the primer pairs SL1178/SL1222 and SL1220/SL1221 respectively. The PCR products were digested with restriction enzymes as indicated in Table 2.2 and ligated with T4 DNA ligase. The ligation product was amplified using the outside primers SL1178/SL1221, and the resulting construct was used to transform *S. gordonii* SecCR1 or *S. gordonii* DL1 Challis as described above. Transformants were selected on BHI containing the appropriate antibiotics, and insertion of *aphA3* was confirmed by PCR.

Complementation of *ciaRH* in the *ΔsdbAΔciaRH* mutant was achieved by introducing functional *ciaRH* genes back onto the chromosome under their native promoter as follows. The *ciaRH* genes and the upstream 130 bp intergenic region were amplified using the primer pair SL1180/SL1221. The resulting PCR fragment was digested with KpnI (New England Biolabs) and ligated to a chloramphenicol acetyl transferase (*cat*) resistance cassette cut from pCopCAT/pUC18 using KpnI and HindIII. pCopCAT/pUC18 was constructed by subcloning the 1.6 kb PstI-BamHI DNA fragment containing the *cat* gene under the control of a *S. mutans cop* promoter from pHSL2/pUC (212) into the same sites on pUC18. Next, a 425 bp fragment of the gene located upstream of *ciaRH*, *sgo.1071*, was amplified by PCR using the primer pair SL1178/1179 and digested with HindIII. The three fragments were ligated together with T4 DNA ligase and amplified by PCR using the primers SL1178/1221. The resulting construct was used to transform *ΔsdbAΔciaRH* cells by homologous recombination, replacing *aphA3* with the *cat* + *ciaRH* construct. Transformants were selected on BHI with chloramphenicol, and replica plating was used to identify kanamycin-sensitive, chloramphenicol-resistant colonies. Complementation was confirmed by PCR.

2.2.5 Site Directed Mutagenesis

All point mutations were generated on the chromosome and expressed from their native promoters.

AtlS

A cysteine to serine point mutation in *atlS* was generated in the parent SecCR1 background by introducing a mutation to replace the codon for cysteine at position 1069 (TGT) to serine (TCC). To achieve this, the upstream region of *atlS* through to the cysteine codon was amplified with Platinum Pfx DNA polymerase (Life Technologies) using the primer pair SL893/SL896. The resulting PCR product was digested with BspEI at 37°C, 1 h. The fragment was then ligated to a second PCR product that contained the downstream portion of *atlS*, from the cysteine codon to the end of the reading frame, amplified with the primer pair SL897/SL898. The resulting construct consisted of the *atlS* gene with a Cys→ Ser mutation, which also created a novel BspEI restriction site (TCCGGA) from the parent sequence (TGTGGA). To enable selection, an *ermAM* cassette was digested with BamHI and ligated to a 628 bp fragment amplified from the region located immediately downstream of *atls* with the primers SL899/SL900. Finally, the two constructs were ligated via an EcoRV restriction site and amplified by PCR using the outside primers SL893/SL900. The PCR product was used to transform *S. gordonii* SecCR1, and transformants were selected on BHI with erythromycin. The mutation was confirmed by PCR and restriction analysis of the BspEI site. Additional evidence to confirm the mutation was obtained by performing alkylation experiments to test the redox status of AtlS produced in the mutant, and reactions with the AtlS antibodies (Fig. 3.7). Alkylation was performed using SDS-extracted surface proteins as described below.

DegP

A serine (ACT) to alanine (ACG) mutation was introduced in the DegP active site at amino acid position 235. The mutation was constructed by overlapping PCR using Phusion high-fidelity DNA polymerase and the primers SL752 and SL991 (upstream), and SL992 and SL993 (downstream) (213). The mutated *degP* gene was digested with

KpnI and ligated to *aphA3* followed by a 531 bp downstream portion of *degP*, as described above. The construct was amplified with the primer pair SL752/SL755 and the PCR product was used to transform the *ΔdegP* mutant by homologous recombination, replacing *ermAM* with the S235A *degP* gene. Transformants were selected on BHI with kanamycin, and replica plating was used to identify kanamycin-resistant, erythromycin-sensitive colonies.

SdbA

A similar approach was used to construct SdbA cysteine point mutants. Overlapping PCR with the primer pairs SL756 and SL1039 (upstream), and SL1038 and SL759 (downstream) was used to construct a cysteine (TGT) to alanine (GCT) mutation at position 89. The two fragments were combined as template for PCR and amplified with the outside primers SL756/SL803. The resulting construct was then cut with BamHI and ligated to fragment containing *aphA3* followed by a 548 bp portion of the region downstream of *sdbA*. The ligated DNA was amplified using the outside primers SL756/SL759. This PCR product was used to transform the *S. gordonii ΔsdbA* mutant by homologous double cross-over recombination, replacing the *ermAM* gene with the SdbA C89A construct. *sdbA* was expressed from its own promoter on the chromosome. Transformants were selected on BHI with kanamycin, and replica plating was used to identify kanamycin-resistant, erythromycin-sensitive colonies. The same approach was used to generate SdbA C86A and C89P mutations using the primer pairs SL1102/SL1103 and SL1104/SL1105 respectively. These fragments were ligated to *aphA3* and used to transform the *ΔsdbA* mutant exactly as described above.

The $sdbA_{C86P}$ mutant was constructed by a slightly different strategy. The upstream portion of *sdbA* amplified by the primer pairs SL756/SL975 and the downstream portion of *sdbA* amplified by the primer pairs SL974/SL803 were cloned into pBluescript. Primers SL974 and SL975 contained the cysteine (TGT) to proline (CAA) mutation. The resulting pBluescript$sdbA_{C86P}$ was digested with BamHI and ligated to *aphA3* and a downstream portion of *sdbA*. The ligated DNA was amplified using primers SL762/SL759 and transformed into the *ΔsdbA* mutant. This strategy was

used because it created a unique MscI site (TGG TGT → TGG CCA) that could be used as a second approach to quickly confirm the mutation.

The $C_{86}PDC_{89}$ double cysteine mutant was generated using overlapping PCR to mutate Cys89 in the $SdbA_{C86P}$ background. Overlapping PCR with the primer pairs SL756/1039 and SL1038/759 was used to construct a cysteine (TGT) to alanine (GCT) mutation at the cysteine codon at position 89. The fragments were combined and amplified with SL756/803. The resulting construct was then ligated to *aphA3* and a downstream portion of *sdbA*. The ligated DNA was amplified using the primers SL756/759. This PCR product was used to transform an $SdbA_{C86P}$ mutant to produce a C86P/C89A double cysteine mutant.

In addition to PCR and restriction analysis, all point mutations were confirmed by DNA sequencing (The McGill University and Génome Québec Innovation Centre).

2.3 Gene Expression Analysis

2.3.1 RNA Isolation and cDNA Synthesis

RNA was isolated using the hot acid phenol method (214). RNA was extracted from cultures grown in 200 ml HTVG to a density of OD_{600}= 0.6 to test for polar effects, and to a density of OD_{600}= 0.2 in BHI with 5% serum to test expression levels of competence genes and the CiaRH two component system. When cultures reached the desired OD value, the cells were harvested by centrifugation at 10 000 x g, 10 min, 4°C. The resulting cell pellets were suspended in 0.5 ml diethyl pyrocarbonate (DEPC)-treated water, followed by 1.5 ml phenol containing 0.1 % (w/v) SDS and saturated with citric acid buffer (0.05 M sodium citrate and 0.05 M citric acid, pH 4.3 with citric acid). The cells were boiled for 10 min and then cooled on ice. The aqueous phase was separated by centrifugation (3000 x g, 10 min), and extracted once with 2 vols acidic phenol/chloroform (1:1, v/v; 3000 x g, 7.5 min), and then with 2 vols chloroform (3000 g, 7.5 min). The RNA was precipitated with 2 vols isopropyl alcohol in the presence of 0.3 M sodium acetate. The precipitated RNA was collected by centrifugation (15 000 g, 20

min), washed with 75 % ethanol, and dissolved in 50 ml DEPC-treated water. The concentration of the RNA was quantified by measuring the OD_{260} of a 1:500 dilution, and calculated using the following equation: OD_{260} reading × 500 × 40 μg/ml.

The RNA (1 μg) was treated with 1 U of amplification grade DNase I (Life Technologies Inc.) for 15 min at room temperature, and removal of DNA was confirmed by PCR with 16S rRNA primers (SL525/SL697). cDNA synthesis was carried out using random primers and Super Script II reverse transcriptase (Life Technologies Inc.) using the following conditions: 25°C 10 min, 42°C 50 min, 70°C 15 min.

2.3.2 Reverse-Transcription PCR

cDNA template (3 μl) was used as the template to amplify *nusG, padA*, *sgo_1071*, *sgo_1074*, and *sthA* with the primers listed in Table 2.2. Total cDNA was assessed by amplification of *16S rRNA* using 1 μl cDNA as template. All PCR reactions were performed using Taq DNA polymerase (NEB Biolabs).

2.3.3 Quantitative Real Time PCR

qPCR to amplify *comC, comE, sthA, ciaR,* and *degP* was carried out using the primers listed in Table 2.2 with iTaq Universal SYBR Green Supermix (Bio-Rad Laboratories, Inc., Hercules, CA) according to the manufacturer's directions. The reactions were performed using a 7900 HT Fast Real-Time PCR system (Applied Biosystems) at 95°C for 30 s, followed by 40 cycles of 95°C for 15 s and 60°C for 60 s. The cycle threshold (C_T) was calculated using SDS 2.2.2 software (Applied Biosystems). The relative expression was calculated using the comparative C_T method (215) using *16S rRNA* as an internal control gene. Each reaction was performed in duplicate using cDNA prepared from at least triplicate bacterial cultures.

2.4 Phenotypic Analysis

2.4.1 Biofilm Formation

2.4.1.1 Crystal Violet Staining

Biofilms were grown as described by Loo et al. (202), with the following modifications. Overnight cultures of *S. gordonii* grown in HTVG for ~12h at 37°C, 5% CO_2. Cells were harvested by centrifugation (3000 *x g* for 10 min) and resuspended to an OD_{600} of 0.200 in Biofilm Medium. Flat bottom 24-well plates (Falcon 3047, Corning Inc.) were inoculated with 1 ml per well of the cell suspension, and the plates were incubated for 24 h at 37C, 5% CO_2. Following incubation, the medium was removed and the wells were washed twice with 1 ml phosphate-buffered saline (PBS) to remove loosely attached cells. A vacuum pump was used for all washing steps to improve the consistency of the treatment for each well. The plates were air dried for 15 min and fixed with 10% (v/v) formaldehyde and 5% (v/v) acetic acid in PBS for an additional 15 min. The biofilms were then stained with 0.5 ml of 0.1% crystal violet. After 15 min, the wells were rinsed three times with PBS and the bound stain was solubilized in 1 ml of acetone/ethanol solution (1:1). The liquid (100 μl) was transferred to clean 96-well microtiter plate and the absorbance was measured at 600 nm in a BioTek microplate reader. The biofilm assays were carried out in triplicate with three or more separate experiments.

2.4.1.2 Scanning Electron Microscopy

Biofilms for SEM analysis were grown in Biofilm Medium on glass cover slips. Following growth for 24 h at 37C, 5% CO_2, the medium was removed and planktonic cells were removed by washing one time with PBS. The biofilms were fixed with 2.5% glutaraldehyde in 90 mM cacodylate buffer (pH 7.3) for 24 h at room temperature. The samples were then osmocated and dehydrated to 100% ethanol by standard methods. The dehydrated samples were processed by critical point drying and gold sputter coated. Biofilms were examined using a Hitachi S-4700 Field Emission Scanning Electron Microscope (Hitachi High-Technologies Canada, Inc.) at the Institute for Research in Materials at Dalhousie University.

2.4.2 Autolysis

Autolysis was tested as described by Ahn and Burne (200) with the following modifications. Overnight cultures of *S. gordonii* were diluted 1:20 into HTVG and grown at 37°C, 5% CO_2, to a density of OD_{600} = 1.0. The cells were pelleted by centrifugation (3000 *x g*, 10 min) and then suspended in pre-warmed (44°C) 20 mM potassium phosphate buffer (pH 6.5) containing 1 M KCl, 1 mM $CaCl_2$ 1 mM $MgCl_2$, 0.4% sodium azide, 0.2% Triton X-100. The cell suspensions were incubated in a 44°C water bath and autolysis was monitored by measuring the OD_{600} at regular intervals.

2.4.3 Zymogram

Zymogram analysis of SDS-extracted surface proteins was carried out as described by Liu and Burne (201). Surface protein extracts were prepared from 100 ml cultures of *S. gordonii* grown in HTVG to OD_{600} = 0.9-1.0. Cells were pelleted by centrifugation (5 000 *x g*, 10 min) and suspended in 1 ml of 4% SDS. After incubation for 60 min at room temperature, the cells were removed by centrifugation (15 000 *x g*, 15 min), and supernatant mixed 1:1 with 50 mM Tris, pH 6.5, 10% glycerol. The zymogram substrate was prepared from 800 ml overnight cultures of *S. gordonii* SecCR1 grown in HTVG. Cells were harvested by centrifugation (5 000 *x g*, 10 min) and washed four times with distilled water. The pellets were then suspended in 60 ml of 4% SDS and boiled for 30 min. The heat-killed cells were washed five times with distilled water and suspended in a final volume of 5 ml.

Zymograms were prepared by adding the heat-killed cells described above to 10% polyacrylamide gels. The concentration of the cells in the polyacrylamide gel was 1% wet weight. Following electrophoresis of the SDS-extracted proteins, the gels were washed twice with distilled water and incubated in 0.2 M sodium phosphate buffer (pH 7.0) for 12 h at room temperature to allow for renaturation of the proteins and enzymatic digestion of the heat-killed cell substrate. To resulting gels were either scanned directly or stained with 0.1% methylene blue and destained with dH_2O to enhance contrast.

2.4.4 Extracellular DNA Release

Extracellular DNA was recovered from stationary phase cultures grown for 24h in HTVG at 37°C, 5% CO_2. Cultures were standardized to OD_{600} = 1.0 and cells were removed from 1 ml volumes by centrifugation (14 000 *x g*, 5 min). The supernatants (750 μl) were mixed 1:1 with cold acetone and incubated on ice for 24 h at 4°C. The precipitated DNA was recovered by centrifugation (14 000 *x g*, 10 min), and suspended in 25 μl of TE buffer. The samples were mixed with loading dye and run on 0.8% agarose gels and stained with ethidium bromide to visualize the DNA.

2.4.5 Bacteriocin Activity

Activity of Sth bacteriocins was tested as described by Heng et al. (188) using *S. mitis* I18 or *S. oralis* 34 as the target strain. Overnight starter cultures of *S. gordonii* were diluted 1:40 into pre-warmed BHI with 5% serum medium and grown to a density of OD_{600} = ~0.200. Cells were removed by centrifugation (14 000 x g, 5 min), and the recovered supernatants were filter sterilized (0.2 μm) and mixed 1:1 with an equal volume of fresh medium. The mixture was warmed at 37°C for 15 min prior to inoculation with a 1:100 dilution of overnight *S. oralis* 34 culture. Cultures were grown for 6 h (*S. mitis*) or 10 h (*S. oralis*) and the OD_{600} was read using a spectrophotometer (Shimadzu UV-1700, Kyoto, Japan).

For assays that included synthetic CSP (DVRSNKIRLWWENIFFNKK; Biomatik, Cambridge, ON, Canada), cultures were grown in BHIS to OD = 0.150 followed by the addition of 10 ng/ml CSP (from a 1 mg/ml stock in MilliQ water). The cultures were then incubated for an additional 30 min at 37 °C to allow for induction and protein expression, and bacteriocin activity was tested as described above. Assays were done in triplicate and repeated at least three times.

2.4.6 Genetic Competence

Genetic competence in *S. gordonii* SecCR1, the *sdbA* mutant, and the complemented mutant was tested by transformation with genomic DNA isolated from *S.*

gordonii Wicky WK1, a strain that contains a spontaneous mutation in the β-subunit of RNA polymerase conferring resistance to rifampin (216). Cultures were grown at 37°C to OD_{600} = 0.200 in BHI with 5% heat inactivated calf serum prior to the addition of 1 μg *S. gordonii* Wicky WK1 genomic DNA. Cultures were incubated for an additional 2 h to allow for DNA uptake, and serial dilutions were dropped plated on either BHI or BHI with 100 μg/ml rifampin. The plates were incubated for 48 h at 37°C, 5% CO_2, and the transformation frequency was calculated as the percentage of rifampin resistant transformants to the total CFU/ml.

2.5 Purification of Sth_1 From Culture Supernatants

Sth_1 specific antibodies were affinity purified from rabbit sera using Sth_1 peptides cross-linked to cyanogen bromide (CNBr)-activated sepharose 4B (GE Healthcare Life Sciences, Mississauga, ON, Canada). Freeze-dried CNBr resin (0.25 g) was prepared for antigen coupling by washing with 1 ml of cold 1 mM HCl for 5 min × 10 washes. The resin was then mixed with 3 mg Sth_1 (AGFTGGIAVGLNRVNRK; Biomatik) in 5 ml coupling buffer (0.1 M $NaHCO_3$ pH 8.3 containing 0.5 M NaCl) and incubated overnight at 4°C to allow coupling to occur. Following the reaction, excess ligand was washed away with 5 volumes of coupling buffer and non-reacted groups were blocked with 0.1 M Tris-HCl buffer pH 8.0 for 2 h. The medium was then washed with 3 ml high pH buffer (0.1 M Tris-HCl buffer pH 8, 0.5 M NaCl), followed by 3 ml low pH buffer (0.1 M acetate buffer pH 3.5, 0.5 M NaCl). The wash cycle was repeated 6 times. Coupling was tested by SDS-PAGE.

To purify anti-Sth_1 antibodies, 3 ml of rabbit anti-Sth_1 antisera was diluted 1:10 with 10 mM Tris, pH 7.5 and applied to the Sth_1-coupled sepharose column 3 times. Unbound antibodies were washed from the column with 20 ml of 10 mM Tris pH 7.5, followed by 20 ml of 10 mM Tris pH 7.5 containing 0.5 M NaCl. Anti-Sth_1 antibodies were eluted from the column with 9 ml of 100 mM glycine pH 2.5 and neutralized by the addition of 1:10 volume of 1 M Tris, pH 8.

Affinity purified anti-Sth_1 was irreversibly cross-linked to protein A-agarose beads (Sigma). Briefly, anti-Sth1 antibodies were incubated with protein A-agarose beads for 1 h at 4°C. The resin was then washed with two volumes of 0.2 M sodium borate, pH 9. Cross-linking was achieved by suspending the resin in freshly prepared 25 mM dimethyl pimilimidate in 0.2 M sodium borate and incubating at room temperature for 30 min. The resin was washed with 0.2 M triethanolamine in PBS for 5 min. The resin was then reacted with dimethyl pimilimidate as described above two more times. After the final wash, the resin was quenched with 50 mM diethanolamine in PBS for 5 min, and unbound antibodies were removed by washing with 0.3 M glycine, pH 2.5 for 10 min, followed by PBS. To test for successful crosslinking, 10 μl aliquots of the resin taken before and after the addition of dimethyl pimilimidate were boiled SDS-PAGE sample buffer and analysed by SDS-PAGE and Coomassie blue staining.

To purify secreted bacteriocins, overnight starter cultures were diluted 1:40 into pre-warmed BHIS and grown to a density of OD_{600} = 0.200, unless otherwise noted. Cells were removed by centrifugation (5,000 *x* g, 10 min, 4 °C) and the supernatant was passed through a 10 ml column packed with anti-Sth_1 protein A sepharose. The column was washed with 10 ml of 10 mM Tris, pH 7.5, followed by 10 ml of 10 mM Tris, pH 7.5, containing 500 mM NaCl. Sth_1 was eluted in 200 μl fractions with 100 mM glycine, pH 2.5 and immediately neutralized with 1:10 volume 1M Tris, pH 8.0. Microtiter plates (Maxisorp, Fischer Scientific, Ottawa, ON, Canada) were coated with 100 μl aliquots of the fractions and incubated overnight at 4 °C. The plates were then blocked with 200 μl 1% (w/v) gelatin in PBS with 0.1% Tween 20 (PBST) at room temperature for 1 h. After blocking, mouse anti-Sth_1 antiserum (1:1000) was added to the wells and incubated overnight at 4°C. Sth_1 was detected using goat anti-mouse IgG-biotin (1: 20 000; Sigma-Aldrich) followed by Extravidin-alkaline phosphatase (1: 60 000; Sigma-Aldrich). The plates were developed with *p*-nitrophenylphosphate (1 mg/ml; Bioshop Canada Inc., Burlington, ON, Canada) in diethanolamine buffer and the absorbance at 405 nm was read using a microplate reader.

2.7 Immunoblotting

Unless otherwise specified, proteins were detected using the following Western blotting protocol. Cells from 3 ml of overnight culture, or 6 ml of mid-exponential phase culture were pelleted by centrifugation (14 000 x g, 5 min, 4°C) and suspended in 50 μl sample buffer (250 mM Tris-HCl pH 6.8, 2% sodium dodecyl sulfate, 10% glycerol, 10% 2-mercaptoethanol, 0.01% bromophenol blue). For samples run under non-reducing conditions, 2-mercaptoethanol was omitted from the buffer. Samples were boiled for 5 min and cells were removed by centrifugation at 14 000 x g, 5 min. The supernatants were electrophoresed on SDS-PAGE gels using the buffer system of Laemmli (217) (Mini PROTEAN electrophoresis system, Bio-Rad ; 200 V, ~1 h) followed by Coomassie blue staining to ensure equal protein loading, and the same volumes were run in duplicate for Western blotting. Proteins were transferred to nitrocellulose membranes (Bio-Rad) using a tank blotting system at 200 mA for 60 min (218) (Mini Trans-Blot, Bio-Rad). Membranes were blocked with 1% gelatin dissolved in PBST, for 1 h. Membranes were incubated with primary antibodies diluted in PBST at 4°C overnight. Unbound antibodies were removed by washing 4 × 1 min with PBST. Proteins were detected with secondary antibodies conjugated to alkaline phosphatase. Methods for blotting small peptides are described in Appendix C.

2.8 Chemical Alkylation

2.8.1 AtlS

Crude surface protein extracts containing the autolysin were obtained from the *sdbA* mutant by extraction with 4% SDS as described above. Attempts to analyze SDS-extracted proteins from the parent strain were unsuccessful due to the high concentration of competing proteins in the sample. Thus, AtlS from the parent strain was obtained by extraction with 5 M LiCl for 60 min at 4°C, which extracted surface proteins with a lower efficiency than SDS, resulting in a less complex sample. This approach was not necessary in the *sdbA* mutant because it produced fewer surface proteins. Alkylation of the protein extracts was carried out as described previously, with the following modifications (219). The protein extracts were precipitated with 9% trichloroacetic acid (TCA) on ice for 30

min, followed by centrifugation at 15 000 x g, 10 min, 4°C and washed twice with acetone. Pellets were then suspended in 5 mM maleimide-PEG_2-biotin (Thermo) in 100 mM Tris (pH 7.0) and 1% SDS, and incubated for 30 min at room temperature, followed by 10 min at 37°C. Excess maleimide was removed by TCA precipitation. The resulting pellets were solubilized in 100 mM Tris (pH 7.0), 1% SDS, 8 M urea. To prepare positive controls, the extracts were reduced with 100 mM dithiothreitol (DTT) in 10 mM Tris (pH 8.1) for 30 min at room temperature and TCA precipitated prior to the addition of maleimide.

To specifically detect disulfide-bonded cysteines, iodoacetamide was used to block the free thiol groups. Surface protein extracts were prepared as described above and subsequently TCA precipitated and washed two times with ice-cold acetone. The resulting pellets were suspended in 200 mM Tris, pH 8.1, 100 mM iodoacetamide and incubated for 20 min on ice in the dark, followed by TCA precipitation to remove excess iodoacetamide. Disulfide bonds were then reduced with DTT and alkylated with maleimide-PEG_2-biotin.

To detect biotinlylated proteins, the samples were boiled in sample buffer and run in duplicate on a 10% SDS-PAGE. Proteins were transferred to a nitrocellulose membrane and reacted with avidin alkaline phosphatase (Sigma). Total AtlS concentration in the samples was used as a loading control and was detected with anti-AtlS antisera (1:1000).

2.8.2 Anti-CR1 scFv

ScFv antibody was purified from the parent and the *ΔdegPΔsdbA* and $sdbA_{C86P}$ mutants by affinity chromatography. Cultures were grown overnight in 500 ml HTVG. Cells were pelleted by centrifugation and suspended in 50 ml of column wash buffer with urea (50 mM NaH_2PO_4, 300 mM NaCl, 5 mM imidiazole, 8 M urea, pH 7) to extract and denature scFv. Denaturing conditions were required to make the hexahistidine tag on the scFv accessible for affinity purification. Following overnight incubation at 4°C, the cells were removed by centrifugation at 20 000 x g, 15 min. The supernatant was applied to a NiCAM affinity column (Sigma-Aldrich) three times to allow binding. Unbound proteins

were removed by washing with 20 ml of column wash buffer and anti-CR1 scFv was eluted with 10 ml of elution buffer (50 mM NaH_2PO_4, 300 mM NaCl, 250 mM imidiazole, 8 M urea, pH 7).

Purified scFv was precipitated with 9% (v/v) TCA and 0.18% (v/v) deoxycholate on ice for 30 min, followed by centrifugation at 15 000 x g, 10 min, 4°C and washed twice with acetone. Pellets were then suspended in 5 mM maleimide-PEG_2-biotin in 100 mM Tris (pH 7.0) and 1% (v/v) SDS, and incubated for 30 min at room temperature, followed by 10 min at 37°C. Excess maleimide-PEG_2-biotin was removed by TCA precipitation. The resulting pellets were solubilized in 100 mM Tris (pH 7.0), 1% (v/v) SDS, 8 M urea. To prepare positive controls, the extracts were reduced with 100 mM DTT in 10 mM Tris (pH 8.1) for 30 min at room temperature and TCA precipitated prior to the addition of maleimide-PEG_2-biotin.

To specifically detect disulfide-bonded cysteines, iodoacetamide was used to block the free thiol groups. Purified scFv was TCA precipitated and washed twice with ice-cold acetone. The resulting pellets were suspended in 200 mM Tris (pH 8.1), 100 mM iodoacetamide and incubated for 20 min on ice in the dark, followed by TCA precipitation to remove excess iodoacetamide. Disulfide bonds were then reduced with DTT and alkylated with maleimide-PEG_2-biotin.

To detect biotinlylated proteins, the samples were boiled in sample buffer and run in duplicate on a 12.5% SDS-PAGE. Proteins were transferred to a nitrocellulose membrane and reacted with avidin alkaline phosphatase (1:60 000; Sigma-Aldrich). Total scFv concentration in the samples was used as a loading control and was detected with anti-HA monoclonal antibodies. Experiments were repeated at least three times to ensure reproducibility.

2.9 Cloning and Expression of Recombinant Proteins

Recombinant plasmids to produce hexahistidine tagged proteins were constructed by cloning in frame fragments of the genes into the expression vector pQE-30 (Qiagen)

behind an N-terminal His_6-tag. The primers and restriction enzymes used for each gene are listed in Table 2.2. Plasmids were transformed into *E. coli* XL-1 Blue and selected on LB with ampicillin, and the constructs were confirmed by restriction analysis.

2.9.1 His_6-SdbA

His_6-SdbA consisted of a 17.13 kDa portion of SdbA after the signal sequence. To express His_6-tagged SdbA, a 50 ml of overnight culture was diluted into 450 ml of pre-warmed LB and incubated at 37°C, 200 rpm, until mid-exponential phase. Expression was induced with a final concentration of 1mM of isopropyl-β-D-thiogalactopyranoside (IPTG), and cultures were incubated at 37°C for an additional 4 h. Cells were harvested by centrifugation (5 000 *x g*, 10 min) and the pellets were stored at -80°C overnight. The frozen pellets were suspended in 10 ml column wash buffer (50 mM NaH_2PO_4, 300 mM NaCl, 20 mM imidazole, pH 7) and the cells were lysed by sonication for 30s x 30 cycles, with cooling on ice for 30 s intervals. Cell debris was removed from the lysate by centrifugation at 27 000 *x g*, 30 min and the supernatant was applied to a 4 ml NiCAM affinity column (Sigma) equilibrated with wash buffer. Unbound proteins were removed with 20 ml of wash buffer and His_6-SdbA was eluted with 10 ml of elution buffer collected in 1 ml fractions (50 mM NaH_2PO_4, 300 mM NaCl, 250 mM imidazole). The $SdbA_{C86P}$, $SdbA_{C89A}$, and $SdbA_{C86P/C89A}$ cysteine variants were prepared using the same approach as described above.

2.9.2 His_6-AtlS

His_6-AtlS contained a 30 kDa portion of C-terminal region of the protein. Purification of His_6-AtlS was carried out as described above, except using denaturing conditions with 8 M urea in all buffers, because His-AtlS was insoluble when produced in *E. coli* XL-1 Blue. Purity of the eluted proteins was confirmed by SDS-PAGE and staining with Coomassie blue.

2.9.3 *E. coli* DsbA

E. coli DsbA was expressed from pDsbAcyt in *E. coli* BL21(DE3) and purified as described by Hennecke et al (220). Cells were grown for 2 h in 2 L LB medium inoculated with 100 ml overnight culture. Expression of DsbA was induced with 1 mM IPTG for an additional 5 h, and the cells were then harvested by centrifugation at 10 000 x g, 10 min. The cell pellet was suspended in 20 ml of 10 mM 3-morpholinopropane-1-sulfonic acid (MOPS) NaOH, pH 7.3. Cells were lysed by sonication and insoluble material wa removed by centrifugation as described above. DsbA was recovered in the soluble fraction and further purified by anion exchange chromatography. Supernatant containing DsbA was applied to a column with 50 ml diethylaminoethyl (DEAE) sepharose Fast Flow resin (GE Life Sciences). The column was washed with 100 ml of MOPS-NaOH pH 7.3, and eluted with a NaCl gradient of 0-400 mM NaCl in MOPS-NaOH buffer, 900 ml total volume. Fractions were collected using a RediFrac fraction collector (GE Healthcare) set to collect 200 drops/fraction. SDS-PAGE and Coomassie blue staining was used to test the fractions for DsbA.

2.10 Production of Antisera

Antibodies were raised against purified recombinant SdbA and AtlS in mice using the same approach. The purified proteins were prepared by adsorption to 2% aluminum hydroxide gel (Sigma) at 4°C for 24 h. BALB/c mice were immunized via intraperitoneal injection with 20 μg of antigen per dose, on days 1, 14, and 21. On day 28, the mice were euthanized and blood was collected by cardiac puncture. To obtain serum, the samples were incubated at 37°C for 1 h, and then on ice at 4°C overnight. Following incubation, serum was collected by centrifugation at 10 000 *x g*, 10 min and stored at -20°C.

Antibodies against oxidized SdbA were also generated in rabbits (ProSci, San Diego, California). Rabbits were initially immunized with 200 μg SdbA in complete Freund's adjuvant on day 0, and subsequently boosted with 100 μg SdbA in incomplete Freund's adjuvant on days 14, 28, and 42, and exsanguinated on day 56.

Antibodies were raised against the reduced and oxidized forms of SdbA in both mice and rabbits. Fully oxidized SdbA was generated as described in section 2.11. Throughout the study, only the antibodies raised against the oxidized form of SdbA were used because antibodies raised against the reduced form failed to recognize SdbA produced in *S. gordonii*.

Antibodies were raised against Sth_1 (AGFTGGIAVGLNRVNRK) and CSP (DVRSNKIRLWWENIFFNKK) conjugated to keyhole limpet hemocyanin (Biomatik, Cambridge, ON) in New Zealand white rabbits and in BALB/c mice. Antigens used to inoculate mice were prepared with aluminum hydroxide and delivered via intraperitoneal injections as described above. Antigens used to inoculate rabbits were dissolved in PBS and mixed 1:1 with incomplete Freund's adjuvant. The antigen was emulsified with the adjuvant using a glass syringe and rabbits were injected subcutaneously with 200 μg of antigen in a total volume of 1 ml (4 × 250 μl) on days 1, 20, 40, 60, and the animals were exsanguinated on day 80. Antibody titers were tested by ELISA.

2.11 Enzyme Assays

2.11.1 Oxidative Folding of Reduced, Denatured RNase A

RNase A refolding assays were carried out as described by Daniels et al. (96). Recombinant SdbA expressed in *E. coli* XL-1 Blue was obtained in a mix of oxidized and reduced forms as shown by alkylation with maleimide-PEG_2-biotin (Thermo). To produce fully oxidized SdbA, 0.5 mg/ml protein in 100 mM Tris (pH 8.8), 200 mM KCl, 1 mM EDTA was incubated with 100 mM oxidized glutathione (Sigma) for 1 h at room temperature (220). Glutathione was then removed by dialysis against 100 mM sodium phosphate buffer (pH 7).

Reduced, denatured RNase A was prepared by incubating 5 mg/ml RNase A in 6 M guanidine HCl, 100 mM Tris acetate, 2 mM EDTA, 130 mM DTT, pH 8 overnight at room temperature. The RNase A was separated from excess DTT and guanidine HCl by gel filtration on a Sephedex G25 column (GE Life Sciences) and eluted with 50 mM

sodium phosphate buffer, pH 7. Reduction was confirmed by alkylation with maleimide or using 5,5'-dithio-bis(2-nitrobenzoic acid) (DTNB) (as described below).

Refolding assays were carried out using 10 μM of purified SdbA or DsbA in a redox buffer containing 0.2 mM oxidized glutathione (GSSG), 0.1 mM reduced glutathione (GSH), 2 mM EDTA, in 100 mM Tris acetate, pH 8. Reduced, denatured RNase A (10 μM) was added and incubated for 2 min prior to the addition of 4.5 mM cCMP substrate. RNase A catalyzed cCMP hydrolysis was detected as the increase in absorbance at 296 nm.

The kinetics of RNase A refolding was calculated using a previously described method (221, 222). The reactions were run as described above, using 5 to 30 μM of reduced denatured RNase A substrate and monitored over a 30 min period. The concentration of active, renatured RNase A (E_t in μM) was calculated at each time point from the first derivative of the absorbance versus time data (ν_t, in μM/min) using the equation described by Lyles and Gilbert, and Rupp *et al*. (222, 223). This equation corrects for the time-dependent depletion of cCMP during the assay and for the competitive inhibition of RNase A by the hydrolysis product (CMP).

$$E_t = \nu_t / \{k_{cat}, [cCMPl_t/([cCMP]_t, + K_{mc}(1 + [CMP]_t / K_i))\} \quad (1)$$

Where ν_t is the reaction velocity at time point *t*, k_{cat} is the turnover number for fully active RNase A [196 μmol of cCMP min^{-1}(μmol of RNase)$^{-1}$], K_{Mc} is the K_M for cCMP under these conditions (8.0 ± 0.5 mM), and K_i is the inhibition constant for CMP (2.1 ± 0.4 mM). The concentration of cCMP and CMP were obtained from the initial concentration of cCMP (4.5 mM), the observed absorbance, and the extinction coefficients of cCMP (ε = 0.19 mM^{-1} cm^{-1}) and CMP (ε = 0.38 mM^{-1} cm^{-1}) at 296 nm, pH 8.0.

The calculated amount of renatured RNase A was plotted against time for each substrate concentration. The resulting slopes (initial velocity) for each reaction curve

were plotted versus the concentration of substrate, and non-linear regression analysis was performed using the Michealis Menton equation in GraphPad Prism 6 (GraphPad Prism Software Inc.).

RNaseA folding was also tested by alkylation with maleimide-PEG_2-biotin. $SdbA_{C86P}$ or $SdbA_{C89A}$ (20 μM) was combined with reduced, denatured RNaseA (10 μM) in 100 mM Tris buffer pH 8.0, 1 mM EDTA. Proteins were incubated at ambient temperature for 20 min and the reaction was quenched by the addition of 9% (v/v) TCA. Following TCA precipitation, protein pellets were suspended in column wash buffer and applied to a NiCAM column to trap SdbA via its N-terminal His_6-tag. RNaseA remaining in the unbound and wash fractions was pooled and reacted with maleimide-PEG_2-biotin as described above. Alkylated proteins were separated on 15% SDS-PAGE gels and stained with Coomassie blue. To test for SdbA-RNaseA mixed disulfides, SdbA was eluted from the column and the eluate was run on a 15% SDS-PAGE gel under non-reducing conditions.

2.11.2 Solvent Accessibility

The solvent accessibility of the individual SdbA cysteine thiols was tested by reaction with dithionitrobenzoic acid (DTNB) (224). A 15 μM solution of purified reduced SdbA, $SdbA_{C86P}$ or $SdbA_{C89A}$ was prepared in 0.1 M sodium phosphate buffer (pH 8.0). The reaction was started by adding 200 μM of DTNB from a 10 mM stock solution prepared in 0.1 M sodium phosphate buffer (pH 8.0), and the absorbance at 412 nm was recorded.

2.11.3 pK_a Determination

The pH-dependent ionization of the *S. gordonii* SdbA C86 thiol, or the *E. coli* DsbA C30, was followed by the absorbance of the thiolate anion at 240 nm as described previously (108). The assay was carried out in a buffer containing 10 mM boric acid, 10 mM sodium succinate, 10 mM K_2HPO_4, 200 mM KCl, 1 mM EDTA. The pH of the buffer was titrated with 0.2 M HCl to generate pH values ranging from 3 – 7.5, and

reduced enzymes (SdbA or DsbA) were added to the buffer at a concentration of 30 μM. The pH dependence of the thiolate-specific absorbance signal was determined using the following equation:

$$S = (A_{240}/A_{280})_{red}/(A_{240}/A_{280})_{ox.} \quad (2)$$

Where $(A_{240}/A_{280})_{ox}$ is a control for the pH-dependent absorbance of the fully oxidized form of DsbA or the cysteine-free $SdbA_{C86P/C89A}$ variant. To determine the cysteine pK_a, the calculated value for S was fitted according to a modified Henderson-Hasselbalch equation in which S_{AH} represents the absorption of the fully protonated form, and S_{A^-} is that of the fully deprotonated form.

$$S = S_{AH}(S_{A-} - S_{AH})/(1 + 10^{(pKa + pH)}) \quad (3)$$

2.12 Detection of Cysteine Modifications

2.12.1 DCP-Bio1

Sulfenylation of SdbA cysteines was detected using the sulfenic acid probe DCP-Bio1 (Millipore), which specifically biotinylates sulfenic acid. Purified His_6-SdbA variants (25 μM) were reacted with 1 mM DCP-Bio1 and 100 μM hydrogen peroxide in PBS for 30 min at room temperature. Excess DCP-Bio1 was removed by TCA precipitation. Samples were analyzed by SDS-PAGE and Western blot by probing with avidin alkaline phosphatase.

2.12.2 Colloidal Coomassie Blue Staining

Proteins were visualized by staining with Colloidal Coomassie blue using a previously described staining protocol (225). After electrophoresis, the gels were fixed with 12% TCA for 1 h. The stain was prepared as follows for a 100 ml solution: 10 ml of phosphoric acid was added to 20 ml of distilled, deionized water. Next, 10 g of ammonium sulfate was added and fully dissolved prior to the addition of 0.12 g of coomassie blue G-250. The stained was stirred for 30 min at room temperature. After

stirring, water was added to bring the volume up to 80 ml, followed by 20 ml of methanol. Gels were stained until the protein bands were visible and destained with dH_2O.

2.12.3 Mass Spectrometry

Modification of the SdbA active site cysteines following reaction with glutathione or hydrogen peroxide were tested separately. SdbA was reacted with glutathione as described above. To test for oxidation of the SdbA active site cysteines following exposure to hydrogen peroxide, 25 μM of $SdbA_{C89A}$ or $SdbA_{C86P}$ was reacted with 100 μM hydrogen peroxide and 10 mM dimedone in PBS for 30 min at room temperature. Dimedone stabilizes sulfenic acid, while sulfinic and sulfonic acid species can be detected without derivatization. Following the reaction, 5 μg of SdbA protein was electrophoresed on an SDS-PAGE gel under non-reducing conditions. The 18 kDa bands corresponding to SdbA were excised from the gel and stored at -80°C.

Mass spectrometry and data acquisition were performed by Alejandro Cohen at the Dalhousie Proteomics and Mass Spectrometry Core Facility. Samples were prepared for mass spectrometry by trypsin digestion according to Shevchenko *et al*. with some modifications (226). Briefly, reduction with DTT and alkylation with iodoacetamide was omitted in the procedure to allow the detection of cysteine residues. Gel bands were digested with trypsin (Promega, Madison, WI) for 12 h at 37°C. Peptides were extracted from the gel bands with 100 μL of a 50% acetonitrile-5% formic acid solution. The extract was dried by vacuum centrifugation (SPD SpeedVac Thermo Electron Corp. Waltham, MA); the tryptic peptides were resuspended in 20 μL of a 3% acetonitrile, 0.5% formic acid solution. Liquid chromatography-tandem mass spectrometry (LC-MS/MS) was performed using a nano flow liquid chromatography system (Ultimate3000, ThermoScientific) interfaced to a hybrid ion trap-orbitrap high-resolution tandem mass spectrometer (VelosPro, ThermoScientific) operated in data dependent acquisition (DDA) mode. Briefly, 1 μL of each sample was injected onto a capillary column (C18 Onyx Monolithic, 0.10 x 150 mm Phenomenex) at a flow rate of 300 nl/min. Samples

electro-sprayed at 1.2 kV using a dynamic nanospray probe with fused silica non-coated emitters (20-um ID with 10-um ID tip PicoTip Emitter from New Objective). Chromatographic separation was carried out using 90 minute linear gradients (Mobile Phase A: 0.1% formic acid in MS-grade water, mobile phase B: 0.1% formic acid in MS-grade acetonitrile,) from 3% B to 35% B over 60 minutes, then increasing to 95%B over 5 minutes. MS/MS spectra were acquired using both collision induced dissociation (CID) and higher-energy collisional dissociation (HCD) for the top 15 peaks in the survey 30000-resolution MS scan. The raw files were acquired (Xcalibur, ThermoFisher) and exported to Proteome Discoverer 2.0 (ThermoFisher) software for peptide and protein identification using SequestHT search algorithm (Full trypsin digestion with 2 maximum missed cleavages, 10 ppm precursor mass tolerance and 0.8 Da fragment mass tolerance). Database searching was done using the UniprotKB *E. coli* or *S. gordonii* databases, with the appended SdbA/thioredoxin C86P and C89A mutations, accordingly. Sulfenic acid with dimedone (+138 Da increase in mass), sulfinylation (+32 Da), sulfonylation (+48 Da), and S-glutathionlyation (+305 Da) and oxidized methionines were selected as dynamic (variable) modifications (Table 2.3).

Semi-quantitative analysis was done using Xcalibur QualBrowser by integrating the extracted ion chromatograms (XIC) of each modified and unmodified peptide. XICs were obtained using a 0.02 Da mass window for each peptide precursor. Comparison across the modified and unmodified peptides was always performed on equally charged precursors, (typically 2+ or 3+) whenever the peptides exhibited multiple charged precursors.

The mass spectrometry proteomics data have been deposited to the ProteomeXchange Consortium (227) via the PRIDE partner repository with the dataset identifier PXD002827.

2.13 Differential Scanning Fluorimetry

Differential scanning fluorimetry and data acquisition was performed with the assistance of Jason LeBlanc. A 25 μl solution of purified SdbA (1 μM) was prepared in

20 mM phosphate buffer (pH 7.5), 150 mM NaCl, 10 mM EDTA and 5x SYPRO orange (Invitrogen). Melting curve analysis was performed using a LightCycler 2.0 real-time PCR instrument (Roche Diagnostics) by increasing the temperature from 37°C to 95°C with a ramp rate of 0.05°C/s. During thermal denaturation, continuous fluorescence was captured in all channels. Data were analyzed with melting temperature (Tm) analysis software provided by the manufacturer (version 4.05). The raw data captured from the 610 nm channel were exported and reanalyzed using the Multicode RTx analysis software version 1.6.4.1 (Eragen BioSciences).

2.14 Sequence Analysis

To identify TDORs in *S. gordonii*, the sequences for *Bacillus subtilis* 168 BdbD and BdbC were used as the query for a BLASTP search in *S. gordonii* Challis DL-1. A second search for proteins similar to Sgo.2006 led to the identification of Sgo.1171, Sgo.1177, and Sgo.1267. Sgo.1216 was identified by a BLASTP search for homologs to *Streptococcus thermophilus* LMD-9 $BlpG_{(ST)}$ (154).

Screening for potential SdbA substrates was carried out using a protocol modified from Daniels *et al*. (96). The *S. gordonii* proteome was downloaded from the UniProtKB database (http://www.uniprot.org). Extracytoplasmic proteins were identified using the prediction servers SignalP 3.0 (228) and LipoP 1.0 (229) to identify predicted secreted proteins and lipoproteins, respectively. Cytoplasmic proteins were discarded, and proteins that were predicted to encode a signal sequence by either the Neural Network or Hidden Markov Model were considered as extracellular and analyzed for cysteine content. Extracellular portions of the proteins were identified using the transmembrane prediction server SCAMPI (230), and proteins with two or more cysteine residues predicted to localize on the outside of the membrane were collected in a list of potential substrates. The annotated functions of the genes were obtained from the Oralgen database (http://www.oralgen.lanl.gov).

To identify homologs of *S. gordonii* SdbA in other Gram-positive species, a DELTA BLAST search was carried out using SdbA (YP_001451255) as the query sequence with a homology cut-off of $e < 10^{-29}$.

2.15 Statistical Analysis

Results were analyzed by one-way analysis variance with Tukey post-tests using GraphPad Prism version 6 (GraphPad Software Inc., La Jolla, California).

Table 2.1 Bacterial strains used in this study

Strains	Relevant characteristics	Source
S. gordonii SecCR1	Secretes anti-CR1 scFv, Tet^R, $Spec^R$	(204)
S. gordonii HppG	*S. gordonii* DL1 *hppG*::tet,	(204)
S. gordonii RJM4	Secretes SpaP-S1, Tet^R, $Spec^R$ Kan^R	(231)
ΔsdbA	*sdbA::ermAM,* Tet^R, $Spec^R$, Erm^R	This study
SdbA Compl	*sdbA* complemented on chromosome and expressed from the native *sdbA* promoter, Tet^R, $Spec^R$, Kan^R	This study
ΔsdbAΔdegP	*ΔsdbA, degP::aphA3,* Tet^R, $Spec^R$, Kan^R, Erm^R	This study
$sdbA_{C86P/C89A}$ (PXXA)	*sdbA* coding for the double cysteine mutation located on the chromosome and expressed from the native *sdbA* promoter, Tet^R, $Spec^R$, Kan^R	This study
$sdbA_{C86P}$ (PXXC)	*sdbA* coding for the cysteine 86 to proline mutation located on the chromosome and expressed from the native *sdbA* promoter, Tet^R, $Spec^R$, Kan^R	This study
$sdbA_{C89A}$ (CXXA)	*sdbA* coding for the cysteine 89 to alanine point mutation located on the chromosome and expressed from the native *sdbA* promoter, Tet^R, $Spec^R$, Kan^R	This study
$sdbA_{C86A}$ (AXXC)	*sdbA* coding for the cysteine 86 to alanine point mutation located on the chromosome and expressed from the native *sdbA* promoter, Tet^R, $Spec^R$, Kan^R	This study
$sdbA_{C89P}$ (CXXP)	*sdbA* coding for the cysteine 89 to proline point mutation located on the chromosome and expressed from the native *sdbA* promoter, Tet^R, $Spec^R$, Kan^R	This study
$sdbA_{C86P/C89A}$ *ΔdegP*	$sdbA_{C86P/C89A}$, *degP::ermAM,* Tet^R, $Spec^R$, Kan^R, Erm^R	This study
$sdbA_{C86P}$*ΔdegP*	$sdbA_{C86P}$, *degP::ermAM,* Tet^R, $Spec^R$, Kan^R, Erm^R	This study
$sdbA_{C89A}$*ΔdegP*	$sdbA_{C89A}$, *degP::ermAM,* Tet^R, $Spec^R$, Kan^R, Erm^R	This study
Δsgo.1267	*Sgo.1267::ermAM,* Tet^R, $Spec^R$, Erm^R	This study
Δsgo.1171	*Sgo.1171::ermAM,* Tet^R, $Spec^R$, Erm^R	This study
Δsgo.1177	*Sgo.1177::ermAM,* Tet^R, $Spec^R$, Erm^R	This study
Δsgo.1216	*Sgo.1216::ermAM,* Tet^R, $Spec^R$, Erm^R	This study

Strains	Relevant characteristics	Source
atlS$_{C1069S}$	SecCR1, *atlS* coding for the cysteine to serine mutation located on the chromosome and expressed from the native promoter, Tet^R, $Spec^R$, Erm^R	This study
ΔspxB	SecCR1, *spxB::aphA3,* Tet^R, $Spec^R$, Kan^R	This study
ΔsdbAΔspxB	*ΔsdbA, spxB::aphA3,* Tet^R, $Spec^R$, Kan^R, Erm^R	This study
ΔdegP	SecCR1, *degP::ermAM,* Tet^R, $Spec^R$, Erm^R	This study
DegP Compl	*ΔsdbAΔdegP*, *degP* complemented on chromosome and expressed from the native *degP* promoter, Tet^R, $Spec^R$, Kan^R, Erm^R	This study
degP$_{S235A}$	*ΔsdbA*, *degP* coding for the serine to alanine mutation located on the chromosome and expressed from the native *degP* promoter, Tet^R, $Spec^R$, Kan^R, Erm^R	This study
ΔciaRH	SecCR1, *ciaRH::aphA3,* Tet^R, $Spec^R$, Kan^R	This study
ΔsdbAΔciaRH	*ΔsdbA, ciaRH::aphA3,* Tet^R, $Spec^R$, Kan^R, Erm^R	This study
ΔsdbA CiaRH Compl	*ΔsdbAΔciaRH, ciaRH* complemented on chromosome, Tet^R, $Spec^R$, Erm^R, Cm^R	This study
S. gordonii Wicky WK1	Contains a spontaneous mutation in the β-subunit of RNA polymerase conferring resistance to rifampin	(216)
S. oralis 34	Indication strain for *S. gordonii* Sth bacteriocins	(188)
S. mitis I18	Indication strain for *S. gordonii* Sth bacteriocins	(188)
E. coli XL-1 Blue	Host for DNA manipulations and expression of recombinant proteins	Stratagene
E. coli BL21(DE3)	Host for DNA manipulations and expression of recombinant proteins	

Table 2.2 Primers

Primer	Gene	Direction	Description	RE*	Sequence (5'→3')
SL525	*16S*	Rev	RT PCR / qPCR		GAATTAAACCACATGCTCCACCGC
SL609	*ermAM*	For	Erythromycin resistance	EcoRV	TGAGATATCCCGGGCCCAAAATTTGTTTGAT
SL697	*16S*	For	RT PCR / qPCR		ATTTATTGGGCGTAAAGCGAGCGC
SL729	*ermAM*	Rev	Erythromycin resistance	BamHI	TACGGATCCAGCGACTCATAGAATTATTT
SL752	*degP*	For	DegP mutant/ sequencing		GTTGCTGGAACATGGGGAT
SL753	*degP*	Rev	DegP mutant	BamHI	TACGGATCCATTCCCTGAGTCACTGTATTAGC
SL754	*degP*	For	DegP mutant	EcoRV	TGAGATATCAGCCGTAATGTTTCTTCACGAT
SL755	*degP*	Rev	DegP mutant		TGTTTGCTCTTTTCCATCACG
SL756	*sdbA*	For	SdbA point mutants		ACCTGAACCAAATCGCAGAAT
SL757	*sdbA*	Rev	Knockout	EcoRV	TGAGATATCTCAAACTCTGGCAACTGCTG
SL758	*sdbA*	For	Knockout and complement	EcoRI	TACGAATTCGGTAGACCAAGCAGGGTATC
SL759	*sdbA*	Rev	SdbA point mutants		CGAACAACTGAAGTCCCCAG
SL762	*sdbA*	For	SdbA point mutants	BamHI	TACGGATCCTTAAAGGAAAAGTGGTGGCTAC
SL763	*sdbA*	Rev	Expression/ sequencing	HindIII	TACAAGCTTAAGCTCTCCCTTCTCTTTCTTT
SL764	*sdbA*	For	Expression/ sequencing	BamHI	TACGGATCCTCAGCTGTAGAACATGAGCTG
SL783	*nusG*	For	RT-PCR		AAGGCTGGTTTGTACTGCAG

Primer	Gene	Direction	Description	RE*	Sequence (5'→3')
SL784	*nusG*	Rev	RT-PCR		TCTGCAATGGTGTC ATTTCCA
SL785	*padA*	For	RT-PCR		GGCAACCCTATCAA AGATGC
SL786	*padA*	Rev	RT-PCR		AATCTTCGCAATGG CTTCTGC
SL801	*aphA3*	For	Kanamycin resistance	BamHI	TACGGATCC GCAAGGAACAGTGA ATTGGA
SL802	*aphA3*	Rev	Kanamycin resistance	EcoRI	TACGAATTCCAGTT GCGGATGTACTTCA G
SL803	*sdbA*	Rev	SdbA point mutants	BamHI	TACGGATCCAAGCT CTCCCTTCTCTTTCT T
SL822	*degP*	For	DegP point mutant/ complement	KpnI	TGAGGTACCAGCCG TAATGTTTCTTCACG AT
SL823	*aphA3*	Rev	Kanamycin resistance	KpnI	TACGGTACCCAGTT GCGGATGTACTTCA G
SL863	*sgo1267*	For	Knockout		ATGGATGAATTAGC CGAAAG
SL864	*sgo1267*	Rev	Knockout	SmaI	TTACCCGGGTGGCA ATAAGGACACCAG
SL865	*sgo1267*	For	Knockout	BamHI	TACGGATCCACAGT TACCGGAGATTCAA A
SL866	*sgo1267*	Rev	Knockout		GTCAACCAAGGATT GGAAAT
SL867	*sgo1171*	For	Knockout		CTCTGGCTTCAAGTT TTGTT
SL868	*sgo1171*	Rev	Knockout	EcoRV	TGAGATATCTACAT GGCCCACACCAAG
SL869	*sgo1171*	For	Knockout	BamHI	TACGGATCCGAAAG AAAGACCGCGATTT C
SL870	*sgo1171*	Rev	Knockout		ACAACTATCAAGCT ATGTACT
SL871	*sgo1177*	For	Knockout		GATGATATGAAGAC TCTTC
SL872	*sgo1177*	Rev	Knockout	EcoRV	TAAGATATCTTCCT GCTCCTTGGCCA

Primer	Gene	Direction	Description	RE*	Sequence (5'→3')
SL873	*sgo1177*	For	Knockout	BamHI	TACGGATCCTATCG GTTGTGTCTCCAAC G
SL874	*sgo1177*	Rev	Knockout		TGCATAGCCGGACT CAGC
SL885	*sgo1216*	For	Knockout		CAGCTATCTCTGTC GTAGA
SL886	*sgo1216*	Rev	Knockout	EcoRV	TGAGATATCTCAGC TACGACACCAGCT
SL887	*sgo1216*	For	Knockout	BamHI	TACGGATCCCAGTG AAGAAGCTAGTGAA
SL889	*sgo1216*	Rev	Knockout		CGCGTCGCCTATAA TTGGA
SL893	*atlS*	For	Point Mutation		GGGAGCTTTGATGT CGTCAT
SL896	*atls*	Rev	Point Mutation	BspEI	TACTCCGGATTCTC GTCCAACTAGA
SL897	*atlS*	For	Point Mutation	BspEI	GAATCCGGAGTAGA ACGTCATATTC
SL898	*atlS*	Rev	Point Mutation and Expression	EcoRV	TAGGATATCCCTAG AGCAACTTTCTTCA ACC
SL899	*atlS*	For	Point Mutation	BamHI	TAGGGATCCGCTTA CTTTCCTCGGCCTT
SL900	*sgo2012*	Rev	Point Mutation		GCCAACAAATACCA GGTCGG
SL901	*atlS*	For	Expression	BamHI	TACGGATCCGCTTA TATTAAAGACGTAA ATT
SL914	*spxB*	For	Pox mutants		GGGATTGAGCATCT CTGAGC
SL915	*spxB*	Rev	Pox mutants	EcoRV	TAGGATATCTTAGA AACCGCAGCACGG
SL916	*spxB*	For	Pox mutants	BamHI	TAGGGATCCAGGTC CAGCTGTTGTTGAA A
SL917	*spxB*	Rev	Pox mutants		ACGCCACCATGGAG TAGATT
SL927	*sthA*	For	RT PCR / qPCR		CCTCACCCTAACCG AAGATG
SL928	*sthA*	Rev	RT PCR / qPCR		AGCAATTCCTCCTG TGAAGC
SL931	*comC*	For	qPCR		AAACAAACAAAATC TATTGCCAAA

Primer	Gene	Direction	Description	RE*	Sequence (5'→3')
SL932	*comC*	Rev	qPCR		AAAGAATATATTTT CCCACCATAATC
SL974	*sdbA*	Rev	SdbA point mutants C86P		AGCTGGCCACCAGA TTGTCAAAAACAGT T
SL975	*sdbA*	For	SdbA point mutants C86P		TGGTGGCCAGCTAG CCCACTCTAC
SL991	*degP*	Rev	DegP point mutant		AGGACCACCAG**C**GT TACC
SL992	*degP*	For	DegP point mutant		GGTAAC**G**CTGGTGG TCCT
SL993	*degP*	Rev	DegP point mutant/ complement/ sequencing	BamHI	TACGGATCCTGTTG ACAGTCTTGTAAAT GG
SL1038	*sdbA*	For	SdbA point mutants C89A		CCAGATGCTCAAAA ACAGTTA
SL1039	*sdbA*	Rev	SdbA point mutants C89A		TAACTGTTTTTGAGC ATCTGG
SL1102	*sdbA*	For	SdbA point mutants C86A		GCTAGCTGGGCTCC AGAT
SL1103	*sdbA*	Rev	SdbA point mutants C86A		ATCTGGAGCCCAGC TAGC
SL1104	*sdbA*	For	SdbA point mutants C89P		TGTCCAGATCCTCA AAAACAGTTA
SL1105	*sdbA*	Rev	SdbA point mutants C89P		TAACTGTTTTTGAG GATCTGGACA
SL1178	*sgo1071*	For	CiaRH mutant / CiaRH complement / RT-PCR		AAAACGCTGCAAAA TAATCA
SL1179	*sgo1071*	Rev	CiaRH complement	HindIII	TACAAGCTTTCTCCT CCTGCTATAAGATA
SL1180	*ciaR*	For	CiaRH complement	KpnI	TACGGTACCTCCAT TTGTTAAAGTCATG AT
SL1212	*comE*	For	qPCR		GCGCAATTTATACG CCAAC
SL1213	*comE*	Rev	qPCR		TCGCAAATTCTGAA TGACTCG
SL1214	*degP*	For	qPCR		TGGGAATAAGGTTC CTGGTG
SL1215	*degP*	Rev	qPCR		CGGCAGGAATTCTG ACTACAG

Primer	Gene	Direction	Description	RE*	Sequence (5'→3')
SL1216	*ciaR*	For	qPCR		CATGCAGGTTTTTG ATGGTG
SL1217	*ciaR*	Rev	qPCR		TCAGGAAGCATCAG ATCCAG
SL1220	*sgo1074*	For	CiaRH mutant / RT-PCR	KpnI	TACGGTACCATGAA AATATTGATTTATG GTGCT
SL1221	*sgo1074*	Rev	CiaRH mutant / CiaRH complement/ RT-PCR		TTCAACCAATTCGC TAAATC
SL1222	*sgo1071*	Rev	CiaRH mutant	BamHI	TACGGATCCTCTCCT CCTGCTATAAGATA
SL1223	*sgo1071*	Rev	RT-PCR		GAATTGCTACCGTT TTCTTG

***restriction site**

Table 2.3 Peptide modifications identified by mass spectrometry						
Sample	**Protein coverage (%)**	**Score**	**Peptide sequence with cysteine**	**Modification**	**Score (XCorr)**	**Probability (PEP)**
$SdbA_{C86P}$ + glutathione	98.73	10253.29	SAEFYNKPMLVVEWA SWPPDCQK	glutathione	5.89	5.109 E-08
				unmodified	4.56	0.0004582
				sulfinylation	2.56	0.0006949
				sulfonylation	4.89	8.083 E-10
$SdbA_{C89A}$ + glutathione	98.73	11910.66	SAEFYNKPMLVVEWA SWCPDAQK	glutathione	6.66	0.0001792
				unmodified	5.76	0.000005799
				sulfinylation	1.87	0.009107
				sulfonylation	5.89	0.000002945
$SdbA_{C86P}$ + dimedone	60.43	2377.13	SAEFYNKPMLVVEWA SWPPDCQK	unmodified	4.97	0.00001442
				dimedone	4.90	5.795 E-07
				glutathione	5.31	0.03874
$SdbA_{C89A}$ + dimedone	58.29	2484.94	SAEFYNKPMLVVEWA SWCPDAQK	unmodified	3.79	0.07844
				dimedone	5.30	0.08786
				sulfinylation	3.57	0.05381
				glutathione	4.82	0.000186

Chapter 3: Functional Analysis Of Paralogous Thiol-Disulphide Oxidoreductases in *Streptococcus gordonii*

Davey L, Ng CKW, Halperin SA, Lee SF. 2013. Functional analysis of paralogous thiol-disulfide oxidoreductases in *Streptococcus gordonii*. J Biol Chem 288:16416–16429.

3.1 Summary

Disulfide bonds are important for the stability of many extracellular proteins, including bacterial virulence factors. Formation of these bonds is catalyzed by thiol-disulfide oxidoreductases (TDORs). Little is known about their formation in Gram-positive bacteria, particularly among facultative anaerobic Firmicutes such as streptococci. To investigate disulfide bond formation in *Streptococcus gordonii*, we identified five putative TDORs from the sequenced genome. Each of the putative TDOR genes was insertionally inactivated with an erythromycin resistance cassette and the mutants were analyzed for autolysis, extracellular DNA release, biofilm formation, bacteriocin production, and genetic competence. This analysis revealed a single TDOR, SdbA, which exhibited a pleiotropic mutant phenotype. Using an *in silico* analysis approach, we identified the major autolysin AtlS as a natural substrate of SdbA, and showed that SdbA is critical to the formation of a disulfide bond that is required for autolytic activity. Analysis by BLAST search revealed homologs to SdbA in other Gram-positive species. This study provides the first *in vivo* evidence of an oxidoreductase, SdbA, that affects multiple phenotypes in a Gram-positive bacterium. SdbA shows low sequence homology to previously identified oxidoreductases, suggesting that it may belong to a different class of enzymes. Our results demonstrate that SdbA is required for disulfide bond formation in *S. gordonii*, and indicate that this enzyme may represent a novel type of oxidoreductase in Gram-positive bacteria.

3.2 Introduction

Disulfide bonds are important for the folding and activity of many extracellular proteins, including bacterial virulence factors such as flagella, secretion systems, pili, and toxins (25). Although spontaneous disulfide bond formation can occur, the process is extremely slow, and most disulfide bonds formed *in vivo* are catalyzed by thiol-disulfide oxidoreductases (TDORs) (232).

The *Escherichia coli* Dsb pathway is the paradigm for disulfide bond formation. In this system, the periplasmic oxidase DsbA forms disulfide bonds in substrate proteins as they are translocated from the reducing environment of the cytoplasm. DsbA contains a catalytic disulfide bond with a Cys-X-X-Cys motif that forms a mixed disulfide intermediate with its substrates, which once resolved, leaves DsbA in a reduced state. Its redox partner DsbB then reoxidizes DsbA back to its active state allowing the cycle to continue (44, 232). DsbA has a broad substrate specificity, with an estimated 300 substrates in *E. coli* (232), and homologs of DsbA appear to be widely distributed among Gram-negative bacteria (24, 25). Additional components of the pathway include a disulfide isomerase, DsbC, and its redox partner DsbD (71, 80), as well as a reductase, DsbE (CcmG), that also partners with DsbD and functions to reduce the cysteines in apo-cytochrome *c* to enable heme to bind (80, 233).

In contrast, little is known about disulfide bond formation in Gram-positive bacteria, which are predicted to have a lower prevalence of disulfide bonded proteins (24, 96). Although Gram-positive DsbA homologs have been identified, few have demonstrated functions, and those that do appear to perform specialized functions in the cell. For example, substrates of the DsbAB homologs in *Bacillus subtilis,* BdbDC, are limited to proteins required for genetic competence, such as the ComGC pseudopilus and ComEC channel protein (117, 123). In *Staphylococcus aureus,* SaDsbA has also been shown to be required for the stable production of ComGC (134), however, no other substrates or phenotypes have been identified despite detailed functional and structural characterization (133, 234). Similarly, the biological function of the *Bacillus brevis* DsbA homolog, Bdb, has not been determined (120).

Emerging evidence suggests that Gram-positive Actinobacteria may use different types of TDORs, with low homology to *E. coli* DsbA, to form disulfide bonds (96, 99, 108). Novel oxidases identified in these species include *Mycobacterium tuberculosis* DsbE and DsbF (99, 108), which show greater homology to *E. coli* reductases than to DsbA, and a TDOR from *Corynebacterium glutamicum*, CG.0026, which is predicted to be widespread among Actinobacteria (96). *In vitro* analyses have confirmed that these enzymes function as oxidases, although no *in vivo* functions or phenotypes have been identified (96, 99, 108).

Bioinformatic screens for TDORs among diverse groups of bacteria have noted that many anaerobic Firmicutes, including streptococci and clostridia, lack homologs to *E. coli* DsbA and DsbB (24, 25, 96). It has been proposed that these bacteria do not engage in disulfide bond formation; however, there are important examples of disulfide bonded proteins produced by these species, including secreted toxins that contribute to virulence (169, 235). Moreover, our laboratory has previously reported the construction of recombinant strain of *Streptococcus gordonii* SecCR1 that secretes a functional single chain variable fragment antibody against complement receptor one (204), a protein known to require two disulfide bonds for stable folding (236). This suggests the possibility that anaerobic Firmicute bacteria also possess unique TDORs that have not been identified.

To gain a better understanding of disulfide bond formation in Gram-positive species, we investigated TDORs using *Streptococcus gordonii* as a model organism. *S. gordonii* is a commensal inhabitant of the human oral cavity. As an adaptation to the fluctuating environment of oral cavity, *S. gordonii* exhibits biofilm formation, extracellular DNA (eDNA) release, autolysis, bacteriocin production, and natural genetic competence. Regulation of these phenotypes is interconnected, and conditions at the cell envelope are closely monitored by multiple two-component systems (188, 201, 202, 237). These diverse and testable phenotypes exhibited by *S. gordonii* create a sensitive system to potentially detect disulfide bond formation.

Here we report a functional analysis of five putative TDORs in *S. gordonii*, and the discovery of a single enzyme that affects multiple phenotypes, that we propose to call SdbA (*Streptococcus* disulfide bond protein A). An *in silico* screening approach to identify potential natural substrates of SdbA identified 36 candidate proteins. One potential substrate was selected for additional analysis, the autolysin AtlS. We demonstrate that AtlS requires SdbA for the formation of an intramolecular disulfide bond between residues C1048 and C1069, and that this bond is essential for processing and enzymatic activity. In addition, sequence analysis revealed homologs of SdbA in a range of other Gram-positive species predicted to lack enzymes with homology to DsbA or SaDsbA, indicating that SdbA may belong to a novel class of TDORs specific to certain Gram-positive bacteria. To our knowledge, this report provides the first *in vivo* evidence of a Gram-positive TDOR that affects multiple cellular processes.

3.3 Results

Identification of Putative TDORs in *S. gordonii*

We hypothesized that previous screens failed to identify TDORs in some Firmicutes because these species use different enzymes, with low homology to DsbA, which could be missed due to overly stringent search criteria. Therefore, we conducted a BLASTP search in *S. gordonii* using *Bacillus subtilis* 168 BdbC and BdbD as a query, looking for proteins with even very low homology.

Although there were no hits to BdbC, a homolog of *E. coli* DsbB (117), the search identified a thioredoxin signature protein with limited homology to BdbD called Sgo.2006 (*e* value of 0.14). A search for additional TDORs, similar to Sgo.2006, identified three uncharacterized thioredoxin family proteins: Sgo.1267, Sgo.1171, and Sgo.1177. The proteins ranged in size from 160 to 187 amino acids, and all were predicted to belong to the TlpA/DsbE/ResA family. We also chose to investigate a fifth protein, Sgo.1216, annotated as a bacteriocin transport accessory protein (Bta), based on its similarity to *Streptococcus thermophilus* LMD-9 $BlpG_{(ST)}$ (BLASTP *e* value of 10^{-8}, 13.2% identity and

23% similarity), a thiol-disulfide oxidase dedicated to disulfide bond formation in the bacteriocin thermophilin-9 (154).

A multiple sequence alignment showed that each of the sequences contained a Cys-X-X-Cys motif, where X indicates any amino acid, characteristic of the active site of TDOR enzymes. The proteins also contained a conserved proline residue located away from the active site, close to the C-terminus (Fig. 3.1). This proline is a common feature of thioredoxin family proteins, which has several reported functions, including prevention of metal binding to the active site cysteines (15) and substrate release (14). Although each of the *S. gordonii* TDORs had similar sequences, only Sgo.2006 and Sgo.1177 were predicted to encode signal peptides (SignalP), and Sgo.1177 was predicted to be a lipoprotein (LipoP).

Based on our findings described below, we named Sgo.2006 *Streptococcus* disulfide bond protein A (SdbA).

SdbA Affects Multiple Biological Processes

To analyze the functions of the predicted TDORs in *S. gordonii*, we constructed mutants in each of the genes by insertional inactivation. A common first line approach to screen TDOR mutants is to test for sensitivity to reducing agents; however, this technique has had limited success in *Bacillus*, possibly due to its intrinsic resistance to oxidative stress (96). Similarly, our mutants did not show increased sensitivity to growth with DTT compared to the parent strain, which grew in the presence of 200 mM DTT (data not shown). In contrast, growth of *E. coli* DsbA mutants and wild-type strains is inhibited at 7 and 20 mM concentrations, respectively (238). As an alternative approach to detect disulfide bond formation, our phenotypic analysis of the mutants focused on traits required for the survival and persistence of *S. gordonii* in oral biofilms.

Biofilm formation was assessed in microtiter plates under aerobic conditions. Although four of the mutants formed similar amounts of biofilm as the parent, one mutant, *ΔsdbA*, showed significantly enhanced biofilm formation (Fig. 3.2A). Analysis by

scanning electron microscopy revealed that the *sdbA* mutant formed thick, multilayered biofilms, in contrast to the monolayer biofilms produced by the parent strain (Fig. 3.2B). Because *S. gordonii* forms thicker biofilms under anaerobic conditions (202) we also tested anaerobic biofilm formation to determine if the enhanced biofilm phenotype of the *ΔsdbA* mutant was related to an inability to sense oxygen in the environment. When biofilms were grown under anaerobic conditions, the parent showed higher levels of biofilm formation as expected, and the *ΔsdbA* mutant also showed a proportionate increase in adhesion, indicating that the enhanced biofilm phenotype is not a result of the atmospheric growth conditions.

An important component of the biofilm matrix is extracellular DNA (eDNA), which contributes to cell-cell adhesion and exchange of genetic material (201, 239, 240). We tested eDNA release by the TDOR mutants to determine if this contributed to the enhanced biofilm phenotype of the *ΔsdbA* mutant, and whether the other TDOR mutants showed changes in eDNA release. Surprisingly, high molecular weight eDNA could be extracted from the medium of stationary phase cultures for all of the mutants except for *sdbA* (Fig. 3.2C). The result suggests that SdbA plays an essential role in eDNA release, and the enhanced biofilm phenotype is a result of additional factors that have been altered in the absence of SdbA.

Next, the mutants were tested for autolysis, which has been reported to be required for both eDNA release and biofilm formation in streptococci (199, 201). Consistent with the absence of eDNA, the autolysis assay showed that the *ΔsdbA* mutant lacked autolytic activity, remaining at 88% of the initial optical density. Two additional mutants, *sgo.1267* and *sgo.1216*, also showed moderate defects in autolysis compared to the parent, which lysed rapidly under the test conditions (Fig. 3.2D).

Given the annotation of Sgo.1216 (Bta) as a bacteriocin transport accessory protein, we sought to test bacteriocin production by the mutants. *S. gordonii* produces two bacteriocins, streptocins Sth_1 and Sth_2 (188); however, these proteins lack cysteines and the role of Sgo.1216 in their production, if any, is unknown. Growth inhibition of the target

strain *S. oralis* 34 was used to test activity of Sth_1. Interestingly, only *ΔsdbA*, and not *sgo.1216* or the other TDOR mutants, showed a defect in bacteriocin activity (Fig. 3.2E). The *sdbA* mutant also lacked Sth_2 activity, as determined by testing inhibition of *S. mitis* I18 as the target strain. This indicates that SdbA is required for either processing or production of both Sth_1 and Sth_2 bacteriocins. Since bacteriocin activity coincides with development of genetic competence, and both are controlled under the ComDE regulon, we tested the transformation frequency of the *ΔsdbA* mutant (188). The *ΔsdbA* mutant showed a dramatic defect in transformation frequency compared to the parent strain (Table 3.1). This suggests that a component of the ComDE regulon may be a natural substrate of SdbA.

In each of the assays, a single mutant, *ΔsdbA*, showed striking differences from the parent strain. The *ΔsdbA* mutant clumped when grown in liquid cultures (Fig. 3.3A) and SDS-PAGE analysis of SDS extracted surface proteins showed that the protein profile of the mutant had diminished intensity compared to the parent (Fig. 3.3B). These results suggest that inactivation of *ΔsdbA* resulted in dramatic changes to the cell surface. A complemented mutant was constructed by introducing a functional *ΔsdbA* gene back onto the chromosome (Fig. 3.3C), which reversed the phenotypes observed in the mutant (Figs. 3.2A-E, 3.3A-B, 3.4A, Table 3.1), and RT-PCR analysis of genes immediately upstream and downstream of *ΔsdbA* confirmed that the mutation was non-polar (Fig. 3.3D). Based on these results, we selected the *ΔsdbA* mutant for additional characterization.

SdbA is Required for Production of the Disulfide Bonded Protein, Anti-CR1 scFv

S. gordonii SecCR1 secretes a functional single chain variable fragment antibody (scFv) against complement receptor 1 (CR1) fused to the signal peptide of *Streptococcus mutans* SpaP (204). Single chain antibodies contain two intramolecular disulfide bonds, one in each of the V_H and V_L domains, and disruption of these bonds prevents stable folding, resulting in aggregation and proteolysis (205). Since correct disulfide bonding is well established as a critical factor in single chain antibody production, anti-CR1 scFv levels were assessed as an indication of the cells' capacity for production of disulfide bonded proteins. Western blots revealed that SdbA is essential to anti-CR1 scFv

production because no protein was detected in the mutant, while complementation restored production to levels similar to the parent (Fig. 3.4A). The other TDOR mutants produced anti-CR1 scFv at similar levels as the parent.

The absence of anti-CR1 scFv production in the *ΔsdbA* mutant indicates a possible role for SdbA in either the formation or isomerization of disulfide bonds necessary to stabilize the protein and prevent degradation. However, an alternative explanation could be that SdbA contributes to the function of the general secretory pathway. To distinguish between these two scenarios, we tested the production of a foreign protein without disulfide bonds. An *ΔsdbA* mutant was generated in *S. gordonii* RJM4, a recombinant strain of *S. gordonii* DL-1 that secretes a fusion protein between SpaP and the N-terminal 179-amino acid fragment of the S1 subunit of pertussis toxin without disulfide bonds (231). Western blots showed that both the parent and the *ΔsdbA* mutant produced similar levels of the SpaP-S1 protein (Fig. 3.4B). These findings indicate that the defect in anti-CR1 scFv production in the *ΔsdbA* mutant is specific to the production of disulfide-bonded proteins, rather than a general defect in secretion.

Next, the oxidase activity of recombinant SdbA was tested *in vitro* using the RNase A folding assay. His_6-tagged SdbA lacking the N-terminus signal sequence and transmembrane domain was expressed in *E. coli* and purified by affinity chromatography (Fig. 3.5A). SdbA was incubated with reduced RNase A and the oxidative folding of RNase A to its active conformation was monitored by cCMP hydrolysis. SdbA successfully catalyzed the correct folding of reduced, denatured RNase A, although the enzyme was slightly less active than *E. coli* DsbA, which served as a positive control (Fig. 3.5B). Taken together, these results indicate that SdbA is an oxidoreductase, which is directly involved in the production of disulfide-bonded proteins in *S. gordonii*.

AtlS is a Natural Substrate of SdbA

The role of SdbA in the production of anti-CR1 scFv suggests that the multiple phenotypes observed in the *ΔsdbA* mutant may be the result of impaired disulfide bond formation. To support this hypothesis, we sought to identify natural substrates of SdbA.

Since there are no known disulfide-bonded proteins in *S. gordonii*, we used a computational approach to screen for candidate substrates. This identified 36 secreted proteins with two or more cysteines that may form disulfide bonds (Table 3.2), representing approximately 10% of the secreted proteins in *S. gordonii*.

Among the predicted substrates was the autolysin AtlS, an 1160 amino acid protein with an N terminal glycosyl hydrolase family 25 (GH25) catalytic domain and two C-terminal cysteines at residues C1048 and C1069. Notably, AtlS was recently demonstrated to be crucial for autolysis in *S. gordonii* (201). Given the lack of autolytic activity in the *ΔsdbA* mutant (Fig. 3.2D), we hypothesized that SdbA is required for the formation of a disulfide bond in AtlS, and that this bond contributes to proper folding into a functional conformation.

Using a zymogram to test autolytic activity of SDS-extracted surface proteins, we found that activity of AtlS from the *ΔsdbA* mutant was dramatically reduced compared to the parent and complemented mutant, which produced distinct bands of clearing at approximately 130 and 90 kDa (Fig. 3.6A). This banding pattern is consistent with previous reports showing that autolysins appear as doublets with full length and processed forms (200, 201) and Western blots confirmed that these bands corresponded to AtlS (Fig. 3.6B). In comparison, only the 130 kDa band was detected in extracts from the *ΔsdbA* mutant (Fig. 3.6B). This suggested that SdbA plays a part in the processing and activity of AtlS, possibly via the formation of a disulfide bond in the C-terminal cysteines.

To determine the *in vivo* disulfide status of AtlS in the parent and *ΔsdbA* mutant, we carried out cysteine alkylation experiments with maleimide-PEG_2-biotin. In this reaction, the maleimide moiety forms a thioether bond with free cysteine thiols, resulting in a biotinylated protein that can be detected with avidin-AP (alkaline phosphatase); whereas disulfide bonded cysteines are blocked from reaction. Bands detected with avidin-AP that corresponded to AtlS were identified based on molecular weight. To ensure that the bands aligned, control experiments were carried out by cutting individual lanes of Western blots in half and reacting with either avidin-AP or anti-AtlS.

Alkylated protein extracts from the same sample were run on Western blots and reacted with either avidin-AP to detect biotinylated proteins or anti-AtlS to determine the total amount of AtlS in the sample, thus serving as a loading control. The results for the parent strain showed a weak band detected by avidin-AP at the same molecular weight as the full length AtlS. However, when samples were reduced with DTT prior to alkylation, there was a marked increase in the intensity of this band, indicating the presence of a disulfide bond (Fig. 3.7A). No reaction was observed in the 90 kDa band, presumably because processing had removed the C-terminal cysteine residues. This is a logical explanation given that the active site of AtlS is located at the N-terminus, and processing at the C-terminus resulting in a reduction in molecular weight from 130 kDa to 90 kDa would entail removal of approximately 360 amino acids, including both cysteine residues. In contrast, cysteines in AtlS from the *ΔsdbA* mutant were efficiently alkylated both with and without DTT treatment, showing that the protein lacked a disulfide bond (Fig. 3.7A).

Our analyses suggested that a portion of AtlS produced in the parent contained a disulfide bond, while the *ΔsdbA* mutant lacked disulfide bonds entirely. To confirm these results, and eliminate background from unbonded thiols, we used a differential thiol-trapping approach (219). Surface protein extracts containing AtlS were reacted with iodoacetamide to block free thiol groups, while cysteine residues already disulfide bonded are protected from reaction. Following the removal of excess iodoacetamide, disulfide bonds were reduced with DTT and the newly generated thiol groups were subsequently alkylated with maleimide-PEG_2-biotin. The results indicated that AtlS generated in the parent contains an intact disulfide bond, because biotinylated proteins were only detected in the sample reduced with DTT (Fig. 3.7B). In contrast, treatment with iodoacetamide efficiently blocked biotinylation of AtlS from the *ΔsdbA* mutant, and reduction with DTT did not generate free thiol groups (Fig. 3.7B). Densitometry analysis indicated that approximately 30% of the 130 kDa AtlS in the parent strain contained a disulfide bond, in contrast to none in the *ΔsdbA* mutant (Fig. 3.7C).

To substantiate the importance of this disulfide bond for AtlS function, we constructed a C1069S point mutation in *atlS* in the parent strain. Importantly, AtlS is not

predicted to contain NlpC/p60 or cysteine, histidine-dependent amidohydrolases/peptidases (CHAP) domains, and it is unlikely that the point mutation eliminated a catalytic cysteine (241).

Similar to the *ΔsdbA* mutant, the C1069S mutation resulted in a loss of autolytic activity (Fig. 3.6C), and zymogram analysis confirmed that AtlS was inactive (Fig. 3.6A). Western blots showed that the C1069S mutant produced three immunoreactive bands, two bands at the same molecular weight as the parent, 130 and 90 kDa, in addition to a strong band at ~85 kDa (Fig. 3.6B). Considering the importance of disulfide bonds to tertiary structure, a plausible explanation for this altered banding pattern is that the disulfide bond in AltS contributes to the native conformation needed for processing, and mutations in this region result in altered processing. This is consistent with our alkylation data, which suggests that processing of AtlS occurs at the C-terminus. Taken together, the results suggest that AtlS fails to acquire a disulfide bond in the *ΔsdbA* mutant, which results in misfolding and a subsequent loss of enzymatic activity.

Homologs of SdbA are Present in Other Gram-Positive Bacteria

Our results demonstrate that disulfide bond formation plays a more important role in *S. gordonii* physiology than previously recognized, and we wondered if this phenomenon extended to other Gram-positive species as well. Unlike the Actinobacteria and aerobic Firmicutes, the majority of facultatively anaerobic and anaerobic Firmicutes are not predicted to form disulfide bonds or to encode DsbA-like proteins (24, 25). Remarkably, a search for SdbA homologs identified similar proteins in a range of other species, including important pathogens such as *Clostridium tetanii* and *Streptococcus pneumoniae* (Fig. 3.8A). The top hit in *Mycobacterium tuberculosis* H37Rv corresponded to Mtb DsbF (22.6% identity/ 37.9% similarity), which has been confirmed to function as an oxidase (99). Analysis with SignalP predicted that all of the SdbA homologs contain a signal peptide. In addition to the CXXC active site and conserved proline residue, the sequences also shared a conserved sequence immediately N-terminus to the CXXC active site with a consensus sequence of WAXW (Fig. 3.8B). Similar motifs have been observed in thioredoxin-like proteins (229), although the functional significance is unknown.

3.4 Discussion

Disulfide bond formation in Gram-positive bacteria is a poorly understood process and investigations have been hindered by a lack of mutant phenotypes and known substrates. Gram-positive bacteria produce fewer disulfide bonded proteins than Gram-negative species (96), and in some cases use covalent amide bonds as an alternative to disulfide bond formation (242–244). Nevertheless, there are examples of disulfide bond containing proteins produced by Gram-positive species, such as diphtheria and tetanus toxins, botulinum neurotoxin A, and streptococcal pyrogenic exotoxin (29, 169, 235). In Gram-negative pathogens, DsbA forms disulfide bonds in secreted toxins, but the machinery that forms these bonds in Gram-positive species has not been identified (114, 245).

Among the few TDORs that have been identified in Gram-positive species, there are several examples of systems dedicated to bacteriocin production, including *B. subtilis* 168 BdbAB, *S. thermophilus* LMD $BlpG_{(ST)}$, and *Streptococcus bovis* HJ50 Sdb1 (125, 154, 156). Despite the annotation as a bacteriocin transport accessory protein, Sgo.1216 did not affect bacteriocin production, and the function of this protein remains unknown. However, it is possible that Sgo.1216 affects production or activity of an unidentified bacteriocin, which inhibits different strains of bacteria from the ones used in our assays. Regardless, these types of TDORs likely perform specialized functions within the cell, although not necessarily related to bacteriocin production.

Two of the predicted TDORs, Sgo.1177 and Sgo.1171, did not exhibit any phenotypes in our assays, but share a high level of homology with a recently reported TlpA protein from *S. pneumoniae* (BLASTP *e* values of 10^{-65} and 10^{-43}, respectively). *S. pneumoniae* TlpA is proposed to work in conjunction with MsrAB and CcdA to reduce oxidized methionines, and Sgo.1177 and Sgo.1171 may have the same function in *S. gordonii* (246). Notably, Sgo.1177 is located immediately upstream of a protein annotated as a methionine sulfoxide reductase (Sgo.1176). Overall, it appears that most of the TDORs investigated here either perform specialized functions in the cell or exhibit

functional redundancy that would require multiple mutations to produce observable phenotypes.

In contrast, SdbA displayed a pleiotropic mutant phenotype, indicative of an important biological function, and possibly broad substrate specificity. SdbA was essential for the production of anti-CR1 scFv, a protein that requires two disulfide bonds for stable folding. This suggests that SdbA directly contributes to disulfide bond formation, and *in vitro* analysis confirmed that SdbA exhibits oxidase activity.

Our results suggest that the autolysin AtlS is a natural substrate of SdbA, and that SdbA contributes to the formation of an intramolecular disulfide bond in AtlS that is required for processing and activity. Consistent with this finding, previous reports of mutations that inhibit processing of the *S. mutans* autolysin, AtlA, also resulted in a loss of autolytic activity (214, 216). Inactivation of AtlS likely contributed directly to several of the phenotypes observed in the mutant, including impaired autolysis and eDNA release (201). However, not all of the *ΔsdbA* mutant phenotypes can be attributed solely to inactivation of AtlS. For example, eDNA release in *S. gordonii* has also been reported to occur without cell lysis, via unknown mechanisms, which appear to be affected by SdbA as well (195, 239). In addition, *atlS* mutants are unable to form biofilms, whereas the *ΔsdbA* mutant showed increased biofilm formation, a discrepancy that likely reflects the impact SdbA on several substrates.

The enhanced biofilm formation by the *ΔsdbA* mutant was unexpected, since it lacked autolytic activity and eDNA, two factors that were previously found to be required for biofilm formation in *S. gordonii* (201). eDNA contributes to surface adhesion and is an important component of the oral biofilm matrix (196). Nevertheless, we found that eDNA was not required the *ΔsdbA* mutant to form biofilms, and DNase treatment had no effect of biofilm stability (data not shown). Although the mechanisms involved are unclear, the increase in biofilm formation might be the result of upregulated surface adhesins, polysaccharide production, or due to general changes in cell surface properties such as charge or hydrophobicity (196). Similar factors might also contribute to the

clumping observed in *ΔsdbA* cultures grown in liquid medium. Further investigation will be required to understand biofilm formation in the *ΔsdbA* mutant.

In addition to substrate proteins directly affected in the *sdbA* mutant, the observed phenotypes may also be the result of indirect effects as well. Since certain adhesins in *S. gordonii* can transcriptionally regulate the levels of others, it is plausible that inactivation of a single SdbA substrate could influence expression of multiple surface proteins (247). This situation is exemplified by a previous report that inactivation of the *S. gordonii* surface antigens SspA and SspB resulted in up-regulation of other surface proteins and a 20% increase biofilm formation (247). Moreover, the lack of competence and bacteriocin activity in the *sdbA* mutant strongly suggests an effect on the ComDE two component system, which in turn could affect all of the genes in the regulon (188). We are currently investigating the relationship between SdbA and the ComDE system.

Along with AtlS, we identified 35 candidate SdbA substrates including surface adhesins, cell wall-binding proteins, transporter proteins and hypothetical proteins. It should be noted that some of these proteins contain catalytic cysteines unlikely to be involved in disulfide bond formation, such as Sgo.2107, a CHAP domain protein, and Sgo.1176, a methionine sulfoxide reductase (241, 248). However, given the ability of *S. gordonii* to produce hydrogen peroxide, it is plausible that the majority of these proteins would form disulfide bonds since single cysteines are vulnerable to irreversible oxidation (195).

SdbA has the highest homology to the TlpA/DsbE/ResA family of proteins, a diverse group of redox active proteins that includes *E. coli* CcmG, a reductase that reduces apo-cytochrome *c* (233), as well as *M. tuberculosis* oxidases, DsbE and DsbF, capable of catalyzing disulfide bonds (99, 108). The results presented here show that SdbA is crucial for disulfide bond formation; however, additional biochemical analysis is required to determine the role SdbA plays in this process. While SdbA exhibits oxidase activity *in vitro*, suggesting that it may catalyze disulfide bond formation *in vivo*, it could also contribute to protein stability through disulfide isomerase activity to ensure correct

disulfide connectivity. We are currently investigating the enzymatic activity of SdbA to address these questions.

SdbA homologs are distributed among a range of Gram-positive species, most of which are anaerobic Firmicutes that lack homologs to DsbA. This suggests that SdbA may belong to a novel class of TDOR that has gone undetected due to its lack of homology with DsbA. SdbA and its homologs are similar to DsbA and BdbD in having a CXXC catalytic domain and a conserved C-terminal proline residue, but distinct from DsbA/BdbD in having a WAXW motif immediately next to the CXXC motif. SdbA is also distinct from the Actinobacteria DsbA recently described by Daniels *et al*. (96), and we did not find homologs to this protein in *S. gordonii*, or in other species with SdbA homologs. Thus, these enzymes may represent alternative strategies for disulfide bond formation, and SdbA may be favoured by anaerobic species. Like *S. gordonii*, some species were found to encode more than one SdbA-like protein. Our analysis of TDORs in *S. gordonii* shows that these types of proteins may have similar sequences, but very different effects on the cell, and experimental investigation is essential to determining the physiological roles of predicted TDORs.

In conclusion, our results show that SdbA plays an important role in disulfide bond formation and that inactivation of SdbA results in a pleiotropic phenotype. In contrast to previously described Gram-positive TDORs, many of which have no substrates or phenotypes associated with them, SdbA is unique in affecting multiple biological processes. This suggests that SdbA represents a novel class of thiol-disulfide oxidoreductase, and a possible functional equivalent to *E. coli* DsbA, specific to certain Gram-positive bacteria.

Acknowledgments

We thank J. Rohde (Dalhousie University) for critically reading the manuscript, G. Tompkins (University of Otago) for providing us with *S. oralis* 34 and *S. mitis* I18, M. Vickerman (University at Buffalo) for *S. gordonii* Wicky WK1, and R. Glockshuber for pDsbActy (ETH Zurich, Institute of Molecular Biology and Biophysics). Funding for this

study was provided by the Natural Sciences and Engineering Research Council of Canada (NSERC). LD is a recipient of a NSERC post-graduate scholarship and an IWK graduate scholarship. CN is a recipient of a NSERC undergraduate student research award.

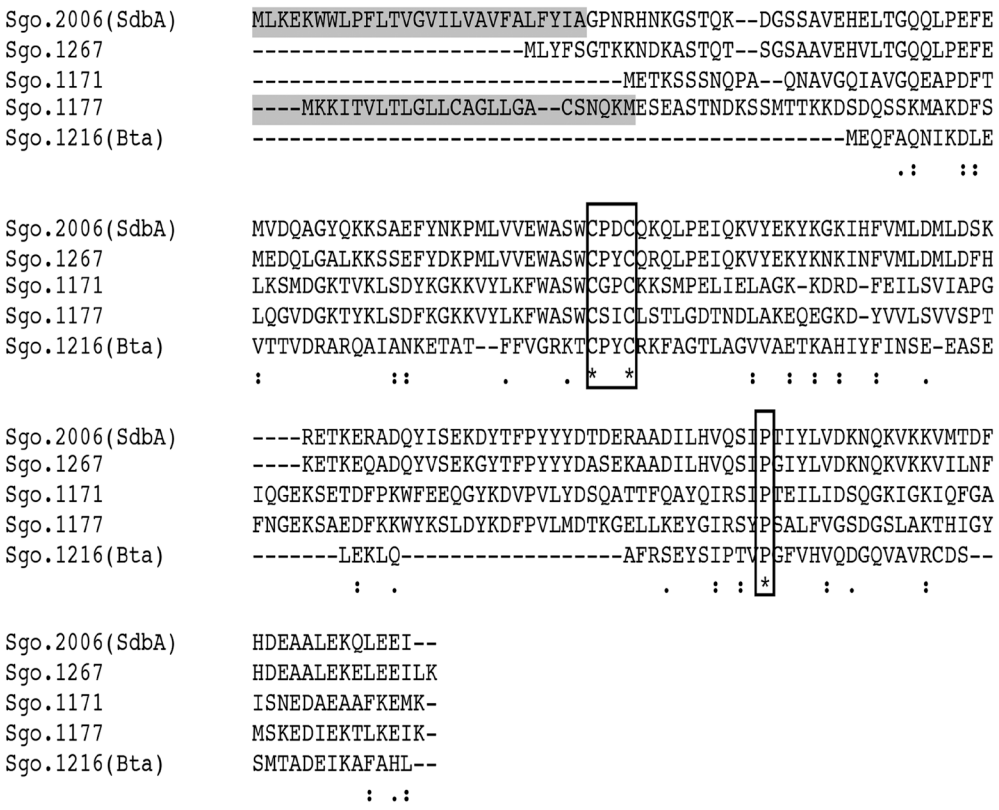

Figure 3. 1 *S. gordonii* TDORs

Putative TDORs identified in *S. gorodnii* by BLASTP search and analysis of the Oralgen database. Sequences were downloaded from NCBI and aligned with Clustal Omega (249). The predicted signal sequences of Sgo.2006 (SdbA) and Sgo.1177 are highlighted (SignalP). Boxes indicate the location of the CXXC active site and conserved *cis*-proline residue characteristic of TDORs.

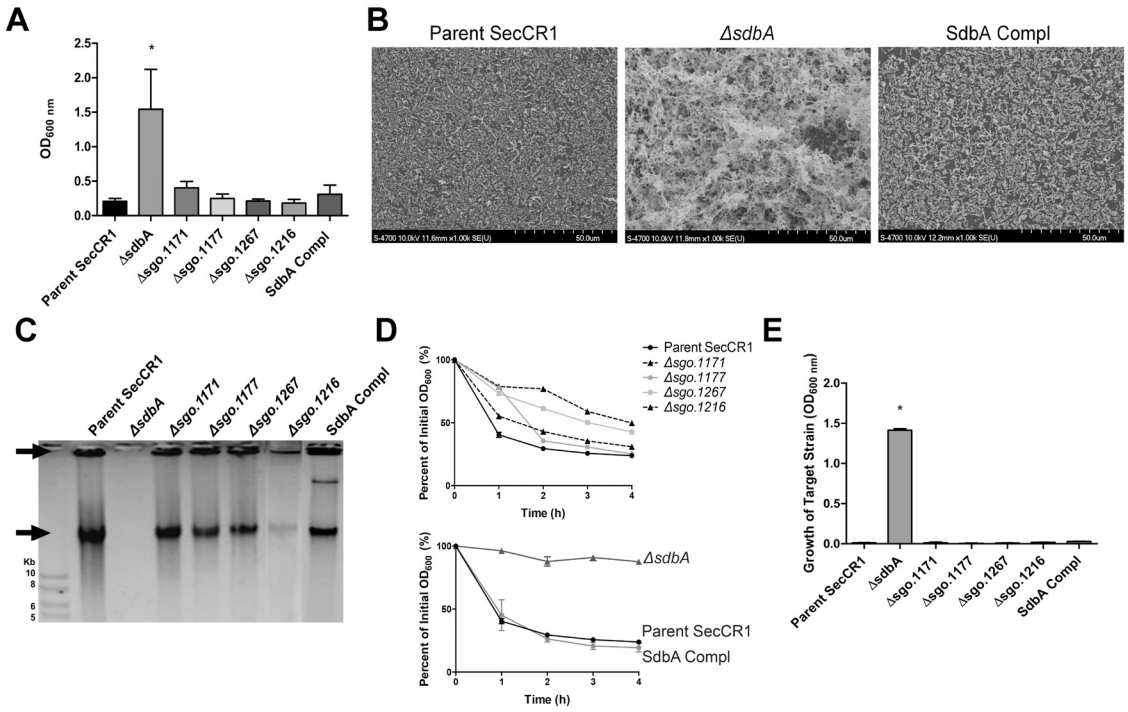

Figure 3. 2 SdbA affects multiple phenotypes

(A) Crystal violet staining of biofilms grown in 24-well microtiter plates. Error bars show standard deviation of triplicates. (B) SEM images of biofilms produced by the parent SecCR1, *sdbA* mutant (*ΔsdbA*), and *sdbA* - complemented mutant (SdbA Compl). (C) Extracellular DNA precipitated from culture supernatants separated on an agarose gel and stained with ethidium bromide. Arrows indicates high molecular weight eDNA. (D) Autolysis of the parent SecCR1 strain and TDOR mutants. Upper panel: Autolysis of TDOR mutants *Δsgo.1171, Δsgo.1177, Δsgo.1267, Δsgo.1216*. Lower panel: Autolysis of the *sdbA* mutant and *sdbA* complemented mutant. (E) Sth_1 bacteriocin activity displayed by the parent SecCR1, TDOR mutants, and *sdbA* complemented mutant. Error bars show standard deviation of triplicates. Asterisks indicate at statistically significant difference ($P < 0.001$, One-way ANOVA).

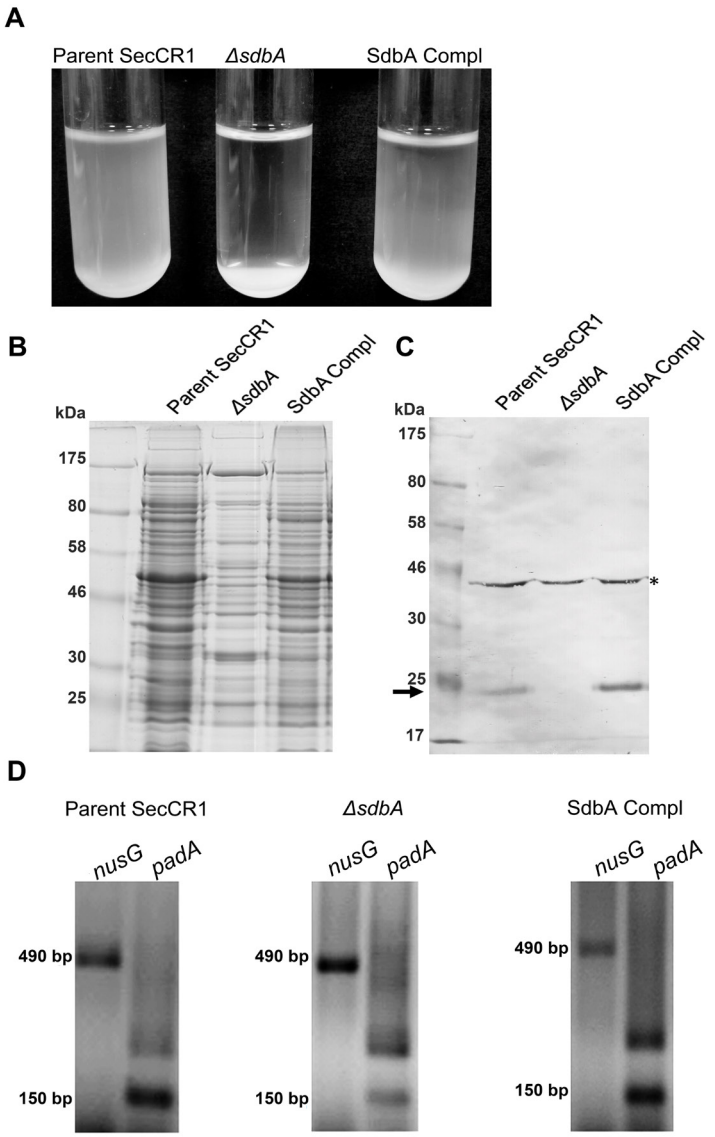

Figure 3. 3 Inactivation of SdbA results in changes to the cell surface

(A) Overnight cultures showing the *sdbA* mutant forms clumps and sediments to the bottom of the tube. (B) SDS-PAGE analysis of SDS-extracted surface proteins stained by Coomassie blue. (C) Western blots of SdbA. The arrow indicates the 21 kDa band corresponding to SdbA. The asterisk indicates a ~40 kDa cross-reactive band to the anti-SdbA antisera. (D) RT-PCR analysis of the genes upstream and downstream from *sdbA*, *nusG* (490 bp) and *padA* (150 bp), respectively.

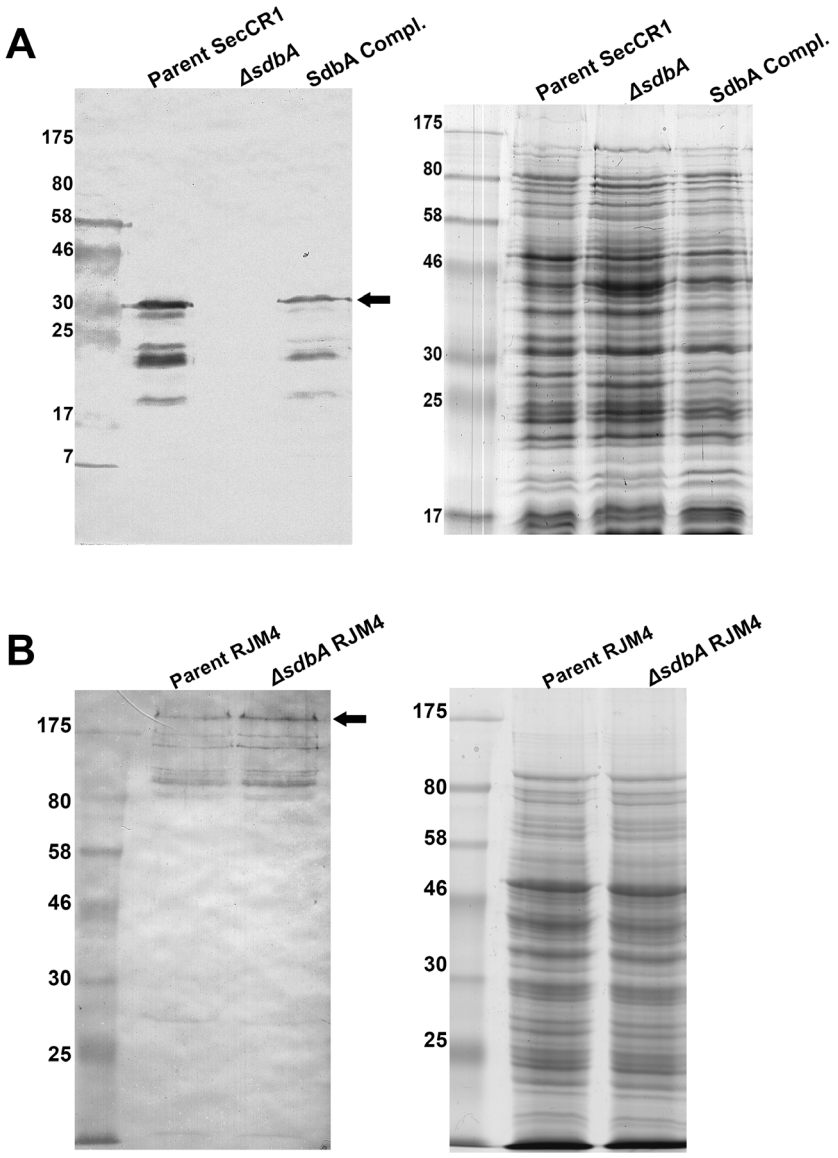

Figure 3. 4 SdbA contributes to the production of a disulfide bonded protein

(A) Production of the 33 kDa anti-CR1 scFv (arrow) was detected by Western blotting using the anti-HA antibody as the probe (left). SDS-PAGE of the same samples used in the Western showing equal loading (right). Lower molecular weight bands recognized by anti-HA represent break down products of anti-CR1 scFv. (B) Western blot to detect 187 kDa SpaP/S1 (arrow) with anti-S1 monoclonal antibody (left). SDS-PAGE for equal loading (right).

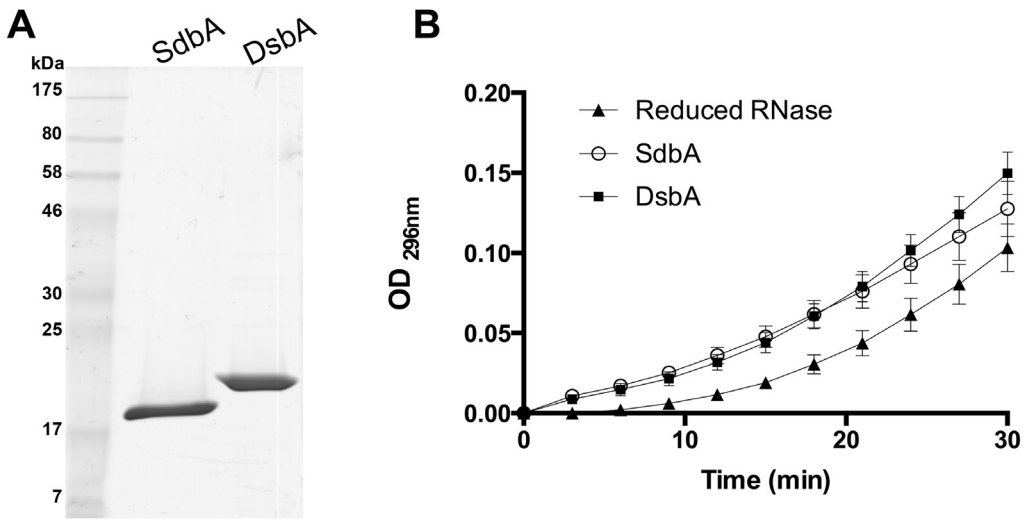

Figure 3. 5 SdbA exhibits oxidase activity

(A) SDS-PAGE of recombinant SdbA and DsbA isolated from *E. coli*. (B) Oxidative folding of reduced, denatured RNase A by the recombinant SdbA and DsbA. SdbA (10 μM) was incubated with reduced RNase A (10 μM) at 22°C and the cleavage of cCMP was monitored at 296 nm. *E. coli* DsbA (10 μM) was used as a positive control and reduced RNase A without added enzyme was used as a negative control. Data show the average from four experiments, error bars represent the standard error.

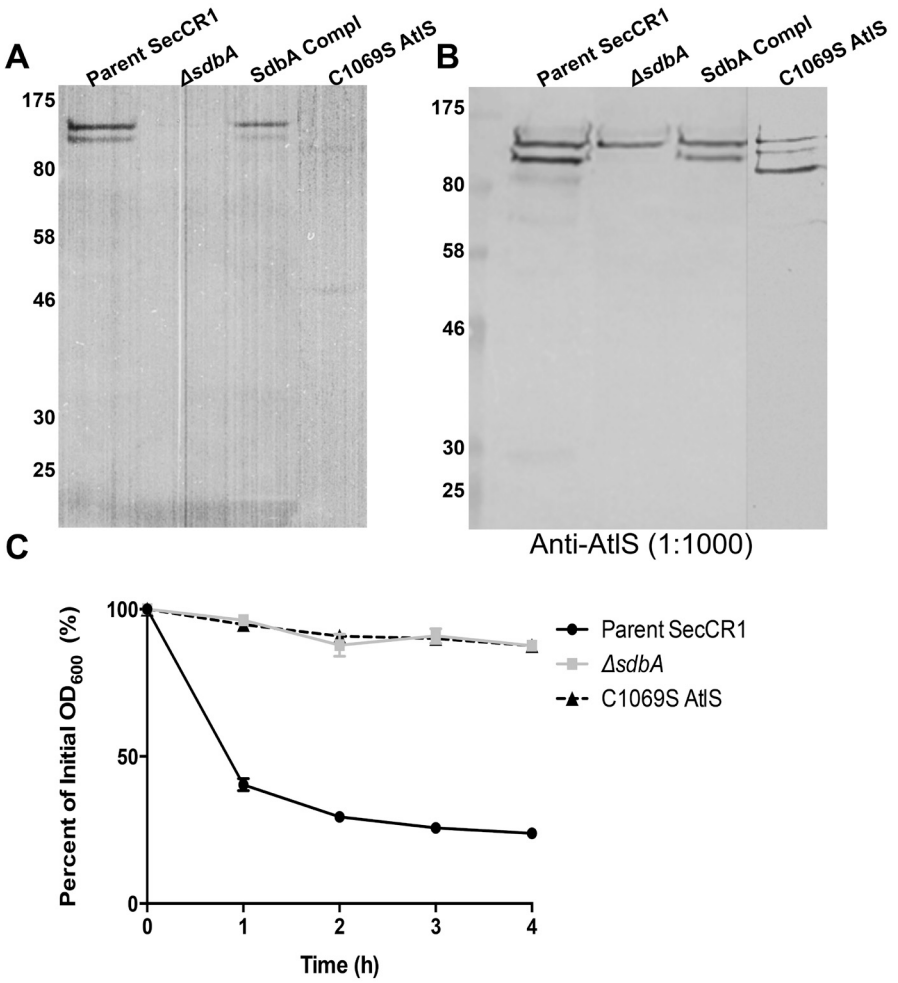

Figure 3. 6 The major autolysin AtlS is inactive in the *sdbA* mutant and the C1069S point mutant

(A) Zymogram analysis of autolytic activity shows the full length (130 kDa) and processed (90 kDa) forms of AltS in the parent strain and *sdbA* complemented mutant (SdbA Compl). These bands are strongly diminished in the *sdbA* mutant and the C1069S point mutant. (B) Western blot of AtlS. Immunoreactive bands were detected at 130 and 90 kDa by the anti-AtlS antisera in the parent and *sdbA* complemented mutant. A single 130 kDa band was detected in the *sdbA* mutant, and the C1069S point mutant produced bands at 130, 90, 85 kDa. For each strain, the proteins used in the zymogram and Western blot originated from the same protein preparation and equal volumes were applied to the gels. (C) Autolysis of the C1069S *atlS* point mutant compared to the parent strain and *sdbA* mutant.

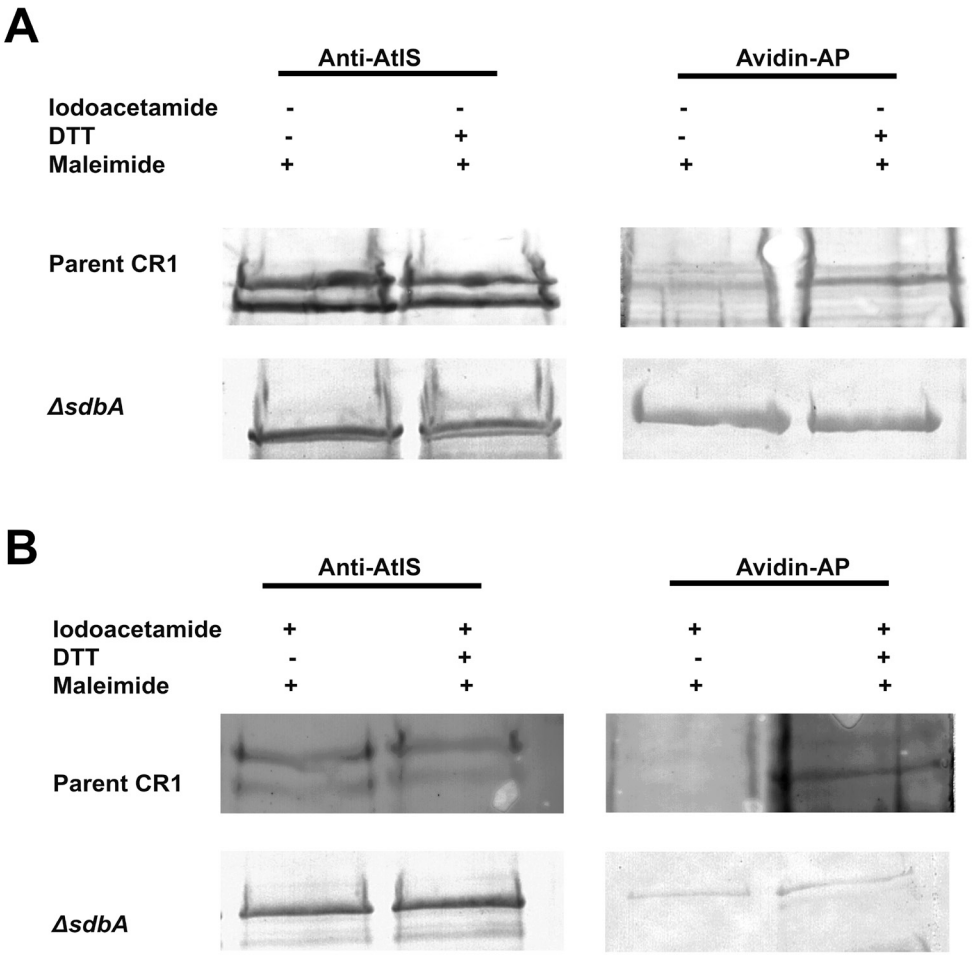
A
Anti-AtlS
Avidin-AP
Iodoacetamide - - - -
DTT - + - +
Maleimide + + + +
Parent CR1
ΔsdbA
B
Anti-AtlS
Avidin-AP
Iodoacetamide + + + +
DTT - + - +
Maleimide + + + +
Parent CR1
ΔsdbA
C
Relative intensity (avidin / anti-AtlS)
80
60
40
20
0
Mal
DTT Mal
IAM Mal
IAM DTT Mal
Parent
ΔsdbA

Figure 3. 7 The AtlS autolysin does not acquire a disulfide bond in the *sdbA* mutant

(A) Surface protein extracts were TCA precipitated and reacted with maleimide-PEG_2-biotin (Mal). Following alkylation, proteins from a single sample were run in duplicate wells and reacted with either avidin-AP to detect biotinylated proteins or with anti-AtlS antisera to detect the total AtlS concentration in the sample (loading control). Positive controls were prepared by reducing the samples with DTT prior to alkylation with maleimide-PEG_2-biotin. (B) A second reaction including iodoacetamide (IAM) was carried out to block free thiols and specifically detect disulfide bonded cysteines. Unbonded cysteine residues were reacted with iodoacetamide (IAM), and DTT was subsequently added to the samples to reduce any disulfide bonds. The cysteine thiol groups formed by reduction with DTT were then labelled with maleimide-PEG_2-biotin. Biotinylated proteins were detected with avidin-AP, and anti-AtlS antisera were used to detect the total amount of AtlS protein in the sample. (C) Densitometry analysis of alkylation was carried out using Image J. The proportion of biotinylated protein was calculated by dividing the signal for bands reacted with avidin-AP by the signal for the 130 kDa band of AtlS. Data is representative of three separate experiments.

A

```
SdbA              MLKEKWWLPFLTVGVILVAV----FAL-FYIAGPNR-----------------HNKGSTQ
SPy_1558          ---MKKGLLVT-TGLACLGLLTACSTQ-DNMAKKEITQDKMSMAAKKKDKMSTSKDKSMM
Ssa_1117          ---MKKLSILT-VSLLCIGLLGACSNQ-KMNSEISK-SD-----------------KSNM
Sp.0659           ---MKKWQTCV-LGAGSLLCLTACSGK-SVTSEHQTKDE-------------------MK
Ssa.1122          ---MKKFVTLL-ATVSAAVFLAACSEQ-EEKPMTMP----------------TTSSSSSE
Sp.1000           ---MKKVMFAG-LSLLSLVVLMACGEE-ETKKTQ----------------------AAQQ
Smu.1070          ---MKKVILPLALGVTLLGI--GLTNQ---------------------------TTSFA
Smt.0346          ---MKKWQTCL-LGVGSICCLAACSAK-NMSDESTMKEQ-------------------TK
dsbF              ---MTHSRLIGALTV-VAIIVTACGSQPKSQPAV-----------------------AP
TlpA              MINLKKKVTIF-L-ILILIIILSSVFYK-FYVDKNQK-----------------DIDNKSNT
H04402_00254      MKNNKRYIY---ISVIMLVLLVGVKFGYDYLSNNYK--------------------SNE

SdbA              KDGSSAVEHEL---TGQQLPEFEMVDQAGYQKKSAEFYNKP-MLVVEWASWCPDCQKQLP
SPy_1558          ADKSSDKKMTN---DGPMAPDFELKGIDGKTYRLSEFKGKK-VYLKEWASWCSICLSTLA
Ssa_1117          Q---TKADSGQ---STKMAKDFSLQGVDGKTYKLSDFKGKK-VYLKEWASWCSICLSTLG
Sp.0659           TEQTASKTSAA---KGKEVADFELMGVDGKTYRLSDYKGKK-VYLKEWASWCSICLASLP
Ssa.1122          TPQTSTVTQVA---VGQEAPDFTLQSMDGKTVKLSDYKGKK-AYLKEWASWCGPCKKSMP
Sp.1000           PKQQTTVQQIA---VGKDAPDFTLQSMDGKEVKLSDFKGKK-VYLKEWASWCGPCKKSMP
Smu.1070          QGKTSPKIVQT---AKNSAPAFKLKNKKGKTVSLSAYKGKK-VYINVWATWCGPCMREIP
Smt.0346          TEQVSS-QTAT---KGQAVADFELTGVDGKTYRLSDYKGKK-VYLKEWASWCSICLASLP
dsbF              TGDAAAATQVPAGQTVPAQLQFSAKTLDGHDFHGESLLGKP-AVLWEWAPWCPTCQGEAP
TlpA              TTQTEISEDKP---KRIASLDFKLKDLNDKEITLSEFKGKK-VMLNEWATWCGYCVQEMP
H04402_00254      A-INNVSDKNS---SFQPAVDFTVYDKDNNEVKLSDYKGKKAVVVNEWASWCSPCKYEMP

SdbA              EIQKVYEKYKGKIHFVMLDMLDSKRET----KERADQYI-------SEKDYTFPYYYDTD
SPy_1558          DTEDLAKM--SDKDYVVLTVVSP-GHQGEKSEADFKKWFQ------GTDYKDLPVLLDPD
Ssa_1117          DTNDLAKE-QSGKDYVVLSVVSP-TFNGEKSADDFKEWYK------SLDYKDFPVLIDNK
Sp.0659           DTDEIAKE--AGDDYVVLTVVSP-GHKGEQSEADFKNWYK------GLDYKNLPVLVDPS
Ssa.1122          ELVELAGK--TDRDFEILTVVAP-GLQGEKSAEEFPKWFQ------EQGYKDVPVLFDTS
Sp.1000           ELMELAAK--PDRDFEILTVIAP-GIQGEKTVEQFPQWFQ------EQGYKDIPVLYDTK
Smu.1070          DLEKIYQTYKHKKDFVFLSVTSP-NDSKYKNSDPIDKDKSTILSKAKDKGITYPILYDYQ
Smt.0346          DTDEIAKD--AGDDYVVLTVVSP-GHKGEQAEADFKNWYK------GLDYKNFPVLIDPS
dsbF              VVGQVAAS-HPEVTFV--GV------AGLDQVPAMQEFVN------KYPVKTFTQLADTD
TlpA              YMQNIHNE-TKDKDIVILAVNV--GEN----KDKIKKFM-------EKKSYDFPVVLDER
H04402_00254      HFQEATNKYN-NEDLEILMVNLTDGMRETK--GSAEEFM-------KEEGYNMNVMFDIN

SdbA              ERAADILHVQSIPTIYLVDKNQKVKKVMTDFHDEAALEKQLEEI---
SPy_1558          GKLLEAYGVRSYPTEVFIGSDGVLAKKHIGYAKKSDIKKTLKGIH--
Ssa_1117          GELLKEYGIRSYPSALFVGSDGSLAKTHIGYMSKEDIEKTLKEIK--
Sp.0659           GKLLETYGVRSYPTQAFIDKEGKLVKTHPGFMEKDAILQTLKELA--
Ssa.1122          GEIFQAYQIRSIPTEILIDSQGKIGKIQFGAISNADAEAAFKEMK--
Sp.1000           ATTFQAYQIRSIPTEYLIDSQGKIGKIQFGAISNADAEAAFKEMN--
Smu.1070          DNFTQAYGIRSIPTHIFINSDGSLSEKIAGGLDEDSLKYYLKKLK--
Smt.0346          GKLLESYGVRSYPTQAFIDKEGKLVKTQPGFMDKDMILKTLKEMG--
dsbF              GSVWANFGVTQQPAYAFVDPHGNVDV-VRGRMSQDELTRRVTALTSR
TlpA              QEVAQNYGVQAFPTTLFIDEEGFVYSGIQGPMTDDIMRKELKIK---
H04402_00254      LDAANKYQLNAIPRTVFIDKEGNLVYDHVGIIDKEILDENIDKIIN-
```

B

Figure 3. 8 SdbA homologs are present in other Gram-positive bacteria

(A) Clustal Omega alignment of homologs to *S. gordonii* SdbA (YP_001451255.1) identified using DELTA BLAST. The CXXC active site and conserved *cis*-proline residue are highlighted. (B) WebLogo (250) showing the consensus sequence of the region surrounding the CXXC motif. Spy, *Streptococcus pyogenes* M1 (NP_269625.1); Ssa, *Streptococcus sanguinis* SK36 (YP_001035078.1, YP_001035083.1); Sp, *Streptococcus pneumoniae* TIG4 (NP_345164.1, NP_345477); Smu, *Streptococcus mutans* UA159 (NP_721554); Smt, *Streptococcus mitis* NCTC 1226 (ZP_07644877); DsbF, *Mycobacterium tuberculosis* H37Rv (NP_216193.1); TlpA, *Clostridium tetani* E88 (NP_780861.1); H04402_00254, *Clostridium botulinum* H04402 065 (YP_005676832.1).

Table 3.1 Transformation frequency of *S. gordonii* parent and mutant strains

Strain	Total CFU/ml	Transformants (CFU/ml)	Frequency (%)[a]
Parent SecCR1	2.20×10^8	1.20×10^5	0.0545
sdbA	5.20×10^7	4×10^1	0.000001
SdbA Compl	1.94×10^8	1.00×10^5	0.0515

[a] Transformation frequency was calculated as the percentage of rifampin resistant transformants divided by the total CFU/ml. Data is representative of at least three separate experiments.

Table 3.2 *S. gordonii* secreted proteins with ≥ 2 extracellular cysteine residues

Gene ID (Sgo)	Gene Name	Annotation*	Cysteine Residues
0014	*pgsA*	CDP-diacylglycerol--glycerol-3-phosphate 3-phosphatidyltransferase	2
0089	*czcD*	Cobalt-zinc-cadmium resistance protein, cation efflux	2
0162	*abpB*	Amylase-binding protein B	2
0231		Glycerophosphoryl diester phosphodiesterase	2
0236		Membrane protein	6
0270		Sodium:dicarboxylate symporter	6
0322		Major facilitator superfamily transporter-permease	4
0385		Exo-beta-D-fructosidase	4
0394		Membrane protein	4
0477		Cell wall binding protein	2
0478		Cell wall binding protein	2
0498	*dsg*	Permease	2
0740		Lipoprotein	5
0770	*btuC*	Vitamin B12 ABC transporter	4
0847		SCP-like extracellular protein	2
0887		Conserved hypothetical protein	4
0899		Hydrolase	3
0952		Conserved hypothetical protein	3
0962		ABC transporter	6
1095		Conserved hypothetical protein	3
1142		Hypothetical protein	2
1176		Peptide methionine sulfoxide reductase	5
1280		Membrane-associated Zn-dependent protease	3
1320	*ntpJ*	Potassium uptake protein	4
1391		Conserved hypothetical protein	2
1416		Two-component system histidine kinase	2
1436		Membrane protein	4
1489		Lipoprotein	3
1790		PTS system, cellobiose-specific IIB component	3
1832		Conserved hypothetical protein	2
1838		ABC-type multidrug/protein/lipid transport system	3
1894		Sugar-binding cell envelope protein	3
2005	*padA*	Collagen adhesion protein	2
2013	*atlS*	N-acetylmuramidase/lysin	2
2094	*comB*	Competence factor transport protein	2
2107		CHAP domain protein	2

***Annotated description obtained from the Oralgen database (http://www.oralgen.lanl.gov)**

Chapter 4: The Disulfide Oxidoreductase SdbA is Active in *Streptococcus gordonii* Using a Single C-Terminal Cysteine of the CXXC Motif

Davey, L., Cohen, A., LeBlanc, J., Halperin, S. A. and Lee, S. F. 2015. The disulfide oxidoreductase SdbA is active in *Streptococcus gordonii* using a single C-terminal cysteine of the CXXC motif. Molecular Microbiology. doi: 10.1111/mmi.13227

4.1 Summary

Recently, we identified a novel disulfide oxidoreductase, SdbA, in the oral bacterium *Streptococcus gordonii*. Disulfide oxidoreductases form disulfide bonds in nascent proteins using a CXXC catalytic motif. Typically, the N-terminal cysteine interacts with substrates, while the C-terminal cysteine is buried and only reacts with the first cysteine of the motif. In this study, we investigated the SdbA $C^{86}P^{87}D^{88}C^{89}$ catalytic motif. *In vitro*, SdbA single cysteine variants at the N or C-terminal position ($SdbA_{C86P}$ and $SdbA_{C89A}$) were active, but displayed different susceptibility to oxidation, and N-terminal cysteine was prone to sulfenylation. In *S. gordonii*, mutants with a single N-terminal were inactive and formed unstable disulfide adducts with other proteins. Activity was partially restored by inactivation of pyruvate oxidase, a hydrogen peroxide generator. Presence of the C-terminal cysteine alone (in the $SdbA_{C86P}$ variant) could complement the Δ*sdbA* mutant and restore disulfide bond formation in recombinant and natural protein substrates. These results provide evidence that certain disulfide oxidoreductases can catalyze disulfide bond formation using a single cysteine of the CXXC motif, including the buried C-terminal cysteine.

4.2 Introduction

Disulfide bonds between cysteine residues are important for the folding and function of secreted proteins, and proteins that are misfolded or lacking disulfide bonds are often unstable and prone to degradation. Disulfide bond formation is an oxidation reaction catalyzed by enzymes called thiol-disulfide oxidoreductases (44). These enzymes belong to the thioredoxin family, which are highly conserved and broadly distributed across all domains of life. In addition to disulfide bond formation, this diverse class of enzymes carries out a range of redox reactions including disulfide reduction, isomerization, S-glutathionylation, and reduction of peroxides (11, 251).

Some of the best characterized thioredoxin family members belong to the disulfide bond (Dsb) pathway of the Gram-negative bacterium *Escherichia coli*. In *E. coli*, disulfide bonds are formed by the periplasmic oxidoreductase DsbA. The active site of DsbA contains a disulfide bond that is transferred to substrate proteins. After each reaction, DsbA is left in a reduced state and the active site must be reoxidized to repeat another catalytic cycle. This function is performed by its redox partner, DsbB (252). Because DsbA is relatively indiscriminate, it can form disulfide bonds between any cysteine residues in a protein, sometimes leading to protein misfolding. The rearrangement of protein disulfides to achieve their proper conformation is catalyzed by the disulfide isomerase DsbC and its redox partner DsbD (69, 76). Additional components of the system include the cytochrome *c* reducing protein CcmG (253), and DsbG, which prevents oxidation of single cysteine residues (79). In the cytoplasm, proteins are maintained in a reduced state with the help of low molecular weight thiols and redox enzymes like thioredoxin and glutaredoxin (70).

Despite their varying activities, all thioredoxin family enzymes share a characteristic thioredoxin fold, consisting of a four-stranded beta sheet between three alpha helices, and most have a Cys-X-X-Cys (CXXC) catalytic motif, where “X” can be any amino acid (11, 22). The two cysteines of the CXXC motif have distinct properties that have been well characterized, and are generally shared by both oxidizing and reducing enzymes. The N-terminal cysteine is solvent exposed and usually has an acidic

pKa, resulting in the formation of a reactive thiolate anion at physiological pH (16). This reactivity contributes to the N-terminal cysteine reacting with both substrate proteins and the redox partner (22). In contrast, the C-terminal cysteine is buried, and as a result substrates are sterically restricted to react with the N-terminal cysteine (254). The C-terminal cysteine reacts solely with the first cysteine of the active site to form an intramolecular disulfide bond. Analyses of diverse disulfide oxidoreductases, ranging from *E. coli* DsbA to eukaryotic protein disulfide isomerase (PDI), have consistently demonstrated that both active site cysteines are required for activity in the cell (115, 255–257).

Unlike *E. coli*, little is known about disulfide bond formation in Gram-positive species and there is considerable diversity in both the prevalence of disulfide bonded proteins and in the machinery used to generate them (24, 96). DsbA homologs in *Staphylococcus aureus* and *Bacillus subtilis* have few substrates or phenotypes associated with them, and appear to play a specialized role in genetic competence (117, 123). In contrast, *Mycobacterium tuberculosis* encodes a DsbA homolog (Rv2969c), that is essential for optimal growth (107). In addition to DsbA-like enzymes, alternative types of disulfide catalysts have been identified, including two CcmG homologs in *M. tuberculosis*, DsbE and DsbF (99, 108), and a dimeric oxidoreductase predicted to be conserved among *Corynebacterium* spp. (96). Although the oxidase activity of these enzymes has been confirmed *in vitro*, no natural substrates or phenotypes have been identified yet.

Gram-positive facultative anaerobes like *Streptococcus* ssp. lack DsbA homologs entirely (24). Nevertheless, pathogenic streptococci produce toxins that are stabilized by disulfide bonds, suggesting that these organisms possess disulfide catalysts that contribute to virulence (169, 258).

To better understand disulfide bond formation in Gram-positive bacteria, we have been investigating thiol-disulfide oxidoreductases in *Streptococcus gordonii*. We recently identified a novel disulfide oxidoreductase, SdbA, in *S. gordonii,* and found that that the

ΔsdbA mutant has a pleiotropic phenotype (101). In this study, we evaluated the enzymatic activity of SdbA using cysteine point mutants in the CXXC catalytic motif. Unexpectedly, we found that SdbA was active *in vitro* using a single active site cysteine, at either the N-terminal or C-terminal position of the active site. In *S. gordonii*, mutants with a single N-terminal cysteine were inactive, whereas the single C-terminal cysteine alone catalyzed disulfide bond formation in both natural and recombinant protein substrates. The remarkable ability of SdbA to catalyze disulfide bond formation using a single cysteine demonstrates that certain disulfide oxidoreductases can carry out the same enzymatic function using different reaction pathways, and suggests the potential existence of naturally occurring oxidoreductases that use a single, buried cysteine to oxidize their substrates.

4.3 Results

DegP Mediates Quality Control Of Disulfide-Bonded Proteins

Virtually all antibodies contain highly conserved disulfide bonds that connect the β-sheets of the immunoglobulin domains in the variable heavy and light chains, and these structural disulfide bonds are critical for stable folding (205, 259). Because of their therapeutic potential, the production of recombinant antibodies has been well studied and disulfide bond formation is often a limiting factor in their production (206). Single chain variable fragment antibodies (scFv) are no exception, and aside from a few unusually stable variants, the proteins typically require two disulfide bonds (205, 206, 236, 259). This instability makes scFv antibodies a useful tool to study disulfide bond formation in *S. gordonii*.

Previously, we found that *S. gordonii* SdbA was essential for the production of a scFv antibody (101). The protein contains four cysteines, which form two consecutive disulfide bonds, one in each variable fragment (204). The absence of scFv in the *ΔsdbA* mutant, and the fact that scFv production could be restored by *sdbA* complementation, indicated that SdbA catalyzed disulfide bond formation in this protein. Thus, to better

understand how SdbA functions in *S. gordonii*, we started by investigating the role of SdbA in scFv production.

To ensure that mutation of SdbA did not have unanticipated effects on the general sec pathway that could account for the absence of the scFv, we first tested production levels of a protein that does not contain disulfide bonds, the extracellular peptidyl-prolyl *cis trans* isomerase PrsA. Western blots showed that PrsA levels were similar between the parent and the *ΔsdbA* mutant, indicating that the sec pathway was functional in the *ΔsdbA* mutant (Fig. 4.1A). Next, we set out to find direct evidence that scFv from the *ΔsdbA* mutant lacked disulfide bonds. To analyze the oxidation state of scFv from the *ΔsdbA* mutant, degradation of the protein had to be prevented. To this end, we inactivated the extracellular serine protease and chaperone DegP in the *ΔsdbA* mutant. DegP has been identified as the sole protease responsible for elimination of unstable foreign proteins in related Gram-positive bacteria, making it a logical candidate for scFv degradation in *S. gordonii* (260). Western blots showed that inactivation of *degP* in the *ΔsdbA* mutant fully restored scFv production, whereas complementation with a functional *degP* gene on the chromosome reversed the effect (Fig. 4.1B). Inactivation of *degP* alone did not alter the level of scFv production. To confirm that degradation required the protease activity of DegP, as opposed to its chaperone function, we introduced a point mutation in the active site serine required for protease activity (261). The catalytically dead *ΔsdbAdegP*$_{S235A}$ mutant produced high levels of the scFv protein, confirming that the protease activity was responsible for degradation (Fig. 4.1B).

SdbA Is Required For Disulfide Bond Formation In *S. gordonii*

Since inactivation of *degP* stabilized scFv in the *ΔsdbA* mutant, we could use this strain to test the oxidation state of the protein. We analyzed disulfide bonding in scFv from the *ΔsdbAΔdegP* mutant using two approaches. First, scFv isolated from the parent and the *ΔsdbAΔdegP* mutant was alkylated with maleimide-PEG$_2$-biotin to detect free thiols. Next, we used a differential thiol-trapping technique to detect disulfide bonds (219). This strategy uses iodoacetamide to block free thiols before reduction of disulfide bonds with dithiothreitol (DTT), and subsequent alkylation of the newly liberated thiols.

The alkylation experiments showed that scFv isolated from the parent was fully oxidized, and free thiols were only detected when samples were reduced with DTT (Fig. 4.2A). In contrast, scFv from the *ΔsdbAΔdegP* mutant clearly contained free thiols indicative of unbonded cysteines. This reaction was blocked by iodoacetamide, which confirmed that the biotinylation was specific to free thiols (Fig. 4.2B). To ensure that the free thiols detected in the double mutant were from the loss of SdbA oxidoreductase activity, and not an accumulation of misfolded protein from the loss of DegP, we also tested the oxidation state of scFv isolated from a *ΔdegP* single mutant as a control. ScFv from the *ΔdegP* mutant was oxidized to a similar extent as the parent, confirming that reduced scFv obtained from the *ΔsdbAΔdegP* mutant was due to the loss of SdbA (Fig. 4.2A). Thus, SdbA is essential for disulfide bonding in the scFv, and DegP alone appears to be responsible for the rapid degradation of the misfolded protein.

The C-terminal Cysteine of the CXXC Motif Alone is Sufficient for SdbA Activity in *S. gordonii*

The conserved CXXC active site motif of thiol disulfide oxidoreductases is critical for their activity (115, 252, 257). To characterize the CXXC motif in SdbA, and confirm that the enzymatic activity of SdbA contributed to the pleiotropic phenotype observed in the *ΔsdbA* mutant, we used site directed mutagenesis to replace one or both active site cysteines, generating $sdbA_{C86P}$, $sdbA_{C89A}$, and $sdbA_{C86P/C89A}$ mutants. The constructs were introduced as single copies onto the chromosome of *ΔsdbA* mutants, and expressed under the native *sdbA* promoter. All mutations were confirmed by DNA sequencing.

To assess the activity of the point mutants, we tested for scFv production. Similar to the *ΔsdbA* mutant, mutation of the SdbA active site C-terminal cysteine (C89A), or of both cysteines C86P/C89A, eliminated scFv production. Inactivation of *degP* rescued production in the mutants, demonstrating that the protein was produced, but was unstable and sensitive to degradation (Fig. 4.2C). Unexpectedly, mutation of the N-terminal cysteine (C86P) did not eliminate scFv production. The $sdbA_{C86P}$ mutant continued to

produce scFv even in the presence of DegP, although inactivation of *degP* did increase the overall yield. The ability of this mutant to generate stable scFv protein suggested that SdbA remained functional using the single C-terminal cysteine (Fig. 4.2C).

When constructing the mutants, the codon for proline was chosen for the $sdbA_{C86P}$ mutation because it generated a unique *Msc*I restriction site that could be used to easily confirm the construct. Given the unexpected activity of the $sdbA_{C86P}$ mutant, we constructed a second of set of SdbA cysteine mutants, in which the amino acid substitutions were reversed to ensure that the proline mutation did not affect activity. Analysis of scFv production by an $sdbA_{C86A}$ mutant showed that, like the $sdbA_{C86P}$ mutant, a low level of stably folded scFv protein was produced (APPENDIX A1). Similarly, mutation of the C-terminal cysteine, Cys89, to either an alanine or a proline abolished scFv production. Thus, the mutants behave similarly, regardless of the amino acid substitution introduced at the Cys86 position. Since the C86P mutation could be easily confirmed by restriction analysis, we used this mutant in all subsequent experiments.

To determine if scFv produced by the $sdbA_{C86P}$ mutant contained disulfide bonds, we tested the oxidation state by alkylation. To improve recovery, we used scFv purified from the $sdbA_{C86P}\Delta degP$ mutant. As expected, the scFv consisted of a mixture of reduced and oxidized protein. Although free thiols were detected, likely corresponding to the portion of reduced scFv degraded by DegP (Fig. 4.2A), a portion of the protein was oxidized (Fig. 4.2B). Similar results were obtained when we tested the oxidation state the autolysin AtlS, a natural substrate of SdbA, which was oxidized to a similar extent in the $sdbA_{C86P}$ mutant and the parent (Fig. 4.2D). This indicated that SdbA could generate correctly folded disulfide bonded proteins using the catalytic C-terminal cysteine alone.

$SdbA_{C86P}$ Complements the *ΔsdbA* Mutant Phenotype

Mutation of either active site cysteine in an oxidoreductase typically eliminates activity, and the same holds true for other members of the thioredoxin family (115, 175, 252, 255, 257, 262, 263). Thus, the oxidase activity in the $sdbA_{C86P}$ mutant was surprising and warranted further investigation.

Previously, we found that *ΔsdbA* mutants have a distinct phenotype that includes enhanced biofilm formation, deficiencies in autolytic activity and bacteriocin production, and clumping in liquid medium (101). To assess oxidase activity in *S. gordonii*, we tested the ability of the SdbA cysteine mutants to complement the *ΔsdbA* mutant phenotype.

Analysis of biofilm formation by crystal violet staining showed that $sdbA_{C86P}$ fully complemented the *ΔsdbA* mutant phenotype, and reduced biofilms levels to that of the parent (Fig. 4.3A). The $sdbA_{C89A}$ partially complemented the *ΔsdbA* mutant, while the $sdbA_{C86P/C89A}$ mutant failed to complement the *ΔsdbA* phenotype and produced significantly more biofilm ($P < 0.0001$).

Another important indicator of SdbA activity is autolysis, given that AtlS is a natural SdbA substrate (101). AtlS contains two cysteines that form a single disulfide bond. An autolysis assay demonstrated that, like the *ΔsdbA* mutant, the $sdbA_{C89A}$ and $sdbA_{C86P/C89A}$ mutants were highly resistant to lysis (Fig. 4.3B). The $sdbA_{C86P}$ mutant, however, restored autolysis and lysed at a rate that was comparable to the parent strain. To look at AtlS activity directly, we used zymography to test enzyme function. While AtlS from the $sdbA_{C89A}$ mutant generated a single, weak band of clearing in a zymogram, the $sdbA_{C86P}$ mutant produced two distinct bands, similar to the parent (Fig. 4.3C). This demonstrated that the $sdbA_{C86P}$ mutant generated enzymatically active AtlS, and agrees with the alkylation data showing that the autolysin had been oxidized in the $sdbA_{C86P}$ mutant (Fig. 4.2D).

Next we tested for complementation of bacteriocin production. *S. gordonii* produces two bacteriocins, Sth_1 and Sth_2 (188), and *ΔsdbA* mutants are deficient in both. Bacteriocins were detected using an activity assay based on growth inhibition of the target strain *S. oralis*. Culture supernatants from the parent inhibited the growth of *S. oralis*, indicating the presence of bacteriocins. In contrast, no inhibitory activity was detected in the *ΔsdbA* and $sdbA_{C86P/C89A}$ mutants, and the $sdbA_{C89A}$ mutant displayed an intermediate phenotype, partially inhibiting the growth of *S. oralis*. The $sdbA_{C86P}$ mutant

behaved similar to the parent and fully restored bacteriocin activity to the *ΔsdbA* mutant (Fig. 4.3D).

Like the parent strain, the $sdbA_{C86P}$ mutant also prevented clumping and sedimentation observed in *ΔsdbA* strains grown in liquid culture (Fig. 4.3E). Taken together, the data support the notion that $SdbA_{C86P}$ was active in the cell with only the single C-terminal active site cysteine.

SdbA Variants With a Single N- Or C-Terminal Cysteine Have Oxidase Activity *In vitro*

In vitro enzyme assays were used to assess the activity of the SdbA cysteine variants. First, we carried out differential scanning fluorimetry to determine if the point mutations introduced major structural changes that might explain the inactivity of the $sdbA_{C89A}$ mutant. Compared to the melting temperature (Tm) of wild-type SdbA at 55.9°C, the inactive $SdbA_{C89A}$ variant was similar to the parent with a Tm of 56.8°C. Thus, the loss of enzyme activity in the $sdbA_{C89A}$ mutant did not appear to be due to misfolding as a result of the mutation. The active $SdbA_{C86P}$ variant had a Tm of 52.4°C, suggesting reduced stability and possible structural changes, but such changes did not affect activity as shown below.

To assess the oxidase activity of the SdbA cysteine variants, we tested the ability of the purified enzymes to catalyze folding of reduced, denatured RNase A in the presence of glutathione. The wild-type enzyme efficiently catalyzed RNase A folding, while the cysteine-free $SdbA_{C86P/C89A}$ variant had lost all activity (Fig. 4.4A). In stark contrast to the activity of the enzymes in *S. gordonii*, where only the $sdbA_{C86P}$ mutant was active, both SdbA single cysteine variants exhibited comparable oxidase activity *in vitro*. Both of the SdbA single cysteine variants accelerated RNase A folding above background levels at approximately the same rate, indicating that either single cysteine of the CXXC active site was sufficient for activity *in vitro* (Fig. 4.4A). Neither mutant was active without prior treatment with GSSG (APPENDIX A3). This suggested that the SdbA single cysteine variants could use glutathione to catalyze disulfide bond formation.

Oxidase activity was also assessed using a modified RNase A folding assay, in which we reacted $SdbA_{C86P}$ or $SdbA_{C89A}$ with reduced denatured RNase A and tested for oxidation by running the RNase A on a gel to visualize a shift in migration. Glutathione was omitted from the reaction buffer to minimize spontaneous refolding, and instead the SdbA single cysteine variants were oxidized with glutathione prior to the reaction. Following the refolding reaction, the RNase A was alkylated with maleimide-PEG_2-biotin, which added 0.5 kDa per thiol to enhance the shift between oxidized and reduced proteins. The SDS-PAGE gel showed a clear shift between RNase A incubated alone versus samples incubated with either $SdbA_{C86P}$ or $SdbA_{C89A}$, signifying that the protein had been oxidized (Fig. 4.4B).

Kinetic analysis of enzyme activity was consistent with the results of the RNase A folding assay, showing that the efficiency of both SdbA single cysteine variants were lower than the parent, but similar to each other (APPENDIX A2A). The k_{cat}/K_m values for the $SdbA_{C89A}$ and $SdbA_{C86P}$ variants with reduced RNase A were 68 and 78% of the wild type protein, respectively.

The CXXC motif of thioredoxin family proteins with oxidoreductase activity usually have an acidic, solvent exposed N-terminal cysteine, and a buried C-terminal cysteine (262). The unexpected activity of the single cysteine variants led us to test whether SdbA shares these characteristics, or if the activity could be attributed to unusual features of the active site. To determine if SdbA has an exposed N-terminal cysteine and buried C-terminal cysteine, solvent accessibility was tested using dithionitrobenzoic acid. Wild type SdbA and $SdbA_{C89A}$ reacted rapidly, while the $SdbA_{C86P}$ variant only reacted after being denatured, confirming that the cysteine was indeed buried in the structure of the protein (Fig. 4.4C). The amount of thionitrobenzoic acid (TNB) released by the wild type was twice that of the single cysteine variants, which is indicative of a dithiol mechanism. During the reaction, the N-terminal cysteine, Cys86, reacts with DTNB to form a mixed disulfide with TNB and released one equivalent of free TNB. This is followed by a second reaction between Cys89 and the mixed disulfide to release a second

unit of TNB. This suggests that despite being active with the single C-terminal cysteine, wild type SdbA probably uses both cysteines. This is also consistent with the fact that both cysteines are conserved in the motif (101). It should also be noted that the N-terminal cysteine was determined to have an acidic pKa of 4.7, similar to other bacterial oxidoreductases (APPENDIX A2B) (108). As such, the SdbA CXXC active site does share some typical characteristics of an oxidoreductase active site, despite the atypical activity of the C-terminal cysteine.

There is evidence that low molecular weight thiols can contribute to oxidase activity by forming intermolecular disulfides, and a previous investigation of an *E. coli* DsbA single cysteine mutant found that it was active *in vitro* using glutathione (224). To determine if the SdbA single cysteine variants could use low molecular weight thiols for activity, we tested for S-glutathionylation of the active site cysteines by mass spectrometry. Peptide fragments containing the catalytic site were analyzed for modifications on the cysteine residue and quantified by comparing the peak intensities. Each modification was expressed as a percentage of the total cysteine content. Surprisingly, both of the SdbA single cysteine variants were found to be almost completely S-glutathionylated, including the buried C-terminal cysteine that was inaccessible to DTNB (Fig. 4.4D and APPENDIX A4). This equivalent reactivity with glutathione likely explains why both enzymes were active *in vitro*, since the disulfide bond between SdbA and glutathione could be transferred to substrate proteins. These data suggest that SdbA can use either single cysteine of the active site to catalyze disulfide bond formation using low molecular weight thiols.

Hydrogen Peroxide Inhibits Oxidase Activity in the $SdbA_{C89A}$ Mutant

Since SdbA was functional using either cysteine of the active site *in vitro*, the results suggested that there was something specific to *S. gordonii* that inhibited activity of the N-terminal cysteine. When cultured under aerobic conditions, *S. gordonii* produces up to 1.6 mM of hydrogen peroxide (H_2O_2) as a metabolic byproduct of pyruvate oxidase (264), which slows the growth of competing bacteria and contributes to the success of *S. gordonii* in colonizing oral biofilms (265). Since the SdbA active site cysteines would be

exposed to endogenous H_2O_2, we hypothesized that cysteine oxidation might contribute to the differences between SdbA activity *in vitro* and in the cell. H_2O_2 can oxidize the sulfhydryl group of thiols to sulfenic acid, a reversible modification that can contribute to disulfide bonding, while further oxidation to sulfinic and sulfonic acid can cause irreversible damage (16, 70).

To test the effect of H_2O_2 on the SdbA cysteine variants, we used mass spectrometry to determine the oxidation state of the enzymes after exposure to H_2O_2 *in vitro*. SdbA was reacted with H_2O_2 in the presence of the sulfenic acid probe dimedone, and the proteins were subjected to trypsin digestion and analyzed by mass spectrometry. Peptide fragments containing the active site cysteines were assessed for modifications and peak intensity integration was used as a semi-quantitative measure of the relative abundance of each modification. Despite their similar reactivity with glutathione, there was a striking difference between the $SdbA_{C89A}$ and $SdbA_{C86P}$ variants in their reactivity with H_2O_2. The cysteine in the $SdbA_{C89A}$ variant was detected almost entirely as sulfenic acid, representing 86.5% of the active site cysteines (Figs. 4.5A, APPENDIX A5, A6). In contrast, the cysteine in the $SdbA_{C86P}$ mutant contained a mixture of sulfenic acid and S-glutathionylated species, corresponding to 37 and 62% of the total cysteine, respectively. The glutathione modification apparently originated from *E. coli* during isolation of the protein.

To confirm the mass spectrometry data, we tested for sulfenylation of the SdbA variants using a biotin-tagged sulfenic acid probe, DCP-Bio1. Western blots showed that the $SdbA_{C89A}$ variant produced a band detected by avidin alkaline phosphatase, indicating that the single N-terminal cysteine had been sulfenylated (Fig. 4.5B). Without H_2O_2, a weak band could still be detected in the $SdbA_{C89A}$ variant, likely due to oxidation by molecular oxygen during protein isolation. Unlike the N-terminal cysteine, the buried C-terminal cysteine was not highly susceptible to sulfenylation.

It was surprising to find that sulfenylation had occurred primarily in the inactive $SdbA_{C89A}$ variant, given that sulfenic acid has been demonstrated to contribute to disulfide

bond formation by proteins with single cysteine residues (177, 266). Despite multiple attempts, we were unable to detect sulfenylation in SdbA immunoprecipitated from *S. gordonii*, possibly due to the low amount of total SdbA protein combined with the high reactivity of sulfenic acid. Therefore, as an alternative approach to investigate the effect of H_2O_2 on disulfide bond formation in the cell, we generated a H_2O_2 null mutant by inactivating the pyruvate oxidase gene *spxB*.

The mutants were tested for scFv production as an indicator of SdbA activity, as described previously. Consistent with the notion that H_2O_2 and sulfenylation was detrimental to SdbA activity, inactivation of *spxB* partially restored scFv production to the $sdbA_{C89A}$ mutant (Fig. 4.5C and 4.5D). Thus, the $SdbA_{C89A}$ variant did have some activity in the cell, as was observed in the biofilm (Fig. 4.3A) and bacteriocin assays (Fig. 4.3D). Eliminating H_2O_2 also increased the scFv yield from the parent and $sdbA_{C86P}$ mutant, indicating that the reactive oxygen species generally inhibits SdbA, either directly or through oxidative damage of the scFv substrate. These results suggest that, in agreement with the *in vitro* data, SdbA has enzymatic activity using either single cysteine of the active site, but that the solvent exposed N-terminal cysteine in $SdbA_{C89A}$ was vulnerable to oxidation that inhibited activity.

The $SdbA_{C89A}$ Mutant Forms Disulfide-linked Complexes that are Degraded by DegP

Oxidoreductases with mutations to the C-terminal cysteine of the CXXC motif, including DsbA (252), PDI (257), and thioredoxin (267) can form disulfide linked complexes with their redox partners and substrates, respectively. We hypothesized that sulfenic acid formation in the $sdbA_{C89A}$ mutant could contribute to complex formation, which if not resolved, would consume the enzyme rendering it inactive. First, we tested for intermolecular disulfide bond formation between SdbA and its natural substrate AtlS. AtlS was extracted by incubating cells in 4% SDS at room temperature and subsequently analyzed by non-reducing Western blots probed with anti-AtlS and anti-SdbA antisera. Extracts from the $sdbA_{C89A}$ mutant contained a ~150-kDa band that was recognized by both antibodies, signifying a complex formed between SdbA (22 kDa) and AtlS (130

kDa) (Fig. 4.6A). The SdbA/AtlS complex was only weakly detected in the active *sdbA*$_{C86P}$ mutant and the parent. Given that AtlS was inactive in the *sdbA*$_{C89A}$ mutant, complex formation did not equate with oxidase activity, and might inhibit function.

Finally, we tested the total disulfide-linked complexes in the cell using cells boiled in non-reducing sample buffer. The samples were run on non-reducing Western blots and reacted with anti-SdbA antisera. Extracts from the *sdbA*$_{C89A}$ mutant produced a distinct banding pattern showing multiple complexes with other cysteine containing proteins (Fig. 4.6B). These complexes were absent in the parent and the active *sdbA*$_{C86P}$ mutant. When we compared complex formation between strains with and without a functional DegP protease, the *sdbA*$_{C89A}$ mutant consistently produced less total SdbA and fewer disulfide complexes, indicating that the complexes were sensitive to degradation.

When we tested complex formation using recombinant SdbA and reduced RNase A *in vitro*, several high molecular weight bands were detected on the gel, however, the intensity and number of these bands was similar in both SdbA single cysteine variants, and the complexes were only a minor component of the total protein sample (APPENDIX A7). This suggested that complex formation was not an intrinsic characteristic of the SdbA$_{C89A}$ variant, but was related to the environment in the cell.

Taken together, the data show SdbA can catalyze disulfide bond formation using a single active site cysteine. Although the N-terminal cysteine in the SdbA$_{C89A}$ variant was active *in vitro*, it was inactive in the cell, apparently because of its propensity to form unstable complexes with other proteins. In contrast, the *sdbA*$_{C86P}$ mutant with a single, buried cysteine was active both *in vitro* and in the cell, and can complement the *ΔsdbA* mutant.

4.4 Discussion

In this study, we analyzed SdbA active site point mutants to confirm that the *ΔsdbA* mutant phenotype was directly related to its oxidoreductase activity. Our characterization of the SdbA active site showed that, unlike previously described thiol-

disulfide oxidoreductases, SdbA is active with only a single cysteine of the CXXC motif. Although SdbA cysteine variants with a single cysteine in either the N-terminal or C-terminal position were active *in vitro*, only variants with a single C-terminal cysteine were active in *S. gordonii* under most conditions. This difference appears to be related to the environment in the cell, the structure of the protein, and the difference between the individual catalytic cysteines in their susceptibility to oxidation.

The single C-terminal cysteine of the $SdbA_{C86P}$ mutant produced disulfide-bonded proteins both *in vitro* and in *S. gordonii*, which was unexpected given that the C-terminal cysteine is buried, and does not typically interact with substrates. *In vitro* activity required glutathione, which suggests that the mechanism of oxidation might involve a transfer of the disulfide bond from S-glutathionylated SdbA to its substrate. This type of mechanism is not unprecedented, and other thioredoxin family proteins, including DsbA mutants (224) and glutaredoxin 3 (175) have been proposed to gain oxidase activity by forming a mixed disulfide between the N-terminal cysteine of the CXXC motif and glutathione. The disulfide bond is then transferred to substrate proteins, with glutathione as the final electron acceptor. We suggest that a similar scenario may occur in the $sdbA_{C86P}$ mutant (Fig. 4.7B). This is also in agreement with the mass spectrometry data, which showed that, despite being buried, the C-terminal cysteine forms a stable disulfide bond with glutathione. This mixed disulfide bond could be transferred to substrate proteins.

Although the $sdbA_{C86P}$ mutant used glutathione to catalyze disulfide formation *in vitro*, it is not clear how the enzyme functioned in *S. gordonii*. Initially, we hypothesized that $sdbA_{C86P}$ might function as a dimer; however, we found that purified $SdbA_{C86P}$ dimers were completely inactive *in vitro*, making it unlikely that they would be active in the cell (data not shown). Similarly, medium components did not contribute to oxidase activity, and the mutant produced similar amounts of scFv protein in both rich and minimal medium (APPENDIX A8). Streptococci do synthesize glutathione (268), which could contribute to $SdbA_{C86P}$ activity, along with other low molecular weight thiols such as

cysteine. Alternatively, $SdbA_{C86P}$ might interact with a redox partner that has not been identified yet.

Interestingly, the C-terminal cysteine was inaccessible to DTNB, yet clearly reacted with glutathione and substrate proteins. A possible explanation for this discrepancy is that binding of a peptide substrate results in a conformation change that alters accessibility of the C-terminal cysteine. At the same time, this buried position might protect the cysteine from damaging oxidation by H_2O_2, allowing it to react preferentially with thiols instead, and maintain its enzymatic activity. Conformation changes induced by substrate binding have been demonstrated for the cytochrome *c* reductase ResA, which increases its catalytic activity in response to substrate binding (130). Some peroxidases also undergo local unfolding around the active site during their catalytic cycle. In these enzymes, the peroxidatic cysteine reacts with substrates in a folded conformation and subsequently unfolds to allow access to the resolving cysteine (269). Intriguingly, the peroxidatic cysteine of peroxidases is in the equivalent position as the C-terminal cysteine in the $SdbA_{C86P}$ variant (269).

In contrast to the C-terminal cysteine, the single N-terminal cysteine of the $sdbA_{C89A}$ mutant was solvent exposed and had an acidic pK_a, two factors that would contribute to its reactivity with endogenous H_2O_2 (269), which appeared to inhibit enzyme activity in the cell. H_2O_2 probably inhibits all of the SdbA variants to some extent, and could potentially cause oxidative damage of SdbA substrates as well, however the effect was most pronounced in the $SdbA_{C89A}$ variant. The ability of the N-terminal cysteine to stabilize sulfenic acid was unexpected, and it is not clear why the cysteine is not equally susceptible to further oxidation to sulfinic or sulfonic acid (Fig. 4.5A).

Our observation that sulfenylation was detrimental to the catalytic activity of the $sdbA_{C89A}$ mutant is counterintuitive, given that sulfenic acid species are highly reactive and can form disulfide bonds. Our data suggest that the sulfenylated N-terminal cysteine of the $sdbA_{C89A}$ mutant does indeed form disulfide bonds, however, the bonds formed via this pathway cannot be resolved and are degraded (Fig. 4.7A). Initially we thought that

SdbA might function like the single cysteine rhodanese PspE, which can use sulfenic acid to catalyze disulfide bond formation in substrate proteins (177). Notably, however, PspE cooperates with the disulfide isomerase DsbC to complete its catalytic cycle and resolve intermolecular bonds between PspE and its substrates (177). Because *S. gordonii* might not have the requisite isomerases needed to resolve disulfide complexes using a similar mechanism, the $SdbA_{C89A}$ mutant ends up trapped with its substrates, resulting in a dead end for the enzyme.

Typically, in thioredoxin family members with oxidase activity, the CXXC motif contains an intramolecular disulfide bond that is transferred to substrate proteins, thereby necessitating both cysteines for activity (44). As such, there are few reports of naturally occurring thioredoxin family proteins with a single C-terminal cysteine. Two eukaryotic PDI-like proteins with SXXC active sites that have been analyzed are human PDILT (270) and EtPDIL from the ampicomplexan *Eimeria tenella* (271). However, neither of these proteins exhibited oxidoreductase activity *in vitro*, although human PDILT might function as a chaperone (270, 271). Generally, the most common thioredoxin family enzymes that use a single C-terminal cysteine are peroxiredoxins, while those that use a single N-terminal cysteine belong to the monothiol glutaredoxins, and there are no known single cysteine oxidoreductases (11). Nevertheless, *in silico* analyses have predicted the existence of DsbA-like thioredoxin family enzymes with single N or C-terminal cysteines, although these enzymes have not been characterized biochemically or biologically (11, 272). Our analysis of SdbA single cysteine variants supports these predictions, by demonstrating that a single cysteine at either position of the CXXC motif has the potential for oxidase activity, even when the C-terminal cysteine is buried.

Virtually all reports of single cysteine mutants with residual activity involve the exposed, N-terminal cysteine. For example, *E. coli* DsbA mutants were found to catalyze the oxidative folding of hirudin *in vitro* using a single N-terminal cysteine (224). Similarly, a DsbA homolog in *Francisella*, FipB, had partial activity using a single N-terminal cysteine (263). PDI mutants also retain some isomerase activity with a single N-terminal active site cysteine (257). In each of these instances, the enzyme activity was

limited to the reactive N-terminal cysteine of the CXXC motif, while variants with a single C-terminal cysteine were inactive. Thus, the activity of the *S. gordonii* single cysteine mutants, and particularly of the C-terminal mutant, was unexpected.

One of the only examples of a mutated CXXC motif protein that did have a low level of activity using a single C-terminal cysteine did not have a typical CXXC active site. Mutants generated in the *Bacillus subtilis* cytochrome c reductase ResA with a single C-terminal cysteine showed a low level of activity in an *in vitro* assay, although they were inactive in the cell (128). ResA, however, has an unusual CXXC motif, where both of the cysteines are sufficiently solvent exposed to react with DTNB, even when fully folded (130). In contrast, our data indicate that SdbA has a typical oxidoreductase active site with an exposed, acidic N-terminal cysteine and buried C-terminal cysteine.

A remaining question is whether wild type SdbA uses the same mechanism as the $SdbA_{C86P}$ mutant. The data suggest that wild type SdbA most likely uses a standard mechanism, using both cysteines, under most conditions (Fig. 4.7C). Although the single cysteine mutant complemented the *ΔsdbA* mutant phenotypes, production of the scFv protein was lower in the $sdbA_{C86P}$ mutant than in the parent. Similarly, kinetic analysis of the single cysteine variants showed that they were less efficient than the wild type. The reactivity of the wild type enzyme with DTNB also indicates that SdbA uses both active site cysteines. Interestingly, the $sdbA_{C86P}$ mutant reached wild type levels of scFv production in the H_2O_2 null *ΔspxB* mutant background, and it is conceivable that SdbA might use different pathways under different conditions (e.g. anaerobic biofilm), or that a single C-terminal cysteine may serve as a backup should the N-terminal cysteine become over oxidized to sulfonic acid. However, additional investigation is required to determine if the wild-type SdbA ever uses a monothiol mechanism in *S. gordonii*.

If SdbA has a typical active site, a remaining question is why SdbA is functional with a single cysteine and what sets it apart from oxidoreductases that require two cysteines. Despite demonstrated oxidase activity, sequence analysis of SdbA reveals that it has a number of features that resemble a reductase. Like thioredoxin, SdbA has a

tryptophan residue adjacent to the CXXC motif and an isoleucine located N-terminus to the conserved *cis*-proline, which has been reported to influence enzymatic activity (13). In addition, the SdbA active site, WCPDC, is identical to the conserved eukaryotic reductase TRP14 (273). The *M. tuberculosis* disulfide oxidase DsbE is also homologous to a Gram-negative reductase, CcmG (108), which suggests that protein homology might not be a good indicator of enzyme function in Gram-positive species. To better understand the catalytic mechanism of SdbA, analyses are underway to solve the enzyme structure.

At this stage we do not know if *S. gordonii* uses additional proteins to catalyze disulfide bond formation, and the identity of SdbA redox partner(s) have yet to be identified. Our data show that SdbA was essential to the production of the scFv antibody and a functional AtlS. This suggests that SdbA was the only oxidoreductase in *S. gordonii* capable of oxidizing these proteins, and therefore it is unlikely that a different enzyme could be forming disulfide bonds in the $sdbA_{C86P}$ mutant. Although stable scFv was not detected in the *ΔsdbA* mutant, our alkylation reactions indicated that a portion of the protein recovered from the *ΔsdbAΔdegP* mutant did contain oxidized cysteines. These could be from non-native disulfide bonds or other types of oxidation reactions, such as sulfenylation, that could give rise to background alkylation after reduction with DTT. Background oxidase activity is also known to occur *E. coli* DsbA mutants, although the mechanisms involved are unknown (45, 177). We do not know if this background oxidation is spontaneous or enzyme catalyzed, or if SdbA is involved in isomerization of non-native bonds. However, we have not found evidence to suggest that SdbA has isomerase activity *in vitro*, and SdbA was inactive in a scrambled RNase A refolding assay, as well as an insulin reduction assay (data not shown).

In summary, we have demonstrated that SdbA can sustain disulfide bond formation using a single cysteine of the CXXC active site motif. Point mutants with a single cysteine at either the N-terminal or C-terminal position of the CXXC motif exhibited oxidase activity *in vitro*, but only mutants with the C-terminal cysteine could maintain activity in *S. gordonii*. Remarkably, mutants with a single C-terminal cysteine

complemented the phenotype of *ΔsdbA* mutants, and generated disulfide bonds in both the native substrate AtlS and a recombinant disulfide bond containing protein. This study shows that certain disulfide oxidoreductases can function with the C-terminal buried cysteine of the CXXC motif.

4.5 Acknowledgements

Funding for this study was provided by the Natural Sciences and Engineering Research Council of Canada (NSERC). LD is a recipient of a NSERC post-graduate scholarship, an IWK graduate studentship, and a Nova Scotia Health Research Foundation Scotia Scholars award.

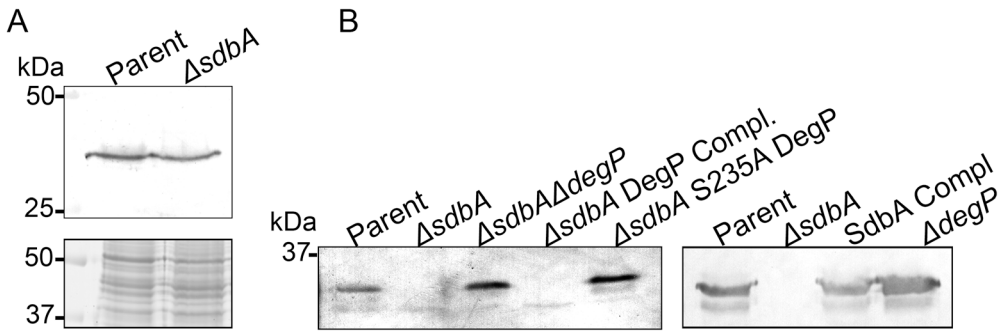

Figure 4. 1 DegP degrades scFv produced in the *ΔsdbA* mutant

(A) Production of the 35 kDa lipoprotein PrsA was detected by Western blotting using anti-PrsA antisera as the probe (upper panel). The same samples were separated by SDS-PAGE and stained with Coomassie blue to show equal protein loading (lower panel). (B) Western blots showing the production of the 33 kDa scFv protein. ScFv was detected using an anti-HA monoclonal antibody. Protein extracts were prepared from the parent, *ΔsdbA,* and *ΔsdbAΔdegP* mutants, as well as a *ΔsdbAΔdegP* mutant complemented with a functional *degP* gene on the chromosome (*ΔsdbA* DegP Compl), and a *ΔsdbA* mutant with a catalytically inactive DegP (*ΔsdbA* S235A DegP) (left panel). The *ΔsdbA* complemented mutant (SdbA Compl.) and single *ΔdegP* mutant are shown on the right panel.

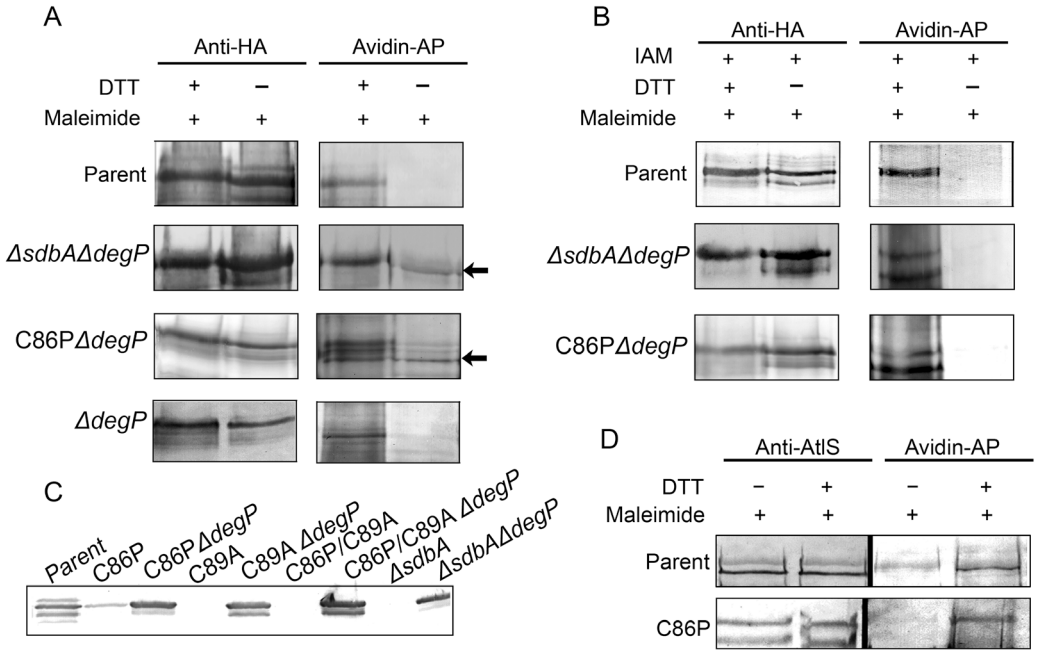
A
Anti-HA
Avidin-AP
DTT
Maleimide
Parent
ΔsdbAΔdegP
C86PΔdegP
ΔdegP
B
Anti-HA
Avidin-AP
IAM
DTT
Maleimide
Parent
ΔsdbAΔdegP
C86PΔdegP
C
Parent
C86P
C86P ΔdegP
C89A
C89A ΔdegP
C86P/C89A
C86P/C89A ΔdegP
ΔsdbA
ΔsdbAΔdegP
D
Anti-AtlS
Avidin-AP
DTT
Maleimide
Parent
C86P

Figure 4. 2 SdbA catalyzes disulfide bond formation

(A) The oxidation state of scFv purified from the parent, *ΔsdbAΔdegP*, *SdbA$_{C86P}$ΔdegP* (C86P*ΔdegP*), and *ΔdegP* mutant was determined by alkylation with maleimide-PEG$_2$-biotin and detected using avidin alkaline phosphatase (Avidin-AP). The same protein samples were run in adjacent lanes and reacted with anti-HA to detect the total scFv protein as a loading control. The lower molecular weight bands recognized by avidin-AP correspond to degradation products that have lost the C-terminal HA-tag, but contain alkylated cysteines. Arrows indicate detection of free thiols. (B) Differential thiol trapping to detect disulfide bonds. Free thiols in proteins were blocked with iodoacetamide (IAM) prior to reduction of disulfide bonds with DTT. The liberated cysteines were then detected by maleimide-PEG$_2$-biotin and avidin-AP. Total protein loading was detected using anti-HA. (C) Western blot to detect scFv produced in the SdbA CXXC active site mutants. Proteins were extracted from the parent, *ΔsdbA*, *sdbA$_{C86P}$* (C86P), and the *sdbA$_{C89A}$* (C89A) mutant, and from their corresponding *ΔdegP* mutants. Lower molecular weight bands are degradation products recognized by anti-HA. (D) The oxidation state of the autolysin AtlS. Protein extracts from the parent and the *sdbA$_{C86P}$* mutant (C86P) were alkylated with maleimide-PEG$_2$-biotin and detected using avidin-AP. The same samples were run in adjacent lanes and reacted with anti-AtlS antisera to detect total AtlS as a loading control.

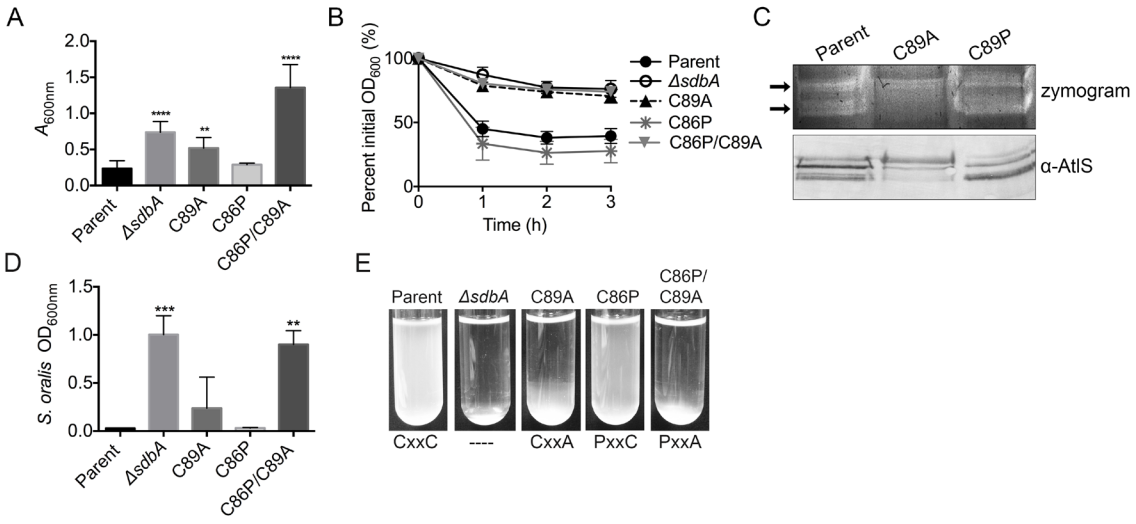

Figure 4. 3 The single C-terminal active site cysteine of $SdbA_{C86P}$ complements a *ΔsdbA* mutant

(A) Crystal violet staining of biofilms grown in 24-well microtiter plates. Biofilms were grown with the parent, *ΔsdbA* mutant, $sdbA_{C86P}$ (C86P), $sdbA_{C89A}$ (C89A), and $sdbA_{C86P/C89A}$ (C86P/C89A) mutants. Bars represent the mean and standard deviation of triplicates. (B) Autolysis of the parent, *ΔsdbA* mutant, and the SdbA cysteine mutants. Each point represents the mean of triplicates (C) Zymogram showing AtlS activity in the parent, $sdbA_{C86P}$ (C86P), and $sdbA_{C89A}$ (C89A) mutants. The zymogram gel was stained with methylene blue to enhance contrast. An equal volume of the autolysin extracts was used for the zymogram (upper panel) and for the Western blot reacted with anti-AtlS antisera as a loading control (lower panel). (D) Sth_1 bacteriocin activity of the parent, *ΔsdbA* mutant, and SdbA cysteine mutants. Bars show the growth of the indicator strain *S. oralis* 34. Error bars show mean and standard deviation of triplicates. (E) Overnight cultures showing mutants that lack SdbA enzymatic activity form clumps and sediment to the bottom of the tube. Asterisks denote a significant difference from the parent (**$P <$ 0.01; ****$P < 0.0001$; One-way ANOVA).

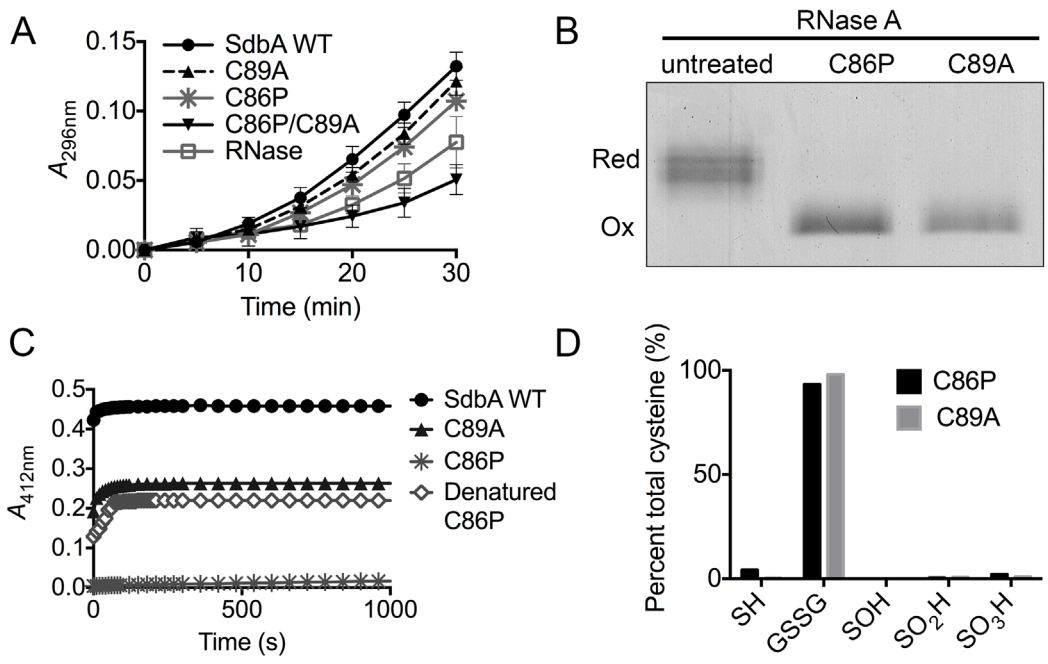

Figure 4. 4 Both SdbA single cysteine variants are active *in vitro*

(A) SdbA catalyzed refolding of reduced denatured RNase A in the presence of glutathione buffer. RNase A was incubated with the parent, $SdbA_{C86P}$ (C86P), $SdbA_{C89A}$ (C89A), $SdbA_{C86P/C89A}$ (C86P/C89A), or in buffer alone (RNase). Refolding was monitored by measuring the increase in absorbance at 296 nm as a result of RNase A catalyzed hydrolysis of cCMP. (B) Alkylation with maleimide-PEG_2-biotin to detect oxidation of RNase A catalyzed by SdbA single cysteine mutants. Maleimide-PEG_2-biotin adds 0.5 kDa to each reduced cysteine, causing the alkylated RNase A (reduced) to migrate slower on a 15% SDS-PAGE gel stained with Coomassie blue. (C) Reactivity of SdbA cysteines with DTNB. Reduced SdbA, the SdbA single cysteine variants, and $SdbA_{C86P}$ denatured with 6M guanidine HCl (Denatured C86P) were reacted with excess DTNB and the absorbance was monitored at 412 nm. (D) Mass spectrometry analysis of the oxidation state of SdbA cysteines following reaction with oxidized glutathione. The bars represent a semi-quantitative analysis of the peak intensities for various modifications on the active site cysteines (SH, thiol; GSSG, S-glutathionylation; SOH, sulfenic acid; SO_2H, sulfinic acid; SO_3H, sulfonic acid). The data are representative of two experiments.

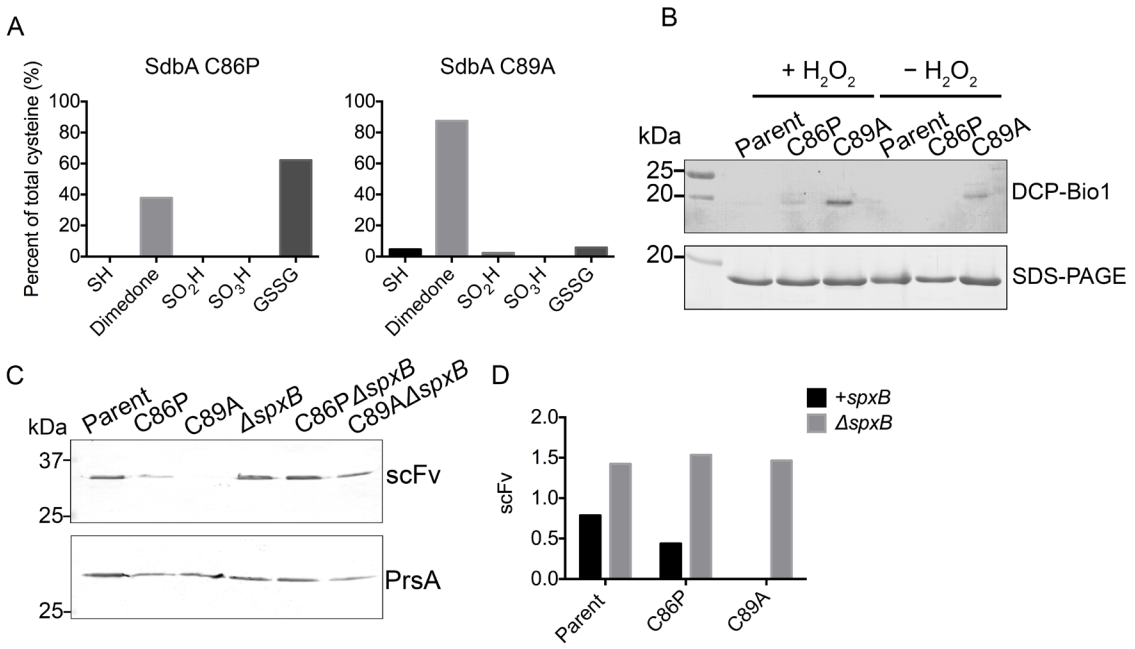

Figure 4. 5 The N-terminal cysteine of the $SdbA_{C89A}$ mutant protein is sensitive to oxidation

(A) Mass spectrometry analysis of the oxidation state of SdbA cysteines following reaction with hydrogen peroxide in the presence of the sulfenic acid probe dimedone. The bars represent a semi-quantitative analysis of the peak intensities for various modifications on the active site cysteines (SH, thiol; dimedone, sulfenic acid; SO_2H, sulfinic acid; SO_3H, sulfonic acid; GSSG, S-glutathionylation). The data are representative of two experiments. (B) Detection of sulfenylated cysteines by Western blot. The SdbA variants were incubated with or without 0.1 mM hydrogen peroxide and detected with a biotin-tagged sulfenic acid probe, DCP-Bio1 and avidin alkaline phosphatase (upper panel). The same samples were separated by 15% SDS-PAGE and stained with Coomassie blue as a loading control (lower panel). (C) Detection of scFv produced in the parent, $sdbA_{C86P}$ (C86P), and $sdbA_{C89A}$ (C89A) mutant, and their corresponding *ΔspxB* mutants. Membranes were probed with anti-HA to detect the scFv protein, and detection with anti-PrsA was used to standardize the protein concentration. (D) The Western blot was analyzed by densitometry using ImageJ. Bars represent the ratio of scFv to PrsA.

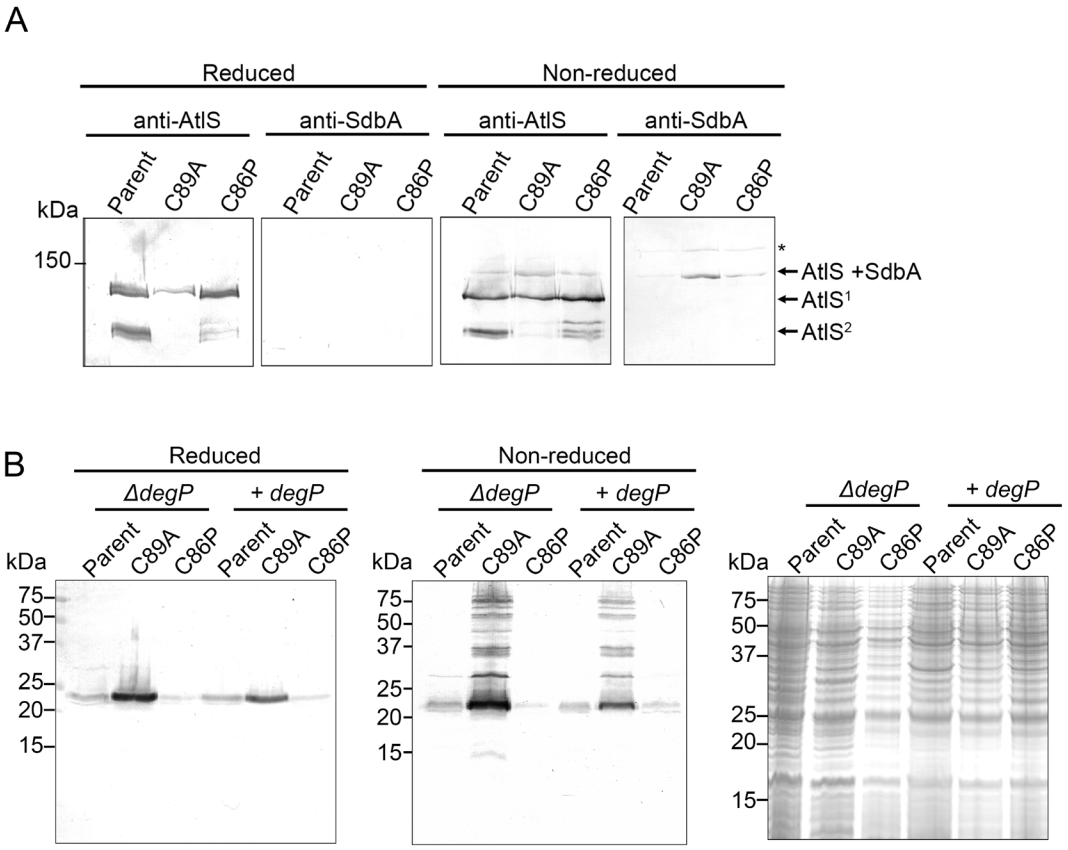
A
Reduced
Non-reduced
anti-AtlS
anti-SdbA
anti-AtlS
anti-SdbA
Parent
C89A
C86P
kDa
150
*
AtlS +SdbA
AtlS1
AtlS2
B
Reduced
Non-reduced
ΔdegP
+ degP
kDa
75
50
37
25
20
15

Figure 4. 6 $SdbA_{C89A}$ forms disulfide-linked complexes in the cell

(A) Complex formation between SdbA and AtlS. Surface proteins extracted with 4% SDS from the parent, $sdbA_{C86P}$ (C86P), or $sdbA_{C89A}$ (C89A) mutant were analyzed under reducing and non-reducing conditions and probed with either anti-AtlS or anti-SdbA antisera. Arrows indicate the AtlS + SdbA complex detected by both anti-SdbA and anti-AtlS antisera, the intact AtlS monomer ($AtlS^1$), and the processed AtlS monomer ($AtlS^2$). The asterisk denotes a second SdbA complex with an unknown protein. (B) Western blot of protein extracts from the parent, the SdbA single cysteine mutants, and their corresponding *ΔdegP* mutants run under non-reducing and reducing conditions and probed with anti-SdbA antisera. Under reducing conditions, SdbA runs at 21 kDa. The same samples were separated on SDS-PAGE and stained with Coomassie blue to show the total protein (right).

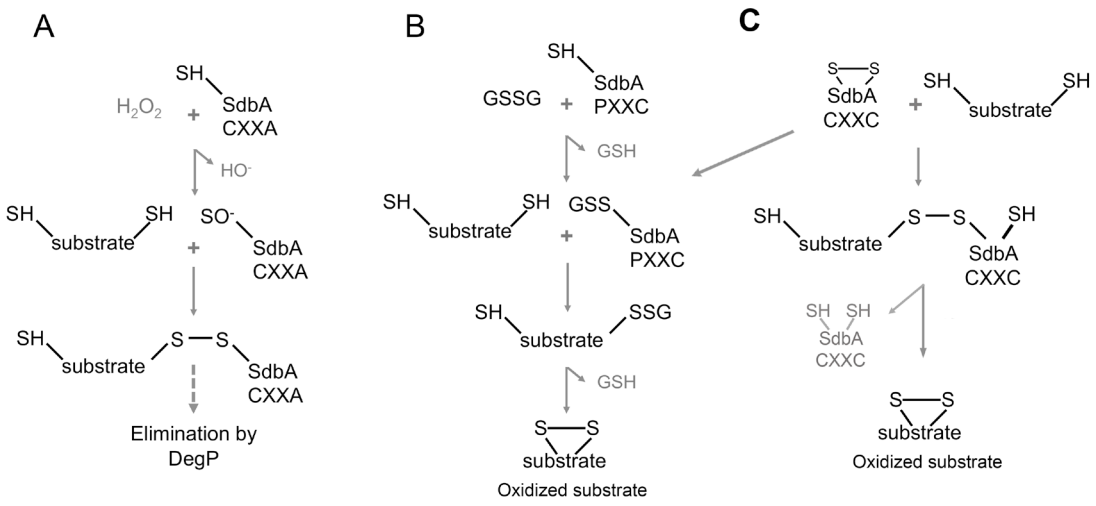

Figure 4. 7 Proposed model for SdbA activity in the cell

(A) Disulfide linked complexes formed by sulfenylated $SdbA_{C89A}$ cannot be resolved and are subsequently degraded by DegP. (B) The $SdbA_{C86P}$ mutant can use low molecular weight thiols to catalyze disulfide bond formation, adapted from (175, 224). (C) Wild type SdbA likely uses a dithiol mechanism, but could potentially also use the same pathway as the $SdbA_{C86P}$ mutant.

Chapter 5: Mutation of the Thiol-disulfide Oxidoreductase SdbA Activates the CiaRH Two-Component System Leading to Bacteriocin Expression Shutdown in *Streptococcus gordonii*

Davey L, Halperin SA, Lee SF. 2016. Mutation of the Thiol-Disulfide Oxidoreductase SdbA Activates the CiaRH Two-Component System, Leading to Bacteriocin Expression Shutdown in *Streptococcus gordonii*. J Bacteriol 198:321–331.

5.1 Summary

Streptococcus gordonii is a commensal inhabitant of the human oral cavity. To maintain its presence as a major component of oral biofilms, *S. gordonii* secretes inhibitory molecules such as hydrogen peroxide and bacteriocins to inhibit competitors. *S. gordonii* produces two non-modified bacteriocins, Sth_1 and Sth_2, that are regulated by the Com two-component regulatory system that also regulates genetic competence. Previously we found that the thiol-disulfide oxidoreductase SdbA is required for bacteriocin activity, however the role of SdbA in Com signaling was not clear. Here, we demonstrate that *ΔsdbA* mutants lacked bacteriocin activity because the bacteriocin gene *sthA* was strongly repressed and the peptides were not secreted. Addition of synthetic competence-stimulating peptide to the medium reversed the phenotype, indicating that the Com pathway was functional, but was not activated in the *ΔsdbA* mutant. Repression of bacteriocin production was mediated by the CiaRH two-component system, which was strongly upregulated in the *ΔsdbA* mutant, and inactivation of CiaRH restored bacteriocin production. The CiaRH induced protease DegP was also upregulated in the *ΔsdbA* mutant, although it was not required to inhibit bacteriocin production. This establishes CiaRH as a regulator of Sth bacteriocin activity, and links the CiaRH and Com systems in *S. gordonii*. It also suggests that either SdbA or one of its substrates is an important factor in regulating activation of the CiaRH system.

5.2 Importance

Streptococcus gordonii is a non-cariogenic colonizer of the human oral cavity. To be competitive in the oral biofilm, *S. gordonii* secretes antimicrobial peptides called bacteriocins that inhibit closely related species. Our previous data showed that mutation of the disulfide oxidoreductase SdbA abolished bacteriocin production. In this study, we show that mutation of SdbA generates a signal that upregulates the CiaRH two-component system, which in turn down-regulates a second two-component system, Com, which regulates bacteriocin expression. Our data show that these systems are also linked in *S. gordonii*, and reveal that the cell's ability to form disulfide bonds is sensed by the CiaRH system.

5.3 Introduction

Oral biofilms are a highly competitive, constantly fluctuating environment. The bacteria that colonize this niche contend with a high density of competing bacteria of an estimated 2000 different taxa and dramatic environmental changes dependent on host behavior (180, 274). *Streptococcus gordonii* is a pioneer colonizer of this environment, where it initiates biofilm formation by binding directly to the acquired salivary pellicle on the tooth surface (180, 275). Once established, *S. gordonii* persists within the host as part of the oral microflora. The presence of *S. gordonii* is associated with oral health (276, 277), and it has been shown to inhibit biofilm formation by cariogenic species (184, 278).

S. gordonii uses several strategies to gain an edge over its competitors and successfully colonize the oral cavity. These include the production of inhibitory molecules to prevent growth and biofilm formation by related species. For example, *S. gordonii* produces hydrogen peroxide as a metabolic byproduct, which inhibits growth of neighboring species that are more sensitive to oxidative stress (185, 265). It also targets closely related species more directly, by secreting small antimicrobial peptides called bacteriocins (188). And to defend itself from similar counter attacks, it secretes a protease that degrades the signaling peptide required for bacteriocin production and biofilm formation in a competitor, *Streptococcus mutans* (279).

S. gordonii DL-1 Challis produces two non-lantibiotic bacteriocins called Sth_1 and Sth_2 encoded by *sthA* and *sthB*, respectively. Sth_1 is active against other *S. gordonii* strains, including C219 and Wicky (194), while Sth_1 and Sth_2 work in conjunction to target other streptococci, such as *S. mitis* and *S. oralis* (188). Sth_1 and Sth_2 are the only known bacteriocins produced by *S. gordonii*, and they are both regulated by the Com two-component regulatory system, which also controls natural genetic competence (187, 188).

With the exception of the Sth bacteriocins, which are unique to *S. gordonii*, the Com signaling system of *S. gordonii* is similar to the pathway in *Streptococcus pneumoniae* (186, 187, 191). Competence in *S. gordonii* occurs during the early exponential growth phase and is activated by competence-stimulating peptide (CSP), a small secreted autoinducer derived from a larger peptide encoded by *comC* (187, 191). Processing and secretion of CSP is mediated by an ABC-transporter, ComAB, which recognizes peptides with a specific double glycine motif (GG-motif) in the N-terminal leader sequence. When the extracellular concentration of CSP surpasses a threshold level, a membrane bound histidine kinase, ComD, phosphorylates its cognate response regulator ComE, thereby activating the Com pathway and ultimately modulating the expression of over 150 genes (187).

The genes controlled by the Com system can be divided into two groups: early genes that are directly activated by ComE, such as *comCDE* and *comAB*, and late genes that are regulated by two alterative sigma factors, ComR1 and ComR2, homologs of *S. pneumoniae* ComX (191). Unlike *S. pneumoniae*, the *S. gordonii comR* genes lack an identifiable ComE binding site and are activated by an unknown mechanism (191). Nevertheless, the ComR sigma factors direct expression of the late genes, which include the DNA uptake machinery for genetic competence and the bacteriocin genes *sthA* and *sthB* (187, 188) (Fig. 5.6A).

The systems regulating bacteriocin production in other streptococci have been studied in greater detail than those in *S. gordonii,* and this has revealed greater

complexity, often involving multiple regulatory systems. *Streptococcus pneumoniae* produces two bacteriocins encoded by the *blp* locus that are controlled by a dedicated quorum sensing and secretion system, however, activity of the Blp system is also modulated by at least two additional regulatory systems, including ComDE (280) and CiaRH (281). Although the mechanisms involved are not fully understood, the serine protease HtrA (DegP) also appears to play an important role in regulating *S. pneumoniae* bacteriocin production (281, 282). Similarly, *S. mutans* produces at least 10 different bacteriocins, that vary by strain and include both lantibiotic and non-lantibiotics (283), and are subject to regulation by complex and overlapping systems, including ComDE (284, 285), CiaRH (286), VicRK (287), HdrRM (288) and BrsRM (289). The effect of regulatory systems other than ComDE on bacteriocin production in *S. gordonii* is not known.

Previously, we found that *S. gordonii* mutants lacking the thiol-disulfide oxidoreductase SdbA did not exhibit bacteriocin activity (101). SdbA catalyzes disulfide bond formation in secreted proteins, and these bonds are important for protein folding and activity. It is not unusual for bacteriocins to contain disulfide bonds, and all class IIa bacteriocins (pediocin-like), which include those produced by *Streptococcus uberis* and *Streptococcus thermophilus*, contain a disulfide bond that is essential for activity (154, 290), as do many lantibiotic bacteriocins, such as bovicin produced by *Streptococcus bovis* HJ50 (156). *S. gordonii* bacteriocins, however, do not contain cysteines to form a disulfide bond and the role of SdbA in their production was unclear.

In this study, we set out to determine how SdbA affects bacteriocin production. Using SdbA active site mutants, we confirmed that bacteriocin production does require the enzyme's disulfide oxidoreductase activity. *ΔsdbA* mutants did not secrete bacteriocins into the medium, and expression of the bacteriocin encoding gene *sthA* was dramatically reduced compared to the parent, as was the gene encoding the CSP autoinducer, *comC*. The effect of SdbA on the Com pathway and bacteriocin production was indirect and required the CiaRH two-component system, which was upregulated in *ΔsdbA* mutants.

5.4 Results

5.4.1 The Thiol-Disulfide Oxidoreductase SdbA is Required for Bacteriocin Production

Previously, we found that *ΔsdbA* mutants were defective in bacteriocin activity (101). To investigate how SdbA affects bacteriocin production, we started by constructing a catalytically dead SdbA active site mutant to determine if bacteriocin production requires SdbA's oxidoreductase activity. The active site of thiol-disulfide oxidoreductases contain a CXXC motif, where X is any amino acid, and the two cysteines are required for activity (44). To eliminate SdbA oxidase activity, the N and C-terminal cysteines were mutated to proline and alanine, respectively, and the loss of enzyme activity was confirmed using an RNase A folding assay (APPENDIX B3).

Bacteriocin production by the active site mutant was tested in an activity assay using the target strains *S. mitis* and *S. oralis* (188, 194). Consistent with our previous results, supernatants obtained from early exponential phase cultures of the *S. gordonii* parent contained active bacteriocins that inhibited the growth of the target strains (Fig. 5.1A and 5.1B). In contrast, supernatants from the *ΔsdbA* mutant and the SdbA active site mutant failed to inhibit growth. When a functional *sdbA* gene was reintroduced onto the chromosome of the *ΔsdbA* mutant, bacteriocin activity was restored, confirming that the enzyme activity of SdbA is required for normal bacteriocin activity.

Because bacteriocin production is a transient, growth phase-dependent phenomenon (194, 291), it was possible that the window of growth where bacteriocin production occurs was altered in the *ΔsdbA* mutant, and that bacteriocins were being produced, but at a different time point than in the parent. Bacteriocin expression peaks at 15 min after exposure to CSP (187), and bacteriocin activity can be detected in culture supernatants during early exponential growth (2 h), but not at the mid to late exponential phase (6 h) (194), suggesting that protein is degraded in older cultures. To determine if the *ΔsdbA* mutant produced bacteriocins at a later growth stage than the parent, we assayed bacteriocin activity against *S. mitis* using *S. gordonii* supernatants harvested at different

time points. Under the conditions used in this study, there was no difference in the growth rate between the parent and the *ΔsdbA* mutant (data not shown). Bacteriocin activity in the parent abruptly shut off as the optical density of the culture increased from OD_{600} = 0.350 to 0.450, and the growth of *S. mitis* was no longer inhibited (Fig. 5.1C). In contrast, the *ΔsdbA* mutant showed no indication of bacteriocin activity at any of the time points tested, even as the culture reached the mid-exponential phase of growth.

An alternative explanation for the lack of bacteriocin activity in the *ΔsdbA* mutant was that the peptides were being produced, but they were not being processed to their active form. *S. gordonii* bacteriocins are produced as small peptides, processed from larger proteins during secretion. Like the CSP autoinducer, Sth bacteriocins contain a GG-motif that directs their secretion via ComAB, which couples transport across the membrane with cysteine protease activity that cleaves at the GG-motif of the signal sequence (189, 292). ComAB is the only transporter of this type encoded by *S. gordonii* (293). Thus, it was possible that the *ΔsdbA* mutant could have a defect in bacteriocin processing and/or secretion that would result in a loss of biological activity. To determine if the *ΔsdbA* mutant secretes an inactive form of Sth_1, we tested for the presence of bacteriocins in culture supernatants by immuno-affinity chromatography. Sth_1 bacteriocins were isolated from supernatants obtained from the parent and an *sdbA* complemented mutant, but were not detected in supernatants from the *ΔsdbA* mutant (Fig. 5.2A). The signal from the *ΔsdbA* mutant was the same as the negative control with medium alone. Even when the volume of supernatant was increased four-fold, Sth_1 was not detected above the background levels, and thus the bacteriocin was either produced at very low levels or not at all (Fig. 5.2B).

Finally, we used quantitative real-time PCR (qPCR) to test expression of the bacteriocin gene *sthA* in the *ΔsdbA* mutant. Expression of *sthA* was markedly lower in the *ΔsdbA* mutant compared to the parent, with an average decrease of more than 1500-fold lower than the parent, indicating that the mutant lacked bacteriocin activity because the gene was not transcribed (Fig. 5.3A).

5.4.2 The Com Pathway is Not Activated in the *ΔsdbA* Mutant

Bacteriocin expression in *S. gordonii* is regulated by the Com two-component system (188). The process is initiated by an autoinducer, encoded by *comC*, which is processed during secretion to produce the mature competence-stimulating peptide (CSP). When CSP levels reach a threshold concentration, the ComDE two-component system becomes activated ultimately inducing expression of the bacteriocin genes, *sthAB* (187, 188). The lack of *sthA* expression in the *ΔsdbA* mutant suggested that the ComDE pathway had not been activated, which is consistent with our previous observation that the *ΔsdbA* mutant is also defective in genetic competence (101) (APPENDIX B1), a phenotype that is regulated by the same system (187).

To assess activity of the Com system in the *ΔsdbA* mutant, we tested expression of *comC*, which encodes the CSP autoinducer that activates the system. CSP is required for expression of the alternative sigma factors *comR1* and *comR2* that induce bacteriocin expression. Consistent with the lack of bacteriocin activity and competence, *comC* expression in the *ΔsdbA* mutant was down regulated by an average of 247-fold relative to the parent. Complementation of *sdbA* reversed the phenotype, suggesting that activation of the Com pathway required SdbA.

Two key elements required for activity of the Com pathway are the ComDE two-component system that senses extracellular CSP, and the ComAB transporter that secretes both CSP and bacteriocins. Inactivation of any of these components would abolish bacteriocin production, and could explain the *ΔsdbA* mutant phenotype. To determine if ComDE was functional in the *ΔsdbA* mutant, we tested the ability of exogenous synthetic CSP to artificially activate the pathway. When exogenous CSP was added to the culture medium, the *ΔsdbA* mutant expressed both *comC* and *sthA* at a level similar to the parent, with a 1.9 and 2.2-fold increase over the parent grown in BHIS (Fig. 5.3C). Induction was somewhat stronger for the parent grown with CSP, with a 3.3-fold increase in *comC* and 5.2-fold increase in *sthA,* compared to BHIS alone. Nevertheless, the ability of the *ΔsdbA* mutant to respond to exogenous CSP confirmed that ComDE was functional.

Heng et al. previously demonstrated that the ComAB transporter is essential for bacteriocin secretion in *S. gordonii*, and that mutation of either ComA or ComB eliminated bacteriocin activity, even when expression of the bacteriocin genes was induced with exogenous CSP (188). Thus, we hypothesized that the ComAB transporter might be inactive in the *ΔsdbA* mutant. If the ComAB transporter was inactive, we would expect to see a strong induction of the bacteriocin genes without a corresponding increase inhibitory activity against Sth sensitive strains. To determine if *sthA* expression induced by exogenous CSP led to bacteriocin secretion in the *ΔsdbA* mutant, we tested for the presence of bacteriocins in culture supernatants by immuno-affinity chromatography. Secreted bacteriocins were successfully purified from culture supernatants obtained from the *ΔsdbA* mutant following induction with CSP, indicating that the transporter was at least partially functional, or that the *ΔsdbA* mutant was secreting the bacteriocins using an unknown mechanism (Fig. 5.2B). The bacteriocins were biologically active, suggesting that they had been properly processed, and supernatant from the *ΔsdbA* mutant efficiently inhibited growth of the target strain *S. mitis* (Fig. 5.3D). Thus, the *ΔsdbA* mutant was capable of bacteriocin production, and the lack of bacteriocin activity appeared to stem from the initial activation of the Com signaling pathway.

5.4.3 Expression of the CiaRH Two-Component System is Upregulated in the *ΔsdbA* Mutant

Given that the components of the Com signaling system appeared to be functional, we reasoned that the lack of bacteriocin activity in the *ΔsdbA* mutant might involve an indirect mechanism. In *S. pneumoniae*, the CiaRH two component system represses both bacteriocin production and the Com signaling system (281, 294), which was strikingly similar to the phenotypes we observed in the *ΔsdbA* mutant (101). Although the signals detected by CiaH, the sensor protein, are not known, certain conditions can increase activity of the system (295–298), and we hypothesized that inactivation of *sdbA* might create a signal that increases CiaRH activity, leading to a loss of bacteriocin production.

To determine if CiaRH is activated in the *ΔsdbA* mutant, we used qPCR to assess expression of known *cia*-induced genes. We tested *ciaR* and *degP* because they have been identified as part of the *cia* regulons in *S. pneumoniae* and *S. mutans* (295, 298), and the *S. gordonii degP* gene contained a CiaR binding motif that matched the sequence and location reported for *S. pneumoniae* (299).

Compared to the parent strain, there was a significant increase in *ciaR* expression in the *ΔsdbA* mutant, with a 4-fold increase over the parent (Fig. 5.4A). Similarly, *degP* expression in the *ΔsdbA* mutant was upregulated 4.5-fold compared to the parent (Fig. 5.4B). This increase was CiaRH dependent, and *degP* was repressed by 6.8-fold in the *ΔsdbA ΔciaRH* mutant. The expression data was confirmed by Western blotting, which showed notably higher levels of DegP protein in the *ΔsdbA* mutant compared to the parent (Fig. 5.4C). In contrast, *ciaR* and *degP* expression in the SdbA complemented mutant was similar to the parent.

Interestingly, cultures induced with exogenous CSP showed even higher levels of *ciaR* and *degP* expression, which increased by 7.5 and 10.6-fold in the *ΔsdbA* mutant (Fig. 5.4D). Although the parent also showed increased *ciaR* and *degP* expression, there was considerable variation and the difference was not significant (Fig. 5.4D). This is consistent with a previous investigation of CSP induced genes in *S. gordonii,* which identified a 2.25 increase in *degP* expression, but did not identify *ciaR* among CSP up-regulated genes (187). Thus, there might be some cross-regulation between the ComDE and CiaRH systems, or the stress of competence induction might affect CiaRH activity. Taken together, the results indicate that mutation of SdbA generates a signal that results in increased CiaRH activity, which is further upregulated with competence induction.

5.4.4 CiaRH Mediates Repression of the Bacteriocin Genes in the *ΔsdbA* Mutant

CiaRH inhibits the Com genetic competence system in *S. pneumoniae* by repressing *comC*, the gene that encodes CSP (294). The mechanism involves small non-coding RNAs that are regulated by CiaRH, which are thought to bind and prevent translation of *comC* mRNA (294). Because the Com system regulates bacteriocin genes

in *S. gordonii*, repression of *comC* could also eliminate bacteriocin production. Thus, we hypothesized that the enhanced CiaRH activity observed in the *ΔsdbA* mutant could lead to repression of the Com pathway. This scenario is consistent with our finding that synthetic CSP activates bacteriocin production in the *ΔsdbA* mutant, despite up-regulating *ciaR* expression, since it would circumvent the need for *comC* to activate the pathway.

Using published sequences for predicted *S. gordonii* csRNAs identified by Marx et al. (300), we searched the genome of *S. gordonii* for potential targets using the program IntaRNA (301). Although the bacteriocin genes *sthAB* were not among the predicted targets, *comC* was identified as a statistically significant ($p = 0.017 – 0.03$) target for multiple csRNAs (csRNA2-1, csRNA2-2, csRNA7) (Fig. 5.5A). The predicted csRNA binding sites centered on the start codon and ribosomal binding site, and are almost identical to the experimentally verified csRNA binding sites on *S. pneumoniae comC* (294).

To verify that CiaRH affected *comC* and *sthA* expression in the *ΔsdbA* mutant, we tested expression in a *ΔsdbAΔciaRH* mutant. Consistent with a role in inhibiting the Com pathway, inactivation of *ciaRH* in the *ΔsdbA* mutant increased expression of *comC* and *comE* to a level that was not significantly different than the parent (Fig. 5.5B). Similarly, *sthA* also showed de-repression in the *ΔsdbAΔciaRH* mutant (Fig. 5.5C). Mutation of *ciaRH* in the parent did not significantly affect expression of *comC* or *sthA* (Fig. 5.5B and 5.5C), which is consistent with previous observations in *S. pneumoniae* (302). Thus, CiaRH influences *comC* and *sthA* expression in the *ΔsdbA* mutant.

5.4.5 Inactivation of CiaRH Restores Bacteriocin Activity to the *ΔsdbA* Mutant

Finally, we used an activity assay to determine if mutation of CiaRH restored bacteriocin production to the *ΔsdbA* mutant. Consistent with the qPCR data, the *ΔsdbAΔciaRH* mutant produced biologically active bacteriocins, sufficient to inhibit the growth of *S. mitis* (Fig. 5.5D). Mutation of *ciaRH* in the parent had no effect on activity, whereas complementation with a single copy of *ciaRH* onto the chromosome of the

ΔsdbAΔciaRH mutant eliminated bacteriocin activity. This confirmed that the CiaRH signaling system mediated the lack of bacteriocin activity in the *ΔsdbA* mutant.

5.5 Discussion

In this study we identified the CiaRH two-component system as an important regulator of *S. gordonii* bacteriocin production, and found that CiaRH was upregulated in mutants lacking the disulfide bond forming enzyme SdbA. Activity assays and immuno-affinity chromatography confirmed that mutation of SdbA abolished bacteriocin production. However, production could be restored by exogenous CSP, suggesting that the individual components required for bacteriocin processing and secretion remained functional, and that these proteins might not require disulfide bonds formed by SdbA. Instead, mutation of SdbA generates a signal that causes increased CiaRH activity, which in turn inhibits bacteriocin production (Fig. 5.6).

The CiaRH system has been found to affect genetic competence, stress resistance, colonization, and bacteriocin production in both *S. pneumoniae* and *S. mutans* (281, 286, 295, 298, 303), however, activity of the CiaRH system in *S. gordonii* has not been investigated as thoroughly. In one of the few studies looking at the *S. gordonii* CiaRH system, Liu and Burne (303) determined that CiaRH was important for survival at low pH and efficient induction of the arginine deiminase system that augments acid tolerance. Our data adds to the roles of CiaRH in *S. gordonii*, showing that it is involved in regulation of the protease DegP and bacteriocin production.

The CiaRH system regulates *htrA* (*degP*) expression in *S. pneumoniae* and *S. mutans* (298, 302, 304, 305), and our results suggest that *degP* is part of the *ciaRH* regulon in *S. gordonii* as well. CiaRH was required for up-regulation of *degP* in the *ΔsdbA* mutant, and mutation of *ciaRH* diminished *degP* expression, suggesting that the system might also affect basal levels of DegP (Fig. 5.4B). This is consistent with observations made in *S. pneumoniae*, where the system was found to have a relatively high level of constitutive activity (299). Sequence analysis of the *degP* promoter region revealed a possible CiaR binding site matching that described by Halfmann et al. which

consists of a consensus sequence of TTTAAG – 5 bp – (T/A)TTAAG located approximately 10 bp up from the -10 position (306).

While regulation of DegP by the CiaRH system appears to be consistent across various streptococci, the role for CiaRH in bacteriocin production is surprisingly species-specific. For example, CiaH positively regulates bacteriocin production in *S. mutans*, and *ciaH* mutants lack mutacin activity (286). In contrast, similar to our findings in *S. gordonii,* the CiaRH system in *S. pneumoniae* represses bacteriocin activity (281, 282). In *S. pneumoniae,* CiaRH inhibits bacteriocin production through HtrA (DegP), which was shown to disrupt the BlpAB transporter required for bacteriocin processing and secretion. Thus, inactivation of HtrA can alleviate CiaRH mediated repression and increase the amount of secreted bacteriocins (282).

Although *degP* was up-regulated in the *S. gordonii ΔsdbA* mutant, the protease does not appear to inhibit bacteriocin production, and mutation of *degP* failed to restore bacteriocin activity to the *ΔsdbA* mutant (Fig. 5.5D). However, DegP might play a minor role in regulating bacteriocin activity, the ComAB transporter, or CSP levels. Despite multiple attempts to detect and quantify CSP in the culture medium using anti-CSP antibodies, we were unable to detect the peptide due to a strong cross-reaction with the BHIS medium required for activation of the Com pathway.

A key difference between bacteriocin production in *S. pneumoniae* and *S. gordonii* is in the systems that regulate their production, and unlike *S. pneumoniae*, the Com pathway controls bacteriocin production in *S. gordonii* (188). The CiaRH system has long been known to influence the Com pathway *S. pneumoniae* (307), where mutations that up-regulate CiaR activity result in a loss of competence, while *ΔciaR* mutants grow poorly and are susceptible to lysis upon exposure to CSP (302). Unlike *S. pneumoniae*, we did not observe any obvious lysis or growth defects in *S. gordonii ΔciaRH* or the *ΔsdbAΔciaR* mutant when CSP was added to the culture. Our finding that mutation of *ciaRH* resulted in de-repression of *comC* in the *ΔsdbA* mutant, but not in overexpression compared to the parent, is consistent with previously reported results for

S. pneumoniae, where *comC* expression in a *ΔciaR* mutant was similar to the parent (302). This might be because CiaR is not inhibiting competence by binding to *comC* to repress transcription, but working via a different mechanism that involves post-transcriptional regulation.

Several studies have analyzed the *S. pneumoniae* CiaRH regulon through microarray analysis (298, 302, 308), and CiaR controls expression of 25 genes including five small non-coding RNAs, called csRNAs (299, 306). Analysis of the csRNAs provided the first direct link between CiaRH signaling and genetic competence, when *comC*, the gene encoding the CSP autoinducer that activates the Com pathway, was identified as a target of multiple csRNAs (294). The csRNAs are thought to work by binding to the Shine-Delgarno sequence of complementary transcripts to prevent translation (294, 309, 310). This mechanism is consistent with our observation that both the parent and the *ΔciaRH* mutant show similar *comC* expression the during competence, a finding that has also been reported for *S. pneumoni*ae (302). *S. gordonii* is predicted to encode several csRNAs (300), and this could be a potential mechanism for CiaRH to influence bacteriocin production. However, additional analysis that is beyond the scope of this study will be required to determine the biological roles of *S. gordonii* csRNAs.

The signals that activate CiaRH are unknown (299), and it is not clear how mutation of SdbA induces CiaRH in *S. gordonii*. Because SdbA is required for disulfide bond formation (101), CiaRH might respond to a general stress created by misfolding of SdbA substrates, or by the loss of function a specific SdbA substrate. Bacteria sense envelope stress using two component systems, and thiol-disulfide oxidoreductases have been linked to these stress responses in both Gram-negative and Gram-positive species (311–313). For example, *Bacillus subtilis* senses envelope stress using a system called CssRS, which, like CiaRH in streptococci, regulates expression of the DegP family proteases HtrA and HtrB (118, 314). Notably, expression of a misfolded disulfide bonded protein, alkaline phosphatase, resulted in a strong induction of the CssRS system and a four-fold increase in *htrB* expression (118). A similar scenario might occur in *S. gordonii*,

where mutation of SdbA causes protein misfolding that either directly or indirectly triggers an increase in CiaRH activity.

Interestingly, protein misfolding has been shown to enhance, rather than repress, ComDE activity in *S. pneumoniae* (315). This increase is mediated by HtrA (DegP), which degrades the *S. pneumoniae* CSP signaling peptide. Under conditions of high ribosomal coding errors, the increased amount of misfolded protein is thought to competitively inhibit HtrA and prevent degradation of CSP (315, 316). Thus, protein quality control, CiaRH, and ComDE appear to be related in various streptococci, although there are clear species-specific differences in how these systems affect one another.

In conclusion, we have demonstrated that mutation of the disulfide oxidoreductase SdbA activates the CiaRH two-component system, which in turn represses bacteriocin expression. Our data reveal a link between CiaRH and the Com system in *S. gordonii*, both of which play important roles in bacteriocin production, genetic competence, stress resistance, and biofilm formation.

5.6 Acknowledgments

This study is funded by the Natural Sciences and Engineering Research Council of Canada. LD is a recipient of a NSERC post-graduate scholarship, an IWK graduate studentship, and a Nova Scotia Health Research Foundation Scotia Scholars award.

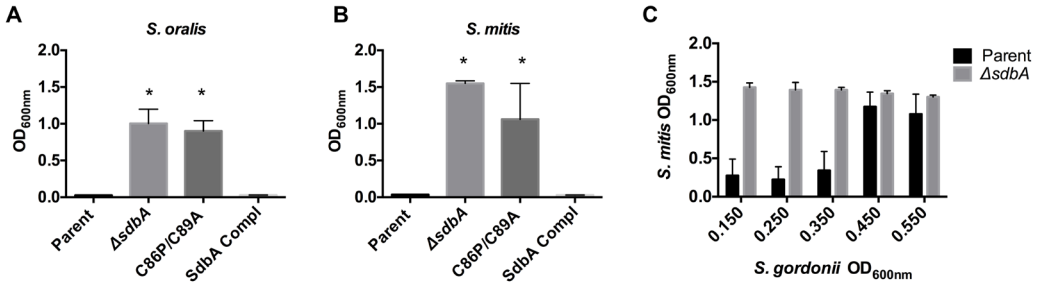

Figure 5. 1 SdbA is required for bacteriocin activity

Inhibitory activity of *S. gordonii* bacteriocins secreted into the medium was tested against two target strains. (A) Growth of *S. oralis* and (B) *S. mitis* in the presence of filter sterilized culture supernatants from the *S. gordonii* parent, *ΔsdbA* mutant, SdbA active site cysteine mutant (C86P/C89A), and an *sdbA* complemented mutant (SdbA Compl) grown to a density of OD_{600} = ~0.200. (C) Growth of *S. mitis* in the presence of culture supernatants obtained from the *S. gordonii* parent or *ΔsdbA* mutant at varying time points. Results are means ± SD of three experiments. Asterisks indicate a significant difference from the parent, $P < 0.001$.

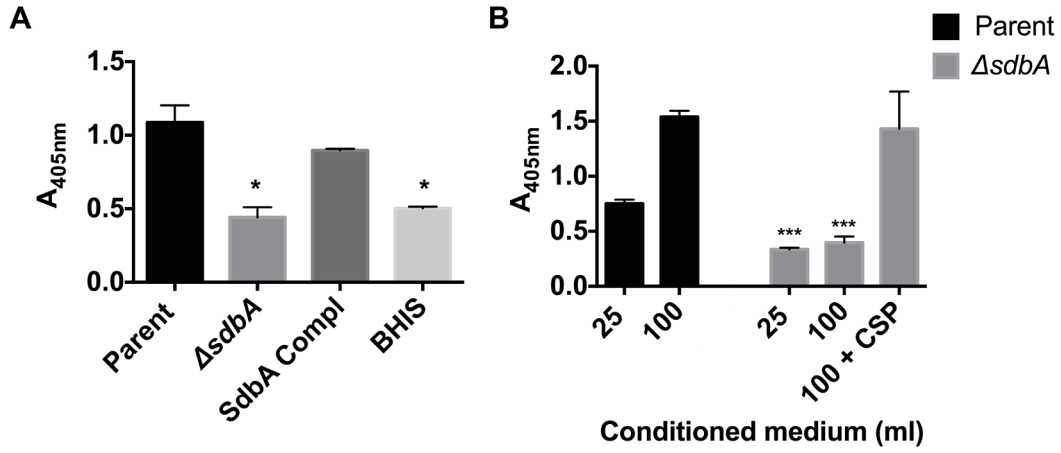

Figure 5. 2 The *ΔsdbA* mutant does not secrete Sth1 bacteriocins

Secreted bacteriocins were isolated from culture supernatants using Sth_1-specific rabbit IgG-protein A sepharose beads and detected by a mouse anti-Sth_1 antibody in ELISA. (A) Detection of Sth_1 captured from 25 ml of culture supernatant prepared from the parent, *ΔsdbA* mutant, or *sdbA* complemented mutant (SdbA Compl). BHI medium with 5% serum (BHIS) was used a negative control. (B) Detection of Sth_1 captured from 25 and 100 ml of culture supernatant from the parent, *ΔsdbA* mutant, and *ΔsdbA* mutant induced with exogenous CSP for 30 min. Results are means ± SD of three experiments. Asterisks indicate a significant difference from the parent (***$P < 0.001$, * $P < 0.05$).

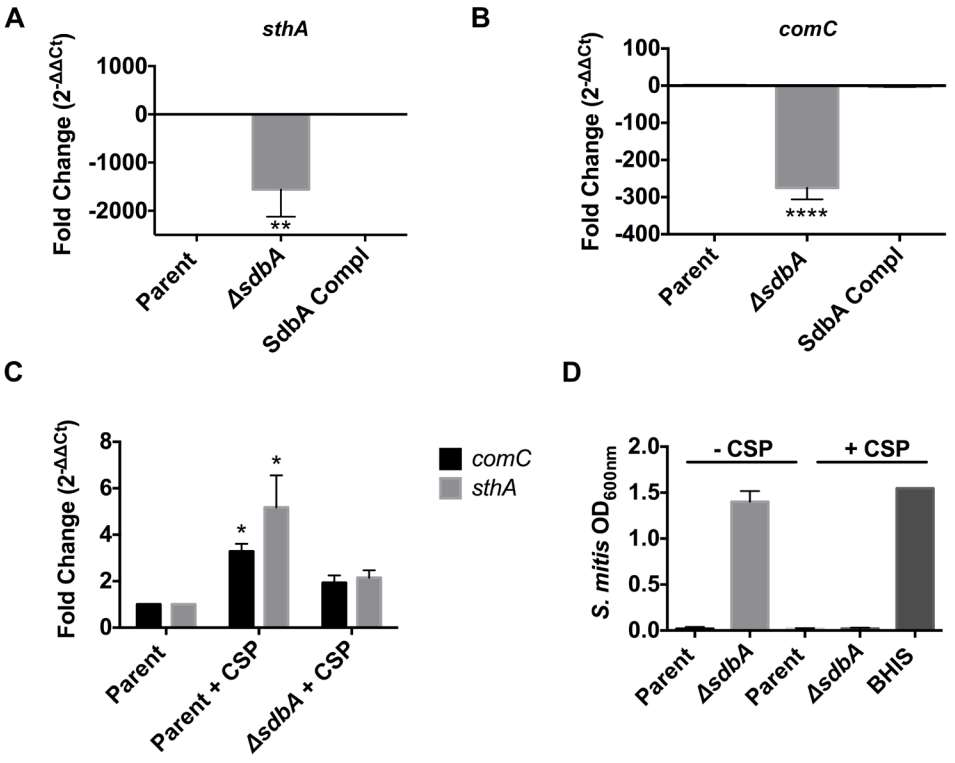

Figure 5. 3 The *ΔsdbA* mutant requires exogenous CSP to activate the Com two-component system

Expression of (A) *sthA* and (B) *comC* in the parent, the *ΔsdbA* mutant, and the *sdbA* complemented mutant (SdbA Compl) grown in BHI with 5% serum. (C) Expression of *comC* and *sthA* following induction with exogenous CSP. Synthetic CSP was added to cultures at a density of OD_{600} = 0.150 and the cultures were grown for an additional 30 min prior to RNA isolation. Bars represent expression levels relative to the parent grown in BHI with 5% serum without exogenous CSP. (D) Bacteriocin activity assay with *S. mitis* as the target strain. CSP was added to *S. gordonii* cultures to induce bacteriocin production 30 min before the culture supernatants were filter sterilized and inoculated with the target strain. BHI medium with synthetic CSP was used as a negative control, and confirms that CSP does not affect growth of *S. mitis*. Results are means ± SD of three experiments. Asterisks indicate a significant difference from the parent (****$P < 0.0001$, **$P < 0.01$, *$P < 0.05$).

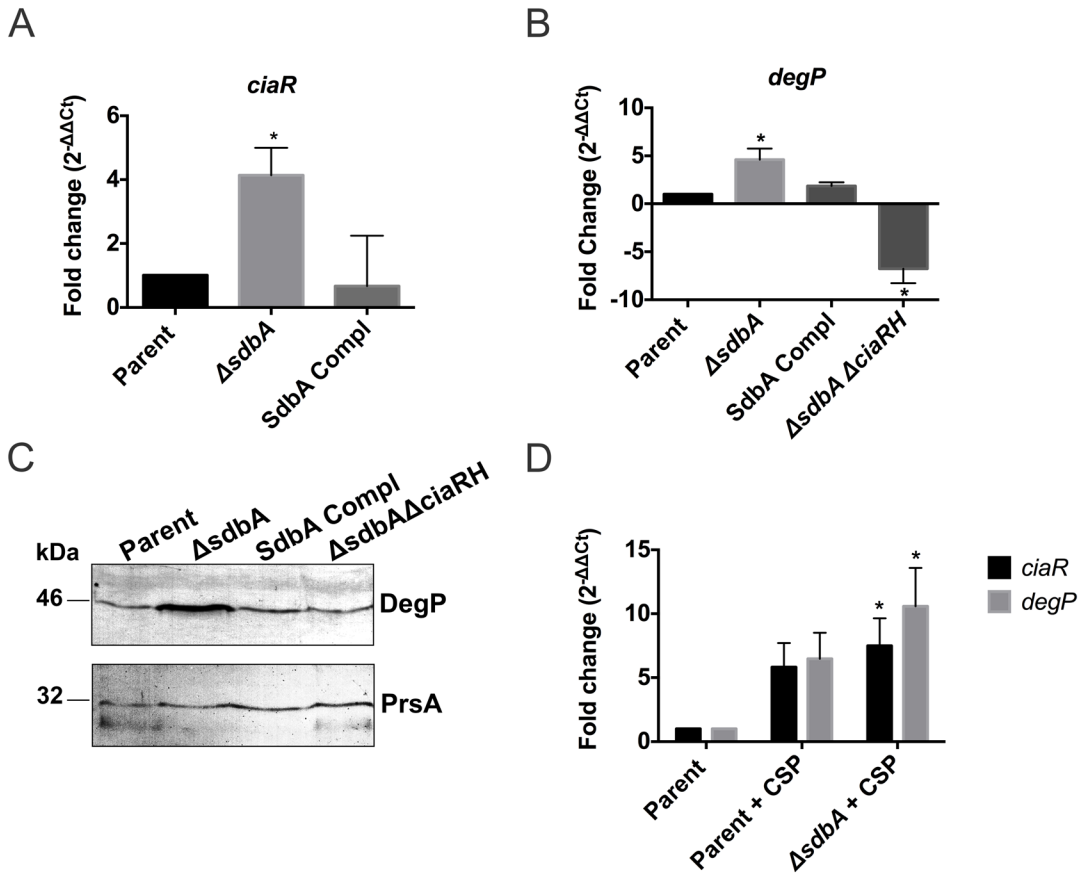

Figure 5. 4 The CiaRH system is activated in the *ΔsdbA* mutant

Expression of the *cia*-induced genes *ciaR* and *degP*. (A) Expression of *ciaR* in the parent, *ΔsdbA* mutant, and SdbA complemented mutant (SdbA Compl). (B) Expression of *degP* in the parent, *ΔsdbA*, *ΔsdbAΔciaRH*, and *sdbA* complemented mutant (SdbA Compl) ($P < 0.05$). (C) Western blot showing DegP detected in cell extracts from the parent, *ΔsdbA*, *ΔsdbAΔciaRH*, and *sdbA* complemented mutant (SdbA Compl). The same samples were electrophoresed on duplicate gels and reacted with either anti-HtrA (DegP) or anti-PrsA antisera as a loading control. (D) Expression of *ciaR* and *degP* in cultures induced with exogenous CSP. Results are means ± SD of three experiments. Asterisks indicate a significant difference from the parent (****$P < 0.0001$, **$P < 0.01$, *$P < 0.05$).

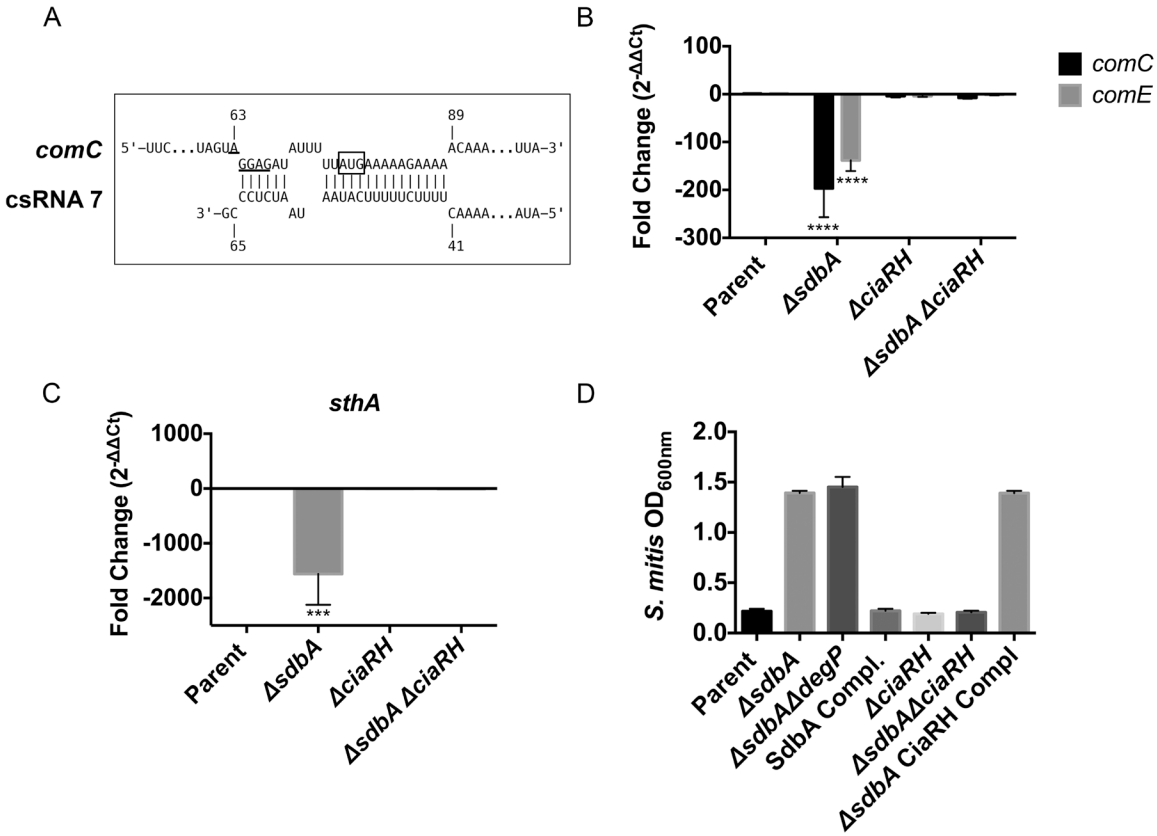

Figure 5. 5 CiaRH represses *comC* and *sthA* in the *ΔsdbA* mutant

(A) Interaction between csRNA7 (300) and *comC* predicted by IntaRNA (301). The csRNA sequence was searched against RefSeq sequence for *S. gordonii* Challis (NC_009785). The ribosomal binding site is underlined and the box indicates the start codon. Expression of (B) *comC* and *comE* (C) *sthA* in the parent, *ΔsdbA*, *ΔciaRH*, and *ΔsdbAΔciaRH* mutants. (D) Bacteriocin activity of the parent, *ΔsdbA* mutant, *ΔsdbAΔdegP, sdbA* complemented mutant (SdbA Compl), *ΔciaRH, ΔsdbAΔciaRH,* and the *ciaRH* complemented mutant (*ΔsdbA* CiaRH Compl). Supernatants were filtered sterilized and inoculated with *S. mitis* as the target strain. Results are means ± SD of three experiments. Asterisks indicate a significant difference from the parent (****$P < 0.0001$, ***$P < 0.001$).

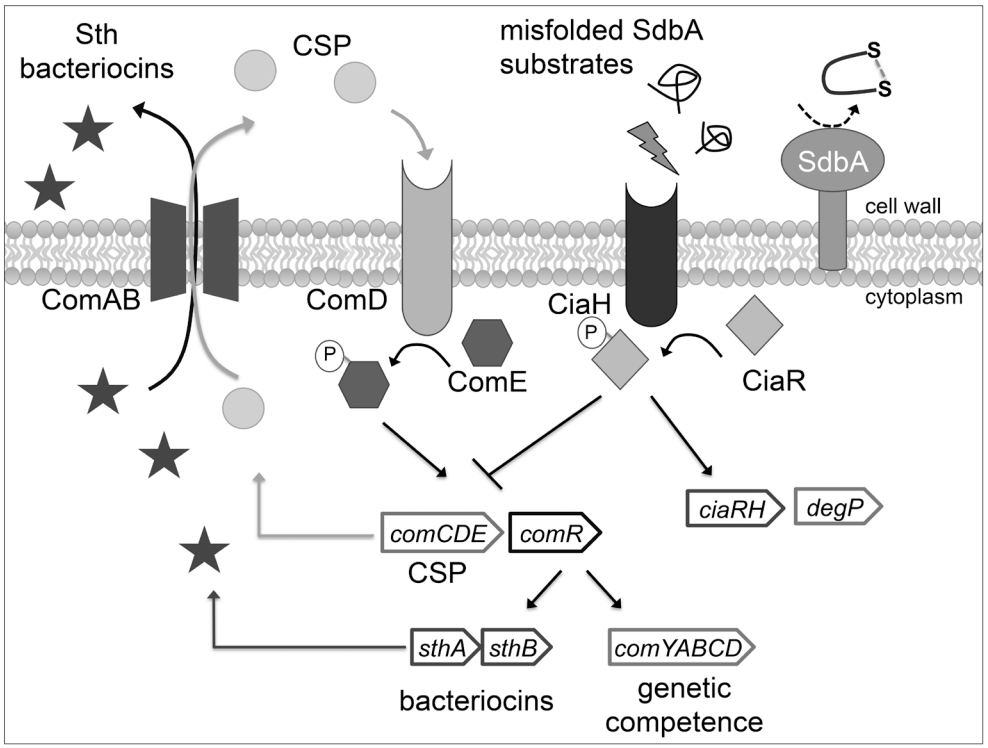
Sth
bacteriocins
CSP
misfolded SdbA
substrates
S
S
SdbA
cell wall
cytoplasm
ComAB
ComD
CiaH
P
P
ComE
CiaR
ciaRH
degP
comCDE
comR
CSP
sthA
sthB
comYABCD
bacteriocins
genetic
competence

Figure 5. 6 Summary of the pathway regulating bacteriocin production in *S. gordonii*

(A) Bacteriocin production in *S. gordonii* is regulated by the Com quorum sensing system that also controls genetic competence. The system is activated by extracellular competence stimulating peptide (CSP), encoded by *comC*. When ComD, a histidine kinase located at the cell surface, binds to CSP it becomes active to phosphorylate its cognate response regulator, ComE. ComE drives the expression of the *comCDE* operon in an auotregulatory loop, as well as the ComAB transporter required for CSP and bacteriocin secretion. In addition to ComE, the Com pathways requires two alternative sigma factors, ComR1 and ComR2, to regulate expression of the genes required for genetic competence (*comYABCD*), and the *sthA* and *sthB* bacteriocins. (B) Mutation of SdbA generates a signal that results in upregulation of the CiaRH two-component regulatory system. Activation of CiaRH represses the Com system, leading to a loss of bacteriocin production.

Chapter 6: Discussion

6.1 Summary

In this thesis we identified a novel thiol-disulfide oxidoreductase, SdbA, that catalyzes disulfide bonds in *S. gordonii*. We analyzed the biological functions of SdbA both directly, by testing disulfide bond formation in a natural substrate and a foreign protein, and indirectly using a thorough phenotypic analysis. We found that the autolysin AtlS is a natural substrate of SdbA. Together, the results revealed that SdbA is crucial for disulfide bond formation and plays a role in multiple cellular processes suggesting that it might have broad substrate specificity (Fig. 6.1).

We took two approaches to better understand how SdbA works. First, we investigated its catalytic mechanisms by analyzing the active site cysteines. We found that SdbA mutants could use a single cysteine to catalyze oxidative protein folding, which is unusual for thioredoxin family proteins. Then, we shifted our focus to investigate the biological roles of SdbA by looking at its effect on bacteriocin production and the CiaRH two component signaling system. This revealed that mutation of SdbA generates an activating signal for CiaRH, and that the CiaRH system can regulate ComDE and bacteriocin production in *S. gordonii*. This allows SdbA to indirectly influence expression of hundreds of genes, even if it only has a limited number of disulfide-bonded substrates.

There is evidence that streptococci generally exclude cysteines from their proteins and form very few disulfide bonds (96), and there has been little research investigating disulfide bond formation in this group of bacteria. However, the disulfide-bonded proteins that they do produce are of significant interest, such as toxins and bacteriocins. The results of this project support the notion that streptococci only form disulfide bonds in a small fraction of their proteins, but that those proteins can play key roles in the biology of the cell.

6.2 Investigating Gram-Positive TDORs

The approach used to identify SdbA relied on the systematic investigation of predicted thioredoxin family enzymes. This strategy was made possible by the availability of genome and proteome sequence data for *S. gordonii*, and by the phenotypes displayed by *S. gordonii* that allowed us to assess enzyme function without prior knowledge of natural substrates. A similar approach should be feasible in other organisms that meet these criteria. However, a limitation to this approach is that the initial selection of candidate proteins is based on homology to known enzymes, and therefore cannot identify enzymes outside of the thioredoxin superfamily. Identification of truly novel enzymes that lack the hallmarks of known oxidoreductase would likely require a random screening strategy. This is exemplified by the work of Chng *et al*. (177), in which analysis of an *E. coli* overexpression library led to the discovery that a rhodanese can catalyze disulfide bonds. Nevertheless, for organisms without known disulfide catalysts, thioredoxin family enzymes are a logical starting point given their universal roles in oxidative protein folding.

Our investigation of thioredoxin family enzymes revealed that *S. gordonii* encodes five highly similar proteins, with different functions that would be difficult to determine by sequence analysis alone. This emphasizes the need to develop biological assays to test enzyme function. Our search for SdbA homologs in other Gram-positive organisms identified several SdbA homologs. However, given the challenges in predicting the function of thioredoxin family enzymes based on sequence data, additional investigation is needed to understand their function. Preliminary data from our laboratory indicates that some of these proteins might be involved in oxidative stress resistance, rather than disulfide bond formation. Similar observations have been made in *S. pneumoniae*, where two proteins with homology *S. gordonii* TDORs were recently determined to have reductase activity (171).

6.3 SdbA Mechanism and Structure

During our investigation of SdbA, we made the surprising discovery that a single active site cysteine was sufficient for activity. This is unusual for a thioredoxin family

protein, and to our knowledge SdbA is the first enzyme of this type to catalyze disulfide bond formation using a single C-terminal cysteine of the CXXC motif. We identified a novel mechanism for the single cysteine variants to catalyze disulfide bond formation using low molecular weight thiols. Although the wild type SdbA enzyme probably uses both of its cysteine residues during its catalytic cycle, a single thiol mechanism might be used under certain growth conditions or as a an alternative pathway if the N-terminal cysteine is over oxidized and damaged. Low molecular weight thiols might also contribute to reoxidation of the SdbA active site.

Our biochemical analysis of SdbA indicated that the C-terminal cysteine was buried in the structure, yet it was enzymatically active both *in vitro* and in *S. gordonii*. The crystal structure of SdbA has recently been determined by our collaborators, Stogios et al (317), and in agreement with our biochemical data, it reveals that the N-terminal cysteine (C86) is surface exposed and that the C-terminal cysteine (C89) is buried (Fig. 6.2). This suggests that substrate binding might result in a conformation change that allows access to the buried cysteine. This type of conformational change has been observed in other thioredoxin family proteins, for example, the active site of ResA undergoes redox dependent conformational changes that affect substrate binding (129), and peroxiredoxins show partial unfolding during their catalytic cycle (269).

Despite the unusual activity of the active site cysteines, the architecture of SdbA is consistent with other thioredoxin family enzymes. SdbA has a thioredoxin fold configuration (β-α-β-α-β-β-α), with the CXXC motif located at the N-terminus of the first α–helix. It also has a conserved *cis*-proline residue in proximity to the active site, along with an adjacent isoleucine. Interestingly, an isoleucine in this position is conserved in cytoplasmic thioredoxins, but is atypical for enzymes that catalyze disulfide bond formation (13). Additional investigation will be required to determine how specific residues affect the activity of SdbA.

6.4 Protein Production and Analysis

Our discovery of SdbA could have useful technical applications. Disulfide bond formation is a rate-limiting step in protein production and manipulation of SdbA expression has potential to enhance production. During our investigation, we noticed that inactivation of both SdbA and the quality control serine protease DegP appears to enhance protein yields, possibly by eliminating a secretion bottleneck. For proteins that do not require accurate disulfide bonds, this strategy could be a useful approach to enhance production, and although it has not been tested, it could potentially increase foreign antigen production in *S. gordonii* based vaccines. Increasing yields of accurately disulfide-bonded proteins, on the other hand, is more challenging, and would likely require overexpression of both SdbA and its redox partner.

During our investigation of bacteriocin production, we developed a method to blot these peptides that is described in Appendix C. This method was developed to enable detection of Sth bacteriocins and CSP, which are small (2.2 to 3.4 kDa), positively charged (pI 11-12) peptides that are undetectable by standard Western blotting techniques. Our method works for CSP and Sth, and for peptides from other streptococci as well. Unfortunately, we were not able to detect Sth in culture supernatants due to difficulties precipitating the rich medium used in our study (BHI, supplemented with 1% peptone and 5% horse serum). However, the approach could be useful to detect bacteriocins in a less complex medium, and could also be applied to other small, charged peptides.

6.5 Future Directions and Conclusions

SdbA Substrates

We demonstrated that the autolysin AtlS is a natural substrate of SdbA, but presumably SdbA has other substrates as well. One likely candidate is the adhesin PadA, located next to SdbA on the genome (318). Our list of candidate substrates could be used as a starting point to identify additional substrates. Alternatively, a proteomics based approach has been used to identify disulfide-bonded proteins in *B. subtilis*, that could also be applied to *S. gordonii* (119).

Another question is how SdbA affects CiaRH, and whether it involves a specific substrate, or misfolding of multiple substrates. CiaRH is associated with cell wall integrity (295), and the effect of SdbA on CiaRH activity might indicate a general stress response to protein misfolding. Although it has not been tested, disulfide oxidoreductases have recently been proposed to form disulfide bonds in the penicillin-binding proteins of Gram-positive bacteria (105). If SdbA substrates include penicillin-binding proteins, in addition to the autolysin AtlS, it is conceivable that mutation of SdbA could alter the cell wall in a way that triggers CiaRH activity.

SdbA Redox Partners

A key question that remains is the identity of SdbA's redox partner. Disulfide bond formation requires a set of enzymes acting in concert, and SdbA is probably just one component in a pathway.

TDORs typically pass electrons to a redox partner, and then into the electron transport chain. Preliminary work from our laboratory suggests that SdbA might interact with homologs of the CcdA-EtrX-MsrA system of *S. pneumoniae* (171). Interestingly, CcdA and related proteins (e.g. DsbD, ScsB) are involved in cytochrome production in many organisms (81, 127), and there is evidence that the cytochrome c maturation and disulfide bond formation pathways are intertwined in both Gram-negative and Gram-positive species (109, 110, 233, 319). Since streptococci and lactococci lack c-type cytochromes and a complete electron transport chain, it is tempting to speculate that perhaps they have evolved to funnel electrons from disulfide bond formation directly into the reducing pathways of the cell.

SdbA Homologs

Another important question is whether or not other bacteria use SdbA homologs to catalyze disulfide bond formation. We identified proteins with homology to SdbA in a range of related Gram-positive bacteria. However, just within *S. gordonii* there are multiple TDORs with similar sequences, that appear to function differently than SdbA.

Additional investigation will be required to determine if other organisms use enzymes like SdbA, and at this point, we cannot rule out the possibility that SdbA might be unique to *S. gordonii*. It is also possible that some predicted TDORs function in disulfide bond formation like SdbA, while others contribute to oxidative stress resistance or other processes. Investigation the biological activities of these enzymes will be essential to determine their functions.

If SdbA homologs can be identified in related Gram-positive pathogens, they would be attractive targets for novel antimicrobials. Disulfide catalysts play a pivotal role in protein stability and function, and virulence factors from important pathogens such as *S. pyogenes* have been demonstrated to require disulfide bonds (136, 170). Targeting a disulfide catalyst is a strategy that could disarm multiple virulence factors at once, and enzymes such as *E. coli* DsbA and DsbB, and *M. tuberculosis* VKOR have been identified as promising targets (36, 37). In species where disulfide catalysts are not essential, inhibitors could abrogate virulence with less selective pressure for resistance than traditional antibiotics (36). An additional advantage is that SdbA and similar proteins are surface localized, making them accessible to potential inhibitors.

In conclusion, we have established SdbA as a novel disulfide oxidoreductase. SdbA appears to be *S. gordonii's* equivalent of *E. coli* DsbA, and it suggests that other related organisms might also possess similar enzymes. Our discovery of SdbA adds to the knowledge of disulfide bond formation in Gram-positive facultative anaerobes, which has been an understudied area of protein production.

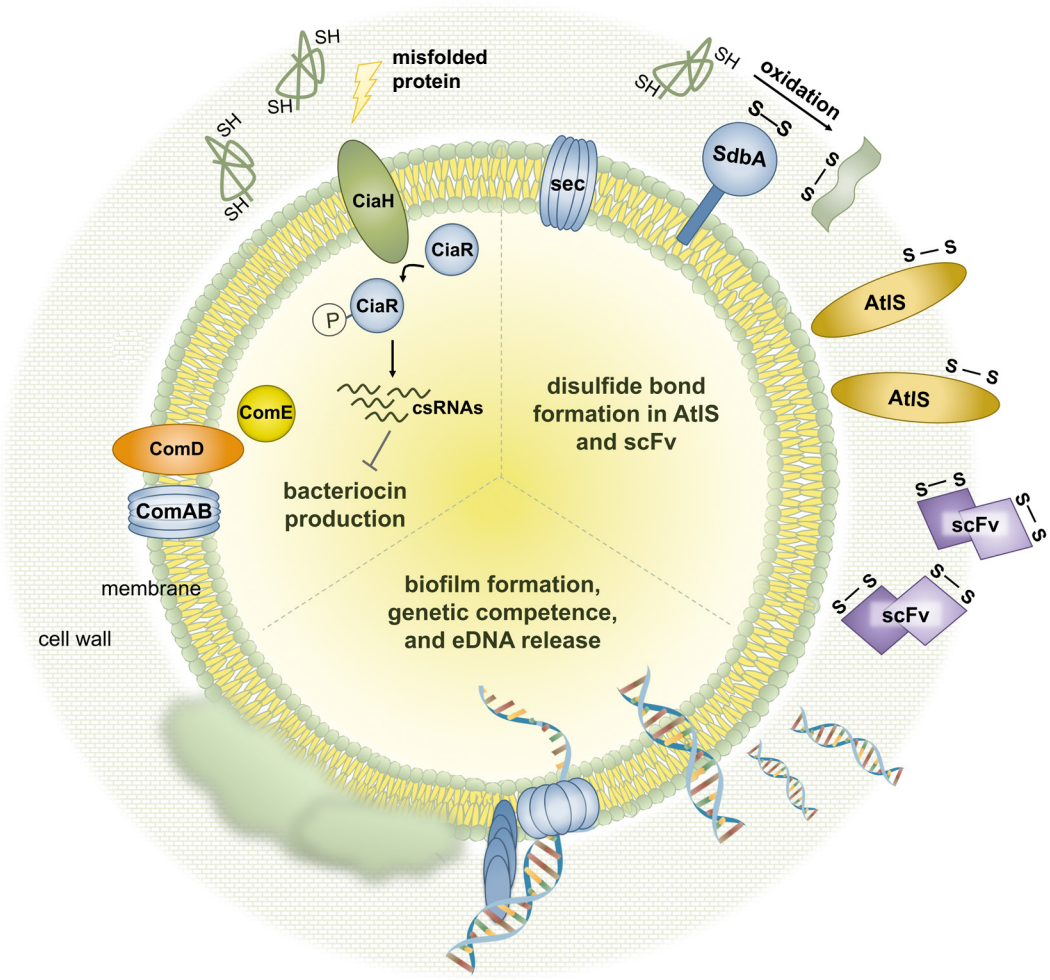
SH
SH
misfolded
protein
SH
SH
SH
SH
oxidation
S—S
SdbA
CiaH
sec
CiaR
CiaR
P
csRNAs
ComE
ComD
ComAB
bacteriocin
production
disulfide bond
formation in AtlS
and scFv
biofilm formation,
genetic competence,
and eDNA release
membrane
cell wall
AtlS
AtlS
scFv
scFv

Figure 6.1 SdbA and oxidative protein folding in *S. gordonii*

SdbA influences multiple processes in the cell through both direct and indirect mechanisms. (i) SdbA introduces disulphide bonds into substrate proteins including the autolysin AtlS and a recombinant single chain variable fragment antibody (scFv). (ii) SdbA can also affect the cell indirectly. Mutation of SdbA generates a signal, possibly misfolded protein, which activates the CiaRH two-component signaling system. CiaRH regulates a set of small RNAs (csRNAs) that act on multiple genes. When CiaRH is upregulated, it represses the ComDE signaling system and shuts down bacteriocin production. (iii) SdbA affects other processes through unknown mechanisms. SdbA mutants show significantly enhanced biofilm formation. Mutants are also deficient in eDNA release and in natural genetic competence.

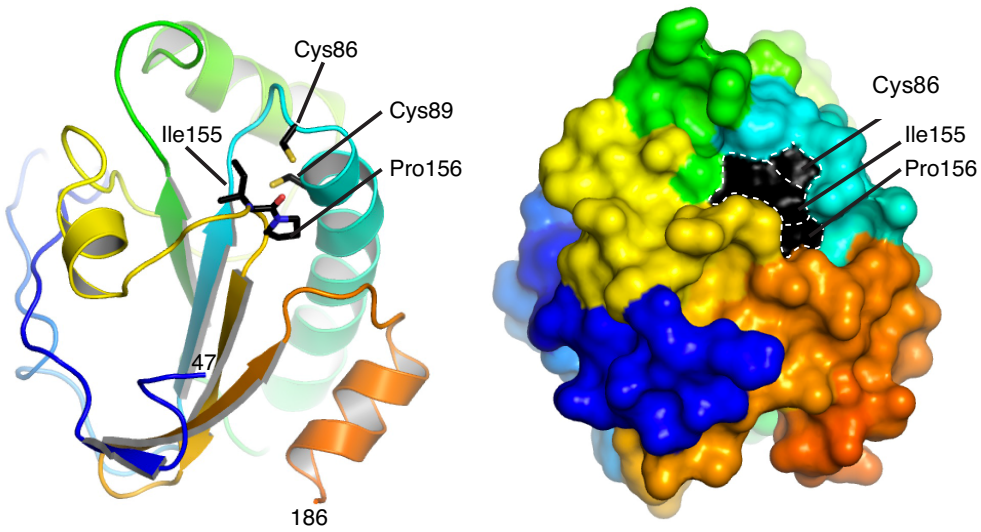

Figure 6.2 Crystal structure of SdbA

The structure shows that the active site cysteines of the CPDC motif are located within a thioredoxin fold (left). The conserved *cis*-proline and adjacent isoleucine localize next to the active site. Surface representation shows that the N-terminal cysteine, C86, is surface exposed, whereas the C-terminal cysteine, C89, is buried (right) (317).

References

1. **Depuydt M**, **Messens J**, **Collet JF**. 2011. How proteins form disulfide bonds. Antioxid Redox Signal **15**:49–66.

2. **Sato Y**, **Inaba K**. 2012. Disulfide bond formation network in the three biological kingdoms, bacteria, fungi and mammals. FEBS J **279**:2262–2271.

3. **Hatahet F**, **Ruddock LW**. 2009. Protein disulfide isomerase: a critical evaluation of its function in disulfide bond formation. Antioxid Redox Signal **11**:2807–2850.

4. **Beckwith J**. 2007. What lies beyond uranus? Preconceptions, ignorance, serendipity and suppressors in the search for biology's secrets. Genetics **176**:733–740.

5. **Sideris DP**, **Tokatlidis K**. 2010. Oxidative protein folding in the mitochondrial intermembrane space. Antioxid Redox Signal **13**:1189–1204.

6. **Hatahet F**, **Boyd D**, **Beckwith J**. 2014. Disulfide bond formation in prokaryotes: History, diversity and design. Biochim Biophys Acta **1844**:1402–1414.

7. **Kouwen TRHM**, **van der Goot A**, **Dorenbos R**, **Winter T**, **Antelmann H**, **Plaisier MC**, **Quax WJ**, **van Dijl JM**, **Dubois J-YF**, **Goot A Van Der**, **Dijl JM Van**. 2007. Thiol-disulphide oxidoreductase modules in the low-GC Gram-positive bacteria. Mol Microbiol **64**:984–999.

8. **Lu J**, **Holmgren A**. 2014. The thioredoxin superfamily in oxidative protein folding. Antioxid Redox Signal **21**:457–470.

9. **Ladenstein R**, **Ren B**. 2006. Protein disulfides and protein disulfide oxidoreductases in hyperthermophiles. FEBS J **273**:4170–4185.

10. **Wouters MA**, **Fan SW**, **Haworth NL**. 2010. Disulfides as redox switches: from molecular mechanisms to functional significance. Antioxid Redox Signal **12**:53–91.

11. **Atkinson HJ**, **Babbitt PC**. 2009. An atlas of the thioredoxin fold class reveals the complexity of function-enabling adaptations. PLoS Comput Biol **5**:e1000541.

12. **Pan JL**, **Bardwell JCA**. 2006. The origami of thioredoxin-like folds. Protein Sci **15**:2217–27.

13. **Ren G**, **Stephan D**, **Xu Z**, **Zheng Y**, **Tang D**, **Harrison RS**, **Kurz M**, **Jarrott R**, **Shouldice SR**, **Hiniker A**, **Martin JL**, **Heras B**, **Bardwell JCA**. 2009. Properties of the thioredoxin fold superfamily are modulated by a single amino acid residue. J Biol Chem **284**:10150–10159.

14. **Kadokura H**, **Tian H**, **Zander T**, **Bardwell JCA**, **Beckwith J**. 2004. Snapshots of DsbA in action: detection of proteins in the process of oxidative folding. Science **303**:534–537.

15. **Su D**, **Berndt C**, **Fomenko DE**, **Holmgren A**, **Gladyshev VN**. 2007. A conserved cis-proline precludes metal binding by the active site thiolates in members of the thioredoxin family of proteins. Biochemistry **46**:6903–6910.

16. **Roos G**, **Foloppe N**, **Messens J**. 2013. Understanding the pK(a) of redox cysteines: the key role of hydrogen bonding. Antioxid Redox Signal **18**:94–127.

17. **Grauschopf U**, **Winther JR**, **Korber P**, **Zander T**, **Dallinger P**, **Bardwell JC**. 1995. Why is DsbA such an oxidizing disulfide catalyst? Cell **83**:947–955.

18. **Quan S**, **Schneider I**, **Pan J**, **Von Hacht A**, **Bardwell JCA**. 2007. The CXXC motif is more than a redox rheostat. J Biol Chem **282**:28823–28833.

19. **Jonda S**, **Huber-Wunderlich M**, **Glockshuber R**, **Mössner E**. 1999. Complementation of DsbA deficiency with secreted thioredoxin variants reveals the crucial role of an efficient dithiol oxidant for catalyzed protein folding in the bacterial periplasm. EMBO J **18**:3271–3281.

20. **Kosuri P**, **Alegre-Cebollada J**, **Feng J**, **Kaplan A**, **Inglés-Prieto A**, **Badilla CL**, **Stockwell BR**, **Sanchez-Ruiz JM**, **Holmgren A**, **Fernández JM**. 2012. Protein folding drives disulfide formation. Cell **151**:794–806.

21. **Gross E**, **Kastner DB**, **Kaiser CA**, **Fass D**. 2004. Structure of Ero1p , source of disulfide bonds for oxidative protein folding in the cell. Cell **117**:601–610.

22. **Shouldice SR**, **Heras B**, **Walden PM**, **Totsika M**, **Schembri MA**, **Martin JL**. 2011. Structure and function of DsbA, a key bacterial oxidative folding catalyst. Antioxid Redox Signal **14**:1729–1760.

23. **Koch JR**, **Schmid FX**. 2014. Mia40 combines thiol oxidase and disulfide isomerase activity to efficiently catalyze oxidative folding in mitochondria. J Mol Biol **426**:4087–4098.

24. **Dutton RJ**, **Boyd D**, **Berkmen M**, **Beckwith J**. 2008. Bacterial species exhibit diversity in their mechanisms and capacity for protein disulfide bond formation. Proc Natl Acad Sci U S A **105**:11933–11938.

25. **Heras B**, **Shouldice SR**, **Totsika M**, **Scanlon MJ**, **Schembri MA**, **Martin JL**. 2009. DSB proteins and bacterial pathogenicity. Nat Rev Microbiol **7**:215–225.

26. **Łasica AM**, **Jagusztyn-Krynicka EK**. 2007. The role of Dsb proteins of Gram-negative bacteria in the process of pathogenesis. FEMS Microbiol Rev **31**:626–636.

27. **Tinsley CR**, **Voulhoux R**, **Beretti JL**, **Tommassen J**, **Nassif X**. 2004. Three homologues, including two membrane-bound proteins, of the disulfide oxidoreductase DsbA in *Neisseria meningitidis*: EFFECTS ON BACTERIAL GROWTH AND BIOGENESIS OF FUNCTIONAL TYPE IV PILI. J Biol Chem **279**:27078–27087.

28. **Crespo MD**, **Puorger C**, **Schärer MA**, **Eidam O**, **Grütter MG**, **Capitani G**, **Glockshuber R**. 2012. Quality control of disulfide bond formation in pilus subunits by the chaperone FimC. Nat Chem Biol **8**:707–713.

29. **Wey J**, **Tang S**, **Wu T**. 2006. Disulfide bond reduction corresponds to dimerization and hydrophobi-city changes of *Clostridium botulinum* type A neurotoxin. Acta Pharmacol Sin **27**:1238–1246.

30. **Dailey FE**, **Berg HC**. 1993. Mutants in disulfide bond formation that disrupt flagellar assembly in *Escherichia coli*. Proc Natl Acad Sci U S A **90**:1043–1047.

31. **Betts-Hampikian HJ**, **Fields KA**. 2011. Disulfide bonding within components of the *Chlamydia* type III secretion apparatus correlates with development. J Bacteriol **193**:6950–6959.

32. **Ha UH**, **Wang Y**, **Jin S**. 2003. DsbA of *Pseudomonas aeruginosa* is essential for multiple virulence factors. Infect Immun **71**:1590–1595.

33. **Miki T**, **Okada N**, **Danbara H**. 2004. Two periplasmic bisulfide oxidoreductases, DsbA and SrgA, target outer membrane protein SpiA, a component of the *Salmonella pathogenicity* island 2 type III secretion system. J Biol Chem **279**:34631–34642.

34. **Kpadeh ZZ**, **Jameson-Lee M**, **Yeh AJ**, **Chertihin O**, **Shumilin IA**, **Dey R**, **Day SR**, **Hoffman PS**. 2013. Disulfide bond oxidoreductase DsbA2 of *Legionella pneumophila* exhibits protein disulfide isomerase activity. J Bacteriol **195**:1825–1833.

35. **Dutton RJ**, **Wayman A**, **Wei JR**, **Rubin EJ**, **Beckwith J**, **Boyd D**. 2010. Inhibition of bacterial disulfide bond formation by the anticoagulant warfarin. Proc Natl Acad Sci U S A **107**:297–301.

36. **Mcmahon RM**, **Premkumar L**, **Martin JL**. 2014. Four structural subclasses of the antivirulence drug target disulfide oxidoreductase DsbA provide a platform for design of subclass-specific inhibitors. Biochim Biophys Acta **1844**:1391–1401.

37. **Landeta C**, **Blazyk JL**, **Hatahet F**, **Meehan BM**, **Eser M**, **Myrick A**, **Bronstain L**, **Minami S**, **Arnold H**, **Ke N**, **Rubin EJ**, **Furie BC**, **Furie B**, **Beckwith J**, **Dutton R**, **Boyd D**. 2015. Compounds targeting disulfide bond forming enzyme DsbB of Gram-negative bacteria. Nat Chem Biol **11**:292–298.

38. **Assenberg R**, **Wan PT**, **Geisse S**, **Mayr LM**. 2013. Advances in recombinant protein expression for use in pharmaceutical research. Curr Opin Struct Biol **23**:393–402.

39. **Zhang Z**, **Li ZH**, **Wang F**, **Fang M**, **Yin CC**, **Zhou ZY**, **Lin Q**, **Huang HL**. 2002. Overexpression of DsbC and DsbG markedly improves soluble and functional expression of single-chain Fv antibodies in *Escherichia coli*. Protein Expr Purif **26**:218–228.

40. **Kouwen TRHM**, **van Dijl JM**. 2009. Applications of thiol-disulfide oxidoreductases for optimized *in vivo* production of functionally active proteins in *Bacillus*. Appl Microbiol Biotechnol **85**:45–52.

41. **Joly JC**, **Leung WS**, **Swartz JR**. 1998. Overexpression of *Escherichia coli* oxidoreductases increases recombinant insulin-like growth factor-I accumulation. Proc Natl Acad Sci U S A **95**:2773–2777.

42. **Delic M**, **Göngrich R**, **Mattanovich D**, **Gasser B**. 2014. Engineering of protein folding and secretion-strategies to overcome bottlenecks for efficient production of recombinant proteins. Antioxid Redox Signal **21**:414–437.

43. **Berkmen M**. 2012. Production of disulfide-bonded proteins in *Escherichia coli*. Protein Expr Purif **82**:240–251.

44. **Kadokura H**, **Beckwith J**. 2010. Mechanisms of oxidative protein folding in the bacterial cell envelope. Antioxid Redox Signal **13**:1231–1246.

45. **Bardwell JC**, **McGovern K**, **Beckwith J**. 1991. Identification of a protein required for disulfide bond formation *in vivo*. Cell **67**:581–589.

46. **Denoncin K**, **Collet JF**. 2013. Disulfide bond formation in the bacterial periplasm: major achievements and challenges ahead. Antioxid Redox Signal **19**:63–71.

47. **Guddat LW**, **Bardwell JC**, **Martin JL**. 1998. Crystal structures of reduced and oxidized DsbA: investigation of domain motion and thiolate stabilization. Structure **6**:757–767.

48. **Martin JL**, **Bardwell JCA**, **Kuriyan J**. 1993. Crystal structure of the DsbA protein required for disulphide bond formation in vivo. Nature **365**:464–468.

49. **Inaba K**, **Murakami S**, **Suzuki M**, **Nakagawa A**, **Yamashita E**, **Okada K**, **Ito K**. 2006. Crystal structure of the DsbB-DsbA complex reveals a mechanism of disulfide bond generation. Cell **127**:789–801.

50. **Paxman JJ**, **Borg NA**, **Horne J**, **Thompson PE**, **Chin Y**, **Sharma P**, **Simpson JS**, **Wielens J**, **Piek S**, **Kahler CM**, **Sakellaris H**, **Pearce M**, **Bottomley SP**, **Rossjohn J**, **Scanlon MJ**. 2009. The structure of the bacterial oxidoreductase enzyme DsbA in complex with a peptide reveals a basis for substrate specificity in the catalytic cycle of DsbA enzymes. J Biol Chem **284**:17835–17845.

51. **Kadokura H**, **Beckwith J**. 2002. Four cysteines of the membrane protein DsbB act in concert to oxidize its substrate DsbA. EMBO J **21**:2354–2363.

52. **Inaba K**, **Ito K**. 2008. Structure and mechanisms of the DsbB-DsbA disulfide bond generation machine. Biochim Biophys Acta **1783**:520–529.

53. **Bader M**, **Muse W**, **Ballou DP**, **Gassner C**, **Bardwell JCA**.1999. Oxidative folding is driven by the electron transport system. Cell **98**:217–227.

54. **Takahashi YH**, **Inaba K**, **Ito K**. 2004. Characterization of the menaquinone-dependent disulfide bond formation pathway of *Escherichia coli*. J Biol Chem **279**:47057–47065.

55. **Wunderlich M**, **Otto A**, **Seckler R**, **Glockshuber R**. 1993. Bacterial protein disulfide isomerase: efficient catalysis of oxidative protein folding at acidic pH. Biochemistry **32**:12251–12256.

56. **Zapun A**, **Bardwell JC**, **Creighton TE**. 1993. The reactive and destabilizing disulfide bond of DsbA, a protein required for protein disulfide bond formation *in vivo*. Biochemistry **32**:5083–5092.

57. **Chivers PT**, **Prehoda KE**, **Raines RT**. 1997. The CXXC motif: A rheostat in the active site. Biochemistry **36**:4061–4066.

58. **Bessette PH**, **Qiu J**, **Bardwell JC**, **Swartz JR**, **Georgiou G**. 2001. Effect of sequences of the active-site dipeptides of DsbA and DsbC on *in vivo* folding of multidisulfide proteins in *Escherichia coli*. J Bacteriol **183**:980–988.

59. **Debarbieux L**, **Beckwith J**. 2000. On the functional interchangeability, oxidant versus reductant, of members of the thioredoxin superfamily. J Bacteriol **182**:723–727.

60. **Frech C**, **Wunderlich M**, **Glockshuber R**, **Schmid FX**. 1996. Preferential binding of an unfolded protein to DsbA. EMBO J **15**:392–398.

61. **Kadokura H**, **Beckwith J**. 2009. Detecting folding intermediates of a protein as it passes through the bacterial translocation channel. Cell **138**:1164–1173.

62. **Hiniker A**, **Bardwell JCA**. 2004. *In vivo* substrate specificity of periplasmic disulfide oxidoreductases. J Biol Chem **279**:12967–12973.

63. **Berkmen M**, **Boyd D**, **Beckwith J**. 2005. The nonconsecutive disulfide bond of *Escherichia coli* phytase (AppA) renders it dependent on the protein-disulfide isomerase, DsbC. J Biol Chem **280**:11387–11394.

64. **Ruiz N**, **Chng SS**, **Hiniker A**, **Kahne D**, **Silhavy TJ**. 2010. Nonconsecutive disulfide bond formation in an essential integral outer membrane protein. Proc Natl Acad Sci U S A **107**:12245–12250.

65. **Hiniker A**, **Collet JF**, **Bardwell JCA**. 2005. Copper stress causes an *in vivo* requirement for the *Escherichia coli* disulfide isomerase DsbC. J Biol Chem **280**:33785–33791.

66. **McCarthy A**, **Haebel P**. 2000. Crystal structure of the protein disulfide bond isomerase, DsbC, from *Escherichia coli*. Nat Struct Biol **7**:7–10.

67. **Shouldice SR**, **Cho SH**, **Boyd D**, **Heras B**, **Eser M**, **Beckwith J**, **Riggs P**, **Martin JL**, **Berkmen M**. 2010. *In vivo* oxidative protein folding can be facilitated by oxidation-reduction cycling. Mol Microbiol **75**:13–28.

68. **Bader MW**, **Hiniker A**, **Regeimbal J**, **Goldstone D**, **Haebel PW**, **Riemer J**, **Metcalf P**, **Bardwell JC**. 2001. Turning a disulfide isomerase into an oxidase: DsbC mutants that imitate DsbA. EMBO J **20**:1555–1562.

69. **Missiakas D**, **Schwager F**, **Raina S**. 1995. Identification and characterization of a new disulfide isomerase-like protein (DsbD) in *Escherichia coli*. EMBO J **14**:3415–3424.

70. **Cho SH**, **Collet JF**. 2013. Many roles of the bacterial envelope reducing pathways. Antioxid Redox Signal **18**:1690–1698.

71. **Rietsch A**, **Bessette P**, **Georgiou G**, **Beckwith J**. 1997. Reduction of the periplasmic disulfide bond isomerase, DsbC, occurs by passage of electrons from cytoplasmic thioredoxin. J Bacteriol **179**:6602–6608.

72. **Stewart EJ**, **Katzen F**, **Beckwith J**. 1999. Six conserved cysteines of the membrane protein DsbD are required for the transfer of electrons from the cytoplasm to the periplasm of *Escherichia coli*. EMBO J **18**:5963–5971.

73. **Haebel PW**, **Goldstone D**, **Katzen F**, **Beckwith J**, **Metcalf P**. 2002. The disulfide bond isomerase DsbC is activated by an immunoglobulin-fold thiol oxidoreductase: crystal structure of the DsbC-DsbDα complex. EMBO J **21**:4774–4784.

74. **Kim JH**, **Kim SJ**, **Jeong DG**, **Son JH**, **Ryu SE**. 2003. Crystal structure of DsbDγ reveals the mechanism of redox potential shift and substrate specificity. FEBS Lett **543**:164–169.

75. **Williamson JA**, **Cho S-H**, **Ye J**, **Collet JF**, **Beckwith JR**, **Chou JJ**. 2015. Structure and multistate function of the transmembrane electron transporter CcdA. Nat Struct Mol Biol **22**:809–814.

76. **Cho SH**, **Porat A**, **Ye J**, **Beckwith J**. 2007. Redox-active cysteines of a membrane electron transporter DsbD show dual compartment accessibility. EMBO J **26**:3509–3520.

77. **Katzen F**, **Beckwith J**. 2000. Transmembrane electron transfer by the membrane protein DsbD occurs via a disulfide bond cascade. Cell **103**:769–779.

78. **Goldstone D**, **Haebel PW**, **Katzen F**, **Bader MW**, **Bardwell JC**, **Beckwith J**, **Metcalf P**. 2001. DsbC activation by the N-terminal domain of DsbD. Proc Natl Acad Sci U S A **98**:9551–9556.

79. **Depuydt M**, **Leonard SE**, **Vertommen D**, **Denoncin K**, **Morsomme P**, **Wahni K**, **Messens J**, **Carroll KS**, **Collet JF**. 2009. A periplasmic reducing system protects single cysteine residues from oxidation. Science **326**:1109–1111.

80. **Stirnimann CU**, **Rozhkova A**, **Grauschopf U**, **Grütter MG**, **Glockshuber R**, **Capitani G**. 2005. Structural basis and kinetics of DsbD-dependent cytochrome c maturation. Structure **13**:985–993.

81. **Bonnard G**, **Corvest V**, **Meyer EH**, **Hamel PP**. 2010. Redox processes controlling the biogenesis of c-type cytochromes. Antioxid Redox Signal **13**:1385–401.

82. **Totsika M**, **Heras B**, **Wurpel DJ**, **Schembri MA.** 2009. Characterization of two homologous disulfide bond systems involved in virulence factor biogenesis in uropathogenic *Escherichia coli* CFT073. J Bacteriol **191**:3901–3908.

83. **Bouwman CW**, **Kohli M**, **Killoran A**, **Touchie GA**, **Kadner RJ**, **Martin NL**. 2003. Characterization of SrgA, a *Salmonella enterica* Serovar Typhimurium virulence plasmid-encoded paralogue of the disulfide oxidoreductase DsbA, essential for biogenesis of plasmid-encoded fimbriae. J Bacteriol **185**:991–1000.

84. **Heras B**, **Totsika M**, **Jarrott R**, **Shouldice SR**, **Guncar G**, **Achard MES**, **Wells TJ**, **Argente MP**, **McEwan AG**, **Schembri MA**. 2010. Structural and functional characterization of three DsbA paralogues from *Salmonella enterica* serovar Typhimurium. J Biol Chem **285**:18423–18432.

85. **Sinha S**, **Langford PR**, **Kroll JS**. 2004. Functional diversity of three different DsbA proteins from *Neisseria meningitidis*. Microbiology **150**:2993–3000.

86. **Vivian JP**, **Scoullar J**, **Rimmer K**, **Bushell SR**, **Beddoe T**, **Wilce MCJ**, **Byres E**, **Boyle TP**, **Doak B**, **Simpson JS**, **Graham B**, **Heras B**, **Kahler CM**, **Rossjohn J**, **Scanlon MJ**. 2009. Structure and function of the oxidoreductase DsbA1 from *Neisseria meningitidis*. J Mol Biol **394**:931–943.

87. **Arts IS**, **Ball G**, **Leverrier P**, **Garvis S**, **Nicolaes V**, **Vertommen D**, **Ize B**, **Tamu Dufe V**, **Messens J**, **Voulhoux R**, **Collet JF**. 2013. Dissecting the machinery that introduces disulfide bonds in *Pseudomonas aeruginosa*. MBio **4**:e00912–13.

88. **Lester J**, **Kichler S**, **Oickle B**, **Fairweather S**, **Oberc A**, **Chahal J**, **Ratnayake D**, **Creuzenet C**. 2015. Characterization of *Helicobacter pylori* HP0231 (DsbK): Role in disulfide bond formation, redox homeostasis and production of *Helicobacter* cystein-rich protein HcpE. Mol Microbiol **96**:110–133.

89. **Roszczenko P**, **Radomska KA**, **Wywial E**, **Collet JF**, **Jagusztyn-Krynicka EK**. 2012. A novel insight into the oxidoreductase activity of *Helicobacter pylori* HP0231 protein. PLoS One **7**:e46563.

90. **Yoon JY**, **Kim J**, **Lee SJ**, **Kim HS**, **Im HN**, **Yoon HJ**, **Kim KH**, **Kim SJ**, **Han BW**, **Suh SW**. 2011. Structural and functional characterization of *Helicobacter pylori* DsbG. FEBS Lett **585**:3862–3867.

91. **Ren G**, **Champion MM**, **Huntley JF**. 2014. Identification of disulfide bond isomerase substrates reveals bacterial virulence factors. Mol Microbiol **94**:926–944.

92. **Kpadeh ZZ**, **Day SR**, **Mills BW**, **Hoffman PS**. 2015. *Legionella pneumophila* utilizes a single-player disulfide-bond oxidoreductase system to manage disulfide bond formation and isomerization. Mol Microbiol **95**:1054–1069.

93. **Jameson-Lee M**, **Garduño RA**, **Hoffman PS**. 2011. DsbA2 (27kDa Com1-like protein) of *Legionella pneumophila* catalyses extracytoplasmic disulphide-bond formation in proteins including the Dot/Icm type IV secretion system. Mol Microbiol **80**:835–852.

94. **Wang X**, **Dutton RJ**, **Beckwith J**, **Boyd D**. 2011. Membrane topology and mutational analysis of *Mycobacterium tuberculosis* VKOR, a protein involved in disulfide bond formation and a homologue of human vitamin K epoxide reductase. Antioxid Redox Signal **14**:1413–1420.

95. **Li W**, **Schulman S**, **Dutton RJ**, **Boyd D**, **Beckwith J**, **Rapoport TA**. 2010. Structure of a bacterial homologue of vitamin K epoxide reductase. Nature **463**:507–512.

96. **Daniels R**, **Mellroth P**, **Bernsel A**, **Neiers F**, **Normark S**, **von Heijne G**, **Henriques-Normark B**. 2010. Disulfide bond formation and cysteine exclusion in Gram-positive bacteria. J Biol Chem **285**:3300–9.

97. **Reardon-Robinson ME**, **Osipiuk J**, **Chang C**, **Wu C**, **Jooya N**, **Joachimiak A**, **Das A**, **Ton-That H**. 2015. A disulfide bond-forming machine is linked to the sortase-mediated pilus assembly pathway in the Gram-positive bacterium *Actinomyces oris*. J Biol Chem **290**:21393–21405.

98. **Reardon-Robinson ME**, **Osipiuk J**, **Jooya N**, **Chang C**, **Joachimiak A**, **Das A**, **Ton-That H**. 2015. A thiol-disulfide oxidoreductase of the Gram-positive pathogen *Corynebacterium diphtheriae* is essential for viability, pilus assembly, toxin production and virulence. Mol Microbiol **98**:1037–1050.

99. **Chim N**, **Riley R**, **The J**, **Im S**, **Segelke B**, **Lekin T**, **Yu M**, **Hung LW**, **Terwilliger T**, **Whitelegge JP**, **Goulding CW**. 2010. An extracellular disulfide bond forming protein (DsbF) from *Mycobacterium tuberculosis*: structural, biochemical, and gene expression analysis. J Mol Biol **396**:1211–1226.

100. **Chim N**, **Harmston CA**, **Guzman DJ**, **Goulding CW**. 2013. Structural and biochemical characterization of the essential DsbA-like disulfide bond forming protein from *Mycobacterium tuberculosis*. BMC Struct Biol **13**:23.

101. **Davey L**, **Ng CKW**, **Halperin SA**, **Lee SF**. 2013. Functional analysis of paralogous thiol-disulfide oxidoreductases in *Streptococcus gordonii*. J Biol Chem **288**:16416–16429.

102. **Crow A**, **Lewin A**, **Hecht O**, **Carlsson Möller M**, **Moore GR**, **Hederstedt L**, **Le Brun NE**. 2009. Crystal structure and biophysical properties of *Bacillus subtilis* BdbD. An oxidizing thiol:disulfide oxidoreductase containing a novel metal site. J Biol Chem **284**:23719–23733.

103. **Dumoulin A**, **Grauschopf U**, **Bischoff M**, **Thöny-Meyer L**, **Berger-Bächi B**. 2005. *Staphylococcus aureus* DsbA is a membrane-bound lipoprotein with thiol-disulfide oxidoreductase activity. Arch Microbiol **184**:117–128.

104. **Hoffmann C**, **Leis A**, **Niederweis M**, **Plitzko JM**, **Engelhardt H**. 2008. Disclosure of the mycobacterial outer membrane: cryo-electron tomography and vitreous sections reveal the lipid bilayer structure. Proc Natl Acad Sci U S A **105**:3963–3967.

105. **Reardon-Robinson ME**, **Ton-That H**. 2015. Disulfide bond-forming pathways in Gram-positive bacteria. J Bacteriol JB.00769–15.

106. **Wang L**, **Li J**, **Wang X**, **Liu W**, **Zhang XC**, **Li X**, **Rao Z**. 2013. Structure analysis of the extracellular domain reveals disulfide bond forming-protein properties of *Mycobacterium tuberculosis* Rv2969c. Protein Cell **4**:628–640.

107. **Premkumar L**, **Heras B**, **Duprez W**, **Walden P**, **Halili M**, **Kurth F**, **Fairlie DP**, **Martin JL**. 2013. Rv2969c, essential for optimal growth in *Mycobacterium tuberculosis*, is a DsbA-like enzyme that interacts with VKOR-derived peptides and has atypical features of DsbA-like disulfide oxidases. Acta Crystallogr Sect D Biol Crystallogr **69**:1981–1994.

108. **Goulding CW**, **Apostol MI**, **Gleiter S**, **Parseghian A**, **Bardwell J**, **Gennaro M**, **Eisenberg D**. 2004. Gram-positive DsbE proteins function differently from Gram-negative DsbE homologs. A structure to function analysis of DsbE from *Mycobacterium tuberculosis*. J Biol Chem **279**:3516–3524.

109. **Small JL**, **Park SW**, **Kana BD**, **Ioerger TR**, **Sacchettini JC**, **Ehrt S**, **Park W**, **Kana BD**, **Ioerger TR**, **Sacchettini JC**. 2013. Perturbation of cytochrome c maturation reveals adaptability of the respiratory chain in *Mycobacterium tuberculosis*. MBio **4**:e00475–13.

110. **Erlendsson LS**, **Hederstedt L**. 2002. Mutations in the thiol-disulfide oxidoreductases BdbC and BdbD can suppress cytochrome c deficiency of CcdA-defective *Bacillus subtilis* cells. J Bacteriol **184**:1423–1429.

111. **Um S**, **Kim JS**, **Song S**, **Kim NA**, **Jeong SH**, **Ha N**. 2015. Crystal structure of DsbA from *Corynebacterium diphtheriae* and its functional implications for CueP in Gram-positive bacteria. Mol Cells **38**:715–722.

112. **Um S-H**, **Kim J-S**, **Lee K**, **Ha N-C**. 2014. Structure of a DsbF homologue from *Corynebacterium diphtheriae*. Acta Crystallogr Sect F Struct Biol Commun **70**:1167–1172.

113. **Kang HJ**, **Baker EN**. 2011. Intramolecular isopeptide bonds: protein crosslinks built for stress? Trends Biochem Sci **36**:229–237.

114. **Stenson TH**, **Weiss AA**. 2002. DsbA and DsbC are required for secretion of pertussis toxin by *Bordetella pertussis* **70**:2297–2303.

115. **Yu J**, **McLaughlin S**, **Freedman RB**, **Hirst TR**. 1993. Cloning and active site mutagenesis of *Vibrio cholerae* DsbA, a periplasmic enzyme that catalyzes disulfide bond formation. J Biol Chem **268**:4326–4330.

116. **Bolhuis A**, **Venema G**, **Quax WJ**, **Bron S**, **van Dijl JM**. 1999. Functional analysis of paralogous thiol-disulfide oxidoreductases in *Bacillus subtilis*. J Biol Chem **274**:24531–24538.

117. **Meima R**, **Eschevins C**, **Fillinger S**, **Bolhuis A**, **Hamoen LW**, **Dorenbos R**, **Quax WJ**, **van Dijl JM**, **Provvedi R**, **Chen I**, **Dubnau D**, **Bron S**. 2002. The *bdbDC* operon of *Bacillus subtilis* encodes thiol-disulfide oxidoreductases required for competence development. J Biol Chem **277**:6994–7001.

118. **Darmon E**, **Dorenbos R**, **Meens J**, **Freudl R**, **Antelmann H**, **Hecker M**, **Kuipers OP**, **Bron S**, **Quax WJ**, **Dubois JYF**, **van Dijl JM**. 2006. A disulfide bond-containing alkaline phosphatase triggers a BdbC-dependent secretion stress response in *Bacillus subtilis*. Appl Environ Microbiol **72**:6876–6885.

119. **Goosens VJ**, **Mars RAT**, **Akeroyd M**, **Vente A**, **Dreisbach A**, **Denham EL**, **Kouwen TRHM**, **van Rij T**, **Olsthoorn M**, **van Dijl JM**. 2013. Is proteomics a reliable tool to probe the oxidative folding of bacterial membrane proteins? Antioxid Redox Signal **18**:1159–1164.

120. **Ishihara T**, **Tomita H**, **Hasegawa Y**, **Tsukagoshi N**, **Yamagata H**, **Udaka S**. 1995. Cloning and characterization of the gene for a protein thiol-disulfide oxidoreductase in *Bacillus brevis*. J Bacteriol **177**:745–749.

121. **Kouwen TRHM**, **van Dijl JM**. 2009. Interchangeable modules in bacterial thiol-disulfide exchange pathways. Trends Microbiol **17**:6–12.

122. **Chen I**, **Provvedi R**, **Dubnau D**. 2006. A macromolecular complex formed by a pilin-like protein in competent *Bacillus subtilis*. J Biol Chem **281**:21720–21727.

123. **Draskovic I**, **Dubnau D**. 2005. Biogenesis of a putative channel protein, ComEC, required for DNA uptake: membrane topology, oligomerization and formation of disulphide bonds. Mol Microbiol **55**:881–896.

124. **Liu Y**, **Carlsson Möller M**, **Petersen L**, **Söderberg CAG**, **Hederstedt L**. 2010. Penicillin-binding protein SpoVD disulphide is a target for StoA in *Bacillus subtilis* forespores. Mol Microbiol **75**:46–60.

125. **Dorenbos R**, **Stein T**, **Kabel J**, **Bruand C**, **Bolhuis A**, **Bron S**, **Quax WJ**, **van Dijl JM**. 2002. Thiol-disulfide oxidoreductases are essential for the production of the lantibiotic sublancin 168. J Biol Chem **277**:16682–16688.

126. **Möller MC**, **Hederstedt L**. 2008. Extracytoplasmic processes impaired by inactivation of trxA (thioredoxin gene) in *Bacillus subtilis*. J Bacteriol **190**:4660–4665.

127. **Cho S**, **Parsonage D**, **Thurston C**, **Dutton RJ**, **Poole LB**, **Collet J**. 2012. A new family of membrane electron transporters and its substrates , including a new cell envelope peroxiredoxin , reveal a broadened reductive capacity of the oxidative bacterial cell envelope. MBio **3**:e00291–11.

128. **Hodson CTC**, **Lewin A**, **Hederstedt L**, **Le Brun NE**. 2008. The active-site cysteinyls and hydrophobic cavity residues of ResA are important for cytochrome c maturation in *Bacillus subtilis*. J Bacteriol **190**:4697–4705.

129. **Colbert CL**, **Wu Q**, **Erbel PJA**, **Gardner KH**, **Deisenhofer J**. 2006. Mechanism of substrate specificity in *Bacillus subtilis* ResA, a thioredoxin-like protein involved in cytochrome c maturation. Proc Natl Acad Sci U S A **103**:4410–4415.

130. **Lewin A**, **Crow A**, **Oubrie A**, **Le Brun NE**. 2006. Molecular basis for specificity of the extracytoplasmic thioredoxin ResA. J Biol Chem **281**:35467–35477.

131. **Ahuja U**, **Kjelgaard P**, **Schulz BL**, **Thöny-Meyer L**, **Hederstedt L**. 2009. Haem-delivery proteins in cytochrome c maturation System II. Mol Microbiol **73**:1058–1071.

132. **Eichenberger P**. 2010. The red-ox status of a penicillin-binding protein is an on/off switch for spore peptidoglycan synthesis in *Bacillus subtilis*. Mol Microbiol **75**:10–12.

133. **Heras B**, **Kurz M**, **Jarrott R**, **Shouldice SR**, **Frei P**, **Robin G**, **Cemazar M**, **Thony-Meyer L**, **Glockshuber R**, **Martin JL**. 2008. *Staphylococcus aureus* DsbA does not have a destabilizing disulfide: A NEW PARADIGM FOR BACTERIAL OXIDATIVE FOLDING. J Biol Chem **283**:4261–4271.

134. **van der Kooi-Pol MM**, **Reilman E**, **Sibbald MJJB**, **Veenstra-Kyuchukova YK**, **Kouwen TRHM**, **Buist G**, **van Dijl JM**. 2012. Requirement of signal peptidase ComC and thiol-disulfide oxidoreductase DsbA for optimal cell surface display of pseudopilin ComGC in *Staphylococcus aureus*. Appl Environ Microbiol **78**:7124–7127.

135. **Morikawa K**, **Takemura AJ**, **Inose Y**, **Tsai M**, **Nguyen Thi LT**, **Ohta T**, **Msadek T**. 2012. Expression of a cryptic secondary sigma factor gene unveils natural competence for DNA transformation in *Staphylococcus aureus*. PLoS Pathog **8**:e1003003.

136. **Spaulding AR**, **Salgado-Pabón W**, **Kohler PL**, **Horswill AR**, **Leung DYM**, **Schlievert PM**. 2013. Staphylococcal and streptococcal superantigen exotoxins. Clin Microbiol Rev **26**:422–447.

137. **Wang X**, **Xu M**, **Cai Y**, **Yang H**, **Zhang H**, **Zhang C**. 2009. Functional analysis of the disulphide loop mutant of staphylococcal enterotoxin C2. Appl Microbiol Biotechnol **82**:861–871.

138. **Hovde CJ**, **Marr JC**, **Hoffmann ML**, **Hackett SP**, **Chi YI**, **Crum KK**, **Stevens DL**, **Stauffacher C V**, **Bohach GA**. 1994. Investigation of the role of the disulphide bond in the activity and structure of staphylococcal enterotoxin C1. Mol Microbiol **13**:897–909.

139. **Grossman D**, **Cook RG**, **Sparrow JT**, **Mollick JA**, **Rich RR**. 1990. Dissociation of the stimulatory activities of staphylococcal enterotoxins for T cells and monocytes. J Exp Med **172**:1831–1841.

140. **Grossman D**, **Van M**, **Mollick JA**, **Highlander SK**, **Rich RR**. 1991. Mutation of the disulphide loop in staphylococcal enterotoxin A. Consequences for T cell recognition. J Immunol **147**:3274–3281.

141. **Papageorgiou AC**, **Acharya KR**, **Shapiro R**, **Passalacqua EF**, **Brehm RD**, **Tranter HS**. 1995. Crystal structure of the superantigen enterotoxin C2 from *Staphylococcus aureus* reveals a zinc-binding site. Structure **3**:769–779.

142. **Schad EM**, **Zaitseva I**, **Zaitsev VN**, **Dohlsten M**, **Kalland T**, **Schlievert PM**, **Ohlendorf DH**, **Svensson LA**. 1995. Crystal structure of the superantigen staphylococcal enterotoxin type A. EMBO J **14**:3292–3301.

143. **Huseby M**, **Shi K**, **Brown CK**, **Digre J**, **Mengistu F**, **Seo KS**, **Bohach GA**, **Schlievert PM**, **Ohlendorf DH**, **Earhart CA**. 2007. Structure and biological activities of beta toxin from *Staphylococcus aureus*. J Bacteriol **189**:8719–8726.

144. **Dziewanowska K**, **Edwards VM**, **Deringer JR**, **Bohach G a**, **Guerra DJ**. 1996. Comparison of the beta-toxins from *Staphylococcus aureus* and *Staphylococcus intermedius*. Arch Biochem Biophys **335**:102–108.

145. **Schiavo G**, **Papini E**, **Genna G**, **Montecucco C**. 1990. An intact interchain disulfide bond is required for the neurotoxicity of tetanus toxin. Infect Immun **58**:4136–4141.

146. **Krieglstein KG**, **Das Gupta BR**, **Henschen AH**. 1994. Covalent structure of botulinum neurotoxin type A: location of sulfhydryl groups, and disulfide bridges and identification of C-termini of light and heavy chains. J Protein Chem **13**:49–57.

147. **Lacy DB**, **Tepp W**, **Cohen AC**, **DasGupta BR**, **Stevens RC**. 1998. Crystal structure of botulinum neurotoxin type A and implications for toxicity. Nat Struct Biol **5**:898–902.

148. **Fischer A**, **Mushrush DJ**, **Lacy DB**, **Montal M**. 2008. Botulinum neurotoxin devoid of receptor binding domain translocates active protease. PLoS Pathog **4**:e1000245.

149. **Simpson LL**, **Maksymowych AB**, **Park JB**, **Bora RS**. 2004. The role of the interchain disulfide bond in governing the pharmacological actions of botulinum toxin. J Pharmacol Exp Ther **308**:857–864.

150. **Montecucco C**, **Rasotto MB**. 2015. On botulinum neurotoxin variability. MBio **6**:e02131–14.

151. **Zuverink M**, **Chen C**, **Przedpelski A**, **Blum FC**, **Barbieri JT**. 2015. A heterologous reporter defines the role of the tetanus toxin interchain disulfide in light-chain translocation. Infect Immun **83**:2714–2724.

152. **Popoff MR**, **Poulain B**. 2010. Bacterial toxins and the nervous system: Neurotoxins and multipotential toxins interacting with neuronal cells. Toxins (Basel) **2**:683–737.

153. **Möller M**, **Hederstedt L**. 2006. Role of membrane-bound thiol–disulfide oxidoreductases in endospore-forming bacteria. Antioxid Redox Signal **8**:823–833.

154. **Fontaine L**, **Hols P**. 2008. The inhibitory spectrum of thermophilin 9 from *Streptococcus thermophilus* LMD-9 depends on the production of multiple peptides and the activity of BlpG(St), a thiol-disulfide oxidase. Appl Environ Microbiol **74**:1102–1110.

155. **Teng K**, **Zhang J**, **Zhang X**, **Ge X**, **Gao Y**, **Wang J**, **Lin Y**, **Zhong J**. 2014. Identification of ligand specificity determinants in lantibiotic bovicin HJ50 and the receptor *bovK*, a multitransmembrane histidine kinase. J Biol Chem **289**:9823–9832.

156. **Liu G**, **Zhong J**, **Ni J**, **Chen M**, **Xiao H**, **Huan L**. 2009. Characteristics of the bovicin HJ50 gene cluster in *Streptococcus bovis* HJ50. Microbiology **155**:584–93.

157. **Lin Y**, **Teng K**, **Huan L**, **Zhong J**. 2011. Dissection of the bridging pattern of bovicin HJ50, a lantibiotic containing a characteristic disulfide bridge. Microbiol Res **166**:146–154.

158. **Wang J**, **Ma H**, **Ge X**, **Zhang J**, **Teng K**, **Sun Z**, **Zhong J**. 2014. Bovicin HJ50-like lantibiotics, a novel subgroup of lantibiotics featured by an indispensable disulfide bridge. PLoS One **9**:e97121.

159. **Heng NCK**. 2006. Dysgalacticin: a novel, plasmid-encoded antimicrobial protein (bacteriocin) produced by *Streptococcus dysgalactiae* subsp. equisimilis. Microbiology **152**:1991–2001.

160. **O'Shea EF**, **O'Connor PM**, **O'Sullivan O**, **Cotter PD**, **Ross RP**, **Hill C**. 2013. Bactofencin A, a new type of cationic bacteriocin with unusual immunity. MBio **4**:1–9.

161. **Sawa N**, **Koga S**, **Okamura K**, **Ishibashi N**, **Zendo T**, **Sonomoto K**. 2013. Identification and characterization of novel multiple bacteriocins produced by *Lactobacillus sakei* D98. J Appl Microbiol **115**:61–69.

162. **Ennahar S**. 2000. Class IIa bacteriocins: biosynthesis, structure and activity. FEMS Microbiol Rev **24**:85–106.

163. **Papagianni M**, **Anastasiadou S**. 2009. Pediocins: The bacteriocins of Pediococci. Sources, production, properties and applications. Microb Cell Fact **8**:3.

164. **Oppegård C**, **Fimland G**, **Anonsen JH**, **Nissen-Meyer J**. 2015. The Pediocin PA-1 accessory protein ensures correct disulfide bond formation in the antimicrobial peptide pediocin PA-1. Biochemistry **54**:2967–2974.

165. **Barnett TC**, **Cole JN**, **Rivera-Hernandez T**, **Henningham A**, **Paton JC**, **Nizet V**, **Walker MJ**. 2015. Streptococcal toxins: role in pathogenesis and disease. Cell Microbiol **17**: 1721–1741.

166. **Proft T**, **Fraser JD**. 2003. Bacterial superantigens. Clin Exp Immunol **133**:299–306.

167. **Nasser W**, **Beres SB**, **Olsen RJ**, **Dean MA**, **Rice KA**, **Long SW**, **Kristinsson KG**, **Gottfredsson M**, **Vuopio J**, **Raisanen K**, **Caugant DA**, **Steinbakk M**, **Low DE**, **McGeer A**, **Darenberg J**, **Henriques-Normark B**, **Van Beneden CA**, **Hoffmann S**, **Musser JM**. 2014. Evolutionary pathway to increased virulence and epidemic group A *Streptococcus* disease derived from 3,615 genome sequences. Proc Natl Acad Sci **111**:E1768–E1776.

168. **Cole JN**, **Barnett TC**, **Nizet V**, **Walker MJ**. 2011. Molecular insight into invasive group A streptococcal disease. Nat Rev Microbiol **9**:724–736.

169. **Baker MD**, **Gendlina I**, **Collins CM**, **Acharya KR**. 2004. Crystal structure of a dimeric form of streptococcal pyrogenic exotoxin A (SpeA1). Protein Sci **1**:2285–2290.

170. **Bradford Kline J**, **Collins CM**, **Kline JB**, **Collins CM**. 1996. Analysis of the superantigenic activity of mutant and allelic forms of streptococcal pyrogenic exotoxin A. Infect Immun **64**:861–869.

171. **Saleh M**, **Bartual SG**, **Abdullah MR**, **Jensch I**, **Asmat TM**, **Petruschka L**, **Pribyl T**, **Gellert M**, **Lillig CH**, **Antelmann H**, **Hermoso JA**, **Hammerschmidt S**. 2013. Molecular architecture of *Streptococcus pneumoniae* surface thioredoxin-fold lipoproteins crucial for extracellular oxidative stress resistance and maintenance of virulence. EMBO Mol Med 1–19.

172. **Bertini I**, **Cavallaro G**, **Rosato A**. 2006. Cytochrome c: Occurrence and functions. Chem Rev **106**:90–115.

173. **Gennaris A**, **Collet JF**. 2013. The "captain of the men of death", *Streptococcus pneumoniae*, fights oxidative stress outside the "city wall." EMBO Mol Med **5**:1798–1800.

174. **Gupta V**, **Carroll KS**. 2014. Sulfenic acid chemistry, detection and cellular lifetime. Biochim Biophys Acta **1840**:847–875.

175. **Eser M**, **Masip L**, **Kadokura H**, **Georgiou G**, **Beckwith J**. 2009. Disulfide bond formation by exported glutaredoxin indicates glutathione's presence in the *E. coli* periplasm. Proc Natl Acad Sci U S A **106**:1572–1577.

176. **Ren G**, **Bardwell JCA**. 2011. Engineered pathways for correct disulfide bond oxidation. Antioxid Redox Signal **14**:2399–2412.

177. **Chng SS**, **Dutton RJ**, **Denoncin K**, **Vertommen D**, **Collet JF**, **Kadokura H**, **Beckwith J**. 2012. Overexpression of the rhodanese PspE, a single cysteine-containing protein, restores disulphide bond formation to an *Escherichia coli* strain lacking DsbA. Mol Microbiol **85**:996–1006.

178. **Liu M**, **Zhou L**, **Xu A**, **Lam KSL**, **Wetzel MD**, **Xiang R**, **Zhang J**, **Xin X**, **Dong LQ**, **Liu F**. 2008. A disulfide-bond A oxidoreductase-like protein (DsbA-L) regulates adiponectin multimerization. Proc Natl Acad Sci U S A **105**:18302–18307.

179. **Kolenbrander PE**. 2000. Oral microbial communities: biofilms, interactions, and genetic systems. Annu Rev Microbiol **54**:413–437.

180. **Kolenbrander PE**, **Palmer RJ**, **Periasamy S**, **Jakubovics NS**. 2010. Oral multispecies biofilm development and the key role of cell-cell distance. Nat Rev Microbiol **8**:471–480.

181. **Nobbs AH**, **Lamont RJ**, **Jenkinson HF**. 2009. Streptococcus adherence and colonization. Microbiol Mol Biol Rev **73**:407–450.

182. **Jakubovics NS**, **Kerrigan SW**, **Nobbs AH**, **Strömberg N**, **van Dolleweerd CJ**, **Cox DM**, **Kelly CG**, **Jenkinson HF**. 2005. Functions of cell surface-anchored antigen I/II family and Hsa polypeptides in interactions of *Streptococcus gordonii* with host receptors. Infect Immun **73**:6629–6638.

183. **Rogers JD**, **Palmer J**, **Kolenbrander PE**, **Scannapieco FA.** 2001. Role of *Streptococcus gordonii* amylase-binding protein A in adhesion to hydroxyapatite, starch metabolism, and biofilm formation. Infect Immun **69**:7046–7056.

184. **Wang B**, **Deutch A**, **Hong J**, **Kuramitsu H**. 2011. Proteases of an early colonizer can hinder *Streptococcus mutans* colonization in vitro. J Dent Res **90**:501–505.

185. **Kreth J**, **Zhang Y**, **Herzberg MC**. 2008. Streptococcal antagonism in oral biofilms: *Streptococcus sanguinis* and *Streptococcus gordonii* interference with *Streptococcus mutans*. J Bacteriol **190**:4632–4640.

186. **Johnston C**, **Martin B**, **Fichant G**, **Polard P**, **Claverys JP**. 2014. Bacterial transformation: distribution, shared mechanisms and divergent control. Nat Rev Microbiol **12**:181–196.

187. **Vickerman MM**, **Iobst S**, **Jesionowski A**, **Gill SR**. 2007. Genome-wide transcriptional changes in *Streptococcus gordonii* in response to competence signaling peptide. J Bacteriol **189**:7799–7807.

188. **Heng NCK**, **Tagg JR**, **Tompkins GR**. 2007. Competence-dependent bacteriocin production by *Streptococcus gordonii* DL1 (Challis). J Bacteriol **189**:1468–1472.

189. **Ishii S**, **Yano T**, **Hayashi H**. 2006. Expression and characterization of the peptidase domain of *Streptococcus pneumoniae* ComA, a bifunctional ATP-binding cassette transporter involved in quorum sensing pathway. J Biol Chem **281**:4726–4731.

190. **Johnston C**, **Martin B**, **Fichant G**, **Polard P**, **Claverys JP**. 2014. Bacterial transformation: distribution, shared mechanisms and divergent control. Nat Rev Microbiol **12**:181–196.

191. **Heng NCK**, **Tagg JR**, **Tompkins GR**. 2006. Identification and characterization of the loci encoding the competence-associated alternative sigma factor of *Streptococcus gordonii*. FEMS Microbiol Lett **259**:27–34.

192. **Lunsford RD**, **Roble AG**. 1997. *comYA*, a gene similar to *comGA* of *Bacillus subtilis*, is essential for competence factor dependent DNA transformation in *Streptococcus gordonii*. J Bacteriol **179**:3122–3126.

193. **Laurenceau R**, **Péhau-Arnaudet G**, **Baconnais S**, **Gault J**, **Malosse C**, **Dujeancourt A**, **Campo N**, **Chamot-Rooke J**, **Le Cam E**, **Claverys JP**, **Fronzes R**. 2013. A type IV pilus mediates DNA binding during natural transformation in *Streptococcus pneumoniae*. PLoS Pathog **9**:e1003473.

194. **Tompkins GR**, **Peavey MA**, **Birchmeier KR**, **Tagg JR**. 1997. Bacteriocin production and sensitivity among coaggregating and noncoaggregating oral streptococci. Oral Microbiol Immunol **12**:98–105.

195. **Kreth J**, **Vu H**, **Zhang Y**, **Herzberg MC**. 2009. Characterization of hydrogen peroxide-induced DNA release by *Streptococcus sanguinis* and *Streptococcus gordonii*. J Bacteriol **191**:6281–6291.

196. **Jakubovics NS**, **Grant Burgess J**. 2015. Extracellular DNA in oral microbial biofilms. Microbes Infect **17**:531–537.

197. **Xu Y**, **Kreth J**. 2013. Role of LytF and AtlS in eDNA release by *Streptococcus gordonii*. PLoS One **8**:e62339.

198. **Berg KH**, **Ohnstad HS**, **Håvarstein LS**. 2012. LytF, a novel competence-regulated murein hydrolase in the genus *Streptococcus*. J Bacteriol **194**:627–635.

199. **Ahn SJ**, **Burne RA.** 2007. Effects of oxygen on biofilm formation and the AtlA autolysin of *Streptococcus mutans*. J Bacteriol **189**:6293–302.

200. **Ahn SJ**, **Burne RA**. 2006. The *atlA* operon of *Streptococcus mutans*: role in autolysin maturation and cell surface biogenesis. J Bacteriol **188**:6877–6888.

201. **Liu Y**, **Burne RA**. 2011. The major autolysin of *Streptococcus gordonii* is subject to complex regulation and modulates stress tolerance, biofilm formation, and extracellular-DNA release. J Bacteriol **193**:2826–2837.

202. **Loo CY**, **Corliss DA**, **Ganeshkumar N**. 2000. *Streptococcus gordonii* biofilm formation: identification of genes that code for biofilm phenotypes. J Bacteriol **182**:1374–1382.

203. **Bermúdez-Humarán LG**, **Langella P**, **Cortes-Perez NG**, **Gruss A**, **Tamez-Guerra RS**, **Oliveira SC**, **Saucedo-Cardenas O**, **Montes de Oca-Luna R**, **Le Loir Y**. 2003. Intranasal immunization with recombinant *Lactococcus lactis* secreting murine interleukin-12 enhances antigen-specific Th1 cytokine production. Infect Immun **71**:1887–1896.

204. **Knight JB**, **Halperin SA**, **West KA**, **Lee SF**. 2008. Expression of a functional single-chain variable-fragment antibody against complement receptor 1 in *Streptococcus gordonii*. Clin Vaccine Immunol **15**:925–931.

205. **Glockshuber R**, **Schmidt T**, **Plueckthun A**. 1992. The disulfide bonds in antibody variable domains: effects on stability, folding in vitro, and functional expression in *Escherichia coli*. Biochemistry **31**:1270–1279.

206. **Jurado P**, **Ritz D**, **Beckwith J**, **de Lorenzo V**, **Fernández LA**. 2002. Production of functional single-chain Fv antibodies in the cytoplasm of *Escherichia coli*. J Mol Biol **320**:1–10.

207. **Dalle-Donne I**, **Rossi R**, **Colombo G**, **Giustarini D**, **Milzani A**. 2009. Protein S-glutathionylation: a regulatory device from bacteria to humans. Trends Biochem Sci **34**:85–96.

208. **Burne RA**, **Wen ZT**, **Chen YM**, **Penders JEC**.1999. Regulation of expression of the fructan hydrolase gene of *Streptococcus mutans* GS-5 by induction and carbon catabolite repression **181**:2863–2871.

209. **Kim J**, **Senadheera D**. 2012. TcyR regulates L-cystine uptake via the TcyABC transporter in *Streptococcus mutans*. FEMS Microbiol Lett **328**:114–121.

210. **Claverys JP**, **Dintilhac A**, **Pestova E V**, **Martin B**, **Morrison DA**. 1995. Construction and evaluation of new drug-resistance cassettes for gene disruption mutagenesis in *Streptococcus pneumoniae*, using an *ami* test platform. Gene **164**:123–128.

211. **Dunny GM**, **Lee LN**, **LeBlanc DJ**. 1991. Improved electroporation and cloning vector system for Gram-positive bacteria. Appl Environ Microbiol **57**:1194–1201.

212. **Vats N**, **Lee SF**. 2001. Characterization of a copper-transport operon, *copYAZ*, from *Streptococcus mutans*. Microbiology **147**:653–662.

213. **Heckman KL**, **Pease LR**. 2007. Gene splicing and mutagenesis by PCR-driven overlap extension. Nat Protoc **2**:924–932.

214. **Tremblay YDN**, **Lo H**, **Li YH**, **Halperin SA**, **Lee SF**. 2009. Expression of the *Streptococcus mutans* essential two-component regulatory system VicRK is pH and growth-phase dependent and controlled by the LiaFSR three-component regulatory system. Microbiology **155**:2856–2865.

215. **Schmittgen TD**, **Livak KJ**. 2008. Analyzing real-time PCR data by the comparative CT method. Nat Protoc **3**:1101–1108.

216. **Lunsford RD**, **London J**. 1996. Natural genetic transformation in *Streptococcus gordonii: comX* imparts spontaneous competence on strain wicky. J Bacteriol **178**: 5831-5835.

217. **Laemmli UK**. 1970. Cleavage of structural proteins during the assembly of the head of bacteriophage T4. Nature **227**:680–685.

218. **Towbin H**, **Staehelin T**, **Gordon J**. 1979. Electrophoretic transfer of proteins from polyacrylamide gels to nitrocellulose sheets: procedure and some applications. Proc Natl Acad Sci U S A **76**:4350–4354.

219. **Leichert LI**, **Jakob U**. 2004. Protein thiol modifications visualized in vivo. PLoS Biol **2**:e333.

220. **Hennecke J**, **Sebbel P**, **Glockshuber R**. 1999. Random circular permutation of DsbA reveals segments that are essential for protein folding and stability. J Mol Biol **286**:1197–215.

221. **Lyles MM**, **Gilbert HF**. 1991. Catalysis of the oxidative folding of ribonuclease A by protein disulfide isomerase: pre-steady-state kinetics and the utilization of the oxidizing equivalents of the isomerase. Biochemistry **30**:619–25.

222. **Rupp K**, **Birnbach U**, **Lundström J**, **Van PN**, **Söling HD**. 1994. Effects of CaBP2, the rat analog of ERp72, and of CaBP1 on the refolding of denatured reduced proteins. Comparison with protein disulfide isomerase. J Biol Chem **269**:2501–2507.

223. **Lyles MM**, **Gilbert HF**. 1991. Catalysis of the oxidative folding of ribonuclease A by protein disulfide isomerase: dependence of the rate on the composition of the redox buffer. Biochemistry **30**:613–619.

224. **Wunderlich M**, **Otto A**, **Maskos K**, **Mücke M**, **Seckler R**, **Glockshuber R**. 1995. Efficient catalysis of disulfide formation during protein folding with a single active-site cysteine. J Mol Biol **247**:28–33.

225. **Candiano G**, **Bruschi M**, **Musante L**, **Santucci L**, **Ghiggeri GM**, **Carnemolla B**, **Orecchia P**, **Zardi L**, **Righetti PG**. 2004. Blue silver: A very sensitive colloidal Coomassie G-250 staining for proteome analysis. Electrophoresis **25**:1327–1333.

226. **Shevchenko A**, **Tomas H**, **Havlis J**, **Olsen J V**, **Mann M**. 2006. In-gel digestion for mass spectrometric characterization of proteins and proteomes. Nat Protoc **1**:2856–2860.

227. **Vizcaíno JA**, **Deutsch EW**, **Wang R**, **Csordas A**, **Reisinger F**, **Ríos D**, **Dianes JA**, **Sun Z**, **Farrah T**, **Bandeira N**, **Binz P-A**, **Xenarios I**, **Eisenacher M**, **Mayer G**, **Gatto L**, **Campos A**, **Chalkley RJ**, **Kraus H-J**, **Albar JP**, **Martinez-Bartolomé S**, **Apweiler R**, **Omenn GS**, **Martens L**, **Jones AR**, **Hermjakob H**. 2014. ProteomeXchange provides globally coordinated proteomics data submission and dissemination. Nat Biotechnol **32**:223–226.

228. **Dyrløv Bendtsen J**, **Nielsen H**, **von Heijne G**, **Brunak S**. 2004. Improved prediction of signal peptides: SignalP 3.0. J Mol Biol **340**:783–795.

229. **Juncker A**, **Willenbrock H**. 2003. Prediction of lipoprotein signal peptides in Gram-negative bacteria. Protein Sci **12**:1652–1662.

230. **Bernsel A**, **Viklund H**, **Falk J**, **Lindahl E**, **von Heijne G**, **Elofsson A**. 2008. Prediction of membrane-protein topology from first principles. Proc Natl Acad Sci **105**:7177–7181.

231. **Lee SF**, **Halperin SA**, **Wang H**, **MacArthur A**. 2002. Oral colonization and immune responses to *Streptococcus gordonii* expressing a pertussis toxin S1 fragment in mice. FEMS Microbiol Lett **208**:175–178.

232. **Kadokura H**, **Katzen F**, **Beckwith J**. 2003. Protein disulfide bond formation in prokaryotes. Annu Rev Biochem **72**:111–135.

233. **Mavridou DAI**, **Ferguson SJ**, **Stevens JM**. 2012. The interplay between the disulfide bond formation pathway and cytochrome c maturation in *Escherichia coli*. FEBS Lett **586**:1702–1707.

234. **Heras B**, **Kurz M**, **Jarrott R**, **Byriel KA**, **Jones A**, **Thöny-Meyer L**, **Martin JL**. 2007. Expression and crystallization of DsbA from *Staphylococcus aureus*. Acta Crystallogr Sect F Struct Biol Cryst Commun **63**:953–956.

235. **Pirazzini M**, **Rossetto O**, **Bolognese P**, **Shone CC**, **Montecucco C**. 2011. Double anchorage to the membrane and intact inter-chain disulfide bond are required for the low pH induced entry of tetanus and botulinum neurotoxins into neurons. Cell Microbiol **13**:1731–1743.

236. **Wörn A**, **Plückthun A**. 2001. Stability engineering of antibody single-chain Fv fragments. J Mol Biol **305**:989–1010.

237. **Zhang Y**, **Whiteley M**, **Kreth J**, **Lei Y**, **Khammanivong A**, **Evavold JN**, **Fan J**, **Herzberg MC**. 2009. The two-component system BfrAB regulates expression of ABC transporters in *Streptococcus gordonii* and *Streptococcus sanguinis*. Microbiology **155**:165–173.

238. **Missiakas D**, **Georgopoulos C**, **Raina S**. 1993. Identification and characterization of the *Escherichia coli* gene *dsbB*, whose product is involved in the formation of disulfide bonds *in vivo*. Proc Natl Acad Sci U S A **90**:7084–7088.

239. **Das T**, **Sharma PK**, **Busscher HJ**, **van der Mei HC**, **Krom BP**. 2010. Role of extracellular DNA in initial bacterial adhesion and surface aggregation. Appl Environ Microbiol **76**:3405–3408.

240. **Itzek A**, **Zheng L**, **Chen Z**, **Merritt J**, **Kreth J**. 2011. Hydrogen peroxide-dependent dna release and transfer of antibiotic resistance genes in *Streptococcus gordonii*. J Bacteriol **193**:6912–6922.

241. **Layec S**, **Decaris B**, **Leblond-Bourget N**. 2008. Characterization of proteins belonging to the CHAP-related superfamily within the Firmicutes. J Mol Microbiol Biotechnol **14**:31–40.

242. **Kang HJ**, **Baker EN**. 2009. Intramolecular isopeptide bonds give thermodynamic and proteolytic stability to the major Pilin protein of *Streptococcus pyogenes*. J Biol Chem **284**:20729–20737.

243. **Budzik JM**, **Poor CB**, **Faull KF**, **Whitelegge JP**, **He C**, **Schneewind O**. 2009. Intramolecular amide bonds stabilize pili on the surface of bacilli. Proc Natl Acad Sci **106**:19992–19997.

244. **Forsgren N**, **Lamont RJ**, **Persson K**. 2010. Two intramolecular isopeptide bonds are identified in the crystal structure of the *Streptococcus gordonii* SspB C-terminal Domain. J Mol Biol **397**:740–751.

245. **Yamanaka H**, **Kameyama M**, **Baba T**, **Fujii Y**, **Okamoto K**. 1994. Maturation pathway of *Escherichia coli* heat-stable enterotoxin I: Requirement of DsbA for disulfide bond formation. J Bacteriol **176**:2906–2913.

246. **Andisi VF**, **Hinojosa CA**, **de Jong A**, **Kuipers OP**, **Orihuela CJ**, **Bijlsma JJE**. 2012. Pneumococcal gene complex involved in resistance to extracellular oxidative stress. Infect Immun **80**:1037–1049.

247. **Zhang Y**, **Lei Y**, **Nobbs A**, **Khammanivong A**, **Herzberg MC**. 2005. Inactivation of *Streptococcus gordonii* SspAB alters expression of multiple adhesin genes. Infect Immun **73**:3351–3357.

248. **Kim YK**, **Shin YJ**, **Lee WH**, **Kim HY**, **Hwang KY**. 2009. Structural and kinetic analysis of an MsrA-MsrB fusion protein from *Streptococcus pneumoniae*. Mol Microbiol **72**:699–709.

249. **Sievers F**, **Wilm A**, **Dineen D**, **Gibson TJ**, **Karplus K**, **Li W**, **Lopez R**, **McWilliam H**, **Remmert M**, **Soding J**, **Thompson JD**, **Higgins DG**. 2014. Fast, scalable generation of high-quality protein multiple sequence alignments using Clustal Omega. Mol Syst Biol **7**:539–539.

250. **Crooks GE**, **Hom G**, **Chandonia J**, **Brenner S**. 2004. WebLogo: A sequence logo generator. Genome Res **14**:1188–1190.

251. **Collet JF**, **Messens J**. 2010. Structure, function, and mechanism of thioredoxin proteins. Antioxid Redox Signal **13**:1205–1216.

252. **Kishigami S**, **Kanaya E**, **Kikuchi M**, **Ito K**. 1995. DsbA-DsbB interaction through their active site cysteines. J Biol Chem **270**:17072–17074.

253. **Reid E**, **Cole J**, **Eaves D**. 2001. The *Escherichia coli* CcmG protein fulfils a specific role in cytochrome c assembly. Biochem J **58**:51–58.

254. **Mössner E**, **Iwai H**, **Glockshuber R**. 2000. Influence of the pK(a) value of the buried, active-site cysteine on the redox properties of thioredoxin-like oxidoreductases. FEBS Lett **477**:21–26.

255. **Tan J**, **Lu Y**, **Bardwell JCA**. 2005. Mutational analysis of the disulfide catalysts DsbA and DsbB. J Bacteriol **187**:1504–1510.

256. **Bardwell JC**, **Lee JO**, **Jander G**, **Martin N**, **Belin D**, **Beckwith J**. 1993. A pathway for disulfide bond formation in vivo. Proc Natl Acad Sci U S A **90**:1038–42.

257. **Walker KW**, **Lyles MM**, **Gilbert HF**. 1996. Catalysis of oxidative protein folding by mutants of protein disulfide isomerase with a single active-site cysteine. Biochemistry **35**:1972–80.

258. **Marvaud JC**, **Eisel U**, **Binz T**, **Niemann H**, **Popoff MR**. 1998. TetR is a positive regulator of the tetanus toxin gene in *Clostridium tetani* and is homologous to *botR*. Infect Immun **66**:5698–702.

259. **Proba K**, **Honegger A**, **Plückthun A**. 1997. A natural antibody missing a cysteine in VH: consequences for thermodynamic stability and folding. J Mol Biol **265**:161–172.

260. **Poquet I**, **Saint V**, **Seznec E**, **Simoes N**, **Bolotin A**, **Gruss A**. 2000. HtrA is the unique surface housekeeping protease in *Lactococcus lactis* and is required for natural protein processing. Mol Microbiol **35**:1042–1051.

261. **Krojer T**, **Sawa J**, **Huber R**, **Clausen T**. 2010. HtrA proteases have a conserved activation mechanism that can be triggered by distinct molecular cues. Nat Struct Mol Biol **17**:844–852.

262. **Zapun A**, **Cooper L**, **Creighton TE**. 1994. Replacement of the active-site cysteine residues of DsbA, a protein required for disulfide bond formation in vivo. Biochemistry **33**:1907–1914.

263. **Qin A**, **Scott DW**, **Rabideau MM**, **Moore EA**, **Mann BJ**. 2011. Requirement of the CXXC motif of novel *Francisella* infectivity potentiator protein B FipB, and FipA in virulence of *F. tularensis* subsp. tularensis. PLoS One **6**:e24611.

264. **Liu X**, **Ramsey MM**, **Chen X**, **Koley D**, **Whiteley M**, **Bard AJ**. 2011. Real-time mapping of a hydrogen peroxide concentration profile across a polymicrobial bacterial biofilm using scanning electrochemical microscopy. Proc Natl Acad Sci U S A **108**:2668–2673.

265. **Jakubovics NS**, **Gill SR**, **Vickerman MM**, **Kolenbrander PE**. 2008. Role of hydrogen peroxide in competition and cooperation between *Streptococcus gordonii* and *Actinomyces naeslundii*. FEMS Microbiol Ecol **66**:637–644.

266. **Wang L**, **Zhang L**, **Niu Y**, **Sitia R**, **Wang C**. 2014. Glutathione peroxidase 7 utilizes hydrogen peroxide generated by Ero1α to promote oxidative protein folding. Antioxid Redox Signal **20**:545–556.

267. **Balmer Y**, **Koller A**, **del Val G**, **Manieri W**, **Schürmann P**, **Buchanan BB**. 2003. Proteomics gives insight into the regulatory function of chloroplast thioredoxins. Proc Natl Acad Sci U S A **100**:370–375.

268. **Zheng X**, **Zhang K**, **Zhou X**, **Liu C**, **Li M**, **Li Y**, **Wang R**, **Li J**, **Shi W**, **Xu X**. 2013. Involvement of *gshAB* in the interspecies competition within oral biofilm. J Dent Res **92**:819–824.

269. **Hall A**, **Nelson K**, **Poole LB**, **Karplus PA**. 2011. Structure-based insights into the catalytic power and conformational dexterity of peroxiredoxins. Antioxid Redox Signal **15**:795–815.

270. **Tokuhiro K**, **Ikawa M**, **Benham AM**, **Okabe M**. 2012. Protein disulfide isomerase homolog PDILT is required for quality control of sperm membrane protein ADAM3 and male fertility [corrected]. Proc Natl Acad Sci U S A **109**:3850–3855.

271. **Han H**, **Dong H**, **Zhu S**, **Zhao Q**, **Jiang L**, **Wang Y**, **Li L**, **Wu Y**, **Huang B**. 2014. Molecular characterization and analysis of a novel protein disulfide isomerase-like protein of *Eimeria tenella*. PLoS One **9**:e99914.

272. **Fomenko DE**, **Gladyshev VN**. 2003. Identity and functions of CxxC-derived motifs. Biochemistry **42**:11214–11225.

273. **Jeong W**, **Jung Y**, **Kim H**, **Park SJ**, **Rhee SG**. 2009. Thioredoxin-related protein 14, a new member of the thioredoxin family with disulfide reductase activity: implication in the redox regulation of TNF-alpha signaling. Free Radic Biol Med **47**:1294–1303.

274. **Nobbs AH**, **Jenkinson HF**. 2015. Interkingdom networking within the oral microbiome. Microbes Infect **17**:484–492.

275. **Dû LD**, **Kolenbrander PE**. 2000. Identification of saliva-regulated genes of *Streptococcus gordonii* DL1 by differential display using random arbitrarily primed PCR. Infect Immun **68**:4834–4837.

276. **Marchant S**, **Brailsford SR**, **Twomey AC**, **Roberts GJ**, **Beighton D**. 2001. The predominant microflora of nursing caries lesions. Caries Res **35**:397–406.

277. **Gross EL**, **Beall CJ**, **Kutsch SR**, **Firestone ND**, **Leys EJ**, **Griffen AL**. 2012. Beyond *Streptococcus mutans*: Dental caries onset linked to multiple species by 16S rRNA community analysis. PLoS One **7**:e47722.

278. **Kuramitsu HK**, **Wang BY**. 2006. Virulence properties of cariogenic bacteria. BMC Oral Health **6 Suppl 1**:S11.

279. **Wang BY**, **Kuramitsu HK**. 2005. Interactions between oral bacteria: Inhibition of *Streptococcus mutans* bacteriocin production by *Streptococcus gordonii*. Appl Environ Microbiol **71**:354–362.

280. **Peterson SN**, **Sung CK**, **Cline R**, **Desai B V**, **Snesrud EC**, **Luo P**, **Walling J**, **Li H**, **Mintz M**, **Tsegaye G**, **Burr PC**, **Do Y**, **Ahn S**, **Gilbert J**, **Fleischmann RD**, **Morrison DA.** 2004. Identification of competence pheromone responsive genes in *Streptococcus pneumoniae* by use of DNA microarrays. Mol Microbiol **51**:1051–1070.

281. **Dawid S**, **Sebert ME**, **Weiser JN**. 2009. Bacteriocin activity of *Streptococcus pneumoniae* is controlled by the serine protease HtrA via posttranscriptional regulation. J Bacteriol **191**:1509–1518.

282. **Kochan TJ**, **Dawid S**. 2013. The HtrA protease of *Streptococcus pneumoniae* controls density-dependent stimulation of the bacteriocin *blp* locus via disruption of pheromone secretion. J Bacteriol **195**:1561–1572.

283. **Merritt J**, **Qi F**. 2012. The mutacins of *Streptococcus mutans*: Regulation and ecology. Mol Oral Microbiol **27**:57–69.

284. **Van Der Ploeg JR**. 2005. Regulation of bacteriocin production in *Streptococcus mutans* by the quorum-sensing system required for development of genetic competence. J Bacteriol **187**:3980–3989.

285. **Kreth J**, **Merritt J**, **Zhu L**, **Shi W**, **Qi F**. 2006. Cell density- and ComE-dependent expression of a group of mutacin and mutacin-like genes in *Streptococcus mutans*. FEMS Microbiol Lett **265**:11–17.

286. **Qi F**, **Merritt J**, **Lux R**, **Shi W**. 2004. Inactivation of the *ciaH* gene in *Streptococcus mutans* diminishes mutacin production and competence development, alters sucrose-dependent biofilm formation, and reduces stress tolerance. Infect Immun **72**:4895–4899.

287. **Senadheera DB**, **Cordova M**, **Ayala EA**, **Chávez de Paz LE**, **Singh K**, **Downey JS**, **Svensäter G**, **Goodman SD**, **Cvitkovitch DG**. 2012. Regulation of bacteriocin production and cell death by the VicRK signaling system in *Streptococcus mutans*. J Bacteriol **194**:1307–1316.

288. **Okinaga T**, **Niu G**, **Xie Z**, **Qi F**, **Merritt J**. 2010. The *hdrRM* operon of *Streptococcus mutans* encodes a novel regulatory system for coordinated competence development and bacteriocin production. J Bacteriol **192**:1844–1852.

289. **Xie Z**, **Okinaga T**, **Niu G**, **Qi F**, **Merritt J**. 2010. Identification of a novel bacteriocin regulatory system in *Streptococcus mutans*. Mol Microbiol **78**:1431–1447.

290. **Heng NCK**, **Burtenshaw GA**, **Jack RW**, **Tagg JR**. 2007. Ubericin A, a class IIa bacteriocin produced by *Streptococcus uberis*. Appl Environ Microbiol **73**:7763–7766.

291. **Schlegel R**, **Slade HD**. 1972. Bacteriocin production by transformable group H streptococci. J Bacteriol **112**:824–829.

292. **Cook LC**, **Federle MJ**. 2014. Peptide pheromone signaling in *Streptococcus* and *Enterococcus*. FEMS Microbiol Rev **38**:473–492.

293. **Claverys JP**, **Martin B**, **Håvarstein LS**. 2007. Competence-induced fratricide in streptococci. Mol Microbiol **64**:1423–1433.

294. **Schnorpfeil A**, **Kranz M**, **Kovács M**, **Kirsch C**, **Gartmann J**, **Brunner I**, **Bittmann S**, **Brückner R**. 2013. Target evaluation of the non-coding csRNAs reveals a link of the two-component regulatory system CiaRH to competence control in *Streptococcus pneumoniae* R6. Mol Microbiol **89**:334–349.

295. **Mascher T**, **Heintz M**, **Zähner D**, **Merai M**, **Hakenbeck R**. 2006. The CiaRH system of *Streptococcus pneumoniae* prevents lysis during stress induced by treatment with cell wall inhibitors and by mutations in *pbp2x* involved in β-lactam resistance. J Bacteriol **188**:1959–1968.

296. **Haas W**, **Kaushal D**, **Sublett J**, **Obert C**, **Tuomanen EI**. 2005. Vancomycin stress response in a sensitive and a tolerant strain of *Streptococcus pneumoniae*. J Bacteriol **187**:8205–8210.

297. **Rogers PD**, **Liu TT**, **Barker KS**, **Hilliard GM**, **English BK**, **Thornton J**, **Swiatlo E**, **McDaniel LS**. 2007. Gene expression profiling of the response of *Streptococcus pneumoniae* to penicillin. J Antimicrob Chemother **59**:616–626.

298. **Sebert ME**, **Palmer LM**, **Rosenberg M**, **Weiser JN**. 2002. Microarray-based identification of *htrA*, a *Streptococcus pneumoniae* gene that is regulated by the ciarh two-component system and contributes to nasopharyngeal colonization. Infect Immun **70**:4059–4067.

299. **Halfmann A**, **Schnorpfeil A**, **Müller M**, **Marx P**, **Günzler U**, **Hakenbeck R**, **Brückner R**. 2011. Activity of the two-component regulatory system CiaRH in *Streptococcus pneumoniae* R6. J Mol Microbiol Biotechnol **20**:96–104.

300. **Marx P**, **Nuhn M**, **Kovács M**, **Hakenbeck R**, **Brückner R**. 2010. Identification of genes for small non-coding RNAs that belong to the regulon of the two-component regulatory system CiaRH in *Streptococcus*. BMC Genomics **11**:661.

301. **Busch A**, **Richter AS**, **Backofen R**. 2008. IntaRNA: Efficient prediction of bacterial sRNA targets incorporating target site accessibility and seed regions. Bioinformatics **24**:2849–2856.

302. **Dagkessamanskaia A**, **Moscoso M**, **Overweg K**, **Reuter M**, **Martin B**, **Wells J**, **Claverys J**. 2004. Interconnection of competence, stress and CiaR regulons in *Streptococcus pneumoniae* : competence triggers stationary phase autolysis of *ciaR* mutant cells. Mol Microbiol **51**:1071–1086.

303. **Liu Y**, **Burne RA.** 2009. Multiple two-component systems modulate alkali generation in *Streptococcus gordonii* in response to environmental stresses. J Bacteriol **191**:7353–7362.

304. **Sebert ME**, **Patel KP**, **Plotnick M**, **Weiser JN**. 2005. Pneumococcal HtrA protease mediates inhibition of competence by the CiaRH two-component signaling system. J Bacteriol **187**:3969–3979.

305. **Ahn S**, **Wen ZT**, **Burne RA**. 2006. Multilevel control of competence development and stress tolerance in *Streptococcus mutans* UA159 **74**:1631–1642.

306. **Halfmann A**, **Kovács M**, **Hakenbeck R**, **Brückner R**. 2007. Identification of the genes directly controlled by the response regulator CiaR in *Streptococcus pneumoniae*: Five out of 15 promoters drive expression of small non-coding RNAs. Mol Microbiol **66**:110–126.

307. **Guenzi E**, **Gasc AM**, **Sicard MA**, **Hakenbeck R**. 1994. A two-component signal-transducing system is involved in competence and penicillin susceptibility in laboratory mutants of *Streptococcus pneumoniae*. Mol Microbiol **12**:505–515.

308. **Mascher T**, **Zähner D**, **Merai M**, **Balmelle N**, **De Saizieu AB**, **Hakenbeck R**. 2003. The *Streptococcus pneumoniae cia* regulon: CiaR target sites and transcription profile analysis. J Bacteriol **185**:60–70.

309. **Brantl S**, **Brückner R**. 2014. Small regulatory RNAs from low-GC Gram-positive bacteria. RNA Biol **11**:443–456.

310. **Wilton J**, **Acebo P**, **Herranz C**, **Gómez A**, **Amblar M**. 2015. Small regulatory RNAs in *Streptococcus pneumoniae*: discovery and biological functions. Front Genet **06**:1–8.

311. **Jordan S**, **Hutchings MI**, **Mascher T**. 2008. Cell envelope stress response in Gram-positive bacteria. FEMS Microbiol Rev **32**:107–146.

312. **Sarvas M**, **Harwood CR**, **Bron S**, **van Dijl JM**. 2004. Post-translocational folding of secretory proteins in Gram-positive bacteria. Biochim Biophys Acta **1694**:311–327.

313. **Raivio TL**. 2005. Envelope stress responses and Gram-negative bacterial pathogenesis. Mol Microbiol **56**:1119–1128.

314. **Westers H**, **Westers L**, **Darmon E**, **Van Dijl JM**, **Quax WJ**, **Zanen G**. 2006. The CssRS two-component regulatory system controls a general secretion stress response in *Bacillus subtilis*. FEBS J **273**:3816–3827.

315. **Stevens KE**, **Chang D**, **Zwack EE**, **Sebert ME**. 2011. Competence in *Streptococcus pneumoniae* is regulated by the rate of ribosomal decoding errors. MBio **2**:1–9.

316. **Cassone M**, **Gagne AL**, **Spruce LA**, **Seeholzer SH**, **Sebert ME**. 2012. The HtrA protease from *Streptococcus pneumoniae* digests both denatured proteins and the competence-stimulating peptide. J Biol Chem **287**:38449–38459.

317. **Stogios P**, **Savchenko A**. 2015. Crystal structure of SdbA. Unpublished.

318. **Petersen HJ**, **Keane C**, **Jenkinson HF**, **Vickerman MM**, **Jesionowski A**, **Waterhouse JC**, **Cox D**, **Kerrigan SW**. 2010. Human platelets recognize a novel surface protein, PadA, on *Streptococcus gordonii* through a unique interaction involving fibrinogen receptor GPIIbIIIa. Infect Immun **78**:413–22.

319. **Roszczenko P**, **Grzeszczuk M**, **Kobierecka P**, **Wywial E**, **Urbanowicz P**, **Wincek P**, **Nowak E**, **Jagusztyn-Krynicka EK**. 2015. *Helicobacter pylori* HP0377, a member of the Dsb family, is an untypical multifunctional CcmG that cooperates with dimeric thioldisulfide oxidase HP0231. BMC Microbiol **15**:135.

320. **Gutiérrez J**, **Criado R**, **Citti R**, **Martín M**, **Herranz C**, **Fernández MF**, **Cintas LM**, **Hernández PE**. 2004. Performance and applications of polyclonal antipeptide antibodies specific for the enterococcal bacteriocin Enterocin P. J Agric Food Chem **52**:2247–2255.

321. **Martínez JM**, **Martínez MI**, **Herranz C**, **Suárez A**, **Fernández MF**, **Cintas LM**, **Rodríguez JM**, **Hernández PE**. 1999. Antibodies to a synthetic 1-9-N-terminal amino acid fragment of mature pediocin PA-1: sensitivity and specificity for pediocin PA-1 and cross-reactivity against Class IIa bacteriocins. Microbiology **145**:2777–87.

322. **Keren T**, **Yarmus M**, **Halevy G**, **Shapira R**. 2004. Immunodetection of the bacteriocin lacticin rm : analysis of the influence of temperature and Tween 80 on its expression and activity. Appl Environ Microbiol **70:**2098-2104.

323. **Qi F**, **Chen P**, **Caufield PW**. 2001. The group I strain of *Streptococcus mutans*, UA140, produces both the lantibiotic mutacin I and a nonlantibiotic bacteriocin, mutacin IV. Appl Environ Microbiol **67**:15–21.

324. **Fontaine L**, **Boutry C**, **Guédon E**, **Guillot A**, **Ibrahim M**, **Grossiord B**, **Hols P**. 2007. Quorum-sensing regulation of the production of Blp bacteriocins in *Streptococcus thermophilus*. J Bacteriol **189**:7195–7205.

325. **Hale JDF**, **Heng NCK**, **Jack RW**, **Tagg JR**. 2005. Identification of *nlmTE*, the locus encoding the ABC transport system required for export of nonlantibiotic mutacins in *Streptococcus mutans*. J Bacteriol **187:** 5036-5039.

326. **Schägger H**. 2006. Tricine-SDS-PAGE. Nat Protoc **1**:16–22.

327. **Davis E**, **Kennedy D**, **Halperin SA**, **Lee SF**. 2011. Role of the cell wall microenvironment in expression of a heterologous SpaP-S1 fusion protein by *Streptococcus gordonii*. Appl Environ Microbiol **77**:1660–1666.

328. **Suzuki Y**, **Takeda Y**, **Ikuta T**. 2008. Immunoblotting conditions for human hemoglobin chains. Anal Biochem **378**:218–220.

329. **Too CK**, **Murphy PR**, **Croll RP**. 1994. Western blotting of formaldehyde-fixed neuropeptides as small as 400 daltons on gelatin-coated nitrocellulose paper. Anal Biochem **219**:341–348.

330. **Mizzen CA**, **Cartel NJ**, **Yu WH**, **Fraser PE**, **McLachlan DR**. 1996. Sensitive detection of metallothioneins-1, -2 and -3 in tissue homogenates by immunoblotting: A method for enhanced membrane transfer and retention. J Biochem Biophys Methods **32**:77–83.

Appendix A: Supporting Material for Chapter 4

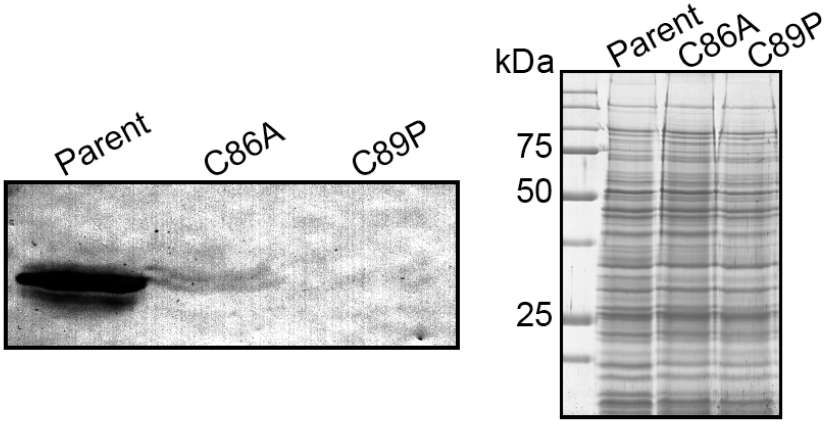

APPENDIX A1. ScFv produced by the C86A mutant. Proteins were extracted from the parent, $sdbA_{C86A}$ (C86A), and $sdbA_{C89P}$ mutants (C89P). Western blot to detect scFv (33 kDa) with an anti-HA monoclonal antibody (left). Coomassie blue stained SDS-PAGE showing total protein loading (right).

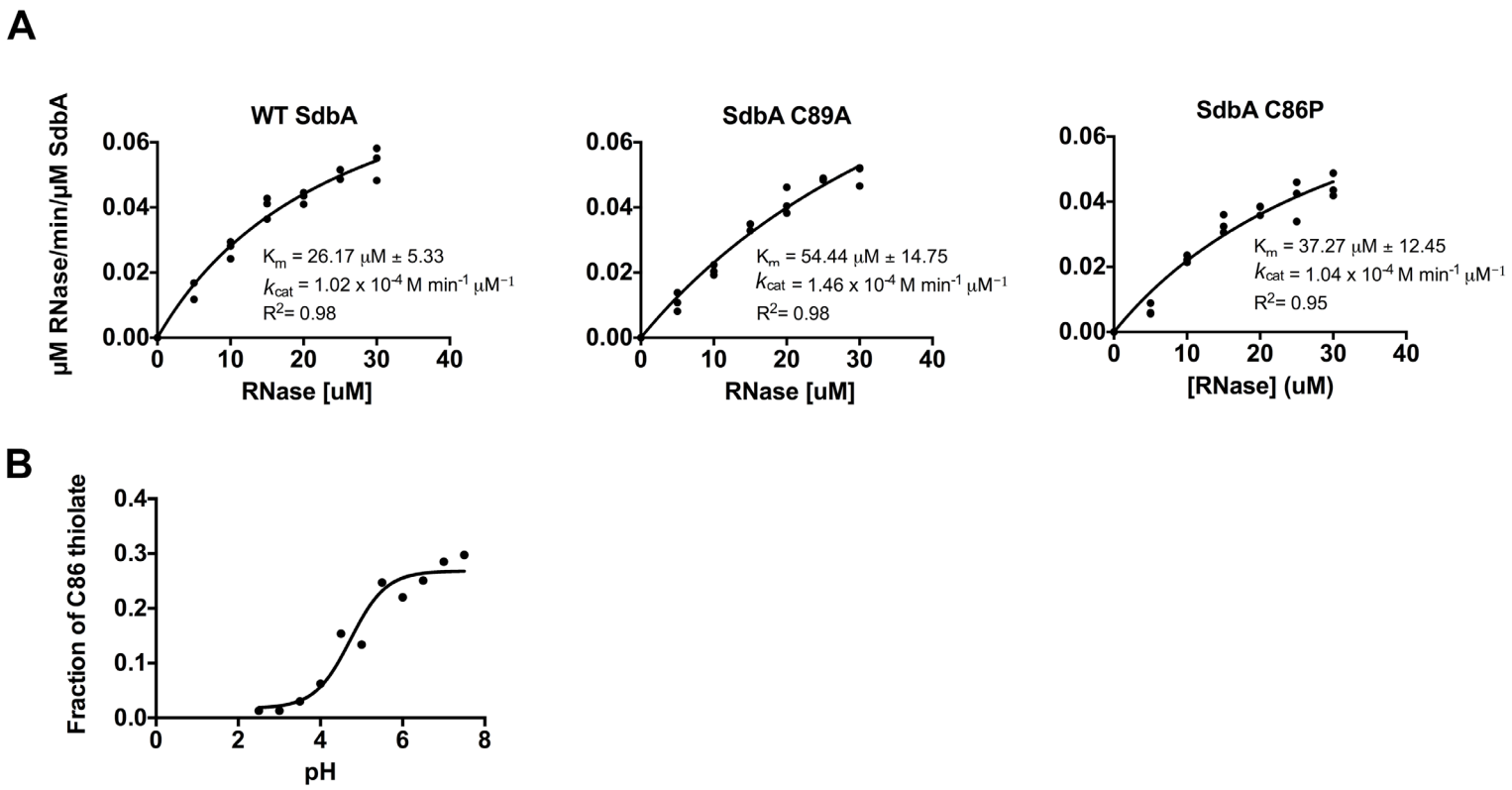

APPENDIX A2. Initial velocity of SdbA catalyzed RNase refolding and cysteine pK_a determination. (A) Michaelis-Menten enzyme kinetics for SdbA and the single cysteine variants reacted with RNase A, the k_{cat} and K_m values were calculated as described previously (222). (B) Determination of the pK_a of the SdbA N-terminal cysteine.

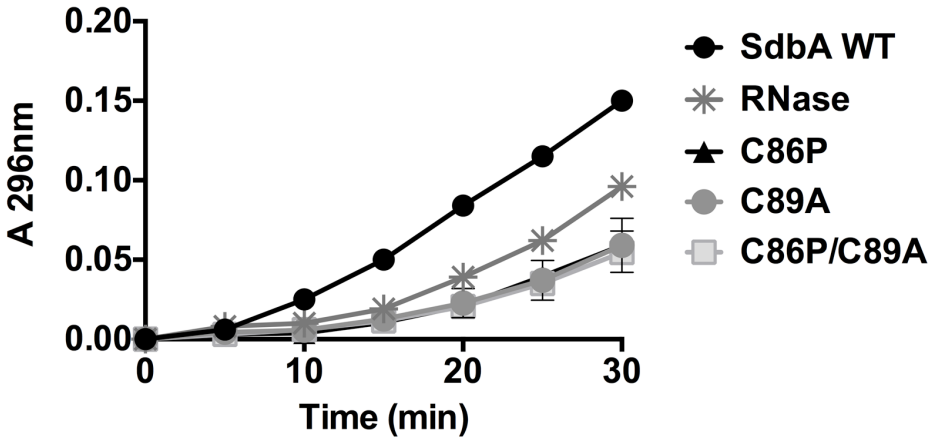

APPENDIX A3. *In vitro* oxidase activity of $SdbA_{C86P}$ and $SdbA_{C89A}$. Refolding of reduced denatured RNase A by wild-type SdbA, $SdbA_{C86P}$ (C86P), $SdbA_{C89A}$ (C89A), and $SdbA_{C86P/C89A}$ (C86P/C89A). The single cysteine variants were not oxidized with glutathione prior to the assay. RNase: RNase A alone.

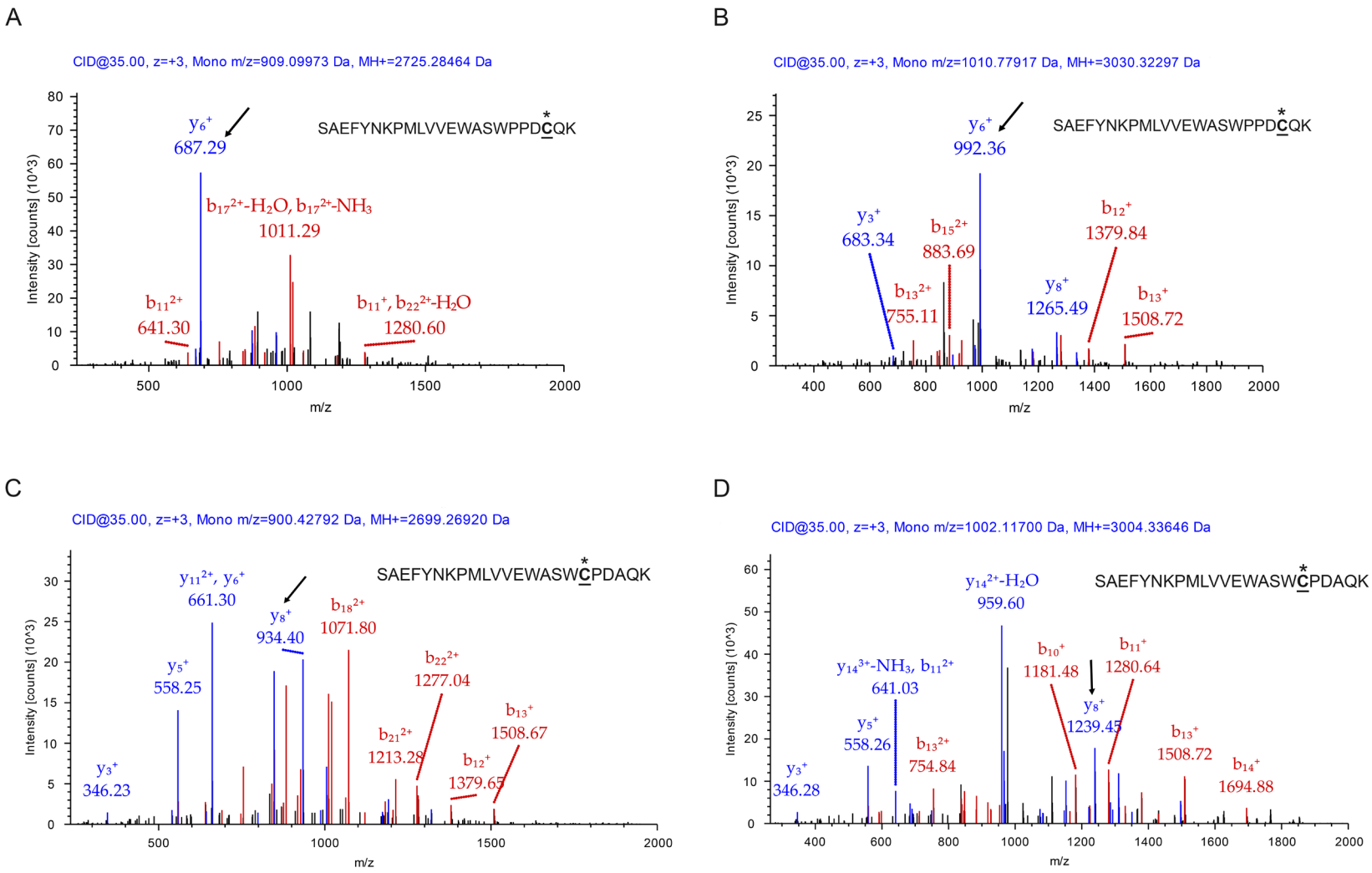
A
CID@35.00, z=+3, Mono m/z=909.09973 Da, MH+=2725.28464 Da
SAEFYNKPMLVVEWASWPPDC*QK
y6+ 687.29
b17 2+-H2O, b17 2+-NH3 1011.29
b11 2+ 641.30
b11+, b22 2+-H2O 1280.60
Intensity [counts] (10^3)
m/z
B
CID@35.00, z=+3, Mono m/z=1010.77917 Da, MH+=3030.32297 Da
SAEFYNKPMLVVEWASWPPDC*QK
y6+ 992.36
y3+ 683.34
b15 2+ 883.69
b13 2+ 755.11
y8+ 1265.49
b12+ 1379.84
b13+ 1508.72
Intensity [counts] (10^3)
m/z
C
CID@35.00, z=+3, Mono m/z=900.42792 Da, MH+=2699.26920 Da
SAEFYNKPMLVVEWASWC*PDAQK
y11 2+, y6+ 661.30
y8+ 934.40
b18 2+ 1071.80
y5+ 558.25
b22 2+ 1277.04
b21 2+ 1213.28
b13+ 1508.67
b12+ 1379.65
y3+ 346.23
Intensity [counts] (10^3)
m/z
D
CID@35.00, z=+3, Mono m/z=1002.11700 Da, MH+=3004.33646 Da
SAEFYNKPMLVVEWASWC*PDAQK
y14 2+-H2O 959.60
y14 3+-NH3, b11 2+ 641.03
b10+ 1181.48
b11+ 1280.64
y8+ 1239.45
y5+ 558.26
b13 2+ 754.84
b13+ 1508.72
b14+ 1694.88
y3+ 346.28
Intensity [counts] (10^3)
m/z

E

SdbA C86P: SAEFYNKPMLVVEWASWPPDC*QK

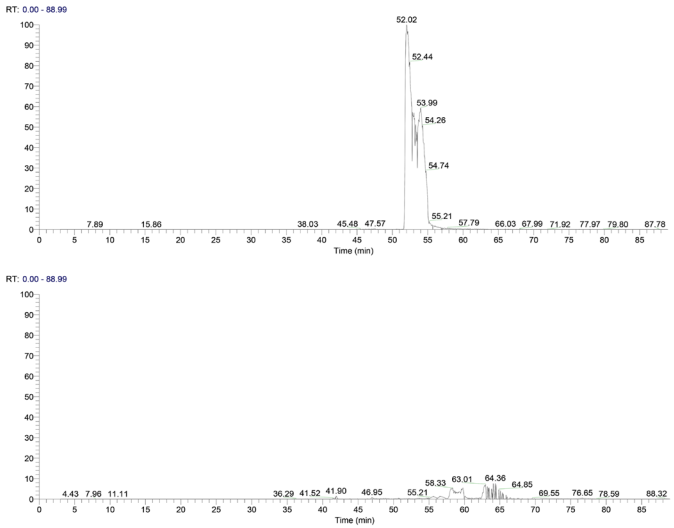

F

SdbA C89A: SAEFYNKPMLVVEWASWC*PDAQK

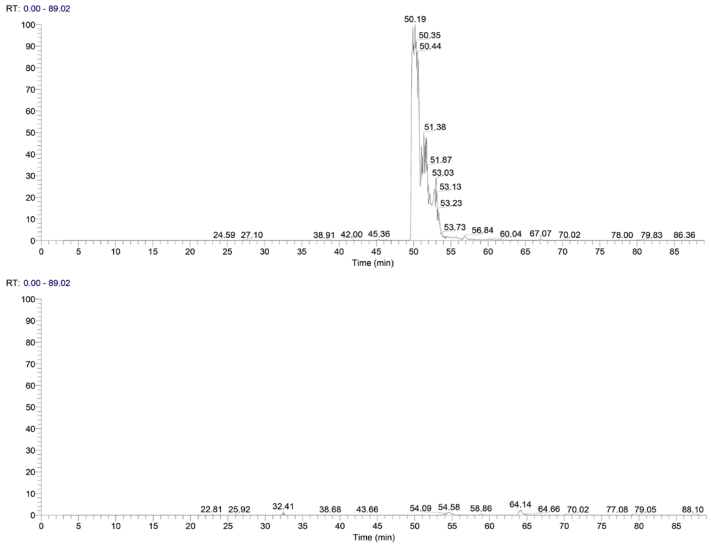

APPENDIX A4. S-glutathionylation of $SdbA_{C86P}$ and $SdbA_{C89A}$. Tandem MS/MS spectra for the cysteine containing peptide of (A) untreated $SdbA_{C86P}$ and (B) S-glutathionylated $SdbA_{C86P}$. The y_6 fragments (arrows) of the untreated and S-glutathionylated samples show a mass increase of +305 Da corresponding to the addition of glutathione. The asterisk indicates the modified cysteine in the peptide. The spectra for the cysteine containing peptide of (C) untreated $SdbA_{C89A}$ and (D) S-glutathionylated $SdbA_{C89A}$ also shows a +305 Da mass increase. This increase can be detected by comparing the y_8 fragments (arrows). The relative abundance of the S-glutathionylated peptides was determined from the extracted ion chromatograms. (E) Chromatograms for the cysteine containing peptide of $SdbA_{C86P}$ showing the S-glutathionylated peptide (upper panel) and untreated (lower panel). (F) Chromatograms for $SdbA_{C89A}$ showing the S-glutathionylated peptide (upper panel) and untreated (lower panel).

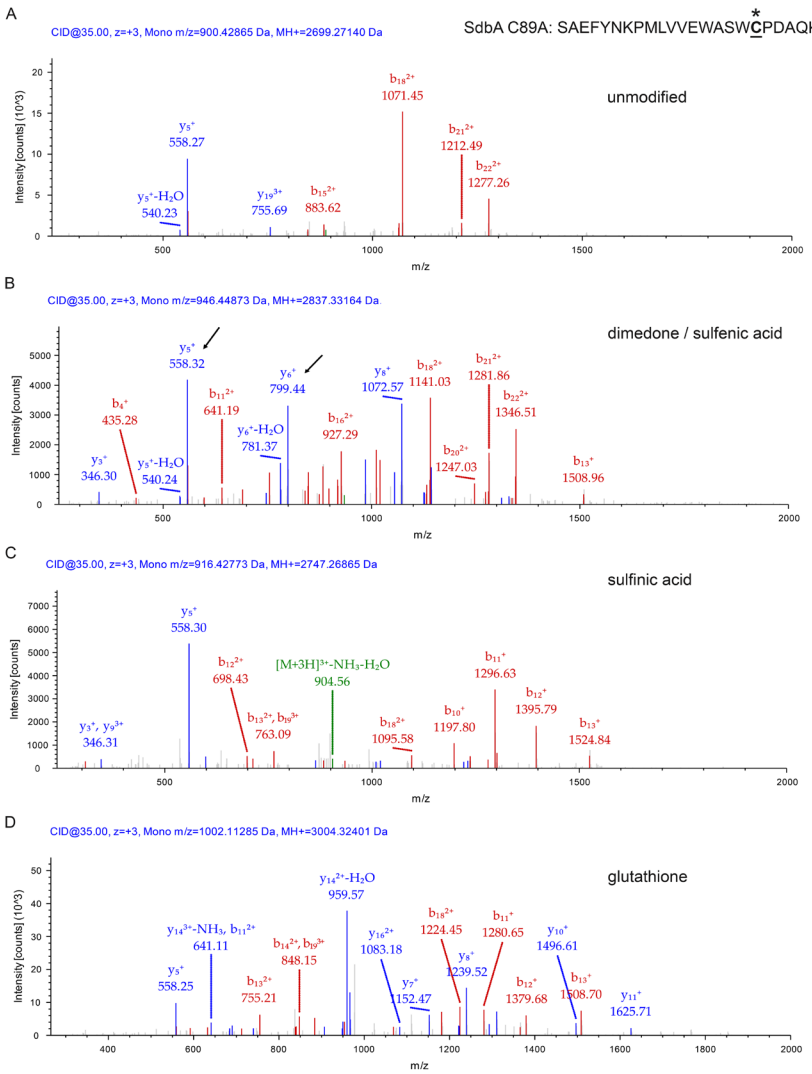
A
CID@35.00, z=+3, Mono m/z=900.42865 Da, MH+=2699.27140 Da
SdbA C89A: SAEFYNKPMLVVEWASWC*PDAQK
unmodified
b18 2+ 1071.45
y5+ 558.27
b21 2+ 1212.49
b22 2+ 1277.26
y5+-H2O 540.23
y19 3+ 755.69
b15 2+ 883.62
Intensity [counts] (10^3)
m/z
B
CID@35.00, z=+3, Mono m/z=946.44873 Da, MH+=2837.33164 Da
dimedone / sulfenic acid
y5+ 558.32
y6+ 799.44
y8+ 1072.57
b18 2+ 1141.03
b21 2+ 1281.86
b11 2+ 641.19
b22 2+ 1346.51
b4+ 435.28
y6+-H2O 781.37
b16 2+ 927.29
b20 2+ 1247.03
y3+ 346.30
y5+-H2O 540.24
b13+ 1508.96
Intensity [counts]
m/z
C
CID@35.00, z=+3, Mono m/z=916.42773 Da, MH+=2747.26865 Da
sulfinic acid
y5+ 558.30
b12 2+ 698.43
[M+3H]3+-NH3-H2O 904.56
b11+ 1296.63
b12+ 1395.79
b13 2+, b19 3+ 763.09
b18 2+ 1095.58
b10+ 1197.80
b13+ 1524.84
y3+, y9 3+ 346.31
Intensity [counts]
m/z
D
CID@35.00, z=+3, Mono m/z=1002.11285 Da, MH+=3004.32401 Da
glutathione
y14 2+-H2O 959.57
b18 2+ 1224.45
b11+ 1280.65
y14 3+-NH3, b11 2+ 641.11
y16 2+ 1083.18
y10+ 1496.61
y8+ 1239.52
b14 2+, b19 3+ 848.15
y5+ 558.25
b13 2+ 755.21
y7+ 152.47
b12+ 1379.68
b13+ 1508.70
y11+ 1625.71
Intensity [counts] (10^3)
m/z
E
SdbA C89A: SAEFYNKPMLVVEWASWC*PDAQK
dimedone
RT: 0.00 - 88.99
66.48
44.25
Time (min)
RT: 0.00 - 88.99
56.47
56.33
52.43
unmodified
57.48
Time (min)

APPENDIX A5. $SdbA_{C89A}$ is susceptible to sulfenylation. Tandem MS/MS spectra for the cysteine containing peptide of $SdbA_{C89A}$ in samples reacted with 100 μM hydrogen peroxide in the presence of the sulfenic acid probe dimedone. (A) Unmodified peptide with a free thiol. (B) Sulfenic acid stabilized by dimedone. The dimedone modification can be detected by comparing the y_5 (558.32 Da) and y_6 (799.44) fragments (arrows). The mass increase of +241 Da corresponds to a cysteine residue (103 Da) and dimedone (138 Da). (C) Sulfinylated peptide. (D) S-glutathionylated peptide. (E) Extracted ion chromatogram of the dimedone modified peptide (upper panel) and unmodified peptide (lower panel). The arrows indicate the peaks corresponding to SdbA.

SdbA C86P: SAEFYNKPMLVVEWASWPPD*C̲QK

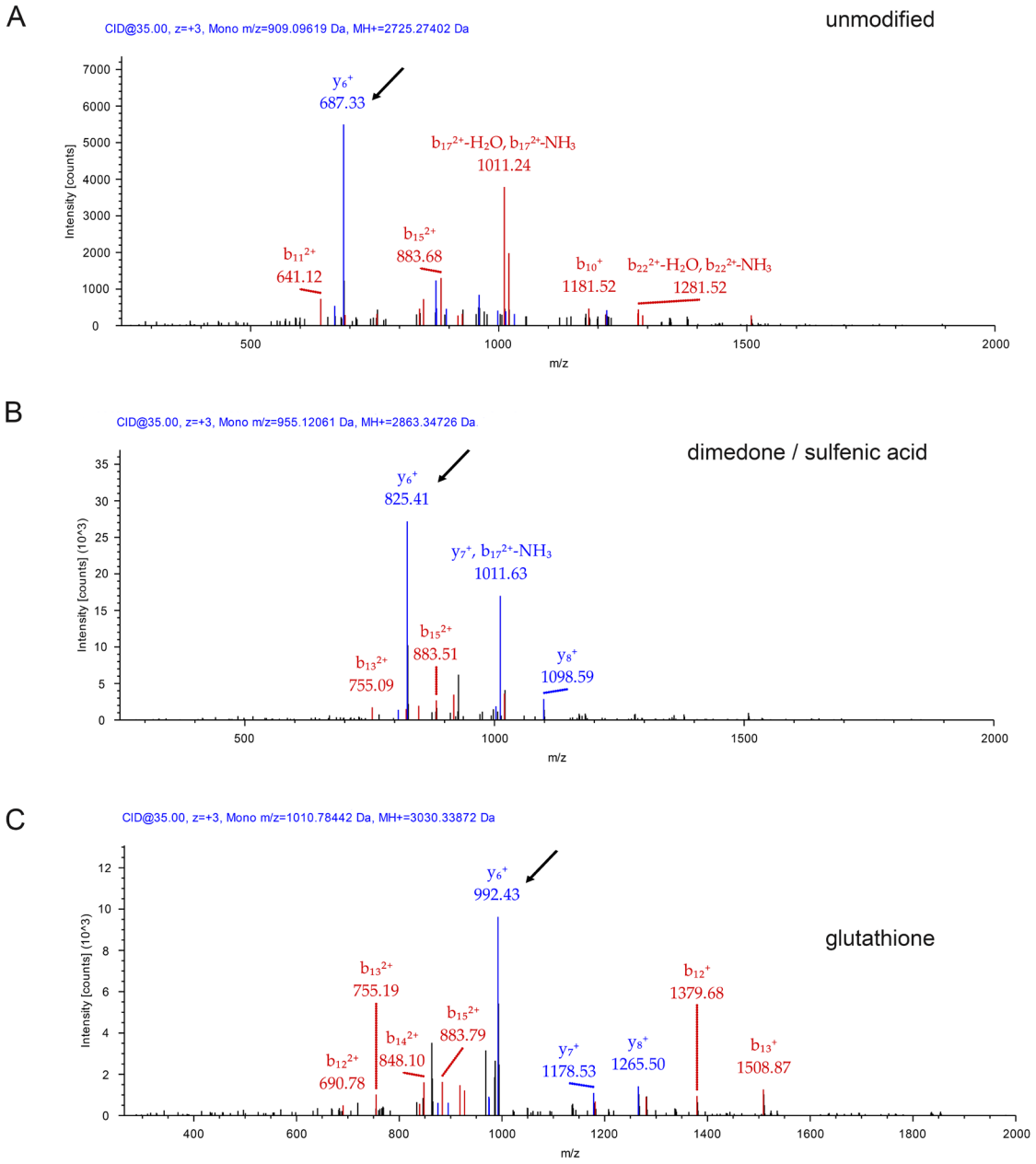

APPENDIX A6. Sulfenylation of $SdbA_{C86P}$. Tandem MS/MS spectra for the cysteine containing peptide of $SdbA_{C86P}$ in samples reacted with 100 μM hydrogen peroxide in the presence of the sulfenic acid probe dimedone. Arrows indicate the y_6 fragment containing the active site cysteine. (A) Unmodified peptide. (B) Sulfenic acid stabilized by dimedone. The addition of dimedone can be detected by comparing the cysteine containing y_6 fragment (825.41 Da) to the y_6 fragment of the unmodified peptide (687.33 Da). The mass increase of +138 Da corresponds to the addition of dimedone. (C) S-glutathionylated peptide showing a +305 Da change in mass on the y_6 fragment.

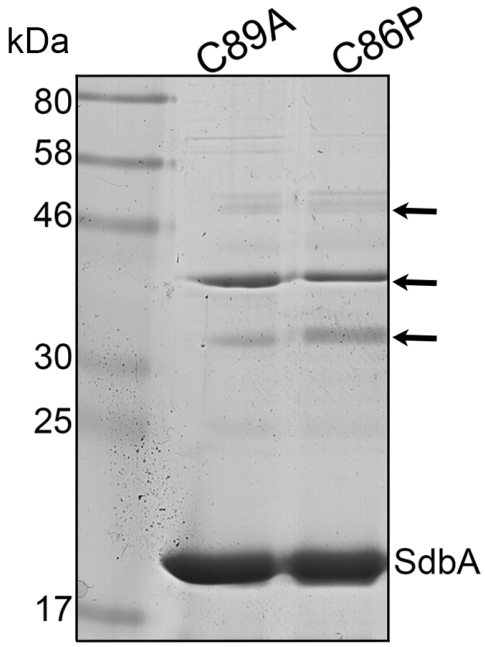

APPENDIX A7. SdbA complexes with RNase A. $SdbA_{C86P}$ and $SdbA_{C89A}$ variants were reacted with reduced denatured RNase A in glutathione buffer. The reaction was quenched by TCA precipitation and SdbA was isolated by affinity purification, followed by non-reducing SDS-PAGE. Arrows indicate disulfide-linked complexes.

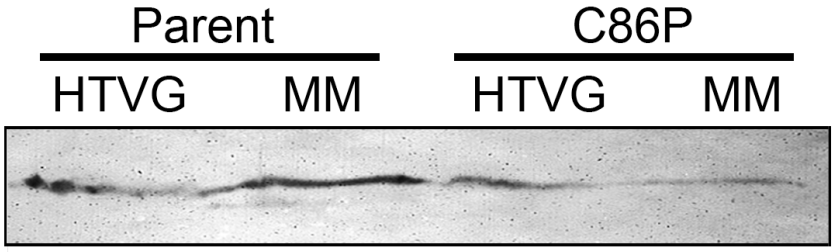

APPENDIX A8. Effect of medium composition on production of a disulfide bonded protein.

Production of scFv produced by the parent and *sdbA*$_{C86P}$ (C86P) mutant grown in a rich medium (HTVG) and in cysteine free minimal medium (MM). Western blot probed with anti-HA antibodies.

Appendix B: Supporting Information for Chapter 5

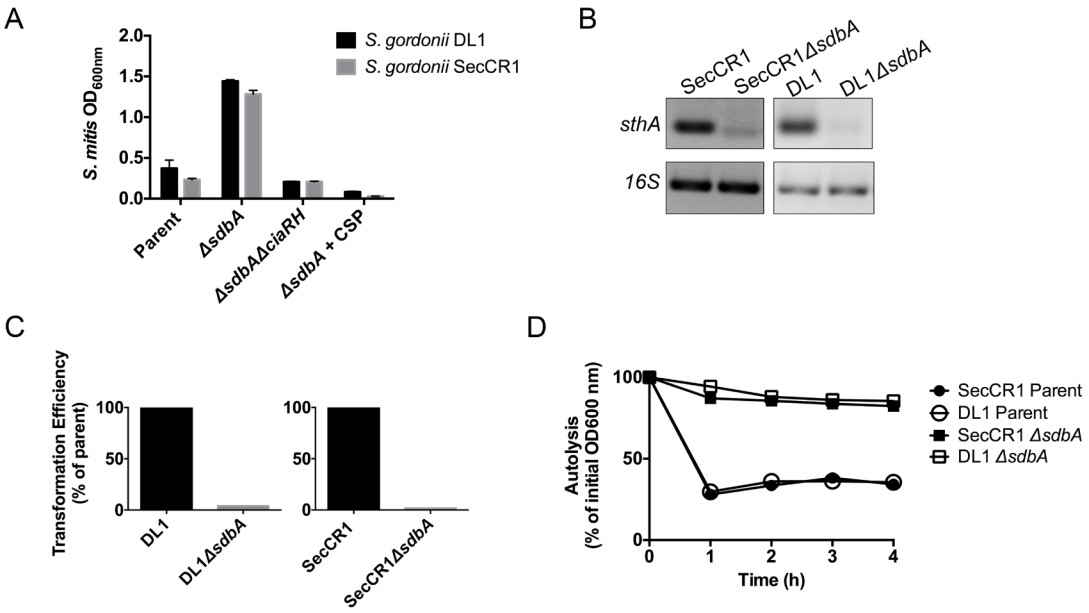

APPENDIX B1. Mutation of *sdbA* and *ciaRH* in *S. gordonii* SecCR1 and *S. gordonii* DL1 Challis produces similar phenotypes in both strains. (A) Bacteriocin activity of culture supernatants from the SecCR1 and DL1 parent and their *ΔsdbA* and *ΔsdbAΔciaRH* mutants. The supernatants were filter sterilized and inoculated with the indicator strain *S. mitis*. Results are means ± SD of three experiments. (B) RT-PCR analysis of *sthA* expression in the DL1 parent, DL1 *ΔsdbA* mutant, SecCR1 parent, and SecCR1 *ΔsdbA* mutant. Amplification of 16S rRNA is shown below as a control. (C) Transformation frequency of the DL1 parent, DL1 *ΔsdbA* mutant, SecCR1 parent and SecCR1 *ΔsdbA* mutant. Bars represent the percentage of transformed cells relative to the parent strains. (D) Autolysis of the SecCR1 and DL1 Challis parent strains and their *ΔsdbA* mutants.

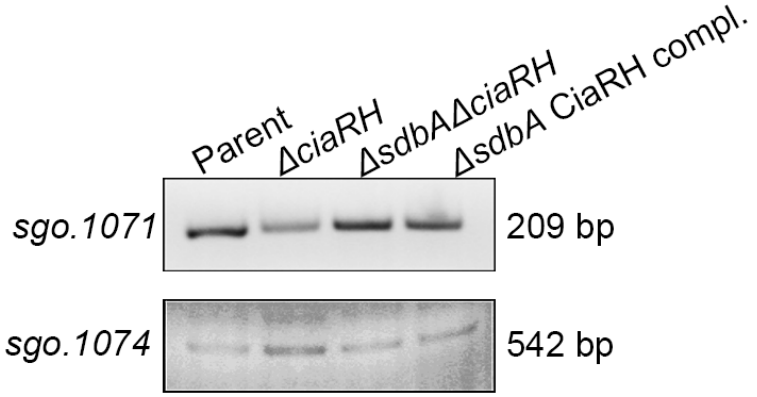

APPENDIX B2. RT-PCR for the upstream and downstream genes flanking *ciaRH*.
RT-PCR was used to amplify *sgo.1071* and *sgo.1074* from the parent, *ΔciaRH*, *ΔsdbAΔciaRH, and ΔsdbA* CiaRH complemented mutant (*ΔsdbA* CiaRH Compl).

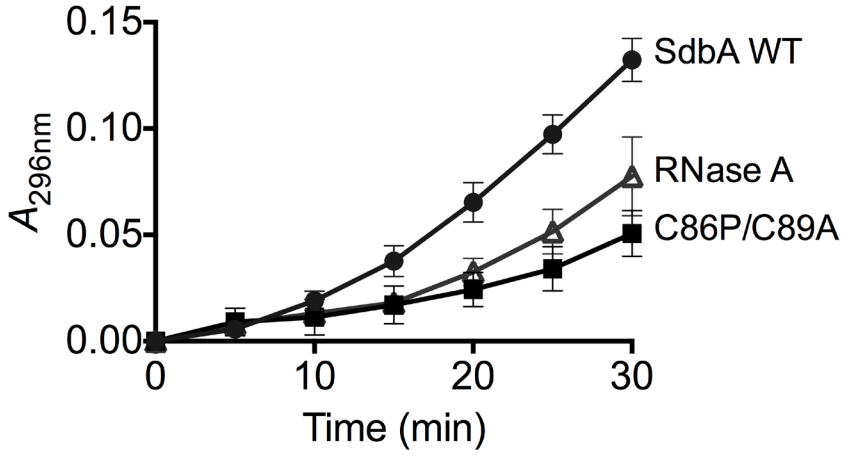

APPENDIX B3. *In vitro* oxidase activity of SdbA and SdbA C86P/C89A. SdbA catalyzed refolding of reduced and denatured RNase A in the presence of glutathione buffer. RNase A was incubated with affinity purified wild-type SdbA (circles), the double cysteine mutant (C86P/C89A) (squares), or without SdbA (triangles) as a negative control. Refolding was monitored by measuring hydrolysis of cCMP by active RNase A as the increase in absorbance at 296 nm.

Appendix C: Immunoblotting Conditions for Small Peptides from Streptococci

Davey L, **Halperin SA**, **Lee SF**. 2015. Immunoblotting conditions for small peptides from streptococci. J Microbiol Methods **114**:40–42

Abstract

Streptococci secrete small peptides with important biological functions. These peptides are not amenable to standard immunoblotting, and are often detected indirectly using activity assays, or by alternative approaches that may be expensive and laborious. Here we describe an immunoblotting method that enables reproducible detection of these small streptococcal peptides.

Streptococci secrete small peptides to mediate complex signaling process such as quorum sensing and genetic competence, and to inhibit the growth of competitors. These small, positively charged peptides are characterized by double glycine processing motif, and include competence signaling peptides (CSP) and class II bacteriocins (292).

Although standard immunoblotting techniques have been used to detect peptides from related bacteria, including the double glycine motif bacteriocins enterocin P (320), pediocin (321), and lactocin (322), similar peptides from streptococci are not typically detected by Western blotting, possibly due to their small size, around 2 kDa, and high isoelectric point, ranging between 10 and 12. Alternative detection strategies have included high performance liquid chromatography (323), mass spectrometry (324), activity assays (188, 325), and the use tags, which facilitate detection, but interfere with biological functions (282).

We found that streptococcal peptides bound poorly to the transfer membrane, washing off before they could be detected. Here we report a method that stably fixes

peptides to the membrane, enabling detection by immunoblotting. All experiments were performed at least three times and the reported results were representative of the experiments.

The method described here can be used to detect streptococcal peptides by Western blotting on polyvinyl difluoride (PVDF) membranes. Synthetic peptides were obtained from Biomatik (Cambridge, ON, Canada) using the amino acid sequences for the *Streptococcus gordonii* bacteriocin Sth1 (AGFTGGIAVGLNRVNRK), and competence signaling peptide (CSP; DVRSNKIRLWWENIFFNKK), *Streptococcus pneumoniae* CSP (EMRLFFRNFILQRKK), and *Streptococcus mutans* CSP (SGSLSTFFRLFNRSFTQALGK). Peptides were boiled for 5 min in SDS-PAGE sample buffer (250 mM Tris-HCl pH 6.8, 2% sodium dodecyl sulfate, 10% glycerol, 10% 2-mercaptoethanol, 0.01% bromophenol blue) and electrophoresed on Tris-tricine, 6 M urea 14% polyacrylamide gels (326). Proteins were transferred to PVDF membranes (Immobilon-P, Millipore) using a tank transfer system with 25 mM Tris, 192 mM glycine buffer for 45 min at a constant 150 mA. Prior to transfer, membranes were pre-wet with 100% methanol for 15 s, followed by Milli-Q water for 2 min and transfer buffer for 15 min. After transfer, membranes were dried for 1 h at 37°C and submerged in freshly prepared 5% paraformaldehyde (BioShop, Burlington, ON, Canada) in phosphate buffered saline (PBS) for 30 min at 37°C. Coomassie blue staining of PVDF membranes was carried out according to the manufacturer's instructions.

For immunoblotting, membranes were rinsed with Milli-Q water following fixation, and blocked with 1% gelatin in PBS with 0.1% Tween-20 (PBST) for 1 h. Antiserum was raised against *S. gordonii* Sth1 and CSP conjugated to keyhole limpet hemocyanin (Biomatik) in New Zealand white rabbits by subcutaneous injection with Freund's incomplete adjuvant (Sigma-Aldrich, Oakville, ON, Canada), using methods similar to those described previously (327). The membranes were incubated with antiserum against either *S. gordonii* Sth1 and CSP (1:500) at 4°C overnight, and subsequently washed 3X with PBST and reacted with goat anti-rabbit IgG-alkaline phosphatase (1:30 000; Sigma-

Aldrich). Pre-immune sera were used as controls and no cross-reactions were observed (data not shown).

Our initial attempts to detect *S. gordonii* Sth1 and CSP by SDS-PAGE with 16% Tris-tricine polyacrylamide gels and immunoblotting to nitrocellulose using standard techniques (218) were unsuccessful. Coomassie blue staining of the gels after transfer revealed that a significant portion of the peptides remained in the gel (data not shown). Transfer out the gel was improved using 14% acrylamide gels with 6 M urea, although the peptides were still not detected on the membrane. One possible explanation was that the peptides were transferring through the membrane due to their small size. We tested for this using multiple layers of membrane and short transfer times, however the peptides were still not detected.

Previous studies found that fixing to the membrane can improve detection of low molecular weight proteins (328–330). We tested fixation using 100% methanol, drying, 5% paraformaldehyde, or drying followed by paraformaldehyde (APPENDIX C1). Although the peptides were not detected after drying or after methanol fixation, 5% paraformaldehyde successfully fixed the peptides to the membrane, and drying the membrane prior to fixation with paraformaldehyde further enhanced detection (APPENDIX C1). The dried membranes were submerged directly into paraformaldehyde without rewetting. Importantly, methanol was found to inhibit peptide binding and was omitted from all steps, with the exception of the initial wetting of the membranes and Coomassie blue staining. Prepared formaldehyde solutions (37% formaldehyde), which contain 10-15% methanol, should be avoided.

We tested transfer and fixation on PVDF (Immobilon-P^{SQ} 0.22 μM and Immobilon-P 0.45 μM, Millipore), nitrocellulose (Bio-Rad Laboratories), and nylon membranes (Hybond-N, Amersham) (APPENDIX C2). Immunoblotting was carried out as described above, except that nylon membranes were blocked with 5% skim milk in 10 mM maleic acid-NaOH pH 7.5 with 15 mM NaCl. PVDF membranes were found to be critical for detection, and no protein was detected on nitrocellulose or nylon membranes

despite following the same fixation procedure. Surprisingly, the membrane pore size did not affect binding, and the peptides were efficiently detected on 0.45 μM PVDF without passing through the membrane. A minor portion of *S. gordonii* CSP, however, was found to migrate in the opposite direction, towards the cathode.

To determine if the protocol could be used for other streptococcal peptides, Western blots were performed using CSP from *S. mutans* and *S. pneumoniae* (APPENDIX C3A). The peptides transferred and bound to the membrane, suggesting that the protocol is broadly applicable to similar peptides. Finally, the sensitivity of the assay was determined by immunoblotting against *S. gordonii* Sth1, and as little as 25 ng of the peptide could be detected (APPENDIX C3B).

In conclusion, we report an efficient method to detect streptococcal peptides by Western blotting which has not been possible previously. Compared to existing techniques, such as HPLC that requires specialized equipment and expertise, the methods described here use simple and inexpensive materials. If the appropriate antibodies are generated, immunoblotting could facilitate detection of secreted peptides without the use of tags that inhibit biological activity.

Acknowledgments

Funding for this study was provided by the Natural Sciences and Engineering Research Council of Canada (NSERC). LD is a recipient of a NSERC post-graduate scholarship, an IWK graduate scholarship, and a Scotia Scholars Award.

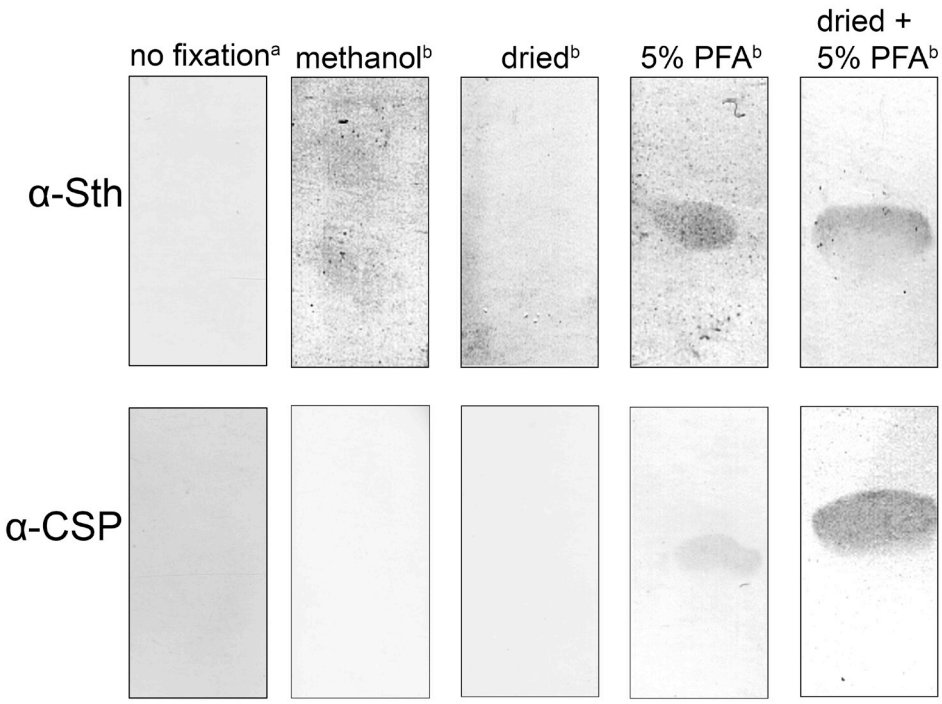

APPENDIX C1. Fixing to the membrane enables detection of *Streptococcus* peptides. *S. gordonii* Sth1 (upper panel) and CSP (lower panel) (1 μg) were transferred to PVDF membranes. After transfer, the membranes were either blocked immediately with 1% gelatin (no fixation), or treated as follows prior to blocking: 100% methanol for 30 min (methanol), dried at 37°C for 1 h (dried), 5% paraformaldehyde for 30 min at 37°C (5% PFA), or dried then fixed with 5% paraformaldehyde (dried + 5% PFA). Peptides were detected with anti-CSP or anti-Sth1 antisera.

[a] 0.22 μM Immobilon-P^{SQ}; [b] 0.45 μM Immonbilon-P

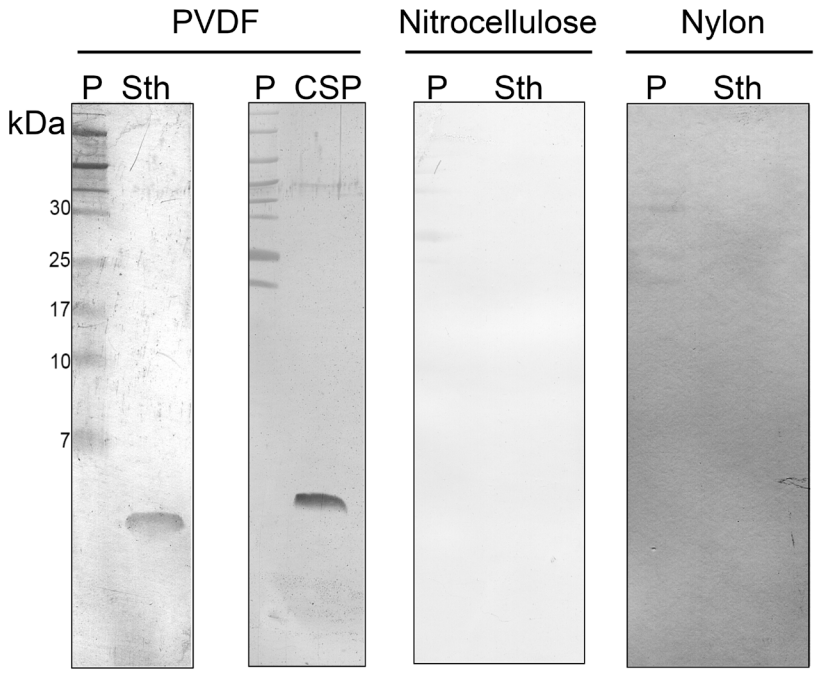

APPENDIX C2. PVDF membranes are required for detection. Detection of *S. gordonii* Sth1 and CSP (1 μg) was tested on PVDF, nitrocellulose, and nylon membranes. The peptides were fixed by drying followed by 5% paraformaldehyde, and detected with either anti-CSP or anti-Sth1 antisera. Protein markers (P).

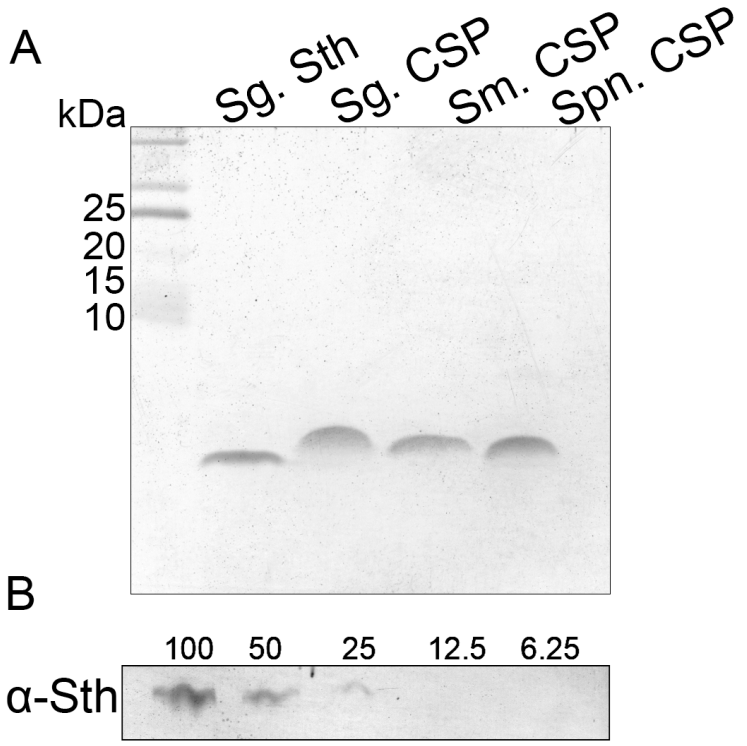

APPENDIX C3. Applicability and sensitivity of peptide blotting. (A) Peptides from *S. gordonii* (Sg), *S. mutans* (Sm), and *S. pneumoniae* (Spn) were transferred to PVDF membranes and fixed by drying followed by 5% paraformaldehyde. Coomassie blue staining was used for detection. (B) Detection of *S. gordonii* Sth1 (ng) with anti-Sth1 antisera.

Appendix D: Copyright Release for Published Material

11200 Rockville Pike
Suite 302
Rockville, Maryland 20852

August 19, 2011

American Society for Biochemistry and Molecular Biology

To whom it may concern,

It is the policy of the American Society for Biochemistry and Molecular Biology to allow reuse of any material published in its journals (the Journal of Biological Chemistry, Molecular & Cellular Proteomics and the Journal of Lipid Research) in a thesis or dissertation at no cost and with no explicit permission needed. Please see our copyright permissions page on the journal site for more information.

Best wishes,

Sarah Crespi

American Society for Biochemistry and Molecular Biology
11200 Rockville Pike, Rockville, MD
Suite 302
240-283-6616
JBC | MCP | JLR

JOHN WILEY AND SONS LICENSE TERMS AND CONDITIONS

Jan 17, 2016

This Agreement between Lauren Davey ("You") and John Wiley and Sons ("John Wiley and Sons") consists of your license details and the terms and conditions provided by John Wiley and Sons and Copyright Clearance Center.

License Number	3791481209570
License date	Jan 17, 2016
Licensed Content Publisher	John Wiley and Sons
Licensed Content Publication	Molecular Microbiology
Licensed Content Title	The disulfide oxidoreductase SdbA is active in Streptococcus gordonii using a single C-terminal cysteine of the CXXC motif
Licensed Content Author	Lauren Davey,Alejandro Cohen,Jason LeBlanc,Scott A. Halperin,Song F. Lee
Licensed Content Date	Oct 30, 2015
Pages	1
Type of use	Dissertation/Thesis
Requestor type	Author of this Wiley article
Format	Print and electronic
Portion	Full article
Will you be translating?	No
Title of your thesis / dissertation	SdbA Catalyzes Disulfide Bond Formation in Streptococcus gordonii
Expected completion date	Feb 2016
Expected size (number of pages)	300
Requestor Location	Lauren Davey 6249 Coburg Rd

AMERICAN SOCIETY FOR MICROBIOLOGY

Title:	Mutation of the Thiol-Disulfide Oxidoreductase SdbA Activates the CiaRH Two-Component System, Leading to Bacteriocin Expression Shutdown in Streptococcus gordonii
Author:	Lauren Davey, Scott A. Halperin, Song F. Lee et al.
Publication:	Journal of Bacteriology
Publisher:	American Society for Microbiology
Date:	Jan 15, 2016

Permissions Request

Authors in ASM journals retain the right to republish discrete portions of his/her article in any other publication (including print, CD-ROM, and other electronic formats) of which he or she is author or editor, provided that proper credit is given to the original ASM publication. ASM authors also retain the right to reuse the full article in his/her dissertation or thesis. For a full list of author rights, please see: http://journals.asm.org/site/misc/ASM_Author_Statement.xhtml

BACK | CLOSE WINDOW

ELSEVIER LICENSE
TERMS AND CONDITIONS

Jan 22, 2016

This is an Agreement between Lauren Davey ("You") and Elsevier ("Elsevier"). It consists of your order details, the terms and conditions provided by Elsevier, and the payment terms and conditions.

All payments must be made in full to CCC. For payment instructions, please see information listed at the bottom of this form.

Supplier	Elsevier Limited The Boulevard,Langford Lane Kidlington,Oxford,OX5 1GB,UK
Registered Company Number	1982084
Customer name	Lauren Davey
Customer address	6249 Coburg Rd Halifax, NS B3H 2A2
License number	3791850695224
License date	Jan 18, 2016
Licensed content publisher	Elsevier
Licensed content publication	Journal of Microbiological Methods
Licensed content title	Immunoblotting conditions for small peptides from streptococci
Licensed content author	Lauren Davey,Scott A. Halperin,Song F. Lee
Licensed content date	July 2015
Licensed content volume number	114
Licensed content issue number	n/a
Number of pages	3
Start Page	40
End Page	42
Type of Use	reuse in a thesis/dissertation
Portion	full article
Format	both print and electronic
Are you the author of this Elsevier article?	Yes
Will you be translating?	No
Title of your thesis/dissertation	SdbA Catalyzes Disulfide Bond Formation in Streptococcus gordonii
Expected completion date	Feb 2016
Estimated size (number of pages)	300
Elsevier VAT number	GB 494 6272 12
Price	0.00 CAD
VAT/Local Sales Tax	0.00 CAD / 0.00 GBP